Initial sequencing and analysis of the human genome

International Human Genome Sequencing Consortium*

* *A partial list of authors appears on the opposite page. Affiliations are listed at the end of the paper.*

The human genome holds an extraordinary trove of information about human development, physiology, medicine and evolution. Here we report the results of an international collaboration to produce and make freely available a draft sequence of the human genome. We also present an initial analysis of the data, describing some of the insights that can be gleaned from the sequence.

The rediscovery of Mendel's laws of heredity in the opening weeks of the 20th century[1–3] sparked a scientific quest to understand the nature and content of genetic information that has propelled biology for the last hundred years. The scientific progress made falls naturally into four main phases, corresponding roughly to the four quarters of the century. The first established the cellular basis of heredity: the chromosomes. The second defined the molecular basis of heredity: the DNA double helix. The third unlocked the informational basis of heredity, with the discovery of the biological mechanism by which cells read the information contained in genes and with the invention of the recombinant DNA technologies of cloning and sequencing by which scientists can do the same.

The last quarter of a century has been marked by a relentless drive to decipher first genes and then entire genomes, spawning the field of genomics. The fruits of this work already include the genome sequences of 599 viruses and viroids, 205 naturally occurring plasmids, 185 organelles, 31 eubacteria, seven archaea, one fungus, two animals and one plant.

Here we report the results of a collaboration involving 20 groups from the United States, the United Kingdom, Japan, France, Germany and China to produce a draft sequence of the human genome. The draft genome sequence was generated from a physical map covering more than 96% of the euchromatic part of the human genome and, together with additional sequence in public databases, it covers about 94% of the human genome. The sequence was produced over a relatively short period, with coverage rising from about 10% to more than 90% over roughly fifteen months. The sequence data have been made available without restriction and updated daily throughout the project. The task ahead is to produce a finished sequence, by closing all gaps and resolving all ambiguities. Already about one billion bases are in final form and the task of bringing the vast majority of the sequence to this standard is now straightforward and should proceed rapidly.

The sequence of the human genome is of interest in several respects. It is the largest genome to be extensively sequenced so far, being 25 times as large as any previously sequenced genome and eight times as large as the sum of all such genomes. It is the first vertebrate genome to be extensively sequenced. And, uniquely, it is the genome of our own species.

Much work remains to be done to produce a complete finished sequence, but the vast trove of information that has become available through this collaborative effort allows a global perspective on the human genome. Although the details will change as the sequence is finished, many points are already clear.

- The genomic landscape shows marked variation in the distribution of a number of features, including genes, transposable elements, GC content, CpG islands and recombination rate. This gives us important clues about function. For example, the developmentally important HOX gene clusters are the most repeat-poor regions of the human genome, probably reflecting the very complex coordinate regulation of the genes in the clusters.
- There appear to be about 30,000–40,000 protein-coding genes in the human genome—only about twice as many as in worm or fly. However, the genes are more complex, with more alternative splicing generating a larger number of protein products.
- The full set of proteins (the 'proteome') encoded by the human genome is more complex than those of invertebrates. This is due in part to the presence of vertebrate-specific protein domains and motifs (an estimated 7% of the total), but more to the fact that vertebrates appear to have arranged pre-existing components into a richer collection of domain architectures.
- Hundreds of human genes appear likely to have resulted from horizontal transfer from bacteria at some point in the vertebrate lineage. Dozens of genes appear to have been derived from transposable elements.
- Although about half of the human genome derives from transposable elements, there has been a marked decline in the overall activity of such elements in the hominid lineage. DNA transposons appear to have become completely inactive and long-terminal repeat (LTR) retroposons may also have done so.
- The pericentromeric and subtelomeric regions of chromosomes are filled with large recent segmental duplications of sequence from elsewhere in the genome. Segmental duplication is much more frequent in humans than in yeast, fly or worm.
- Analysis of the organization of Alu elements explains the long-standing mystery of their surprising genomic distribution, and suggests that there may be strong selection in favour of preferential retention of Alu elements in GC-rich regions and that these 'selfish' elements may benefit their human hosts.
- The mutation rate is about twice as high in male as in female meiosis, showing that most mutation occurs in males.
- Cytogenetic analysis of the sequenced clones confirms suggestions that large GC-poor regions are strongly correlated with 'dark G-bands' in karyotypes.
- Recombination rates tend to be much higher in distal regions (around 20 megabases (Mb)) of chromosomes and on shorter chromosome arms in general, in a pattern that promotes the occurrence of at least one crossover per chromosome arm in each meiosis.
- More than 1.4 million single nucleotide polymorphisms (SNPs) in the human genome have been identified. This collection should allow the initiation of genome-wide linkage disequilibrium mapping of the genes in the human population.

In this paper, we start by presenting background information on the project and describing the generation, assembly and evaluation of the draft genome sequence. We then focus on an initial analysis of the sequence itself: the broad chromosomal landscape; the repeat elements and the rich palaeontological record of evolutionary and biological processes that they provide; the human genes and proteins and their differences and similarities with those of other

© 2001 Macmillan Magazines Ltd

EX1041

Genome Sequencing Centres (Listed in order of total genomic sequence contributed, with a partial list of personnel. A full list of contributors at each centre is available as Supplementary Information.)

Whitehead Institute for Biomedical Research, Center for Genome Research: Eric S. Lander[1*], Lauren M. Linton[1], Bruce Birren[1*], Chad Nusbaum[1*], Michael C. Zody[1*], Jennifer Baldwin[1], Keri Devon[1], Ken Dewar[1], Michael Doyle[1], William FitzHugh[1*], Roel Funke[1], Diane Gage[1], Katrina Harris[1], Andrew Heaford[1], John Howland[1], Lisa Kann[1], Jessica Lehoczky[1], Rosie LeVine[1], Paul McEwan[1], Kevin McKernan[1], James Meldrim[1], Jill P. Mesirov[1*], Cher Miranda[1], William Morris[1], Jerome Naylor[1], Christina Raymond[1], Mark Rosetti[1], Ralph Santos[1], Andrew Sheridan[1], Carrie Sougnez[1], Nicole Stange-Thomann[1], Nikola Stojanovic[1], Aravind Subramanian[1] & Dudley Wyman[1]

The Sanger Centre: Jane Rogers[2], John Sulston[2*], Rachael Ainscough[2], Stephan Beck[2], David Bentley[2], John Burton[2], Christopher Clee[2], Nigel Carter[2], Alan Coulson[2], Rebecca Deadman[2], Panos Deloukas[2], Andrew Dunham[2], Ian Dunham[2], Richard Durbin[2*], Lisa French[2], Darren Grafham[2], Simon Gregory[2], Tim Hubbard[2*], Sean Humphray[2], Adrienne Hunt[2], Matthew Jones[2], Christine Lloyd[2], Amanda McMurray[2], Lucy Matthews[2], Simon Mercer[2], Sarah Milne[2], James C. Mullikin[2*], Andrew Mungall[2], Robert Plumb[2], Mark Ross[2], Ratna Shownkeen[2] & Sarah Sims[2]

Washington University Genome Sequencing Center: Robert H. Waterston[3*], Richard K. Wilson[3], LaDeana W. Hillier[3*], John D. McPherson[3], Marco A. Marra[3], Elaine R. Mardis[3], Lucinda A. Fulton[3], Asif T. Chinwalla[3*], Kymberlie H. Pepin[3], Warren R. Gish[3], Stephanie L. Chissoe[3], Michael C. Wendl[3], Kim D. Delehaunty[3], Tracie L. Miner[3], Andrew Delehaunty[3], Jason B. Kramer[3], Lisa L. Cook[3], Robert S. Fulton[3], Douglas L. Johnson[3], Patrick J. Minx[3] & Sandra W. Clifton[3]

US DOE Joint Genome Institute: Trevor Hawkins[4], Elbert Branscomb[4], Paul Predki[4], Paul Richardson[4], Sarah Wenning[4], Tom Slezak[4], Norman Doggett[4], Jan-Fang Cheng[4], Anne Olsen[4], Susan Lucas[4], Christopher Elkin[4], Edward Uberbacher[4] & Marvin Frazier[4]

Baylor College of Medicine Human Genome Sequencing Center: Richard A. Gibbs[5*], Donna M. Muzny[5], Steven E. Scherer[5], John B. Bouck[5*], Erica J. Sodergren[5], Kim C. Worley[5*], Catherine M. Rives[5], James H. Gorrell[5], Michael L. Metzker[5], Susan L. Naylor[6], Raju S. Kucherlapati[7], David L. Nelson, & George M. Weinstock[8]

RIKEN Genomic Sciences Center: Yoshiyuki Sakaki[9], Asao Fujiyama[9], Masahira Hattori[9], Tetsushi Yada[9], Atsushi Toyoda[9], Takehiko Itoh[9], Chiharu Kawagoe[9], Hidemi Watanabe[9], Yasushi Totoki[9] & Todd Taylor[9]

Genoscope and CNRS UMR-8030: Jean Weissenbach[10], Roland Heilig[10], William Saurin[10], Francois Artiguenave[10], Philippe Brottier[10], Thomas Bruls[10], Eric Pelletier[10], Catherine Robert[10] & Patrick Wincker[10]

GTC Sequencing Center: Douglas R. Smith[11], Lynn Doucette-Stamm[11], Marc Rubenfield[11], Keith Weinstock[11], Hong Mei Lee[11] & JoAnn Dubois[11]

Department of Genome Analysis, Institute of Molecular Biotechnology: André Rosenthal[12], Matthias Platzer[12], Gerald Nyakatura[12], Stefan Taudien[12] & Andreas Rump[12]

Beijing Genomics Institute/Human Genome Center: Huanming Yang[13], Jun Yu[13], Jian Wang[13], Guyang Huang[14] & Jun Gu[15]

Multimegabase Sequencing Center, The Institute for Systems Biology: Leroy Hood[16], Lee Rowen[16], Anup Madan[16] & Shizen Qin[16]

Stanford Genome Technology Center: Ronald W. Davis[17], Nancy A. Federspiel[17], A. Pia Abola[17] & Michael J. Proctor[17]

Stanford Human Genome Center: Richard M. Myers[18], Jeremy Schmutz[18], Mark Dickson[18], Jane Grimwood[18] & David R. Cox[18]

University of Washington Genome Center: Maynard V. Olson[19], Rajinder Kaul[19] & Christopher Raymond[19]

Department of Molecular Biology, Keio University School of Medicine: Nobuyoshi Shimizu[20], Kazuhiko Kawasaki[20] & Shinsei Minoshima[20]

University of Texas Southwestern Medical Center at Dallas: Glen A. Evans[21]†, Maria Athanasiou[21] & Roger Schultz[21]

University of Oklahoma's Advanced Center for Genome Technology: Bruce A. Roe[22], Feng Chen[22] & Huaqin Pan[22]

Max Planck Institute for Molecular Genetics: Juliane Ramser[23], Hans Lehrach[23] & Richard Reinhardt[23]

Cold Spring Harbor Laboratory, Lita Annenberg Hazen Genome Center: W. Richard McCombie[24], Melissa de la Bastide[24] & Neilay Dedhia[24]

GBF—German Research Centre for Biotechnology: Helmut Blöcker[25], Klaus Hornischer[25] & Gabriele Nordsiek[25]

* **Genome Analysis Group (listed in alphabetical order, also includes individuals listed under other headings):** Richa Agarwala[26], L. Aravind[26], Jeffrey A. Bailey[27], Alex Bateman[2], Serafim Batzoglou[1], Ewan Birney[28], Peer Bork[29,30], Daniel G. Brown[1], Christopher B. Burge[31], Lorenzo Cerutti[28], Hsiu-Chuan Chen[26], Deanna Church[26], Michele Clamp[2], Richard R. Copley[30], Tobias Doerks[29,30], Sean R. Eddy[32], Evan E. Eichler[27], Terrence S. Furey[33], James Galagan[1], James G. R. Gilbert[2], Cyrus Harmon[34], Yoshihide Hayashizaki[35], David Haussler[36], Henning Hermjakob[28], Karsten Hokamp[37], Wonhee Jang[26], L. Steven Johnson[32], Thomas A. Jones[32], Simon Kasif[38], Arek Kaspryzk[28], Scot Kennedy[39], W. James Kent[40], Paul Kitts[26], Eugene V. Koonin[26], Ian Korf[3], David Kulp[34], Doron Lancet[41], Todd M. Lowe[42], Aoife McLysaght[37], Tarjei Mikkelsen[38], John V. Moran[43], Nicola Mulder[28], Victor J. Pollara[1], Chris P. Ponting[44], Greg Schuler[26], Jörg Schultz[30], Guy Slater[28], Arian F. A. Smit[45], Elia Stupka[28], Joseph Szustakowki[38], Danielle Thierry-Mieg[26], Jean Thierry-Mieg[26], Lukas Wagner[26], John Wallis[3], Raymond Wheeler[34], Alan Williams[34], Yuri I. Wolf[26], Kenneth H. Wolfe[37], Shiaw-Pyng Yang[3] & Ru-Fang Yeh[31]

Scientific management: National Human Genome Research Institute, US National Institutes of Health: Francis Collins[46*], Mark S. Guyer[46], Jane Peterson[46], Adam Felsenfeld[46*] & Kris A. Wetterstrand[46]; **Office of Science, US Department of Energy:** Aristides Patrinos[47]; **The Wellcome Trust:** Michael J. Morgan[48]

© 2001 Macmillan Magazines Ltd

organisms; and the history of genomic segments. (Comparisons are drawn throughout with the genomes of the budding yeast *Saccharomyces cerevisiae*, the nematode worm *Caenorhabditis elegans*, the fruitfly *Drosophila melanogaster* and the mustard weed *Arabidopsis thaliana*; we refer to these for convenience simply as yeast, worm, fly and mustard weed.) Finally, we discuss applications of the sequence to biology and medicine and describe next steps in the project. A full description of the methods is provided as Supplementary Information on *Nature*'s web site (http://www.nature.com).

We recognize that it is impossible to provide a comprehensive analysis of this vast dataset, and thus our goal is to illustrate the range of insights that can be gleaned from the human genome and thereby to sketch a research agenda for the future.

Background to the Human Genome Project

The Human Genome Project arose from two key insights that emerged in the early 1980s: that the ability to take global views of genomes could greatly accelerate biomedical research, by allowing researchers to attack problems in a comprehensive and unbiased fashion; and that the creation of such global views would require a communal effort in infrastructure building, unlike anything previously attempted in biomedical research. Several key projects helped to crystallize these insights, including:

(1) The sequencing of the bacterial viruses ΦX174[4,5] and lambda[6], the animal virus SV40[7] and the human mitochondrion[8] between 1977 and 1982. These projects proved the feasibility of assembling small sequence fragments into complete genomes, and showed the value of complete catalogues of genes and other functional elements.

(2) The programme to create a human genetic map to make it possible to locate disease genes of unknown function based solely on their inheritance patterns, launched by Botstein and colleagues in 1980 (ref. 9).

(3) The programmes to create physical maps of clones covering the yeast[10] and worm[11] genomes to allow isolation of genes and regions based solely on their chromosomal position, launched by Olson and Sulston in the mid-1980s.

(4) The development of random shotgun sequencing of complementary DNA fragments for high-throughput gene discovery by Schimmel[12] and Schimmel and Sutcliffe[13], later dubbed expressed sequence tags (ESTs) and pursued with automated sequencing by Venter and others[14–20].

The idea of sequencing the entire human genome was first proposed in discussions at scientific meetings organized by the US Department of Energy and others from 1984 to 1986 (refs 21, 22). A committee appointed by the US National Research Council endorsed the concept in its 1988 report[23], but recommended a broader programme, to include: the creation of genetic, physical and sequence maps of the human genome; parallel efforts in key model organisms such as bacteria, yeast, worms, flies and mice; the development of technology in support of these objectives; and research into the ethical, legal and social issues raised by human genome research. The programme was launched in the US as a joint effort of the Department of Energy and the National Institutes of Health. In other countries, the UK Medical Research Council and the Wellcome Trust supported genomic research in Britain; the Centre d'Etude du Polymorphisme Humain and the French Muscular Dystrophy Association launched mapping efforts in France; government agencies, including the Science and Technology Agency and the Ministry of Education, Science, Sports and Culture supported genomic research efforts in Japan; and the European Community helped to launch several international efforts, notably the programme to sequence the yeast genome. By late 1990, the Human Genome Project had been launched, with the creation of genome centres in these countries. Additional participants subsequently joined the effort, notably in Germany and China. In addition, the Human Genome Organization (HUGO) was founded to provide a forum for international coordination of genomic research. Several books[24–26] provide a more comprehensive discussion of the genesis of the Human Genome Project.

Through 1995, work progressed rapidly on two fronts (Fig. 1). The first was construction of genetic and physical maps of the human and mouse genomes[27–31], providing key tools for identification of disease genes and anchoring points for genomic sequence. The second was sequencing of the yeast[32] and worm[33] genomes, as

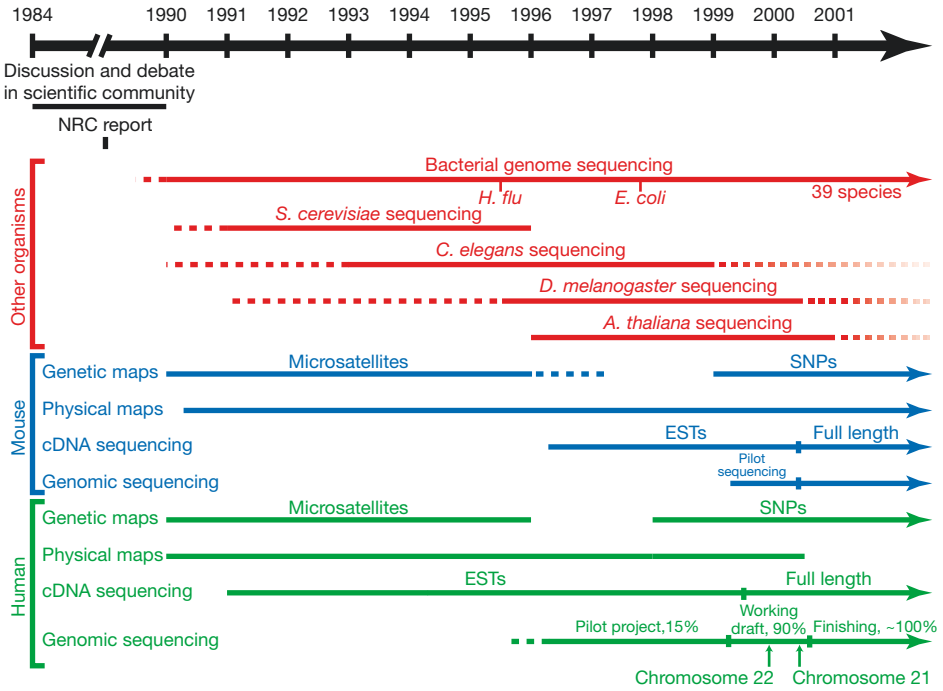

Figure 1 Timeline of large-scale genomic analyses. Shown are selected components of work on several non-vertebrate model organisms (red), the mouse (blue) and the human (green) from 1990; earlier projects are described in the text. SNPs, single nucleotide polymorphisms; ESTs, expressed sequence tags.

© 2001 Macmillan Magazines Ltd

well as targeted regions of mammalian genomes[34–37]. These projects showed that large-scale sequencing was feasible and developed the two-phase paradigm for genome sequencing. In the first, 'shotgun', phase, the genome is divided into appropriately sized segments and each segment is covered to a high degree of redundancy (typically, eight- to tenfold) through the sequencing of randomly selected subfragments. The second is a 'finishing' phase, in which sequence gaps are closed and remaining ambiguities are resolved through directed analysis. The results also showed that complete genomic sequence provided information about genes, regulatory regions and chromosome structure that was not readily obtainable from cDNA studies alone.

In 1995, genome scientists considered a proposal[38] that would have involved producing a draft genome sequence of the human genome in a first phase and then returning to finish the sequence in a second phase. After vigorous debate, it was decided that such a plan was premature for several reasons. These included the need first to prove that high-quality, long-range finished sequence could be produced from most parts of the complex, repeat-rich human genome; the sense that many aspects of the sequencing process were still rapidly evolving; and the desirability of further decreasing costs.

Instead, pilot projects were launched to demonstrate the feasibility of cost-effective, large-scale sequencing, with a target completion date of March 1999. The projects successfully produced finished sequence with 99.99% accuracy and no gaps[39]. They also introduced bacterial artificial chromosomes (BACs)[40], a new large-insert cloning system that proved to be more stable than the cosmids and yeast artificial chromosomes (YACs)[41] that had been used previously. The pilot projects drove the maturation and convergence of sequencing strategies, while producing 15% of the human genome sequence. With successful completion of this phase, the human genome sequencing effort moved into full-scale production in March 1999.

The idea of first producing a draft genome sequence was revived at this time, both because the ability to finish such a sequence was no longer in doubt and because there was great hunger in the scientific community for human sequence data. In addition, some scientists favoured prioritizing the production of a draft genome sequence over regional finished sequence because of concerns about commercial plans to generate proprietary databases of human sequence that might be subject to undesirable restrictions on use[42–44].

The consortium focused on an initial goal of producing, in a first production phase lasting until June 2000, a draft genome sequence covering most of the genome. Such a draft genome sequence, although not completely finished, would rapidly allow investigators to begin to extract most of the information in the human sequence. Experiments showed that sequencing clones covering about 90% of the human genome to a redundancy of about four- to fivefold ('half-shotgun' coverage; see Box 1) would accomplish this[45,46]. The draft genome sequence goal has been achieved, as described below.

The second sequence production phase is now under way. Its aims are to achieve full-shotgun coverage of the existing clones during 2001, to obtain clones to fill the remaining gaps in the physical map, and to produce a finished sequence (apart from regions that cannot be cloned or sequenced with currently available techniques) no later than 2003.

Strategic issues

Hierarchical shotgun sequencing

Soon after the invention of DNA sequencing methods[47,48], the shotgun sequencing strategy was introduced[49–51]; it has remained the fundamental method for large-scale genome sequencing[52–54] for the past 20 years. The approach has been refined and extended to make it more efficient. For example, improved protocols for fragmenting and cloning DNA allowed construction of shotgun libraries with more uniform representation. The practice of sequencing from both ends of double-stranded clones ('double-barrelled' shotgun sequencing) was introduced by Ansorge and others[37] in 1990, allowing the use of 'linking information' between sequence fragments.

The application of shotgun sequencing was also extended by applying it to larger and larger DNA molecules—from plasmids (~4 kilobases (kb)) to cosmid clones[37] (40 kb), to artificial chromosomes cloned in bacteria and yeast[55] (100–500 kb) and bacterial genomes[56] (1–2 megabases (Mb)). In principle, a genome of arbitrary size may be directly sequenced by the shotgun method, provided that it contains no repeated sequence and can be uniformly sampled at random. The genome can then be assembled using the simple computer science technique of 'hashing' (in which one detects overlaps by consulting an alphabetized look-up table of all *k*-letter words in the data). Mathematical analysis of the expected number of gaps as a function of coverage is similarly straightforward[57].

Practical difficulties arise because of repeated sequences and cloning bias. Small amounts of repeated sequence pose little problem for shotgun sequencing. For example, one can readily assemble typical bacterial genomes (about 1.5% repeat) or the euchromatic portion of the fly genome (about 3% repeat). By contrast, the human genome is filled (>50%) with repeated sequences, including interspersed repeats derived from transposable elements, and long genomic regions that have been duplicated in tandem, palindromic or dispersed fashion (see below). These include large duplicated segments (50–500 kb) with high sequence identity (98–99.9%), at which mispairing during recombination creates deletions responsible for genetic syndromes. Such features complicate the assembly of a correct and finished genome sequence.

There are two approaches for sequencing large repeat-rich genomes. The first is a whole-genome shotgun sequencing approach, as has been used for the repeat-poor genomes of viruses, bacteria and flies, using linking information and computational

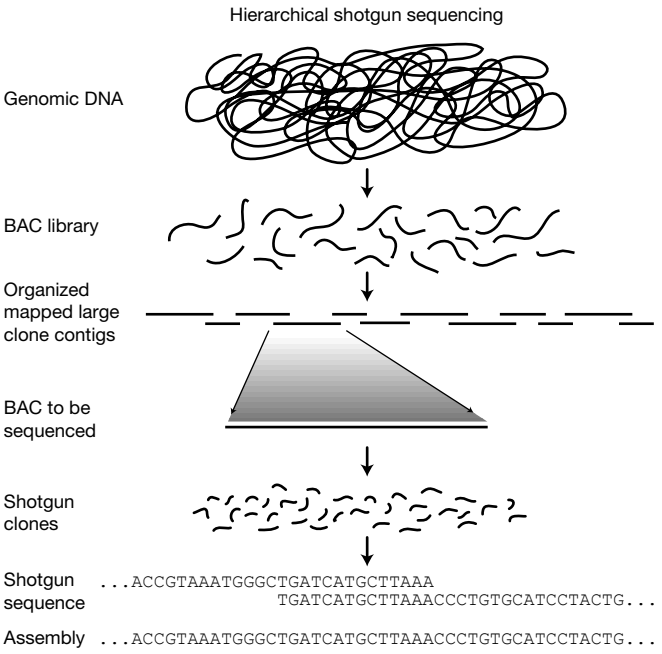

Figure 2 Idealized representation of the hierarchical shotgun sequencing strategy. A library is constructed by fragmenting the target genome and cloning it into a large-fragment cloning vector; here, BAC vectors are shown. The genomic DNA fragments represented in the library are then organized into a physical map and individual BAC clones are selected and sequenced by the random shotgun strategy. Finally, the clone sequences are assembled to reconstruct the sequence of the genome.

© 2001 Macmillan Magazines Ltd

analysis to attempt to avoid misassemblies. The second is the 'hierarchical shotgun sequencing' approach (Fig. 2), also referred to as 'map-based', 'BAC-based' or 'clone-by-clone'. This approach involves generating and organizing a set of large-insert clones (typically 100–200 kb each) covering the genome and separately performing shotgun sequencing on appropriately chosen clones. Because the sequence information is local, the issue of long-range misassembly is eliminated and the risk of short-range misassembly is reduced. One caveat is that some large-insert clones may suffer rearrangement, although this risk can be reduced by appropriate quality-control measures involving clone fingerprints (see below).

The two methods are likely to entail similar costs for producing finished sequence of a mammalian genome. The hierarchical approach has a higher initial cost than the whole-genome approach, owing to the need to create a map of clones (about 1% of the total cost of sequencing) and to sequence overlaps between clones. On the other hand, the whole-genome approach is likely to require much greater work and expense in the final stage of producing a finished sequence, because of the challenge of resolving misassemblies. Both methods must also deal with cloning biases, resulting in under-representation of some regions in either large-insert or small-insert clone libraries.

There was lively scientific debate over whether the human genome sequencing effort should employ whole-genome or hierarchical shotgun sequencing. Weber and Myers[58] stimulated these discussions with a specific proposal for a whole-genome shotgun approach, together with an analysis suggesting that the method could work and be more efficient. Green[59] challenged these conclusions and argued that the potential benefits did not outweigh the likely risks.

In the end, we concluded that the human genome sequencing effort should employ the hierarchical approach for several reasons. First, it was prudent to use the approach for the first project to sequence a repeat-rich genome. With the hierarchical approach, the ultimate frequency of misassembly in the finished product would probably be lower than with the whole-genome approach, in which it would be more difficult to identify regions in which the assembly was incorrect.

Second, it was prudent to use the approach in dealing with an outbred organism, such as the human. In the whole-genome shotgun method, sequence would necessarily come from two different copies of the human genome. Accurate sequence assembly could be complicated by sequence variation between these two copies—both SNPs (which occur at a rate of 1 per 1,300 bases) and larger-scale structural heterozygosity (which has been documented in human chromosomes). In the hierarchical shotgun method, each large-insert clone is derived from a single haplotype.

Third, the hierarchical method would be better able to deal with inevitable cloning biases, because it would more readily allow targeting of additional sequencing to under-represented regions. And fourth, it was better suited to a project shared among members of a diverse international consortium, because it allowed work and responsibility to be easily distributed. As the ultimate goal has always been to create a high-quality, finished sequence to serve as a foundation for biomedical research, we reasoned that the advantages of this more conservative approach outweighed the additional cost, if any.

A biotechnology company, Celera Genomics, has chosen to incorporate the whole-genome shotgun approach into its own efforts to sequence the human genome. Their plan[60,61] uses a mixed strategy, involving combining some coverage with whole-genome shotgun data generated by the company together with the publicly available hierarchical shotgun data generated by the International Human Genome Sequencing Consortium. If the raw sequence reads from the whole-genome shotgun component are made available, it may be possible to evaluate the extent to which the sequence of the human genome can be assembled without the need for clone-based information. Such analysis may help to refine sequencing strategies for other large genomes.

Technology for large-scale sequencing

Sequencing the human genome depended on many technological improvements in the production and analysis of sequence data. Key innovations were developed both within and outside the Human Genome Project. Laboratory innovations included four-colour fluorescence-based sequence detection[62], improved fluorescent dyes[63–66], dye-labelled terminators[67], polymerases specifically designed for sequencing[68–70], cycle sequencing[71] and capillary gel electrophoresis[72–74]. These studies contributed to substantial improvements in the automation, quality and throughput of collecting raw DNA sequence[75,76]. There were also important advances in the development of software packages for the analysis of sequence data. The PHRED software package[77,78] introduced the concept of assigning a 'base-quality score' to each base, on the basis of the probability of an erroneous call. These quality scores make it possible to monitor raw data quality and also assist in determining whether two similar sequences truly overlap. The PHRAP computer package (http://bozeman.mbt.washington.edu/phrap.docs/phrap.html) then systematically assembles the sequence data using the base-quality scores. The program assigns 'assembly-quality scores' to each base in the assembled sequence, providing an objective criterion to guide sequence finishing. The quality scores were based on and validated by extensive experimental data.

Another key innovation for scaling up sequencing was the development by several centres of automated methods for sample preparation. This typically involved creating new biochemical protocols suitable for automation, followed by construction of appropriate robotic systems.

Coordination and public data sharing

The Human Genome Project adopted two important principles with regard to human sequencing. The first was that the collaboration would be open to centres from any nation. Although potentially less efficient, in a narrow economic sense, than a centralized approach involving a few large factories, the inclusive approach was strongly favoured because we felt that the human genome sequence is the common heritage of all humanity and the work should transcend national boundaries, and we believed that scientific progress was best assured by a diversity of approaches. The collaboration was coordinated through periodic international meetings (referred to as 'Bermuda meetings' after the venue of the first three gatherings) and regular telephone conferences. Work was shared flexibly among the centres, with some groups focusing on particular chromosomes and others contributing in a genome-wide fashion.

The second principle was rapid and unrestricted data release. The centres adopted a policy that all genomic sequence data should be made publicly available without restriction within 24 hours of assembly[79,80]. Pre-publication data releases had been pioneered in mapping projects in the worm[11] and mouse genomes[30,81] and were prominently adopted in the sequencing of the worm, providing a direct model for the human sequencing efforts. We believed that scientific progress would be most rapidly advanced by immediate and free availability of the human genome sequence. The explosion of scientific work based on the publicly available sequence data in both academia and industry has confirmed this judgement.

Generating the draft genome sequence

Generating a draft sequence of the human genome involved three steps: selecting the BAC clones to be sequenced, sequencing them and assembling the individual sequenced clones into an overall draft genome sequence. A glossary of terms related to genome sequencing and assembly is provided in Box 1.

The draft genome sequence is a dynamic product, which is regularly updated as additional data accumulate en route to the

© 2001 Macmillan Magazines Ltd

ultimate goal of a completely finished sequence. The results below are based on the map and sequence data available on 7 October 2000, except as otherwise noted. At the end of this section, we provide a brief update of key data.

Clone selection

The hierarchical shotgun method involves the sequencing of overlapping large-insert clones spanning the genome. For the Human Genome Project, clones were largely chosen from eight large-insert libraries containing BAC or P1-derived artificial chromosome (PAC) clones (Table 1; refs 82–88). The libraries were made by partial digestion of genomic DNA with restriction enzymes. Together, they represent around 65-fold coverage (redundant sampling) of the genome. Libraries based on other vectors, such as cosmids, were also used in early stages of the project.

The libraries (Table 1) were prepared from DNA obtained from anonymous human donors in accordance with US Federal Regulations for the Protection of Human Subjects in Research (45CFR46) and following full review by an Institutional Review Board. Briefly, the opportunity to donate DNA for this purpose was broadly advertised near the two laboratories engaged in library

Box 1

Genome glossary

Sequence

Raw sequence Individual unassembled sequence reads, produced by sequencing of clones containing DNA inserts.

Paired-end sequence Raw sequence obtained from both ends of a cloned insert in any vector, such as a plasmid or bacterial artificial chromosome.

Finished sequence Complete sequence of a clone or genome, with an accuracy of at least 99.99% and no gaps.

Coverage (or depth) The average number of times a nucleotide is represented by a high-quality base in a collection of random raw sequence. Operationally, a 'high-quality base' is defined as one with an accuracy of at least 99% (corresponding to a PHRED score of at least 20).

Full shotgun coverage The coverage in random raw sequence needed from a large-insert clone to ensure that it is ready for finishing; this varies among centres but is typically 8–10-fold. Clones with full shotgun coverage can usually be assembled with only a handful of gaps per 100 kb.

Half shotgun coverage Half the amount of full shotgun coverage (typically, 4–5-fold random coverage).

Clones

BAC clone Bacterial artificial chromosome vector carrying a genomic DNA insert, typically 100–200 kb. Most of the large-insert clones sequenced in the project were BAC clones.

Finished clone A large-insert clone that is entirely represented by finished sequence.

Full shotgun clone A large-insert clone for which full shotgun sequence has been produced.

Draft clone A large-insert clone for which roughly half-shotgun sequence has been produced. Operationally, the collection of draft clones produced by each centre was required to have an average coverage of fourfold for the entire set and a minimum coverage of threefold for each clone.

Predraft clone A large-insert clone for which some shotgun sequence is available, but which does not meet the standards for inclusion in the collection of draft clones.

Contigs and scaffolds

Contig The result of joining an overlapping collection of sequences or clones.

Scaffold The result of connecting contigs by linking information from paired-end reads from plasmids, paired-end reads from BACs, known messenger RNAs or other sources. The contigs in a scaffold are ordered and oriented with respect to one another.

Fingerprint clone contigs Contigs produced by joining clones inferred to overlap on the basis of their restriction digest fingerprints.

Sequenced-clone layout Assignment of sequenced clones to the physical map of fingerprint clone contigs.

Initial sequence contigs Contigs produced by merging overlapping sequence reads obtained from a single clone, in a process called sequence assembly.

Merged sequence contigs Contigs produced by taking the initial sequence contigs contained in overlapping clones and merging those found to overlap. These are also referred to simply as 'sequence contigs' where no confusion will result.

Sequence-contig scaffolds Scaffolds produced by connecting sequence contigs on the basis of linking information.

Sequenced-clone contigs Contigs produced by merging overlapping sequenced clones.

Sequenced-clone-contig scaffolds Scaffolds produced by joining sequenced-clone contigs on the basis of linking information.

Draft genome sequence The sequence produced by combining the information from the individual sequenced clones (by creating merged sequence contigs and then employing linking information to create scaffolds) and positioning the sequence along the physical map of the chromosomes.

N50 length A measure of the contig length (or scaffold length) containing a 'typical' nucleotide. Specifically, it is the maximum length L such that 50% of all nucleotides lie in contigs (or scaffolds) of size at least L.

Computer programs and databases

PHRED A widely used computer program that analyses raw sequence to produce a 'base call' with an associated 'quality score' for each position in the sequence. A PHRED quality score of X corresponds to an error probability of approximately $10^{-X/10}$. Thus, a PHRED quality score of 30 corresponds to 99.9% accuracy for the base call in the raw read.

PHRAP A widely used computer program that assembles raw sequence into sequence contigs and assigns to each position in the sequence an associated 'quality score', on the basis of the PHRED scores of the raw sequence reads. A PHRAP quality score of X corresponds to an error probability of approximately $10^{-X/10}$. Thus, a PHRAP quality score of 30 corresponds to 99.9% accuracy for a base in the assembled sequence.

GigAssembler A computer program developed during this project for merging the information from individual sequenced clones into a draft genome sequence.

Public sequence databases The three coordinated international sequence databases: GenBank, the EMBL data library and DDBJ.

Map features

STS Sequence tagged site, corresponding to a short (typically less than 500 bp) unique genomic locus for which a polymerase chain reaction assay has been developed.

EST Expressed sequence tag, obtained by performing a single raw sequence read from a random complementary DNA clone.

SSR Simple sequence repeat, a sequence consisting largely of a tandem repeat of a specific k-mer (such as $(CA)_{15}$). Many SSRs are polymorphic and have been widely used in genetic mapping.

SNP Single nucleotide polymorphism, or a single nucleotide position in the genome sequence for which two or more alternative alleles are present at appreciable frequency (traditionally, at least 1%) in the human population.

Genetic map A genome map in which polymorphic loci are positioned relative to one another on the basis of the frequency with which they recombine during meiosis. The unit of distance is centimorgans (cM), denoting a 1% chance of recombination.

Radiation hybrid (RH) map A genome map in which STSs are positioned relative to one another on the basis of the frequency with which they are separated by radiation-induced breaks. The frequency is assayed by analysing a panel of human–hamster hybrid cell lines, each produced by lethally irradiating human cells and fusing them with recipient hamster cells such that each carries a collection of human chromosomal fragments. The unit of distance is centirays (cR), denoting a 1% chance of a break occuring between two loci.

© 2001 Macmillan Magazines Ltd

construction. Volunteers of diverse backgrounds were accepted on a first-come, first-taken basis. Samples were obtained after discussion with a genetic counsellor and written informed consent. The samples were made anonymous as follows: the sampling laboratory stripped all identifiers from the samples, applied random numeric labels, and transferred them to the processing laboratory, which then removed all labels and relabelled the samples. All records of the labelling were destroyed. The processing laboratory chose samples at random from which to prepare DNA and immortalized cell lines. Around 5–10 samples were collected for every one that was eventually used. Because no link was retained between donor and DNA sample, the identity of the donors for the libraries is not known, even by the donors themselves. A more complete description can be found at http://www.nhgri.nih.gov/Grant_info/Funding/Statements/RFA/human_subjects.html.

During the pilot phase, centres showed that sequence-tagged sites (STSs) from previously constructed genetic and physical maps could be used to recover BACs from specific regions. As sequencing expanded, some centres continued this approach, augmented with additional probes from flow sorting of chromosomes to obtain long-range coverage of specific chromosomes or chromosomal regions[89–94].

For the large-scale sequence production phase, a genome-wide physical map of overlapping clones was also constructed by systematic analysis of BAC clones representing 20-fold coverage of the human genome[86]. Most clones came from the first three sections of the RPCI-11 library, supplemented with clones from sections of the RPCI-13 and CalTech D libraries (Table 1). DNA from each BAC clone was digested with the restriction enzyme *Hin*dIII, and the sizes of the resulting fragments were measured by agarose gel electrophoresis. The pattern of restriction fragments provides a 'fingerprint' for each BAC, which allows different BACs to be distinguished and the degree of overlaps to be assessed. We used these restriction-fragment fingerprints to determine clone overlaps, and thereby assembled the BACs into fingerprint clone contigs.

The fingerprint clone contigs were positioned along the chromosomes by anchoring them with STS markers from existing genetic and physical maps. Fingerprint clone contigs were tied to specific STSs initially by probe hybridization and later by direct search of the sequenced clones. To localize fingerprint clone contigs that did not contain known markers, new STSs were generated and placed onto chromosomes[95]. Representative clones were also positioned by fluorescence *in situ* hybridization (FISH) (ref. 86 and C. McPherson, unpublished).

We selected clones from the fingerprint clone contigs for sequencing according to various criteria. Fingerprint data were reviewed[86,90] to evaluate overlaps and to assess clone fidelity (to bias against rearranged clones[83,96]). STS content information and BAC end sequence information were also used[91,92]. Where possible, we tried to select a minimally overlapping set spanning a region. However, because the genome-wide physical map was constructed concurrently with the sequencing, continuity in many regions was low in early stages. These small fingerprint clone contigs were nonetheless useful in identifying validated, nonredundant clones

Table 1 Key large-insert genome-wide libraries

Library name*	GenBank abbreviation	Vector type	Source DNA	Library segment or plate numbers	Enzyme digest	Average insert size (kb)	Total number of clones in library	Number of fingerprinted clones†	BAC-end sequence (ends/clones/clones with both ends sequenced)‡	Number of clones in genome layout§	Sequenced clones used in construction of the draft genome sequence		
											Number‖	Total bases (Mb)¶	Fraction of total from library
Caltech B	CTB	BAC	987SK cells	All	*Hin*dIII	120	74,496	16	2/1/1	528	518	66.7	0.016
Caltech C	CTC	BAC	Human sperm	All	*Hin*dIII	125	263,040	144	21,956/14,445/7,255	621	606	88.4	0.021
Caltech D1 (CITB-H1)	CTD	BAC	Human sperm	All	*Hin*dIII	129	162,432	49,833	403,589/226,068/156,631	1,381	1,367	185.6	0.043
Caltech D2 (CITB-E1)		BAC	Human sperm	All									
				2,501–2,565	*Eco*RI	202	24,960						
				2,566–2,671	*Eco*RI	182	46,326						
				3,000–3,253	*Eco*RI	142	97,536						
RPCI-1	RP1	PAC	Male, blood	All	*Mbo*I	110	115,200	3,388		1,070	1,053	117.7	0.028
RPCI-3	RP3	PAC	Male, blood	All	*Mbo*I	115	75,513			644	638	68.5	0.016
RPCI-4	RP4	PAC	Male, blood	All	*Mbo*I	116	105,251			889	881	95.5	0.022
RPCI-5	RP5	PAC	Male, blood	All	*Mbo*I	115	142,773			1,042	1,033	116.5	0.027
RPCI-11	RP11	BAC	Male, blood	All		178	543,797	267,931	379,773/243,764/134,110	19,405	19,145	3,165.0	0.743
				1	*Eco*RI	164	108,499						
				2	*Eco*RI	168	109,496						
				3	*Eco*RI	181	109,657						
				4	*Eco*RI	183	109,382						
				5	*Mbo*I	196	106,763						
Total of top eight libraries							1,482,502	321,312	805,320/484,278/297,997	25,580	25,241	3,903.9	0.916
Total all libraries								354,510	812,594/488,017/100,775	30,445	29,298	4,260.5	1

* For the CalTech libraries[82], see http://www.tree.caltech.edu/lib_status.html; for RPCI libraries[83], see http://www.chori.org/bacpac/home.htm.
† For the FPC map and fingerprinting[84–86], see http://genome.wustl.edu/gsc/human/human_database.shtml.
‡ The number of raw BAC end sequences (clones/ends/clones with both ends sequenced) available for use in human genome sequencing. Typically, for clones in which sequence was obtained from both ends, more than 95% of both end sequences contained at least 100 bp of nonrepetitive sequence. BAC-end sequencing of RPCI-11 and of the CalTech libraries was done at The Institute for Genomic Research, the California Institute of Technology and the University of Washington High Throughput Sequencing Center. The sources for the Table were http://www.ncbi.nlm.nih.gov/genome/clone/BESstat.shtml and refs 87, 88.
§ These are the clones in the sequenced-clone layout map (http://genome.wustl.edu/gsc/human/Mapping/index.shtml) that were pre-draft, draft or finished.
‖ The number of sequenced clones used in the assembly. This number is less than that in the previous column owing to removal of a small number of obviously contaminated, combined or duplicated projects; in addition, not all of the clones from completed chromosomes 21 and 22 were included here because only the available finished sequence from those chromosomes was used in the assembly.
¶ The number reported is the total sequence from the clones indicated in the previous column. Potential overlap between clones was not removed here, but Ns were excluded.

© 2001 Macmillan Magazines Ltd

that were used to 'seed' the sequencing of new regions. The small fingerprint clone contigs were extended or merged with others as the map matured.

The clones that make up the draft genome sequence therefore do not constitute a minimally overlapping set—there is overlap and redundancy in places. The cost of using suboptimal overlaps was justified by the benefit of earlier availability of the draft genome sequence data. Minimizing the overlap between adjacent clones would have required completing the physical map before undertaking large-scale sequencing. In addition, the overlaps between BAC clones provide a rich collection of SNPs. More than 1.4 million SNPs have already been identified from clone overlaps and other sequence comparisons[97].

Because the sequencing project was shared among twenty centres in six countries, it was important to coordinate selection of clones across the centres. Most centres focused on particular chromosomes or, in some cases, larger regions of the genome. We also maintained a clone registry to track selected clones and their progress. In later phases, the global map provided an integrated view of the data from all centres, facilitating the distribution of effort to maximize coverage of the genome. Before performing extensive sequencing on a clone, several centres routinely examined an initial sample of 96 raw sequence reads from each subclone library to evaluate possible overlap with previously sequenced clones.

Figure 3 The automated production line for sample preparation at the Whitehead Institute, Center for Genome Research. The system consists of custom-designed factory-style conveyor belt robots that perform all functions from purifying DNA from bacterial cultures through setting up and purifying sequencing reactions.

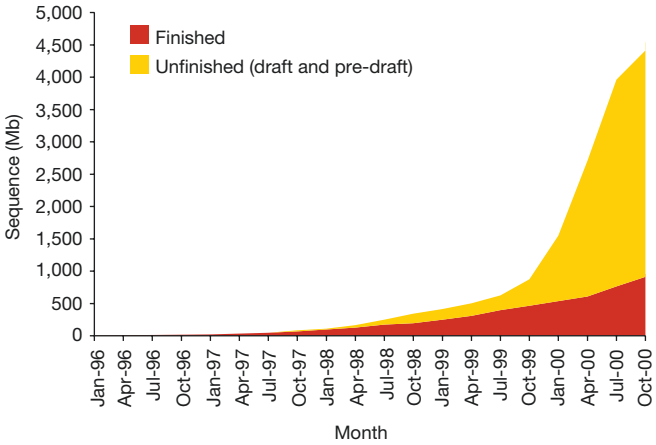

Figure 4 Total amount of human sequence in the High Throughput Genome Sequence (HTGS) division of GenBank. The total is the sum of finished sequence (red) and unfinished (draft plus predraft) sequence (yellow).

Sequencing

The selected clones were subjected to shotgun sequencing. Although the basic approach of shotgun sequencing is well established, the details of implementation varied among the centres. For example, there were differences in the average insert size of the shotgun libraries, in the use of single-stranded or double-stranded cloning vectors, and in sequencing from one end or both ends of each insert. Centres differed in the fluorescent labels employed and in the degree to which they used dye-primers or dye-terminators. The sequence detectors included both slab gel- and capillary-based devices. Detailed protocols are available on the web sites of many of the individual centres (URLs can be found at www.nhgri.nih.gov/genome_hub). The extent of automation also varied greatly among the centres, with the most aggressive automation efforts resulting in factory-style systems able to process more than 100,000 sequencing reactions in 12 hours (Fig. 3). In addition, centres differed in the amount of raw sequence data typically obtained for each clone (so-called half-shotgun, full shotgun and finished sequence). Sequence information from the different centres could be directly integrated despite this diversity, because the data were analysed by a common computational procedure. Raw sequence traces were processed and assembled with the PHRED and PHRAP software packages[77,78] (P. Green, unpublished). All assembled contigs of more than 2 kb were deposited in public databases within 24 hours of assembly.

The overall sequencing output rose sharply during production (Fig. 4). Following installation of new sequence detectors beginning in June 1999, sequencing capacity and output rose approximately eightfold in eight months to nearly 7 million samples processed per month, with little or no drop in success rate (ratio of useable reads to attempted reads). By June 2000, the centres were producing raw sequence at a rate equivalent to onefold coverage of the entire human genome in less than six weeks. This corresponded to a continuous throughput exceeding 1,000 nucleotides per second, 24 hours per day, seven days per week. This scale-up resulted in a concomitant increase in the sequence available in the public databases (Fig. 4).

A version of the draft genome sequence was prepared on the basis of the map and sequence data available on 7 October 2000. For this version, the mapping effort had assembled the fingerprinted BACs into 1,246 fingerprint clone contigs. The sequencing effort had sequenced and assembled 29,298 overlapping BACs and other large-insert clones (Table 2), comprising a total length of 4.26 gigabases (Gb). This resulted from around 23 Gb of underlying raw shotgun sequence data, or about 7.5-fold coverage averaged across the genome (including both draft and finished sequence). The various contributions to the total amount of sequence deposited in the HTGS division of GenBank are given in Table 3.

Table 2 Total genome sequence from the collection of sequenced clones, by sequence status

Sequence status	Number of clones	Total clone length (Mb)	Average number of sequence reads per kb*	Average sequence depth†	Total amount of raw sequence (Mb)
Finished	8,277	897	20–25	8–12	9,085
Draft	18,969	3,097	12	4.5	13,395
Predraft	2,052	267	6	2.5	667
Total					23,147

*The average number of reads per kb was estimated based on information provided by each sequencing centre. This number differed among sequencing centres, based on the actual protocols used.

†The average depth in high quality bases (≥99% accuracy) was estimated from information provided by each sequencing centre. The average varies among the centres, and the number may vary considerably for clones with the same sequencing status. For draft clones in the public databases (keyword: HTGS_draft), the number can be computed from the quality scores listed in the database entry.

© 2001 Macmillan Magazines Ltd

By agreement among the centres, the collection of draft clones produced by each centre was required to have fourfold average sequence coverage, with no clone below threefold. (For this purpose, sequence coverage was defined as the average number of times that each base was independently read with a base-quality score corresponding to at least 99% accuracy.) We attained an overall average of 4.5-fold coverage across the genome for draft clones. A few of the sequenced clones fell below the minimum of threefold sequence coverage or have not been formally designated by centres as meeting draft standards; these are referred to as predraft (Table 2). Some of these are clones that span remaining gaps in the draft genome sequence and were in the process of being sequenced on 7 October 2000; a few are old submissions from centres that are no longer active.

The lengths of the initial sequence contigs in the draft clones vary as a function of coverage, but half of all nucleotides reside in initial sequence contigs of at least 21.7 kb (see below). Various properties of the draft clones can be assessed from instances in which there was substantial overlap between a draft clone and a finished (or nearly finished) clone. By examining the sequence alignments in the overlap regions, we estimated that the initial sequence contigs in a draft sequence clone cover an average of about 96% of the clone and are separated by gaps with an average size of about 500 bp.

Although the main emphasis was on producing a draft genome sequence, the centres also maintained sequence finishing activities during this period, leading to a twofold increase in finished sequence from June 1999 to June 2000 (Fig. 4). The total amount of human sequence in this final form stood at more than 835 Mb on 7 October 2000, or more than 25% of the human genome. This includes the finished sequences of chromosomes 21 and 22 (refs 93, 94). As centres have begun to shift from draft to finished sequencing in the last quarter of 2000, the production of finished sequence has increased to an annualized rate of 1 Gb per year and is continuing to rise.

Table 3 Total human sequence deposited in the HTGS division of GenBank

Sequencing centre	Total human sequence (kb)	Finished human sequence (kb)
Whitehead Institute, Center for Genome Research*	1,196,888	46,560
The Sanger Centre*	970,789	284,353
Washington University Genome Sequencing Center*	765,898	175,279
US DOE Joint Genome Institute	377,998	78,486
Baylor College of Medicine Human Genome Sequencing Center	345,125	53,418
RIKEN Genomic Sciences Center	203,166	16,971
Genoscope	85,995	48,808
GTC Sequencing Center	71,357	7,014
Department of Genome Analysis, Institute of Molecular Biotechnology	49,865	17,788
Beijing Genomics Institute/Human Genome Center	42,865	6,297
Multimegabase Sequencing Center; Institute for Systems Biology	31,241	9,676
Stanford Genome Technology Center	29,728	3,530
The Stanford Human Genome Center and Department of Genetics	28,162	9,121
University of Washington Genome Center	24,115	14,692
Keio University	17,364	13,058
University of Texas Southwestern Medical Center at Dallas	11,670	7,028
University of Oklahoma Advanced Center for Genome Technology	10,071	9,155
Max Planck Institute for Molecular Genetics	7,650	2,940
GBF – German Research Centre for Biotechnology	4,639	2,338
Cold Spring Harbor Laboratory Lita Annenberg Hazen Genome Center	4,338	2,104
Other	59,574	35,911
Total	4,338,224	842,027

Total human sequence deposited in GenBank by members of the International Human Genome Sequencing Consortium, as of 8 October 2000.The amount of total sequence (finished plus draft plus predraft) is shown in the second column and the amount of finished sequence is shown in the third column. Total sequence differs from totals in Tables 1 and 2 because of inclusion of padding characters and of some clones not used in assembly. HTGS, high throughput genome sequence.
*These three centres produced an additional 2.4 Gb of raw plasmid paired-end reads (see Table 4), consisting of 0.99 Gb from Whitehead Institute, 0.66 Gb from The Sanger Centre and 0.75 Gb from Washington University.

In addition to sequencing large-insert clones, three centres generated a large collection of random raw sequence reads from whole-genome shotgun libraries (Table 4; ref. 98). These 5.77 million successful sequences contained 2.4 Gb of high-quality bases; this corresponds to about 0.75-fold coverage and would be statistically expected to include about 50% of the nucleotides in the human genome (data available at http://snp.cshl.org/data). The primary objective of this work was to discover SNPs, by comparing these random raw sequences (which came from different individuals) with the draft genome sequence. However, many of these raw sequences were obtained from both ends of plasmid clones and thereby also provided valuable 'linking' information that was used in sequence assembly. In addition, the random raw sequences provide sequence coverage of about half of the nucleotides not yet represented in the sequenced large-insert clones; these can be used as probes for portions of the genome not yet recovered.

Assembly of the draft genome sequence

We then set out to assemble the sequences from the individual large-insert clones into an integrated draft sequence of the human genome. The assembly process had to resolve problems arising from the draft nature of much of the sequence, from the variety of clone sources, and from the high fraction of repeated sequences in the human genome. This process involved three steps: filtering, layout and merging.

The entire data set was filtered uniformly to eliminate contamination from nonhuman sequences and other artefacts that had not already been removed by the individual centres. (Information about contamination was also sent back to the centres, which are updating the individual entries in the public databases.) We also identified instances in which the sequence data from one BAC clone was substantially contaminated with sequence data from another (human or nonhuman) clone. The problems were resolved in most instances; 231 clones remained unresolved, and these were eliminated from the assembly reported here. Instances of lower levels of cross-contamination (for example, a single 96-well microplate misassigned to the wrong BAC) are more difficult to detect; some undoubtedly remain and may give rise to small spurious sequence contigs in the draft genome sequence. Such issues are readily resolved as the clones progress towards finished sequence, but they necessitate some caution in certain applications of the current data.

The sequenced clones were then associated with specific clones on the physical map to produce a 'layout'. In principle, sequenced clones that correspond to fingerprinted BACs could be directly assigned by name to fingerprint clone contigs on the fingerprint-based physical map. In practice, however, laboratory mixups occasionally resulted in incorrect assignments. To eliminate such problems, sequenced clones were associated with the fingerprint clone contigs in the physical map by using the sequence data to calculate a

Table 4 Plasmid paired-end reads

	Total reads deposited*	Read pairs†	Size range of inserts (kb)
Random-sheared	3,227,685	1,155,284	1.8–6
Enzyme digest	2,539,222	761,010	0.8–4.7
Total	5,766,907	1,916,294	

The plasmid paired-end reads used a mixture of DNA from a set of 24 samples from the DNA Polymorphism Discovery Resource (http://locus.umdnj.edu/nigms/pdr.html). This set of 24 anonymous US residents contains samples from European-Americans, African-Americans, Mexican-Americans, Native Americans and Asian-Americans, although the ethnicities of the individual samples are not identified. Informed consent to contribute samples to the DNA Polymorphism Discovery Resource was obtained from all 450 individuals who contributed samples. Samples from the European-American, African-American and Mexican-American individuals came from NHANES (http://www.cdc.gov/nchs/nhanes.htm); individuals were recontacted to obtain their consent for the Resource project. New samples were obtained from Asian-Americans whose ancestry was from a variety of East and South Asian countries. New samples were also obtained for the Native Americans; tribal permission was obtained first, and then individual consents. See http://www.nhgri.nih.gov/Grant_info/Funding/RFA/discover_polymorphisms.html and ref. 98.
*Reflects data deposited with and released by The SNP Consortium (see http://snp.cshl.org/data).
† Read pairs represents the number of cases in which sequence from both ends of a genomic cloned fragment was determined and used in this study as linking information.

© 2001 Macmillan Magazines Ltd

partial list of restriction fragments *in silico* and comparing that list with the experimental database of BAC fingerprints. The comparison was feasible because the experimental sizing of restriction fragments was highly accurate (to within 0.5–1.5% of the true size, for 95% of fragments from 600 to 12,000 base pairs (bp))[84,85]. Reliable matching scores could be obtained for 16,193 of the clones. The remaining sequenced clones could not be placed on the map by this method because they were too short, or they contained too many small initial sequence contigs to yield enough restriction fragments, or possibly because their sequences were not represented in the fingerprint database.

An independent approach to placing sequenced clones on the physical map used the database of end sequences from fingerprinted BACs (Table 1). Sequenced clones could typically be reliably mapped if they contained multiple matches to BAC ends, with all corresponding to clones from a single genomic region (multiple matches were required as a safeguard against errors known to exist in the BAC end database and against repeated sequences). This approach provided useful placement information for 22,566 sequenced clones.

Altogether, we could assign 25,403 sequenced clones to fingerprint clone contigs by combining *in silico* digestion and BAC end sequence match data. To place most of the remaining sequenced clones, we exploited information about sequence overlap or BAC-end paired links of these clones with already positioned clones. This left only a few, mostly small, sequenced clones that could not be placed (152 sequenced clones containing 5.5 Mb of sequence out of 29,298 sequenced clones containing more than 4,260 Mb of sequence); these are being localized by radiation hybrid mapping of STSs derived from their sequences.

The fingerprint clone contigs were then mapped to chromosomal locations, using sequence matches to mapped STSs from four human radiation hybrid maps[95,99,100], one YAC and radiation hybrid map[29], and two genetic maps[101,102], together with data from FISH[86,90,103]. The mapping was iteratively refined by comparing the order and orientation of the STSs in the fingerprint clone contigs and the various STS-based maps, to identify and refine discrepancies (Fig. 5). Small fingerprint clone contigs (< 1 Mb) were difficult to orient and, sometimes, to order using these methods. In all, 942 fingerprint clone contigs contained sequenced clones. (An additional 304 of the 1,246 fingerprint clone contigs did not contain sequenced clones, but these tended to be extremely small and together contain less than 1% of the mapped clones. About one-third have been targeted for sequencing. A few derive from the Y chromosome, for which the map was constructed separately[89]. Most of the remainder are fragments of other larger contigs or represent other artefacts. These are being eliminated in subsequent versions of the database.) Of these 942 contigs with sequenced clones, 852 (90%, containing 99.2% of the total sequence) were localized to specific chromosome locations in this way. An additional 51 fingerprint clone contigs, containing 0.5% of the sequence, could be assigned to a specific chromosome but not to a precise position.

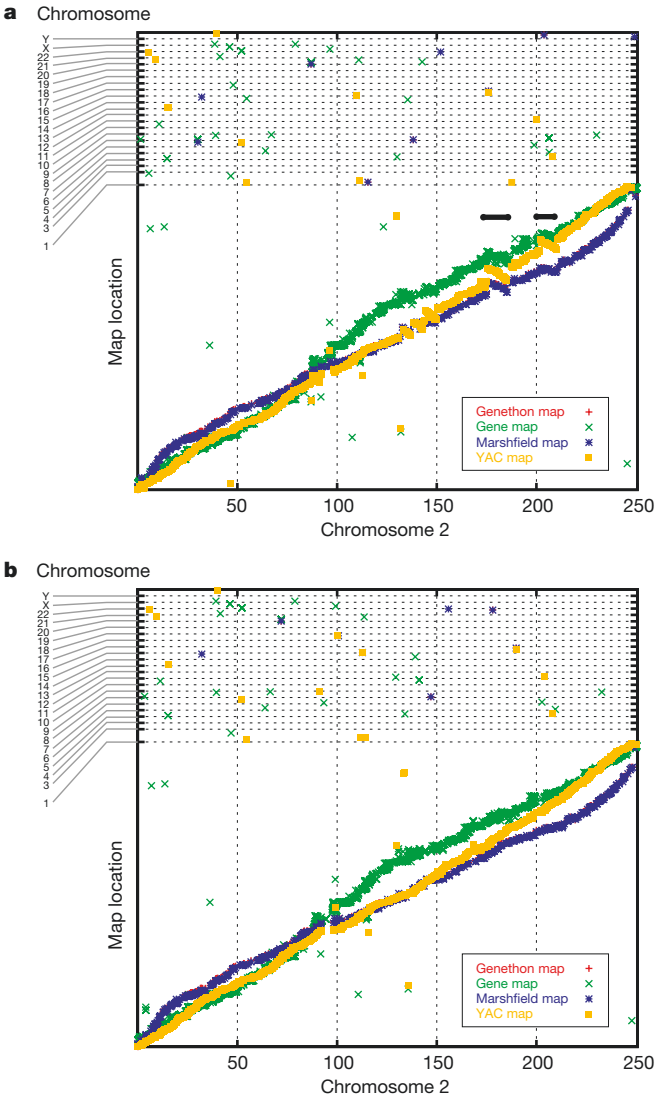

Figure 5 Positions of markers on previous maps of the genome (the Genethon[101] genetic map and Marshfield genetic map (http://research.marshfieldclinic.org/genetics/genotyping_service/mgsver2.htm), the GeneMap99 radiation hybrid map[100], and the Whitehead YAC and radiation hybrid map[29]) plotted against their derived position on the draft sequence for chromosome 2. The horizontal units are Mb but the vertical units of each map vary (cM, cR and so on) and thus all were scaled so that the entire map spans the full vertical range. Markers that map to other chromosomes are shown in the chromosome lines at the top.The data sets generally follow the diagonal, indicating that order and orientation of the marker sets on the different maps largely agree (note that the two genetic maps are completely superimposed). In **a**, there are two segments (bars) that are inverted in an earlier version draft sequence relative to all the other maps. **b,** The same chromosome after the information was used to reorient those two segments.

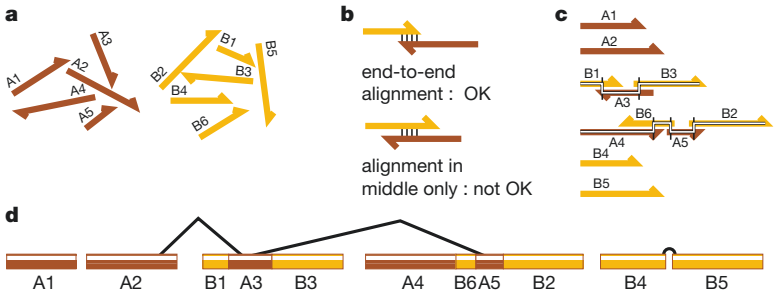

Figure 6 The key steps (**a–d**) in assembling individual sequenced clones into the draft genome sequence. A1–A5 represent initial sequence contigs derived from shotgun sequencing of clone A, and B1–B6 are from clone B.

© 2001 Macmillan Magazines Ltd

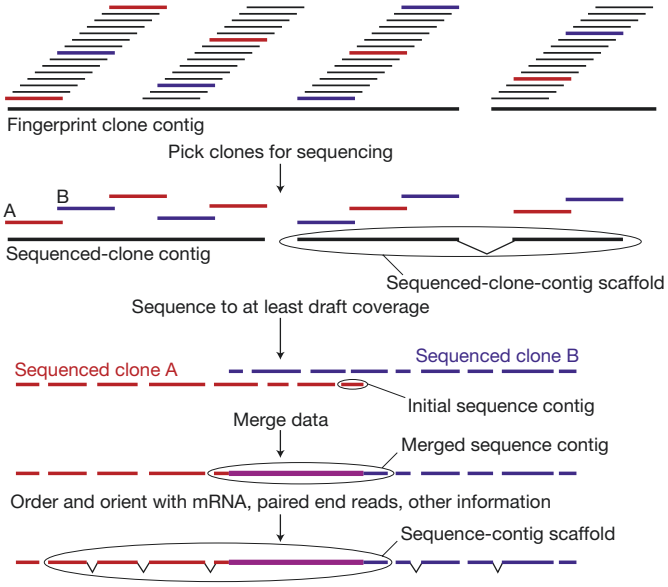

Figure 7 Levels of clone and sequence coverage. A 'fingerprint clone contig' is assembled by using the computer program FPC[84,451] to analyse the restriction enzyme digestion patterns of many large-insert clones. Clones are then selected for sequencing to minimize overlap between adjacent clones. For a clone to be selected, all of its restriction enzyme fragments (except the two vector-insert junction fragments) must be shared with at least one of its neighbours on each side in the contig. Once these overlapping clones have been sequenced, the set is a 'sequenced-clone contig'. When all selected clones from a fingerprint clone contig have been sequenced, the sequenced-clone contig will be the same as the fingerprint clone contig. Until then, a fingerprint clone contig may contain several sequenced-clone contigs. After individual clones (for example, A and B) have been sequenced to draft coverage and the clones have been mapped, the data are analysed by GigAssembler (Fig. 6), producing merged sequence contigs from initial sequence contigs, and linking these to form sequence-contig scaffolds (see Box 1).

The remaining 39 contigs containing 0.3% of the sequence were not positioned at all.

We then merged the sequences from overlapping sequenced clones (Fig. 6), using the computer program GigAssembler[104]. The program considers nearby sequenced clones, detects overlaps between the initial sequence contigs in these clones, merges the overlapping sequences and attempts to order and orient the sequence contigs. It begins by aligning the initial sequence contigs from one clone with those from other clones in the same fingerprint clone contig on the basis of length of alignment, per cent identity of the alignment, position in the sequenced clone layout and other factors. Alignments are limited to one end of each initial sequence contig for partially overlapping contigs or to both ends of an initial sequence contig contained entirely within another; this eliminates internal alignments that may reflect repeated sequence or possible misassembly (Fig. 6b). Beginning with the highest scoring pairs, initial sequence contigs are then integrated to produce 'merged sequence contigs' (usually referred to simply as 'sequence contigs'). The program refines the arrangement of the clones within the fingerprint clone contig on the basis of the extent of sequence overlap between them and then rebuilds the sequence contigs. Next, the program selects a sequence path through the sequence contigs (Fig. 6c). It tries to use the highest quality data by preferring longer initial sequence contigs and avoiding the first and last 250 bases of initial sequence contigs where possible. Finally, it attempts to order and orient the sequence contigs by using additional information, including sequence data from paired-end plasmid and BAC reads, known messenger RNAs and ESTs, as well as additional linking information provided by centres. The sequence contigs are thereby linked together to create 'sequence-contig scaffolds' (Fig. 6d). The process also joins overlapping sequenced clones into sequenced-clone contigs and links sequenced-clone contigs to form sequenced-clone-contig scaffolds. A fingerprint clone contig may contain several sequenced-clone contigs, because bridging clones remain to be sequenced. The assembly contained 4,884 sequenced-clone

Table 5 The draft genome sequence

Chromosome	Sequence from clones (kb)			Sequence from contigs (kb)		
	Finished clones	Draft clones	Pre-draft clones	Contigs containing finished clones	Deep coverage sequence contigs	Draft/predraft sequence contigs
All	826,441	1,734,995	131,476	958,922	840,815	893,175
1	50,851	149,027	12,356	61,001	78,773	72,461
2	46,909	167,439	7,210	53,775	81,569	86,214
3	22,350	152,840	11,057	26,959	79,649	79,638
4	15,914	134,973	17,261	19,096	66,165	82,887
5	37,973	129,581	2,160	48,895	61,387	59,431
6	75,312	76,082	6,696	93,458	28,204	36,428
7	94,845	47,328	4,047	103,188	14,434	28,597
8	14,538	102,484	7,236	16,659	47,198	60,400
9	18,401	77,648	10,864	24,030	42,653	40,230
10	16,889	99,181	11,066	21,421	54,054	51,662
11	13,162	111,092	4,352	16,145	65,147	47,314
12	32,156	84,653	7,651	37,519	43,995	42,946
13	16,818	68,983	7,136	22,191	38,319	32,429
14	58,989	27,370	565	78,302	3,267	5,355
15	2,739	67,453	3,211	3,112	34,758	35,533
16	22,987	48,997	1,143	27,751	20,892	24,484
17	29,881	36,349	6,600	33,531	14,671	24,628
18	5,128	65,284	2,352	6,656	40,947	25,160
19	28,481	26,568	369	32,228	7,188	16,003
20	54,217	5,302	976	56,534	1,065	2,896
21	33,824	0	0	33,824	0	0
22	33,786	0	0	33,786	0	0
X	77,630	45,100	4,941	83,796	14,056	29,820
Y	18,169	3,221	363	20,222	333	1,198
NA	2,434	1,858	844	2,446	122	2,568
UL	2,056	6,182	1,020	2,395	1,969	4,894

The table presents summary statistics for the draft genome sequence over the entire genome and by individual chromosome. NA, clones that could not be placed into the sequenced clone layout. UL, clones that could be placed in the layout, but that could not reliably be placed on a chromosome. First three columns, data from finished clones, draft clones and predraft clones. The last three columns break the data down according to the type of sequence contig. Contigs containing finished clones represent sequence contigs that consist of finished sequence plus any (small) extensions from merged sequence contigs that arise from overlap with flanking draft clones. Deep coverage sequence contigs include sequence from two or more overlapping unfinished clones; they consist of roughly full shotgun coverage and thus are longer than the average unfinished sequence contig. Draft/predraft sequence contigs are all of the other sequence contigs in unfinished clones. Thus, the draft genome sequence consists of approximately one-third finished sequence, one-third deep coverage sequence and one-third draft/pre-draft coverage sequence. In all of the statistics, we count only nonoverlapping bases in the draft genome sequence.

© 2001 Macmillan Magazines Ltd

contigs in 942 fingerprint clone contigs.

The hierarchy of contigs is summarized in Fig. 7. Initial sequence contigs are integrated to create merged sequence contigs, which are then linked to form sequence-contig scaffolds. These scaffolds reside within sequenced-clone contigs, which in turn reside within fingerprint clone contigs.

The draft genome sequence

The result of the assembly process is an integrated draft sequence of the human genome. Several features of the draft genome sequence are reported in Tables 5–7, including the proportion represented by finished, draft and predraft categories. The Tables also show the numbers and lengths of different types of contig, for each chromosome and for the genome as a whole.

The contiguity of the draft genome sequence at each level is an important feature. Two commonly used statistics have significant drawbacks for describing contiguity. The 'average length' of a contig is deflated by the presence of many small contigs comprising only a small proportion of the genome, whereas the 'length-weighted average length' is inflated by the presence of large segments of finished sequence. Instead, we chose to describe the contiguity as a property of the 'typical' nucleotide. We used a statistic called the 'N50 length', defined as the largest length L such that 50% of all nucleotides are contained in contigs of size at least L.

The continuity of the draft genome sequence reported here and the effectiveness of assembly can be readily seen from the following: half of all nucleotides reside within an initial sequence contig of at least 21.7 kb, a sequence contig of at least 82 kb, a sequence-contig scaffold of at least 274 kb, a sequenced-clone contig of at least 826 kb and a fingerprint clone contig of at least 8.4 Mb (Tables 6, 7). The cumulative distributions for each of these measures of contiguity are shown in Fig. 8, in which the N50 values for each measure can be seen as the value at which the cumulative distributions cross 50%. We have also estimated the size of each chromosome, by estimating the gap sizes (see below) and the extent of missing heterochromatic sequence[93,94,105–108] (Table 8). This is undoubtedly an oversimplification and does not adequately take into account the sequence status of each chromosome. Nonetheless, it provides a useful way to relate the draft sequence to the chromosomes.

Quality assessment

The draft genome sequence already covers the vast majority of the genome, but it remains an incomplete, intermediate product that is regularly updated as we work towards a complete finished sequence. The current version contains many gaps and errors. We therefore sought to evaluate the quality of various aspects of the current draft genome sequence, including the sequenced clones themselves, their assignment to a position in the fingerprint clone contigs, and the assembly of initial sequence contigs from the individual clones into sequence-contig scaffolds.

Nucleotide accuracy is reflected in a PHRAP score assigned to each base in the draft genome sequence and available to users through the Genome Browsers (see below) and public database entries. A summary of these scores for the unfinished portion of the genome is shown in Table 9. About 91% of the unfinished draft genome sequence has an error rate of less than 1 per 10,000 bases (PHRAP score > 40), and about 96% has an error rate of less than 1 in 1,000 bases (PHRAP > 30). These values are based only on the quality scores for the bases in the sequenced clones; they do not reflect additional confidence in the sequences that are represented in overlapping clones. The finished portion of the draft genome sequence has an error rate of less than 1 per 10,000 bases.

Individual sequenced clones. We assessed the frequency of misassemblies, which can occur when the assembly program PHRAP joins two nonadjacent regions in the clone into a single initial sequence contig. The frequency of misassemblies depends heavily on the depth and quality of coverage of each clone and the nature of the underlying sequence; thus it may vary among genomic regions and among individual centres. Most clone misassemblies are readily corrected as coverage is added during finishing, but they may have been propagated into the current version of the draft genome sequence and they justify caution for certain applications.

We estimated the frequency of misassembly by examining instances in which there was substantial overlap between a draft clone and a finished clone. We studied 83 Mb of such overlaps, involving about 9,000 initial sequence contigs. We found 5.3 instances per Mb in which the alignment of an initial sequence contig to the finished sequence failed to extend to within 200 bases

Table 6 Clone level contiguity of the draft genome sequence

Chromosome	Sequenced-clone contigs		Sequenced-clone-contig scaffolds		Fingerprint clone contigs with sequence	
	Number	N50 length (kb)	Number	N50 length (kb)	Number	N50 length (kb)
All	4,884	826	2,191	2,279	942	8,398
1	453	650	197	1,915	106	3,537
2	348	1,028	127	3,140	52	10,628
3	409	672	201	1,550	73	5,077
4	384	606	163	1,659	41	6,918
5	385	623	164	1,642	48	5,747
6	292	814	98	3,292	17	24,680
7	224	1.074	86	3,527	29	20,401
8	292	542	115	1,742	43	6,236
9	143	1,242	78	2,411	21	29,108
10	179	1,097	105	1,952	16	30,284
11	224	887	89	3,024	31	9,414
12	196	1,138	76	2,717	28	9,546
13	128	1,151	56	3,257	13	25,256
14	54	3,079	27	8,489	14	22,128
15	123	797	56	2,095	19	8,274
16	159	620	92	1,317	57	2,716
17	138	831	58	2,138	43	2,816
18	137	709	47	2,572	24	4,887
19	159	569	79	1,200	51	1,534
20	42	2,318	20	6,862	9	23,489
21	5	28,515	5	28,515	5	28,515
22	11	23,048	11	23,048	11	23,048
X	325	572	181	1,082	143	1,436
Y	27	1,539	20	3,290	8	5,135
UL	47	227	40	281	40	281

Number and size of sequenced-clone contigs, sequenced-clone-contig scaffolds and those fingerprint clone contigs (see Box 1) that contain sequenced clones; some small fingerprint clone contigs do not as yet have associated sequence. UL, fingerprint clone contigs that could not reliably be placed on a chromosome. These length estimates are from the draft genome sequence, in which gaps between sequence contigs are arbitrarily represented with 100 Ns and gaps between sequence clone contigs with 50,000 Ns for 'bridged gaps' and 100,000 Ns for 'unbridged gaps'. These arbitrary values differ minimally from empirical estimates of gap size (see text), and using the empirically derived estimates would change the N50 lengths presented here only slightly. For unfinished chromosomes, the N50 length ranges from 1.5 to 3 times the arithmetic mean for sequenced-clone contigs, 1.5 to 3 times for sequenced-clone-contig scaffolds, and 1.5 to 6 times for fingerprint clone contigs with sequence.

© 2001 Macmillan Magazines Ltd

of the end of the contig, suggesting a possible false join in the assembly of the initial sequence contig. In about half of these cases, the potential misassembly involved fewer than 400 bases, suggesting that a single raw sequence read may have been incorrectly joined. We found 1.9 instances per Mb in which the alignment showed an internal gap, again suggesting a possible misassembly; and 0.5 instances per Mb in which the alignment indicated that two initial sequence contigs that overlapped by at least 150 bp had not been merged by PHRAP. Finally, there were another 0.9 instances per Mb with various other problems. This gives a total of 8.6 instances per Mb of possible misassembly, with about half being relatively small issues involving a few hundred bases.

Some of the potential problems might not result from misassembly, but might reflect sequence polymorphism in the population, small rearrangements during growth of the large-insert clones, regions of low-quality sequence or matches between segmental duplications. Thus, the frequency of misassemblies may be overstated. On the other hand, the criteria for recognizing overlap between draft and finished clones may have eliminated some misassemblies.

Layout of the sequenced clones. We assessed the accuracy of the layout of sequenced clones onto the fingerprinted clone contigs by calculating the concordance between the positions assigned to a sequenced clone on the basis of *in silico* digestion and the position assigned on the basis of BAC end sequence data. The positions agreed in 98% of cases in which independent assignments could be made by both methods. The results were also compared with well studied regions containing both finished and draft genome sequence. These results indicated that sequenced clone order in the fingerprint map was reliable to within about half of one clone length (~100 kb).

A direct test of the layout is also provided by the draft genome sequence assembly itself. With extensive coverage of the genome, a correctly placed clone should usually (although not always) show sequence overlap with its neighbours in the map. We found only 421 instances of 'singleton' clones that failed to overlap a neighbouring clone. Close examination of the data suggests that most of these are correctly placed, but simply do not yet overlap an adjacent sequenced clone. About 150 clones appeared to be candidates for being incorrectly placed.

Alignment of the fingerprint clone contigs. The alignment of the fingerprint clone contigs with the chromosomes was based on the radiation hybrid, YAC and genetic maps of STSs. The positions of most of the STSs in the draft genome sequence were consistent with these previous maps, but the positions of about 1.7% differed from one or more of them. Some of these disagreements may be due to errors in the layout of the sequenced clones or in the underlying

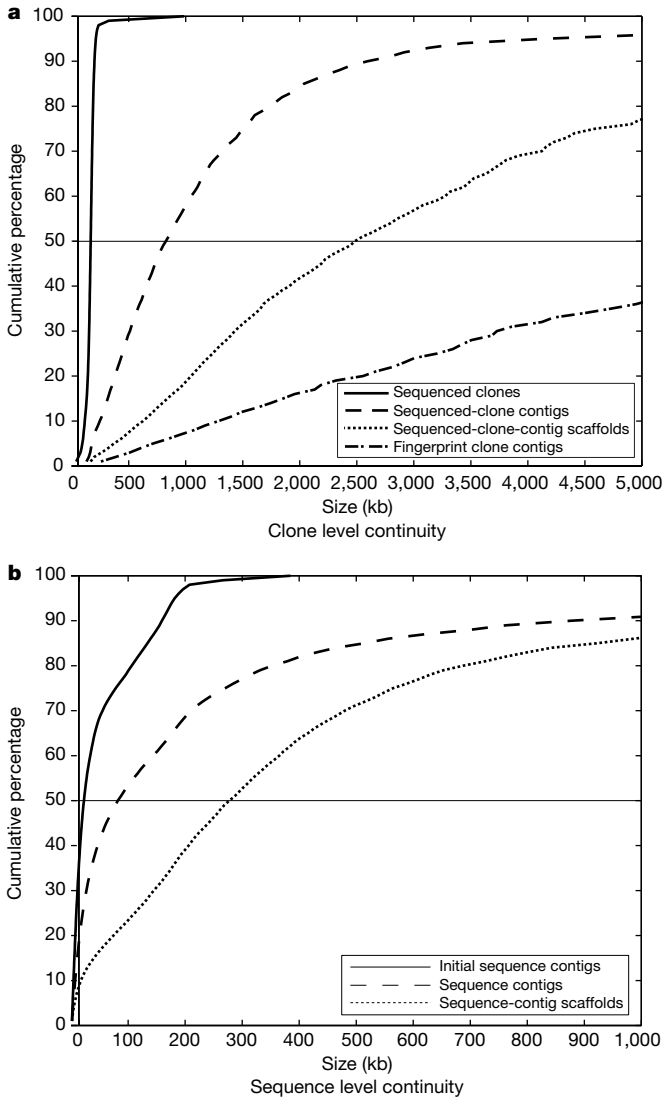

Figure 8 Cumulative distributions of several measures of clone level contiguity and sequence contiguity. The figures represent the proportion of the draft genome sequence contained in contigs of at most the indicated size. **a**, Clone level contiguity. The clones have a tight size distribution with an N50 of ~160 kb (corresponding to 50% on the cumulative distribution). Sequenced-clone contigs represent the next level of continuity, and are linked by mRNA sequences or pairs of BAC end sequences to yield the sequenced-clone-contig scaffolds. The underlying contiguity of the layout of sequenced clones against the fingerprinted clone contigs is only partially shown at this scale. **b**, Sequence contiguity. The input fragments have low continuity (N50 = 21.7 kb). After merging, the sequence contigs grow to an N50 length of about 82 kb. After linking, sequence-contig scaffolds with an N50 length of about 274 kb are created.

Figure 9 Overview of features of draft human genome. The Figure shows the occurrences of twelve important types of feature across the human genome. Large grey blocks represent centromeres and centromeric heterochromatin (size not precisely to scale). Each of the feature types is depicted in a track, from top to bottom as follows. (1) Chromosome position in Mb. (2) The approximate positions of Giemsa-stained chromosome bands at the 800 band resolution. (3) Level of coverage in the draft genome sequence. Red, areas covered by finished clones; yellow, areas covered by predraft sequence. Regions covered by draft sequenced clones are in orange, with darker shades reflecting increasing shotgun sequence coverage. (4) GC content. Percentage of bases in a 20,000 base window that are C or G. (5) Repeat density. Red line, density of SINE class repeats in a 100,000-base window; blue line, density of LINE class repeats in a 100,000-base window. (6) Density of SNPs in a 50,000-base window. The SNPs were detected by sequencing and alignments of random genomic reads. Some of the heterogeneity in SNP density reflects the methods used for SNP discovery. Rigorous analysis of SNP density requires comparing the number of SNPs identified to the precise number of bases surveyed. (7) Non-coding RNA genes. Brown, functional RNA genes such as tRNAs, snoRNAs and rRNAs; light orange, RNA pseudogenes. (8) CpG islands. Green ticks represent regions of ~200 bases with CpG levels significantly higher than in the genome as a whole, and GC ratios of at least 50%. (9) Exofish ecores. Regions of homology with the pufferfish *T. nigroviridis*[292] are blue. (10) ESTs with at least one intron when aligned against genomic DNA are shown as black tick marks. (11) The starts of genes predicted by Genie or Ensembl are shown as red ticks. The starts of known genes from the RefSeq database[110] are shown in blue. (12) The names of genes that have been uniquely located in the draft genome sequence, characterized and named by the HGM Nomenclature Committee. Known disease genes from the OMIM database are red, other genes blue. This Figure is based on an earlier version of the draft genome sequence than analysed in the text, owing to production constraints. We are aware of various errors in the Figure, including omissions of some known genes and misplacements of others. Some genes are mapped to more than one location, owing to errors in assembly, close paralogues or pseudogenes. Manual review was performed to select the most likely location in these cases and to correct other regions. For updated information, see http://genome.ucsc.edu/ and http://www.ensembl.org/.

© 2001 Macmillan Magazines Ltd

Table 7 Sequence level contiguity of the draft genome sequence

Chromosome	Initial sequence contigs		Sequence contigs		Sequence-contig scaffolds	
	Number	N50 length (kb)	Number	N50 length (kb)	Number	N50 length (kb)
All	396,913	21.7	149,821	81.9	87,757	274.3
1	37,656	16.5	12,256	59.1	5,457	278.4
2	32,280	19.9	13,228	57.3	6,959	248.5
3	38,848	15.6	15,098	37.7	8,964	167.4
4	28,600	16.0	13,152	33.0	7,402	158.9
5	30,096	20.4	10,689	72.9	6,378	241.2
6	17,472	43.6	5,547	180.3	2,554	485.0
7	12,733	86.4	4,562	335.7	2,726	591.3
8	19,042	18.1	8,984	38.2	4,631	198.9
9	15,955	20.1	6,226	55.6	3,766	216.2
10	21,762	18.7	9,126	47.9	6,886	133.0
11	29,723	14.3	8,503	40.0	4,684	193.2
12	22,050	19.1	8,422	63.4	5,526	217.0
13	13,737	21.7	5,193	70.5	2,659	300.1
14	4,470	161.4	829	1,371.0	541	2,009.5
15	13,134	15.3	5,840	30.3	3,229	149.7
16	10,297	34.4	4,916	119.5	3,337	356.3
17	10,369	22.9	4,339	90.6	2,616	248.9
18	16,266	15.3	4,461	51.4	2,540	216.1
19	6,009	38.4	2,503	134.4	1,551	375.5
20	2,884	108.6	511	1,346.7	312	813.8
21	103	340.0	5	28,515.3	5	28,515.3
22	526	113.9	11	23,048.1	11	23,048.1
X	11,062	58.8	4,607	218.6	2,610	450.7
Y	557	154.3	140	1,388.6	106	1,439.7
UL	1,282	21.4	613	46.0	297	166.4

This Table is similar to Table 6 but shows the number and N50 length for various types of sequence contig (see Box 1). See legend to Table 6 concerning treatment of gaps. For sequence contigs in the draft genome sequence, the N50 length ranges from 1.7 to 5.5 times the arithmetic mean for initial sequence contigs, 2.5 to 8.2 times for merged sequence contigs, and 6.1 to 10 times for sequence-contig scaffolds.

Table 8 Chromosome size estimates

Chromosome*	Sequenced bases† (Mb)	FCC gaps‡		SCC gaps‖		Sequence gaps#		Heterochromatin and short arm adjustments**(Mb)	Total estimated chromosome size (including artefactual duplication in draft genome sequence)†† (Mb)	Previously estimated chromosome size‡‡ (Mb)
		Number	Total bases in gaps§ (Mb)	Number	Total bases in gaps¶ (Mb)	Number	Total bases in gaps✲ (Mb)			
All	2,692.9	897	152.0	4,076	142.7	145,514	80.6	212	3,289	3,286
1	212.2	104	17.7	347	12.1	11,803	6.5	30	279	263
2	221.6	50	8.5	296	10.4	12,880	7.1	3	251	255
3	186.2	71	12.1	336	11.8	14,689	8.1	3	221	214
4	168.1	39	6.6	343	12.0	12,768	7.1	3	197	203
5	169.7	46	7.8	337	11.8	10,304	5.7	3	198	194
6	158.1	15	2.6	275	9.6	5,225	2.9	3	176	183
7	146.2	27	4.6	195	6.8	4,338	2.4	3	163	171
8	124.3	41	7.0	249	8.7	8,692	4.8	3	148	155
9	106.9	19	3.2	122	4.3	6,083	3.4	22	140	145
10	127.1	14	2.4	163	5.7	8,947	5.0	3	143	144
11	128.6	29	4.9	193	6.8	8,279	4.6	3	148	144
12	124.5	26	4.4	168	5.9	8,226	4.6	3	142	143
13	92.9	12	2.0	115	4.0	5,065	2.8	16	118	114
14	86.9	13	2.2	40	1.4	775	0.4	16	107	109
15	73.4	18	3.1	104	3.6	5,717	3.2	17	100	106
16	73.1	55	9.4	102	3.6	4,757	2.6	15	104	98
17	72.8	41	7.0	95	3.3	4,261	2.4	3	88	92
18	72.9	22	3.7	113	4.0	4,324	2.4	3	86	85
19	55.4	49	8.3	108	3.8	2,344	1.3	3	72	67
20	60.5	7	1.2	33	1.2	469	0.3	3	66	72
21	33.8	4	0.1	0	0.0	0	0.0	11	45	50
22	33.8	10	1.0	0	0.0	0	0.0	13	48	56
X	127.7	141	24.0	182	6.4	4,282	2.4	3	163	164
Y	21.8	6	1.0	19	0.7	113	0.1	27	51	59
NA	5.1	0	0	134	0.0	577	0.3	0	0	0
UL	9.3	38	0	7	0.0	566	0.3	0	0	0

* NA, sequenced clones that could not be associated with fingerprint clone contigs. UL, clone contigs that could not be reliably placed on a chromosome.
† Total number of bases in the draft genome sequence, excluding gaps. Total length of scaffold (including gaps contained within clones) is 2.916 Gb.
‡ Gaps between those fingerprint clone contigs that contain sequenced clones excluding gaps for centromeres.
§ For unfinished chromosomes, we estimate an average size of 0.17 Mb per FCC gap, based on retrospective estimates of the clone coverage of chromosomes 21 and 22. Gap estimates for chromosomes 21 and 22 are taken from refs 93, 94.
‖ Gaps between sequenced-clone contigs within a fingerprint clone contig.
¶ For unfinished chromosomes, we estimate sequenced clone gaps at 0.035 Mb each, based on evaluation of a sample of these gaps.
# Gaps between two sequence contigs within a sequenced-clone contig.
✲ We estimate the average number of bases in sequence gaps from alignments of the initial sequence contigs of unfinished clones (see text) and extrapolation to the whole chromosome.
** Including adjustments for estimates of the sizes of the short arms of the acrocentric chromosomes 13, 14, 15, 21 and 22 (ref. 105), estimates for the centromere and heterochromatic regions of chromosomes 1, 9 and 16 (refs 106, 107) and estimates of 3 Mb for the centromere and 24 Mb for telomeric heterochromatin for the Y chromosome[108].
†† The sum of the five lengths in the preceding columns. This is an overestimate, because the draft genome sequence contains some artefactual sequence owing to inability to correctly to merge all underlying sequence contigs. The total amount of artefactual duplication varies among chromosomes; the overall amount is estimated by computational analysis to be about 100 Mb, or about 3% of the total length given, yielding a total estimated size of about 3,200 Mb for the human genome.
‡‡ Including heterochromatic regions and acrocentric short arm(s)[105].

© 2001 Macmillan Magazines Ltd

fingerprint map. However, many involve STSs that have been localized on only one or two of the previous maps or that occur as isolated discrepancies in conflict with several flanking STSs. Many of these cases are probably due to errors in the previous maps (with error rates for individual maps estimated at 1–2%[100]). Others may be due to incorrect assignment of the STSs to the draft genome sequence (by the electronic polymerase chain reaction (e-PCR) computer program) or to database entries that contain sequence data from more than one clone (owing to cross-contamination).

Graphical views of the independent data sets were particularly useful in detecting problems with order or orientation (Fig. 5). Areas of conflict were reviewed and corrected if supported by the underlying data. In the version discussed here, there were 41 sequenced clones falling in 14 sequenced-clone contigs with STS content information from multiple maps that disagreed with the flanking clones or sequenced-clone contigs; the placement of these clones thus remains suspect. Four of these instances suggest errors in the fingerprint map, whereas the others suggest errors in the layout of sequenced clones. These cases are being investigated and will be corrected in future versions.

Assembly of the sequenced clones. We assessed the accuracy of the assembly by using a set of 148 draft clones comprising 22.4 Mb for which finished sequence subsequently became available[104]. The initial sequence contigs lack information about order and orientation, and GigAssembler attempts to use linking data to infer such information as far as possible[104]. Starting with initial sequence contigs that were unordered and unoriented, the program placed 90% of the initial sequence contigs in the correct orientation and 85% in the correct order with respect to one another. In a separate test, GigAssembler was tested on simulated draft data produced from finished sequence on chromosome 22 and similar results were obtained.

Some problems remain at all levels. First, errors in the initial sequence contigs persist in the merged sequence contigs built from them and can cause difficulties in the assembly of the draft genome sequence. Second, GigAssembler may fail to merge some overlapping sequences because of poor data quality, allelic differences or misassemblies of the initial sequence contigs; this may result in apparent local duplication of a sequence. We have estimated by various methods the amount of such artefactual duplication in the assembly from these and other sources to be about 100 Mb. On the other hand, nearby duplicated sequences may occasionally be incorrectly merged. Some sequenced clones remain incorrectly placed on the layout, as discussed above, and others ($<0.5\%$) remain unplaced. The fingerprint map has undoubtedly failed to resolve some closely related duplicated regions, such as the Williams region and several highly repetitive subtelomeric and pericentric regions (see below). Detailed examination and sequence finishing may be required to sort out these regions precisely, as has been done with chromosome Y[89]. Finally, small sequenced-clone contigs with limited or no STS landmark content remain difficult to place. Full utilization of the higher resolution radiation hybrid map (the TNG map) may help in this[95]. Future targeted FISH experiments and increased map continuity will also facilitate positioning of these sequences.

Table 9 Distribution of PHRAP scores in the draft genome sequence

PHRAP score	Percentage of bases in the draft genome sequence
0–9	0.6
10–19	1.3
20–29	2.2
30–39	4.8
40–49	8.1
50–59	8.7
60–69	9.0
70–79	12.1
80–89	17.3
>90	35.9

PHRAP scores are a logarithmically based representation of the error probability. A PHRAP score of X corresponds to an error probability of $10^{-X/10}$. Thus, PHRAP scores of 20, 30 and 40 correspond to accuracy of 99%, 99.9% and 99.99%, respectively. PHRAP scores are derived from quality scores of the underlying sequence reads used in sequence assembly. See http://www.genome.washington.edu/UWGC/analysistools/phrap.htm.

Genome coverage

We next assessed the nature of the gaps within the draft genome sequence, and attempted to estimate the fraction of the human genome not represented within the current version.

Gaps in draft genome sequence coverage. There are three types of gap in the draft genome sequence: gaps within unfinished sequenced clones; gaps between sequenced-clone contigs, but within fingerprint clone contigs; and gaps between fingerprint clone contigs. The first two types are relatively straightforward to close simply by performing additional sequencing and finishing on already identified clones. Closing the third type may require screening of additional large-insert clone libraries and possibly new technologies for the most recalcitrant regions. We consider these three cases in turn.

We estimated the size of gaps within draft clones by studying instances in which there was substantial overlap between a draft clone and a finished clone, as described above. The average gap size in these draft sequenced clones was 554 bp, although the precise estimate was sensitive to certain assumptions in the analysis. Assuming that the sequence gaps in the draft genome sequence are fairly represented by this sample, about 80 Mb or about 3% (likely range 2–4%) of sequence may lie in the 145,514 gaps within draft sequenced clones.

The gaps between sequenced-clone contigs but within fingerprint clone contigs are more difficult to evaluate directly, because the draft genome sequence flanking many of the gaps is often not precisely aligned with the fingerprinted clones. However, most are much smaller than a single BAC. In fact, nearly three-quarters of these gaps are bridged by one or more individual BACs, as indicated by linking information from BAC end sequences. We measured the sizes of a subset of gaps directly by examining restriction fragment fingerprints of overlapping clones. A study of 157 'bridged' gaps and 55 'unbridged' gaps gave an average gap size of 25 kb. Allowing for the possibility that these gaps may not be fully representative and that some restriction fragments are not included in the calculation, a more conservative estimate of gap size would be 35 kb. This would indicate that about 150 Mb or 5% of the human genome may reside in the 4,076 gaps between sequenced-clone contigs. This sequence should be readily obtained as the clones spanning them are sequenced.

The size of the gaps between fingerprint clone contigs was estimated by comparing the fingerprint maps to the essentially completed chromosomes 21 and 22. The analysis shows that the fingerprinted BAC clones in the global database cover 97–98% of the sequenced portions of those chromosomes[86]. The published sequences of these chromosomes also contain a few small gaps (5 and 11, respectively) amounting to some 1.6% of the euchromatic sequence, and do not include the heterochromatic portion. This suggests that the gaps between contigs in the fingerprint map contain about 4% of the euchromatic genome. Experience with closure of such gaps on chromosomes 20 and 7 suggests that many of these gaps are less than one clone in length and will be closed by clones from other libraries. However, recovery of sequence from these gaps represents the most challenging aspect of producing a complete finished sequence of the human genome.

As another measure of the representation of the BAC libraries, Riethman[109] has found BAC or cosmid clones that link to telomeric half-YACs or to the telomeric sequence itself for 40 of the 41 non-satellite telomeres. Thus, the fingerprint map appears to have no substantial gaps in these regions. Many of the pericentric regions are also represented, but analysis is less complete here (see below).

Representation of random raw sequences. In another approach to measuring coverage, we compared a collection of random raw sequence reads to the existing draft genome sequence. In principle,

© 2001 Macmillan Magazines Ltd

the fraction of reads matching the draft genome sequence should provide an estimate of genome coverage. In practice, the comparison is complicated by the need to allow for repeat sequences, the imperfect sequence quality of both the raw sequence and the draft genome sequence, and the possibility of polymorphism. Nonetheless, the analysis provides a reasonable view of the extent to which the genome is represented in the draft genome sequence and the public databases.

We compared the raw sequence reads against both the sequences used in the construction of the draft genome sequence and all of GenBank using the BLAST computer program. Of the 5,615 raw sequence reads analysed (each containing at least 100 bp of contiguous non-repetitive sequence), 4,924 had a match of $\geq 97\%$ identity with a sequenced clone, indicating that $88 \pm 1.5\%$ of the genome was represented in sequenced clones. The estimate is subject to various uncertainties. Most serious is the proportion of repeat sequence in the remainder of the genome. If the unsequenced portion of the genome is unusually rich in repeated sequence, we would underestimate its size (although the excess would be comprised of repeated sequence).

We examined those raw sequences that failed to match by comparing them to the other publicly available sequence resources. Fifty (0.9%) had matches in public databases containing cDNA sequences, STSs and similar data. An additional 276 (or 43% of the remaining raw sequence) had matches to the whole-genome shotgun reads discussed above (consistent with the idea that these reads cover about half of the genome).

We also examined the extent of genome coverage by aligning the cDNA sequences for genes in the RefSeq dataset[110] to the draft genome sequence. We found that 88% of the bases of these cDNAs could be aligned to the draft genome sequence at high stringency (at least 98% identity). (A few of the alignments with either the random raw sequence reads or the cDNAs may be to a highly similar region in the genome, but such matches should affect the estimate of genome coverage by considerably less than 1%, based on the estimated extent of duplication within the genome (see below).)

These results indicate that about 88% of the human genome is represented in the draft genome sequence and about 94% in the combined publicly available sequence databases. The figure of 88% agrees well with our independent estimates above that about 3%, 5% and 4% of the genome reside in the three types of gap in the draft genome sequence.

Finally, a small experimental check was performed by screening a large-insert clone library with probes corresponding to 16 of the whole genome shotgun reads that failed to match the draft genome sequence. Five hybridized to many clones from different fingerprint clone contigs and were discarded as being repetitive. Of the remaining eleven, two fell within sequenced clones (presumably within sequence gaps of the first type), eight fell in fingerprint clone contigs but between sequenced clones (gaps of the second type) and one failed to identify clones in the fingerprint map (gaps of the third type) but did identify clones in another large-insert library. Although these numbers are small, they are consistent with the view that the much of the remaining genome sequence lies within already identified clones in the current map.

Estimates of genome and chromosome sizes. Informed by this analysis of genome coverage, we proceeded to estimate the sizes of the genome and each of the chromosomes (Table 8). Beginning with the current assigned sequence for each chromosome, we corrected for the known gaps on the basis of their estimated sizes (see above). We attempted to account for the sizes of centromeres and heterochromatin, neither of which are well represented in the draft sequence. Finally, we corrected for around 100 Mb of artefactual duplication in the assembly. We arrived at a total human genome size estimate of around 3,200 Mb, which compares favourably with previous estimates based on DNA content.

We also independently estimated the size of the euchromatic portion of the genome by determining the fraction of the 5,615 random raw sequences that matched the finished portion of the human genome (whose total length is known with greater precision). Twenty-nine per cent of these raw sequences found a match among 835 Mb of nonredundant finished sequence. This leads to an estimate of the euchromatic genome size of 2.9 Gb. This agrees reasonably with the prediction above based on the length of the draft genome sequence (Table 8).

Update. The results above reflect the data on 7 October 2000. New data are continually being added, with improvements being made to the physical map, new clones being sequenced to close gaps and draft clones progressing to full shotgun coverage and finishing. The draft genome sequence will be regularly reassembled and publicly released.

Currently, the physical map has been refined such that the number of fingerprint clone contigs has fallen from 1,246 to 965; this reflects the elimination of some artefactual contigs and the closure of some gaps. The sequence coverage has risen such that 90% of the human genome is now represented in the sequenced clones and more than 94% is represented in the combined publicly available sequence databases. The total amount of finished sequence is now around 1 Gb.

Broad genomic landscape

What biological insights can be gleaned from the draft sequence? In this section, we consider very large-scale features of the draft genome sequence: the distribution of GC content, CpG islands and recombination rates, and the repeat content and gene content of the human genome. The draft genome sequence makes it possible to integrate these features and others at scales ranging from individual

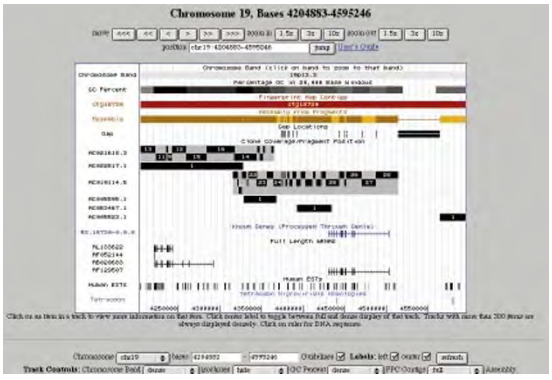

Figure 10 Screen shot from UCSC Draft Human Genome Browser. See http://genome.ucsc.edu/.

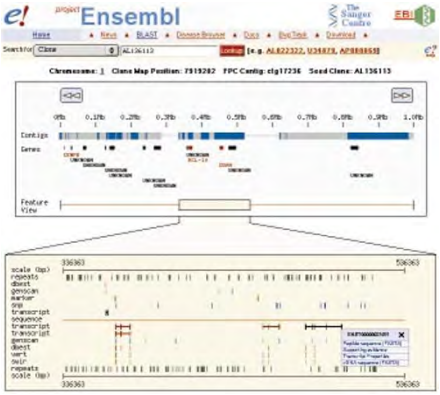

Figure 11 Screen shot from the Genome Browser of Project Ensembl. See http://www.ensembl.org.

© 2001 Macmillan Magazines Ltd

nucleotides to collections of chromosomes. Unless noted, all analyses were conducted on the assembled draft genome sequence described above.

Figure 9 provides a high-level view of the contents of the draft genome sequence, at a scale of about 3.8 Mb per centimetre. Of course, navigating information spanning nearly ten orders of magnitude requires computational tools to extract the full value. We have created and made freely available various 'Genome Browsers'. Browsers were developed and are maintained by the University of California at Santa Cruz (Fig. 10) and the EnsEMBL project of the European Bioinformatics Institute and the Sanger Centre (Fig. 11). Additional browsers have been created; URLs are listed at www.nhgri.nih.gov/genome_hub. These web-based computer tools allow users to view an annotated display of the draft genome sequence, with the ability to scroll along the chromosomes and zoom in or out to different scales. They include: the nucleotide sequence, sequence contigs, clone contigs, sequence coverage and finishing status, local GC content, CpG islands, known STS markers from previous genetic and physical maps, families of repeat sequences, known genes, ESTs and mRNAs, predicted genes, SNPs and sequence similarities with other organisms (currently the pufferfish *Tetraodon nigroviridis*). These browsers will be updated as the draft genome sequence is refined and corrected as additional annotations are developed.

In addition to using the Genome Browsers, one can download from these sites the entire draft genome sequence together with the annotations in a computer-readable format. The sequences of the underlying sequenced clones are all available through the public sequence databases. URLs for these and other genome websites are listed in Box 2. A larger list of useful URLs can be found at www.nhgri.nih.gov/genome_hub. An introduction to using the draft genome sequence, as well as associated databases and analytical tools, is provided in an accompanying paper[111].

In addition, the human cytogenetic map has been integrated with the draft genome sequence as part of a related project. The BAC Resource Consortium[103] established dense connections between the maps using more than 7,500 sequenced large-insert clones that had been cytogenetically mapped by FISH; the average density of the map is 2.3 clones per Mb. Although the precision of the integration is limited by the resolution of FISH, the links provide a powerful tool for the analysis of cytogenetic aberrations in inherited diseases and cancer. These cytogenetic links can also be accessed through the Genome Browsers.

Box 2

Sources of publicly available sequence data and other relevant genomic information

http://genome.ucsc.edu/
University of California at Santa Cruz
Contains the assembly of the draft genome sequence used in this paper and updates

http://genome.wustl.edu/gsc/ human/Mapping/
Washington University
Contains links to clone and accession maps of the human genome

http://www.ensembl.org
EBI/Sanger Centre
Allows access to DNA and protein sequences with automatic baseline annotation

http://www.ncbi.nlm.nih.gov/ genome/guide/
NCBI
Views of chromosomes and maps and loci with links to other NCBI resources

http://www.ncbi.nlm.nih.gov/ genemap99/
Gene map 99: contains data and viewers for radiation hybrid maps of EST-based STSs

http://compbio.ornl.gov/channel/index.html
Oak Ridge National Laboratory
Java viewers for human genome data

http://hgrep.ims.u-tokyo.ac.jp/
RIKEN and the University of Tokyo
Gives an overview of the entire human genome structure

http://snp.cshl.org/
The SNP Consortium
Includes a variety of ways to query for SNPs in the human genome

http://www.ncbi.nlm.nih.gov/Omim/
Online *Mendelian Inheritance in Man*
Contain information about human genes and disease

http://www.nhgri.nih.gov/ELSI/ and http://www.ornl.gov/hgmis/elsi/elsi.html
NHGRI and DOE
Contains information, links and articles on a wide range of social, ethical and legal issues

Long-range variation in GC content

The existence of GC-rich and GC-poor regions in the human genome was first revealed by experimental studies involving density gradient separation, which indicated substantial variation in average GC content among large fragments. Subsequent studies have indicated that these GC-rich and GC-poor regions may have different biological properties, such as gene density, composition of repeat sequences, correspondence with cytogenetic bands and recombination rate[112–117]. Many of these studies were indirect, owing to the lack of sufficient sequence data.

The draft genome sequence makes it possible to explore the variation in GC content in a direct and global manner. Visual inspection (Fig. 9) confirms that local GC content undergoes substantial long-range excursions from its genome-wide average of 41%. If the genome were drawn from a uniform distribution of GC content, the local GC content in a window of size n bp should be $41 \pm \sqrt{((41)(59)/n)}$%. Fluctuations would be modest, with the standard deviation being halved as the window size is quadrupled—for example, 0.70%, 0.35%, 0.17% and 0.09% for windows of size 5, 20, 80 and 320 kb.

The draft genome sequence, however, contains many regions with much more extreme variation. There are huge regions (> 10 Mb) with GC content far from the average. For example, the most distal 48 Mb of chromosome 1p (from the telomere to about STS marker D1S3279) has an average GC content of 47.1%, and chromosome 13 has a 40-Mb region (roughly between STS marker A005X38 and

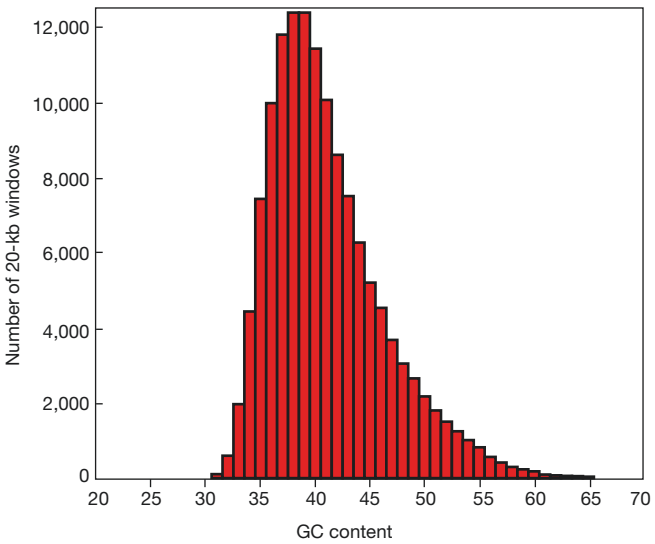

Figure 12 Histogram of GC content of 20-kb windows in the draft genome sequence.

© 2001 Macmillan Magazines Ltd

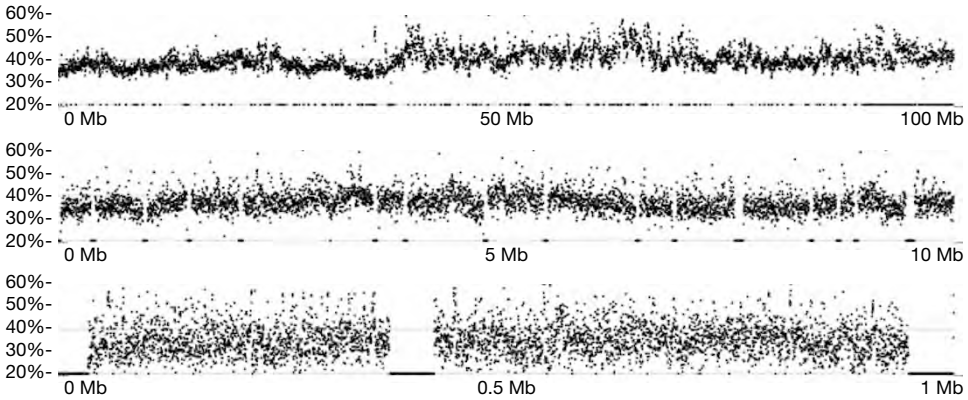

Figure 13 Variation in GC content at various scales. The GC content in subregions of a 100-Mb region of chromosome 1 is plotted, starting at about 83 Mb from the beginning of the draft genome sequence. This region is AT-rich overall. Top, the GC content of the entire 100-Mb region analysed in non-overlapping 20-kb windows. Middle, GC content of the first 10 Mb, analysed in 2-kb windows. Bottom, GC content of the first 1 Mb, analysed in 200-bp windows. At this scale, gaps in the sequence can be seen.

stsG30423) with only 36% GC content. There are also examples of large shifts in GC content between adjacent multimegabase regions. For example, the average GC content on chromosome 17q is 50% for the distal 10.3 Mb but drops to 38% for the adjacent 3.9 Mb. There are regions of less than 300 kb with even wider swings in GC content, for example, from 33.1% to 59.3%.

Long-range variation in GC content is evident not just from extreme outliers, but throughout the genome. The distribution of average GC content in 20-kb windows across the draft genome sequence is shown in Fig. 12. The spread is 15-fold larger than predicted by a uniform process. Moreover, the standard deviation barely decreases as window size increases by successive factors of four—5.9%, 5.2%, 4.9% and 4.6% for windows of size 5, 20, 80 and 320 kb. The distribution is also notably skewed, with 58% below the average and 42% above the average of 41%, with a long tail of GC-rich regions.

Bernardi and colleagues[118,119] proposed that the long-range variation in GC content may reflect that the genome is composed of a mosaic of compositionally homogeneous regions that they dubbed 'isochores'. They suggested that the skewed distribution is composed of five normal distributions, corresponding to five distinct types of isochore (L1, L2, H1, H2 and H3, with GC contents of $<$ 38%, 38–42%, 42–47%, 47–52% and $>$ 52%, respectively).

We studied the draft genome sequence to see whether strict isochores could be identified. For example, the sequence was divided into 300-kb windows, and each window was subdivided into 20-kb subwindows. We calculated the average GC content for each window and subwindow, and investigated how much of the variance in the GC content of subwindows across the genome can be statistically 'explained' by the average GC content in each window. About three-quarters of the genome-wide variance among 20-kb windows can be statistically explained by the average GC content of 300-kb windows that contain them, but the residual variance among subwindows (standard deviation, 2.4%) is still far too large to be consistent with a homogeneous distribution. In fact, the hypothesis of homogeneity could be rejected for each 300-kb window in the draft genome sequence.

Similar results were obtained with other window and subwindow sizes. Some of the local heterogeneity in GC content is attributable to transposable element insertions (see below). Such repeat elements typically have a higher GC content than the surrounding sequence, with the effect being strongest for the most recent insertions.

These results rule out a strict notion of isochores as compositionally homogeneous. Instead, there is substantial variation at many different scales, as illustrated in Fig. 13. Although isochores do not appear to merit the prefix 'iso', the genome clearly does contain large regions of distinctive GC content and it is likely to be worth redefining the concept so that it becomes possible rigorously to partition the genome into regions. In the absence of a precise definition, we will loosely refer to such regions as 'GC content domains' in the context of the discussion below.

Fickett *et al.*[120] have explored a model in which the underlying preference for a particular GC content drifts continuously throughout the genome, an approach that bears further examination. Churchill[121] has proposed that the boundaries between GC content domains can in some cases be predicted by a hidden Markov model, with one state representing a GC-rich region and one representing an AT-rich region. We found that this approach tended to identify only very short domains of less than a kilobase (data not shown), but variants of this approach deserve further attention.

The correlation between GC content domains and various biological properties is of great interest, and this is likely to be the most fruitful route to understanding the basis of variation in GC content. As described below, we confirm the existence of strong correlations with both repeat content and gene density. Using the integration between the draft genome sequence and the cytogenetic map described above, it is possible to confirm a statistically significant correlation between GC content and Giemsa bands (G-bands). For example, 98% of large-insert clones mapping to the darkest G-bands are in 200-kb regions of low GC content (average 37%), whereas more than 80% of clones mapping to the lightest G-bands are in regions of high GC content (average 45%)[103]. Estimated band locations can be seen in Fig. 9 and viewed in the context of other genome annotation at http://genome.ucsc.edu/goldenPath/mapPlots/ and http://genome.ucsc.edu/goldenPath/hgTracks.html.

CpG islands

A related topic is the distribution of so-called CpG islands across the genome. The dinucleotide CpG is notable because it is greatly under-represented in human DNA, occurring at only about one-fifth of the roughly 4% frequency that would be expected by simply multiplying the typical fraction of Cs and Gs (0.21×0.21). The deficit occurs because most CpG dinucleotides are methylated on the cytosine base, and spontaneous deamination of methyl-C residues gives rise to T residues. (Spontaneous deamination of ordinary cytosine residues gives rise to uracil residues that are readily recognized and repaired by the cell.) As a result, methyl-CpG dinucleotides steadily mutate to TpG dinucleotides. However, the genome contains many 'CpG islands' in which CpG dinucleotides are not methylated and occur at a frequency closer to that predicted by the local GC content. CpG islands are of particular interest because many are associated with the 5′ ends of genes[122–127].

We searched the draft genome sequence for CpG islands. Ideally, they should be defined by directly testing for the absence of cytosine methylation, but that was not practical for this report. There are

© 2001 Macmillan Magazines Ltd

Table 10 Number of CpG islands by GC content

GC content of island	Number of islands	Percentage of islands	Nucleotides in islands	Percentage of nucleotides in islands
Total	28,890	100	19,818,547	100
>80%	22	0.08	5,916	0.03
70–80%	5,884	20	3,111,965	16
60–70%	18,779	65	13,110,924	66
50–60%	4,205	15	3,589,742	18

Potential CpG islands were identified by searching the draft genome sequence one base at a time, scoring each dinucleotide (+17 for GC, –1 for others) and identifying maximally scoring segments. Each segment was then evaluated to determine GC content (≥50%), length (>200) and ratio of observed proportion of GC dinucleotides to the expected proportion on the basis of the GC content of the segment (>0.60), using a modification of a program developed by G. Micklem (personal communication).

various computer programs that attempt to identify CpG islands on the basis of primary sequence alone. These programs differ in some important respects (such as how aggressively they subdivide long CpG-containing regions), and the precise correspondence with experimentally undermethylated islands has not been validated. Nevertheless, there is a good correlation, and computational analysis thus provides a reasonable picture of the distribution of CpG islands in the genome.

To identify CpG islands, we used the definition proposed by Gardiner-Garden and Frommer[128] and embodied in a computer program. We searched the draft genome sequence for CpG islands, using both the full sequence and the sequence masked to eliminate repeat sequences. The number of regions satisfying the definition of a CpG island was 50,267 in the full sequence and 28,890 in the repeat-masked sequence. The difference reflects the fact that some repeat elements (notably Alu) are GC-rich. Although some of these repeat elements may function as control regions, it seems unlikely that most of the apparent CpG islands in repeat sequences are functional. Accordingly, we focused on those in the non-repeated sequence. The count of 28,890 CpG islands is reasonably close to the previous estimate of about 35,000 (ref. 129, as modified by ref. 130). Most of the islands are short, with 60–70% GC content (Table 10). More than 95% of the islands are less than 1,800 bp long, and more than 75% are less than 850 bp. The longest CpG island (on chromosome 10) is 36,619 bp long, and 322 are longer than 3,000 bp. Some of the larger islands contain ribosomal pseudogenes, although RNA genes and pseudogenes account for only a small proportion of all islands (< 0.5%). The smaller islands are consistent with their previously hypothesized function, but the role of these larger islands is uncertain.

The density of CpG islands varies substantially among some of the chromosomes. Most chromosomes have 5–15 islands per Mb, with a mean of 10.5 islands per Mb. However, chromosome Y has an unusually low 2.9 islands per Mb, and chromosomes 16, 17 and 22 have 19–22 islands per Mb. The extreme outlier is chromosome 19, with 43 islands per Mb. Similar trends are seen when considering the percentage of bases contained in CpG islands. The relative density of CpG islands correlates reasonably well with estimates of relative gene density on these chromosomes, based both on previous mapping studies involving ESTs (Fig. 14) and on the distribution of gene predictions discussed below.

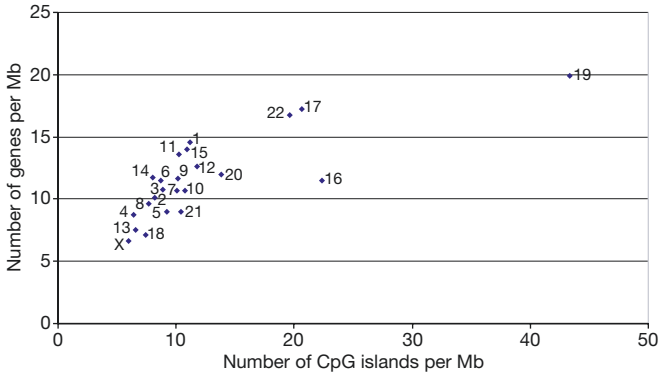

Figure 14 Number of CpG islands per Mb for each chromosome, plotted against the number of genes per Mb (the number of genes was taken from GeneMap98 (ref. 100)). Chromosomes 16, 17, 22 and particularly 19 are clear outliers, with a density of CpG islands that is even greater than would be expected from the high gene counts for these four chromosomes.

Comparison of genetic and physical distance

The draft genome sequence makes it possible to compare genetic and physical distances and thereby to explore variation in the rate of recombination across the human chromosomes. We focus here on large-scale variation. Finer variation is examined in an accompanying paper[131].

The genetic and physical maps are integrated by 5,282 polymorphic loci from the Marshfield genetic map[102], whose positions are known in terms of centimorgans (cM) and Mb along the chromosomes. Figure 15 shows the comparison of the draft genome sequence for chromosome 12 with the male, female and sex-averaged maps. One can calculate the approximate ratio of cM per Mb across a chromosome (reflected in the slopes in Fig. 15) and the average recombination rate for each chromosome arm.

Two striking features emerge from analysis of these data. First, the average recombination rate increases as the length of the chromosome arm decreases (Fig. 16). Long chromosome arms have an average recombination rate of about 1 cM per Mb, whereas the shortest arms are in the range of 2 cM per Mb. A similar trend has been seen in the yeast genome[132,133], despite the fact that the physical scale is nearly 200 times as small. Moreover, experimental studies have shown that lengthening or shortening yeast chromosomes results in a compensatory change in recombination rate[132].

The second observation is that the recombination rate tends to be suppressed near the centromeres and higher in the distal portions of most chromosomes, with the increase largely in the terminal

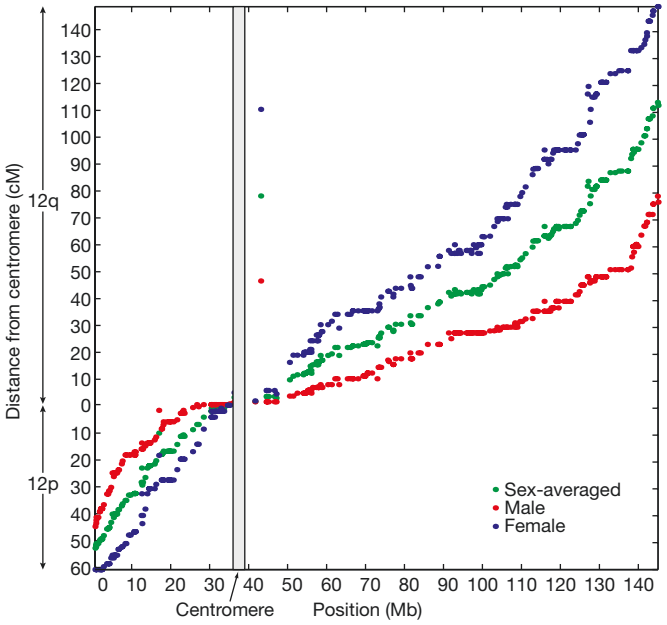

Figure 15 Distance in cM along the genetic map of chromosome 12 plotted against position in Mb in the draft genome sequence. Female, male and sex-averaged maps are shown. Female recombination rates are much higher than male recombination rates. The increased slopes at either end of the chromosome reflect the increased rates of recombination per Mb near the telomeres. Conversely, the flatter slope near the centromere shows decreased recombination there, especially in male meiosis. This is typical of the other chromosomes as well (see http://genome.ucsc.edu/goldenPath/mapPlots). Discordant markers may be map, marker placement or assembly errors.

© 2001 Macmillan Magazines Ltd

20–35 Mb. The increase is most pronounced in the male meiotic map. The effect can be seen, for example, from the higher slope at both ends of chromosome 12 (Fig. 15). Regional and sex-specific effects have been observed for chromosome 21 (refs 110, 134).

Why is recombination higher on smaller chromosome arms? A higher rate would increase the likelihood of at least one crossover during meiosis on each chromosome arm, as is generally observed in human chiasmata counts[135]. Crossovers are believed to be necessary for normal meiotic disjunction of homologous chromosome pairs in eukaryotes. An extreme example is the pseudoautosomal regions on chromosomes Xp and Yp, which pair during male meiosis; this physical region of only 2.6 Mb has a genetic length of 50 cM (corresponding to 20 cM per Mb), with the result that a crossover is virtually assured.

Mechanistically, the increased rate of recombination on shorter chromosome arms could be explained if, once an initial recombination event occurs, additional nearby events are blocked by positive crossover interference on each arm. Evidence from yeast mutants in which interference is abolished shows that interference plays a key role in distributing a limited number of crossovers among the various chromosome arms in yeast[136]. An alternative possibility is that a checkpoint mechanism scans for and enforces the presence of at least one crossover on each chromosome arm.

Variation in recombination rates along chromosomes and between the sexes is likely to reflect variation in the initiation of meiosis-induced double-strand breaks (DSBs) that initiate recombination. DSBs in yeast have been associated with open chromatin[137,138], rather than with specific DNA sequence motifs. With the availability of the draft genome sequence, it should be possible to explore in an analogous manner whether variation in human recombination rates reflects systematic differences in chromosome accessibility during meiosis.

Repeat content of the human genome

A puzzling observation in the early days of molecular biology was that genome size does not correlate well with organismal complexity. For example, *Homo sapiens* has a genome that is 200 times as large as that of the yeast *S. cerevisiae*, but 200 times as small as that of *Amoeba dubia*[139,140]. This mystery (the C-value paradox) was largely resolved with the recognition that genomes can contain a large quantity of repetitive sequence, far in excess of that devoted to protein-coding genes (reviewed in refs 140, 141).

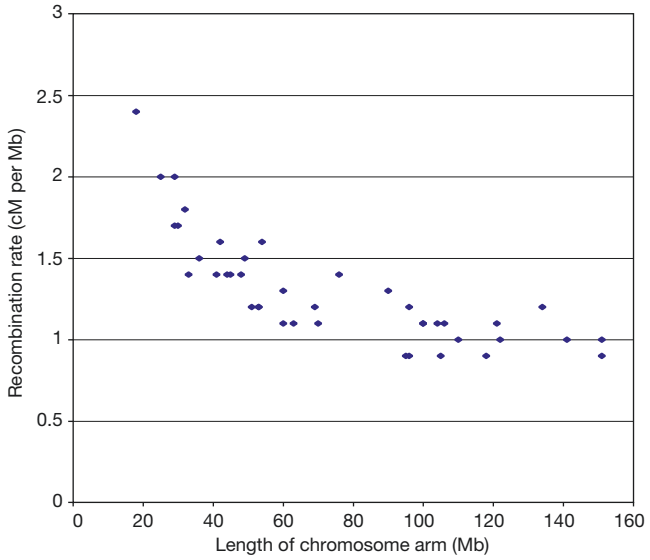

Figure 16 Rate of recombination averaged across the euchromatic portion of each chromosome arm plotted against the length of the chromosome arm in Mb. For large chromosomes, the average recombination rates are very similar, but as chromosome arm length decreases, average recombination rates rise markedly.

In the human, coding sequences comprise less than 5% of the genome (see below), whereas repeat sequences account for at least 50% and probably much more. Broadly, the repeats fall into five classes: (1) transposon-derived repeats, often referred to as interspersed repeats; (2) inactive (partially) retroposed copies of cellular genes (including protein-coding genes and small structural RNAs), usually referred to as processed pseudogenes; (3) simple sequence repeats, consisting of direct repetitions of relatively short *k*-mers such as $(A)_n$, $(CA)_n$ or $(CGG)_n$; (4) segmental duplications, consisting of blocks of around 10–300 kb that have been copied from one region of the genome into another region; and (5) blocks of tandemly repeated sequences, such as at centromeres, telomeres, the short arms of acrocentric chromosomes and ribosomal gene clusters. (These regions are intentionally under-represented in the draft genome sequence and are not discussed here.)

Repeats are often described as 'junk' and dismissed as uninteresting. However, they actually represent an extraordinary trove of information about biological processes. The repeats constitute a rich palaeontological record, holding crucial clues about evolutionary events and forces. As passive markers, they provide assays for studying processes of mutation and selection. It is possible to recognize cohorts of repeats 'born' at the same time and to follow their fates in different regions of the genome or in different species. As active agents, repeats have reshaped the genome by causing ectopic rearrangements, creating entirely new genes, modifying and reshuffling existing genes, and modulating overall GC content. They also shed light on chromosome structure and dynamics, and provide tools for medical genetic and population genetic studies.

The human is the first repeat-rich genome to be sequenced, and so we investigated what information could be gleaned from this majority component of the human genome. Although some of the general observations about repeats were suggested by previous studies, the draft genome sequence provides the first comprehensive view, allowing some questions to be resolved and new mysteries to emerge.

Transposon-derived repeats

Most human repeat sequence is derived from transposable elements[142,143]. We can currently recognize about 45% of the genome as belonging to this class. Much of the remaining 'unique' DNA must also be derived from ancient transposable element copies that have diverged too far to be recognized as such. To describe our analyses of interspersed repeats, it is necessary briefly to review the relevant features of human transposable elements.

Classes of transposable elements. In mammals, almost all transposable elements fall into one of four types (Fig. 17), of which three transpose through RNA intermediates and one transposes directly as DNA. These are long interspersed elements (LINEs), short interspersed elements (SINEs), LTR retrotransposons and DNA transposons.

LINEs are one of the most ancient and successful inventions in eukaryotic genomes. In humans, these transposons are about 6 kb long, harbour an internal polymerase II promoter and encode two open reading frames (ORFs). Upon translation, a LINE RNA assembles with its own encoded proteins and moves to the nucleus, where an endonuclease activity makes a single-stranded nick and the reverse transcriptase uses the nicked DNA to prime reverse transcription from the 3′ end of the LINE RNA. Reverse transcription frequently fails to proceed to the 5′ end, resulting in many truncated, nonfunctional insertions. Indeed, most LINE-derived repeats are short, with an average size of 900 bp for all LINE1 copies, and a median size of 1,070 bp for copies of the currently active LINE1 element (L1Hs). New insertion sites are flanked by a small

© 2001 Macmillan Magazines Ltd

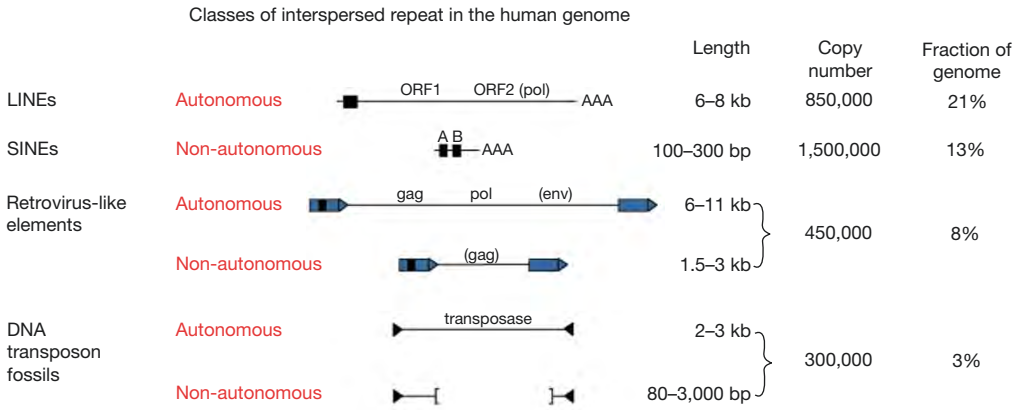

Figure 17 Almost all transposable elements in mammals fall into one of four classes. See text for details.

target site duplication of 7–20 bp. The LINE machinery is believed to be responsible for most reverse transcription in the genome, including the retrotransposition of the non-autonomous SINEs[144] and the creation of processed pseudogenes[145,146]. Three distantly related LINE families are found in the human genome: LINE1, LINE2 and LINE3. Only LINE1 is still active.

SINEs are wildly successful freeloaders on the backs of LINE elements. They are short (about 100–400 bp), harbour an internal polymerase III promoter and encode no proteins. These non-autonomous transposons are thought to use the LINE machinery for transposition. Indeed, most SINEs 'live' by sharing the 3′ end with a resident LINE element[144]. The promoter regions of all known SINEs are derived from tRNA sequences, with the exception of a single monophyletic family of SINEs derived from the signal recognition particle component 7SL. This family, which also does not share its 3′ end with a LINE, includes the only active SINE in the human genome: the Alu element. By contrast, the mouse has both tRNA-derived and 7SL-derived SINEs. The human genome contains three distinct monophyletic families of SINEs: the active Alu, and the inactive MIR and Ther2/MIR3.

LTR retroposons are flanked by long terminal direct repeats that contain all of the necessary transcriptional regulatory elements. The autonomous elements (retrotransposons) contain *gag* and *pol* genes, which encode a protease, reverse transcriptase, RNAse H and integrase. Exogenous retroviruses seem to have arisen from endogenous retrotransposons by acquisition of a cellular *envelope* gene (*env*)[147]. Transposition occurs through the retroviral mechanism with reverse transcription occurring in a cytoplasmic virus-like particle, primed by a tRNA (in contrast to the nuclear location and chromosomal priming of LINEs). Although a variety of LTR retrotransposons exist, only the vertebrate-specific endogenous retroviruses (ERVs) appear to have been active in the mammalian genome. Mammalian retroviruses fall into three classes (I–III), each comprising many families with independent origins. Most (85%) of the LTR retroposon-derived 'fossils' consist only of an isolated LTR, with the internal sequence having been lost by homologous recombination between the flanking LTRs.

DNA transposons resemble bacterial transposons, having terminal inverted repeats and encoding a transposase that binds near the inverted repeats and mediates mobility through a 'cut-and-paste' mechanism. The human genome contains at least seven major classes of DNA transposon, which can be subdivided into many families with independent origins[148] (see RepBase, http://www.girinst.org/~server/repbase.html). DNA transposons tend to have short life spans within a species. This can be explained by contrasting the modes of transposition of DNA transposons and LINE elements. LINE transposition tends to involve only functional elements, owing to the *cis*-preference by which LINE proteins assemble with the RNA from which they were translated. By contrast, DNA transposons cannot exercise a *cis*-preference: the encoded transposase is produced in the cytoplasm and, when it returns to the nucleus, it cannot distinguish active from inactive elements. As inactive copies accumulate in the genome, transposition becomes less efficient. This checks the expansion of any DNA transposon family and in due course causes it to die out. To survive, DNA transposons must eventually move by horizontal transfer to virgin genomes, and there is considerable evidence for such transfer[149–153].

Transposable elements employ different strategies to ensure their evolutionary survival. LINEs and SINEs rely almost exclusively on vertical transmission within the host genome[154] (but see refs 148, 155). DNA transposons are more promiscuous, requiring relatively frequent horizontal transfer. LTR retroposons use both strategies, with some being long-term active residents of the human genome (such as members of the ERVL family) and others having only short residence times.

Table 11 Number of copies and fraction of genome for classes of interspersed repeat

	Number of copies (× 1,000)	Total number of bases in the draft genome sequence (Mb)	Fraction of the draft genome sequence (%)	Number of families (subfamilies)
SINEs	1,558	359.6	13.14	
Alu	1,090	290.1	10.60	1 (~20)
MIR	393	60.1	2.20	1 (1)
MIR3	75	9.3	0.34	1 (1)
LINEs	868	558.8	20.42	
LINE1	516	462.1	16.89	1 (~55)
LINE2	315	88.2	3.22	1 (2)
LINE3	37	8.4	0.31	1 (2)
LTR elements	443	227.0	8.29	
ERV-class I	112	79.2	2.89	72 (132)
ERV(K)-class II	8	8.5	0.31	10 (20)
ERV (L)-class III	83	39.5	1.44	21 (42)
MaLR	240	99.8	3.65	1 (31)
DNA elements	294	77.6	2.84	
hAT group				
MER1-Charlie	182	38.1	1.39	25 (50)
Zaphod	13	4.3	0.16	4 (10)
Tc-1 group				
MER2-Tigger	57	28.0	1.02	12 (28)
Tc2	4	0.9	0.03	1 (5)
Mariner	14	2.6	0.10	4 (5)
PiggyBac-like	2	0.5	0.02	10 (20)
Unclassified	22	3.2	0.12	7 (7)
Unclassified	3	3.8	0.14	3 (4)
Total interspersed repeats		1,226.8	44.83	

The number of copies and base pair contributions of the major classes and subclasses of transposable elements in the human genome. Data extracted from a RepeatMasker analysis of the draft genome sequence (RepeatMasker version 09092000, sensitive settings, using RepBase Update 5.08). In calculating percentages, RepeatMasker excluded the runs of Ns linking the contigs in the draft genome sequence. In the last column, separate consensus sequences in the repeat databases are considered subfamilies, rather than families, when the sequences are closely related or related through intermediate subfamilies.

© 2001 Macmillan Magazines Ltd

Census of human repeats. We began by taking a census of the transposable elements in the draft genome sequence, using a recently updated version of the RepeatMasker program (version 09092000) run under sensitive settings (see http://repeatmasker.genome.washington.edu). This program scans sequences to identify full-length and partial members of all known repeat families represented in RepBase Update (version 5.08; see http://www.girinst.org/~server/repbase.html and ref. 156). Table 11 shows the number of copies and fraction of the draft genome sequence occupied by each of the four major classes and the main subclasses.

The precise count of repeats is obviously underestimated because the genome sequence is not finished, but their density and other properties can be stated with reasonable confidence. Currently recognized SINEs, LINEs, LTR retroposons and DNA transposon copies comprise 13%, 20%, 8% and 3% of the sequence, respectively. We expect these densities to grow as more repeat families are recognized, among which will be lower copy number LTR elements and DNA transposons, and possibly high copy number ancient (highly diverged) repeats.

Age distribution. The age distribution of the repeats in the human genome provides a rich 'fossil record' stretching over several hundred million years. The ancestry and approximate age of each fossil can be inferred by exploiting the fact that each copy is derived from, and therefore initially carried the sequence of, a then-active transposon and, being generally under no functional constraint, has accumulated mutations randomly and independently of other copies. We can infer the sequence of the ancestral active elements by clustering the modern derivatives into phylogenetic trees and building a consensus based on the multiple sequence alignment of a cluster of copies. Using available consensus sequences for known repeat subfamilies, we calculated the per cent divergence from the inferred ancestral active transposon for each of three million interspersed repeats in the draft genome sequence.

The percentage of sequence divergence can be converted into an approximate age in millions of years (Myr) on the basis of evolutionary information. Care is required in calibrating the clock, because the rate of sequence divergence may not be constant over time or between lineages[139]. The relative-rate test[157] can be used to calculate the sequence divergence that accumulated in a lineage after a given timepoint, on the basis of comparison with a sibling species that diverged at that time and an outgroup species. For example, the substitution rate over roughly the last 25 Myr in the human lineage can be calculated by using old world monkeys (which diverged about 25 Myr ago) as a sibling species and new world monkeys as an outgroup. We have used currently available calibrations for the human lineage, but the issue should be revisited as sequence information becomes available from different mammals.

Figure 18a shows the representation of various classes of trans-

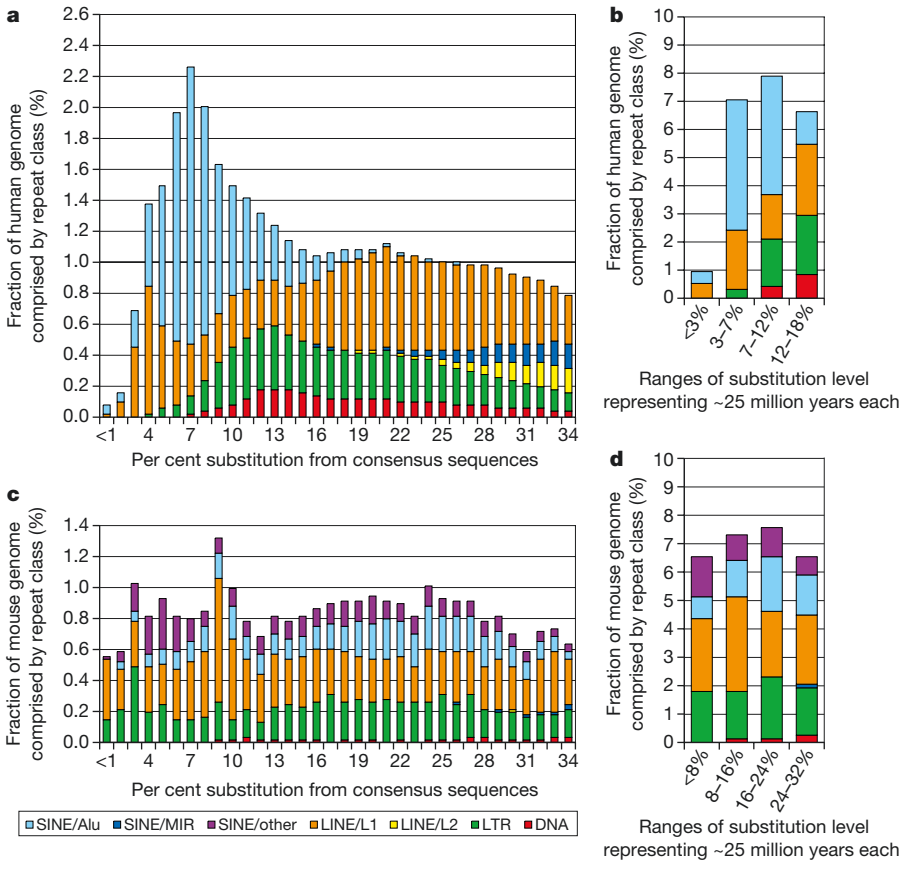

Figure 18 Age distribution of interspersed repeats in the human and mouse genomes. Bases covered by interspersed repeats were sorted by their divergence from their consensus sequence (which approximates the repeat's original sequence at the time of insertion). The average number of substitutions per 100 bp (substitution level, K) was calculated from the mismatch level p assuming equal frequency of all substitutions (the one-parameter Jukes–Cantor model, $K = -3/4\ln(1 - 4/3p)$). This model tends to underestimate higher substitution levels. CpG dinucleotides in the consensus were excluded from the substitution level calculations because the C→T transition rate in CpG pairs is about tenfold higher than other transitions and causes distortions in comparing transposable elements with high and low CpG content. **a**, The distribution, for the human genome, in bins corresponding to 1% increments in substitution levels. **b**, The data grouped into bins representing roughly equal time periods of 25 Myr. **c**,**d**, Equivalent data for available mouse genomic sequence. There is a different correspondence between substitution levels and time periods owing to different rates of nucleotide substitution in the two species. The correspondence between substitution levels and time periods was largely derived from three-way species comparisons (relative rate test[139,157]) with the age estimates based on fossil data. Human divergence from gibbon 20–30 Myr; old world monkey 25–35 Myr; prosimians 55–80 Myr; eutherian mammalian radiation ~100 Myr.

© 2001 Macmillan Magazines Ltd

posable elements in categories reflecting equal amounts of sequence divergence. In Fig. 18b the data are grouped into four bins corresponding to successive 25-Myr periods, on the basis of an approximate clock. Figure 19 shows the mean ages of various subfamilies of DNA transposons. Several facts are apparent from these graphs. First, most interspersed repeats in the human genome predate the eutherian radiation. This is a testament to the extremely slow rate with which nonfunctional sequences are cleared from vertebrate genomes (see below concerning comparison with the fly).

Second, LINE and SINE elements have extremely long lives. The monophyletic LINE1 and Alu lineages are at least 150 and 80 Myr old, respectively. In earlier times, the reigning transposons were LINE2 and MIR[148,158]. The SINE MIR was perfectly adapted for reverse transcription by LINE2, as it carried the same 50-base sequence at its 3′ end. When LINE2 became extinct 80–100 Myr ago, it spelled the doom of MIR.

Third, there were two major peaks of DNA transposon activity (Fig. 19). The first involved Charlie elements and occurred long before the eutherian radiation; the second involved Tigger elements and occurred after this radiation. Because DNA transposons can produce large-scale chromosome rearrangements[159–162], it is possible that widespread activity could be involved in speciation events.

Fourth, there is no evidence for DNA transposon activity in the past 50 Myr in the human genome. The youngest two DNA transposon families that we can identify in the draft genome sequence (MER75 and MER85) show 6–7% divergence from their respective consensus sequences representing the ancestral element (Fig. 19), indicating that they were active before the divergence of humans and new world monkeys. Moreover, these elements were relatively unsuccessful, together contributing just 125 kb to the draft genome sequence.

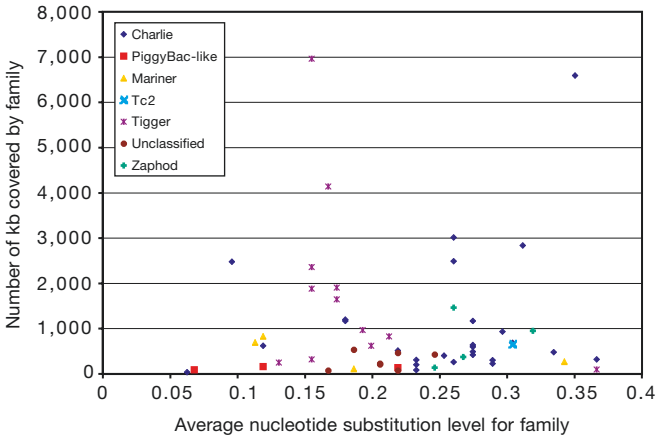

Figure 19 Median ages and per cent of the genome covered by subfamilies of DNA transposons. The Charlie and Zaphod elements were hobo-Activator-Tam3 (hAT) DNA transposons; Mariner, Tc2 and Tigger were Tc1-like elements. Unlike retroposons, DNA transposons are thought to have a short life span in a genome. Thus, the average or median divergence of copies from the consensus is a particularly accurate measure of the age of the DNA transposon copies.

Finally, LTR retroposons appear to be teetering on the brink of extinction, if they have not already succumbed. For example, the most prolific elements (ERVL and MaLRs) flourished for more than 100 Myr but appear to have died out about 40 Myr ago[163,164]. Only a single LTR retroposon family (HERVK10) is known to have transposed since our divergence from the chimpanzee 7 Myr ago, with only one known copy (in the HLA region) that is not shared between all humans[165]. In the draft genome sequence, we can identify only three full-length copies with all ORFs intact (the final total may be slightly higher owing to the imperfect state of the draft genome sequence).

More generally, the overall activity of all transposons has declined markedly over the past 35–50 Myr, with the possible exception of LINE1 (Fig. 18). Indeed, apart from an exceptional burst of activity of Alus peaking around 40 Myr ago, there would appear to have been a fairly steady decline in activity in the hominid lineage since the mammalian radiation. The extent of the decline must be even greater than it appears because old repeats are gradually removed by random deletion and because old repeat families are harder to recognize and likely to be under-represented in the repeat databases. (We confirmed that the decline in transposition is not an artefact arising from errors in the draft genome sequence, which, in principle, could increase the divergence level in recent elements. First, the sequence error rate (Table 9) is far too low to have a significant effect on the apparent age of recent transposons; and second, the same result is seen if one considers only finished sequence.)

What explains the decline in transposon activity in the lineage leading to humans? We return to this question below, in the context of the observation that there is no similar decline in the mouse genome.

Comparison with other organisms. We compared the complement of transposable elements in the human genome with those of the other sequenced eukaryotic genomes. We analysed the fly, worm and mustard weed genomes for the number and nature of repeats (Table 12) and the age distribution (Fig. 20). (For the fly, we analysed the 114 Mb of unfinished 'large' contigs produced by the whole-genome shotgun assembly[166], which are reported to represent euchromatic sequence. Similar results were obtained by analysing 30 Mb of finished euchromatic sequence.) The human genome stands in stark contrast to the genomes of the other organisms.

(1) The euchromatic portion of the human genome has a much higher density of transposable element copies than the euchromatic DNA of the other three organisms. The repeats in the other organisms may have been slightly underestimated because the repeat databases for the other organisms are less complete than for the human, especially with regard to older elements; on the other hand, recent additions to these databases appear to increase the repeat content only marginally.

(2) The human genome is filled with copies of ancient transposons, whereas the transposons in the other genomes tend to be of more recent origin. The difference is most marked with the fly, but is clear for the other genomes as well. The accumulation of old repeats is likely to be determined by the rate at which organisms engage in 'housecleaning' through genomic deletion. Studies of pseudogenes

Table 12 Number and nature of interspersed repeats in eukaryotic genomes

	Human		Fly		Worm		Mustard weed	
	Percentage of bases	Approximate number of families	Percentage of bases	Approximate number of families	Percentage of bases	Approximate number of families	Percentage of bases	Approximate number of families
LINE/SINE	33.40%	6	0.70%	20	0.40%	10	0.50%	10
LTR	8.10%	100	1.50%	50	0.00%	4	4.80%	70
DNA	2.80%	60	0.70%	20	5.30%	80	5.10%	80
Total	44.40%	170	3.10%	90	6.50%	90	10.50%	160

The complete genomes of fly, worm, and chromosomes 2 and 4 of mustard weed (as deposited at ncbi.nlm.nih.gov/genbank/genomes) were screened against the repeats in RepBase Update 5.02 (September 2000) with RepeatMasker at sensitive settings.

© 2001 Macmillan Magazines Ltd

have suggested that small deletions occur at a rate that is 75-fold higher in flies than in mammals; the half-life of such nonfunctional DNA is estimated at 12 Myr for flies and 800 Myr for mammals[167]. The rate of large deletions has not been systematically compared, but seems likely also to differ markedly.

(3) Whereas in the human two repeat families (LINE1 and Alu) account for 60% of all interspersed repeat sequence, the other organisms have no dominant families. Instead, the worm, fly and mustard weed genomes all contain many transposon families, each consisting of typically hundreds to thousands of elements. This difference may be explained by the observation that the vertically transmitted, long-term residential LINE and SINE elements represent 75% of interspersed repeats in the human genome, but only 5–25% in the other genomes. In contrast, the horizontally transmitted and shorter-lived DNA transposons represent only a small portion of all interspersed repeats in humans (6%) but a much larger fraction in fly, mustard weed and worm (25%, 49% and 87%, respectively). These features of the human genome are probably general to all mammals. The relative lack of horizontally transmitted elements may have its origin in the well developed immune system of mammals, as horizontal transfer requires infectious vectors, such as viruses, against which the immune system guards.

We also looked for differences among mammals, by comparing the transposons in the human and mouse genomes. As with the human genome, care is required in calibrating the substitution clock for the mouse genome. There is considerable evidence that the rate of substitution per Myr is higher in rodent lineages than in the hominid lineages[139,168,169]. In fact, we found clear evidence for different rates of substitution by examining families of transposable elements whose insertions predate the divergence of the human and mouse lineages. In an analysis of 22 such families, we found that the substitution level was an average of 1.7-fold higher in mouse than human (not shown). (This is likely to be an underestimate because of an ascertainment bias against the most diverged copies.) The faster clock in mouse is also evident from the fact that the ancient LINE2 and MIR elements, which transposed before the mammalian radiation and are readily detectable in the human genome, cannot be readily identified in available mouse genomic sequence (Fig. 18).

We used the best available estimates to calibrate substitution levels and time[169]. The ratio of substitution rates varied from about 1.7-fold higher over the past 100 Myr to about 2.6-fold higher over the past 25 Myr.

The analysis shows that, although the overall density of the four transposon types in human and mouse is similar, the age distribution is strikingly different (Fig. 18). Transposon activity in the mouse genome has not undergone the decline seen in humans and proceeds at a much higher rate. In contrast to their possible extinction in humans, LTR retroposons are alive and well in the mouse with such representatives as the active IAP family and putatively active members of the long-lived ERVL and MaLR families. LINE1 and a variety of SINEs are quite active. These evolutionary findings are consistent with the empirical observations that new spontaneous mutations are 30 times more likely to be caused by LINE insertions in mouse than in human (~3% versus 0.1%)[170] and 60 times more likely to be caused by transposable elements in general. It is estimated that around 1 in 600 mutations in human are due to transpositions, whereas 10% of mutations in mouse are due to transpositions (mostly IAP insertions).

The contrast between human and mouse suggests that the explanation for the decline of transposon activity in humans may lie in some fundamental difference between hominids and rodents. Population structure and dynamics would seem to be likely suspects. Rodents tend to have large populations, whereas hominid populations tend to be small and may undergo frequent bottlenecks. Evolutionary forces affected by such factors include inbreeding and genetic drift, which might affect the persistence of active transposable elements[171]. Studies in additional mammalian lineages may shed light on the forces responsible for the differences in the activity of transposable elements[172].

Variation in the distribution of repeats. We next explored variation in the distribution of repeats across the draft genome sequence, by calculating the repeat density in windows of various sizes across the genome. There is striking variation at smaller scales.

Some regions of the genome are extraordinarily dense in repeats. The prizewinner appears to be a 525-kb region on chromosome Xp11, with an overall transposable element density of 89%. This region contains a 200-kb segment with 98% density, as well as a segment of 100 kb in which LINE1 sequences alone comprise 89% of the sequence. In addition, there are regions of more than 100 kb with extremely high densities of Alu (> 56% at three loci, including one on 7q11 with a 50-kb stretch of > 61% Alu) and the ancient transposons MIR (> 15% on chromosome 1p36) and LINE2 (> 18% on chromosome 22q12).

In contrast, some genomic regions are nearly devoid of repeats. The absence of repeats may be a sign of large-scale *cis*-regulatory elements that cannot tolerate being interrupted by insertions. The four regions with the lowest density of interspersed repeats in the human genome are the four homeobox gene clusters, HOXA, HOXB, HOXC and HOXD (Fig. 21). Each locus contains regions of around 100 kb containing less than 2% interspersed repeats. Ongoing sequence analysis of the four HOX clusters in mouse, rat and baboon shows a similar absence of transposable elements, and reveals a high density of conserved noncoding elements (K. Dewar and B. Birren, manuscript in preparation). The presence of a complex collection of regulatory regions may explain why individual HOX genes carried in transgenic mice fail to show proper regulation.

It may be worth investigating other repeat-poor regions, such as a region on chromosome 8q21 (1.5% repeat over 63 kb) containing a gene encoding a homeodomain zinc-finger protein (homologous to mouse pID 9663936), a region on chromosome 1p36 (5% repeat over 100 kb) with no obvious genes and a region on chromosome 18q22 (4% over 100 kb) containing three genes of unknown function (among which is KIAA0450). It will be interesting to see whether the homologous regions in the mouse genome have

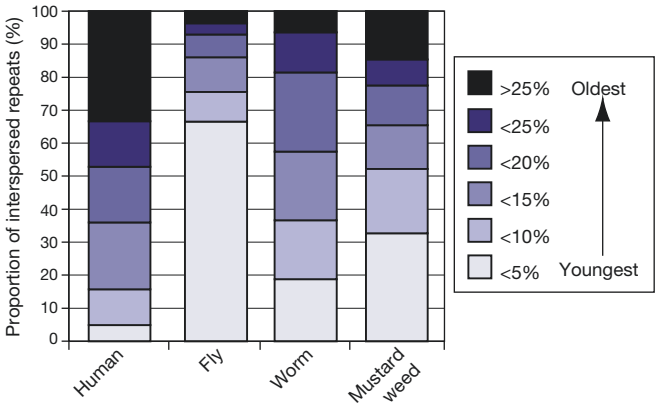

Figure 20 Comparison of the age of interspersed repeats in eukaryotic genomes. The copies of repeats were pooled by their nucleotide substitution level from the consensus.

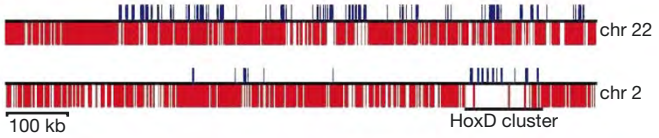

Figure 21 Two regions of about 1 Mb on chromosomes 2 and 22. Red bars, interspersed repeats; blue bars, exons of known genes. Note the deficit of repeats in the HoxD cluster, which contains a collection of genes with complex, interrelated regulation.

© 2001 Macmillan Magazines Ltd

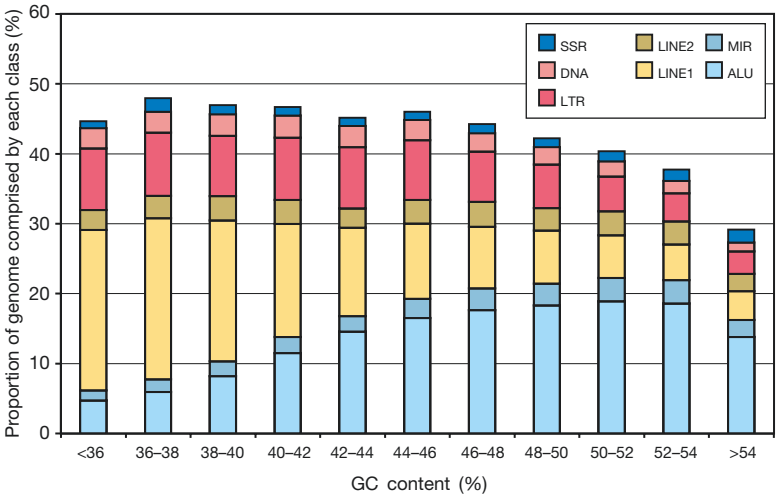

Figure 22 Density of the major repeat classes as a function of local GC content, in windows of 50 kb.

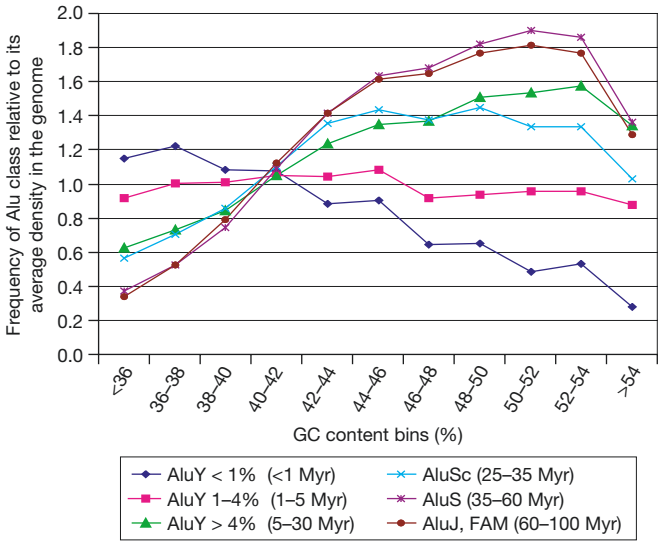

Figure 23 Alu elements target AT-rich DNA, but accumulate in GC-rich DNA. This graph shows the relative distribution of various Alu cohorts as a function of local GC content. The divergence levels (including CpG sites) and ages of the cohorts are shown in the key.

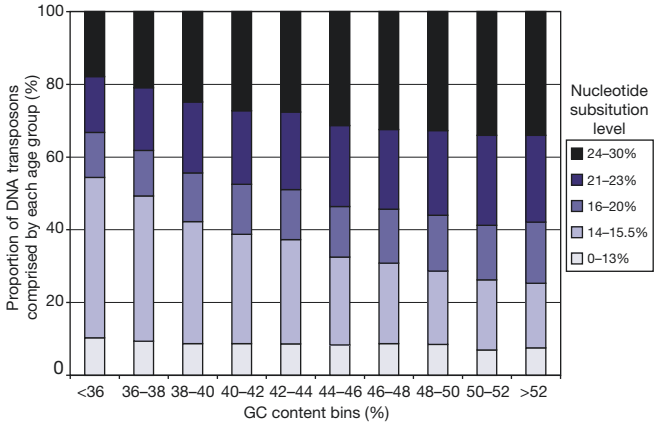

Figure 24 DNA transposon copies in AT-rich DNA tend to be younger than those in more GC-rich DNA. DNA transposon families were grouped into five age categories by their median substitution level (see Fig. 19). The proportion attributed to each age class is shown as a function of GC content. Similar patterns are seen for LINE1 and LTR elements.

similarly resisted the insertion of transposable elements during rodent evolution.

Distribution by GC content. We next focused on the correlation between the nature of the transposons in a region and its GC content. We calculated the density of each repeat type as a function of the GC content in 50-kb windows (Fig. 22). As has been reported[142,173–176], LINE sequences occur at much higher density in AT-rich regions (roughly fourfold enriched), whereas SINEs (MIR, Alu) show the opposite trend (for Alu, up to fivefold lower in AT-rich DNA). LTR retroposons and DNA transposons show a more uniform distribution, dipping only in the most GC-rich regions.

The preference of LINEs for AT-rich DNA seems like a reasonable way for a genomic parasite to accommodate its host, by targeting gene-poor AT-rich DNA and thereby imposing a lower mutational burden. Mechanistically, selective targeting is nicely explained by the fact that the preferred cleavage site of the LINE endonuclease is TTTT/A (where the slash indicates the point of cleavage), which is used to prime reverse transcription from the poly(A) tail of LINE RNA[177].

The contrary behaviour of SINEs, however, is baffling. How do SINEs accumulate in GC-rich DNA, particularly if they depend on the LINE transposition machinery[178]? Notably, the same pattern is seen for the Alu-like B1 and the tRNA-derived SINEs in mouse and for MIR in human[142]. One possibility is that SINEs somehow target GC-rich DNA for insertion. The alternative is that SINEs initially insert with the same proclivity for AT-rich DNA as LINEs, but that the distribution is subsequently reshaped by evolutionary forces[142,179].

We used the draft genome sequence to investigate this mystery by comparing the proclivities of young, adolescent, middle-aged and old Alus (Fig. 23). Strikingly, recent Alus show a preference for AT-rich DNA resembling that of LINEs, whereas progressively older Alus show a progressively stronger bias towards GC-rich DNA. These results indicate that the GC bias must result from strong pressure: Fig. 23 shows that a 13-fold enrichment of Alus in GC-rich DNA has occurred within the last 30 Myr, and possibly more recently.

These results raise a new mystery. What is the force that produces the great and rapid enrichment of Alus in GC-rich DNA? One explanation may be that deletions are more readily tolerated in gene-poor AT-rich regions than in gene-rich GC-rich regions, resulting in older elements being enriched in GC-rich regions. Such an enrichment is seen for transposable elements such as

© 2001 Macmillan Magazines Ltd

DNA transposons (Fig. 24). However, this effect seems too slow and too small to account for the observed remodelling of the Alu distribution. This can be seen by performing a similar analysis for LINE elements (Fig. 25). There is no significant change in the LINE distribution over the past 100 Myr, in contrast to the rapid change seen for Alu. There is an eventual shift after more than 100 Myr, although its magnitude is still smaller than seen for Alus.

These observations indicate that there may be some force acting particularly on Alus. This could be a higher rate of random loss of Alus in AT-rich DNA, negative selection against Alus in AT-rich DNA or positive selection in favour of Alus in GC-rich DNA. The first two possibilities seem unlikely because AT-rich DNA is gene-poor and tolerates the accumulation of other transposable elements. The third seems more feasible, in that it involves selecting in favour of the minority of Alus in GC-rich regions rather than against the majority that lie in AT-rich regions. But positive selection for Alus in GC-rich regions would imply that they benefit the organism.

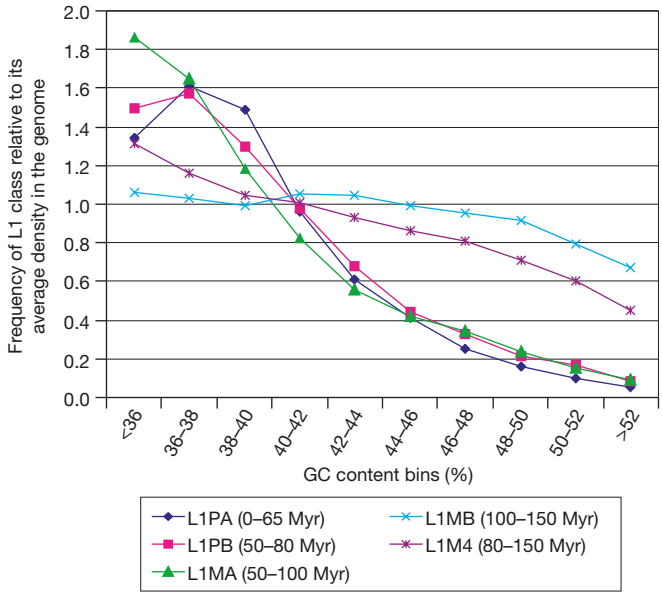

Figure 25 Distribution of various LINE cohorts as a function of local GC content. The divergence levels and ages of the cohorts are shown in the key. (The divergence levels were measured for the 3′ UTR of the LINE1 element only, which is best characterized evolutionarily. This region contains almost no CpG sites, and thus 1% divergence level corresponds to a much longer time than for CpG-rich Alu copies).

Schmid[180] has proposed such a function for SINEs. This hypothesis is based on the observation that in many species SINEs are transcribed under conditions of stress, and the resulting RNAs specifically bind a particular protein kinase (PKR) and block its ability to inhibit protein translation[181–183]. SINE RNAs would thus promote protein translation under stress. SINE RNA may be well suited to such a role in regulating protein translation, because it can be quickly transcribed in large quantities from thousands of elements and it can function without protein translation. Under this theory, there could be positive selection for SINEs in readily transcribed open chromatin such as is found near genes. This could explain the retention of Alus in gene-rich GC-rich regions. It is also consistent with the observation that SINE density in AT-rich DNA is higher near genes[142].

Further insight about Alus comes from the relationship between Alu density and GC content on individual chromosomes (Fig. 26). There are two outliers. Chromosome 19 is even richer in Alus than predicted by its (high) GC content; the chromosome comprises 2% of the genome, but contains 5% of Alus. On the other hand, chromosome Y shows the lowest density of Alus relative to its GC content, being higher than average for GC content less than 40% and lower than average for GC content over 40%. Even in AT-rich DNA, Alus are under-represented on chromosome Y compared with other young interspersed repeats (see below). These phenomena may be related to an unusually high gene density on chromosome 19 and an unusually low density of somatically active genes on chromosome Y (both relative to GC content). This would be consistent with the idea that Alu correlates not with GC content but with actively transcribed genes.

Our results may support the controversial idea that SINEs actually earn their keep in the genome. Clearly, much additional work will be needed to prove or disprove the hypothesis that SINEs are genomic symbionts.

Biases in human mutation. Indirect studies have suggested that nucleotide substitution is not uniform across mammalian

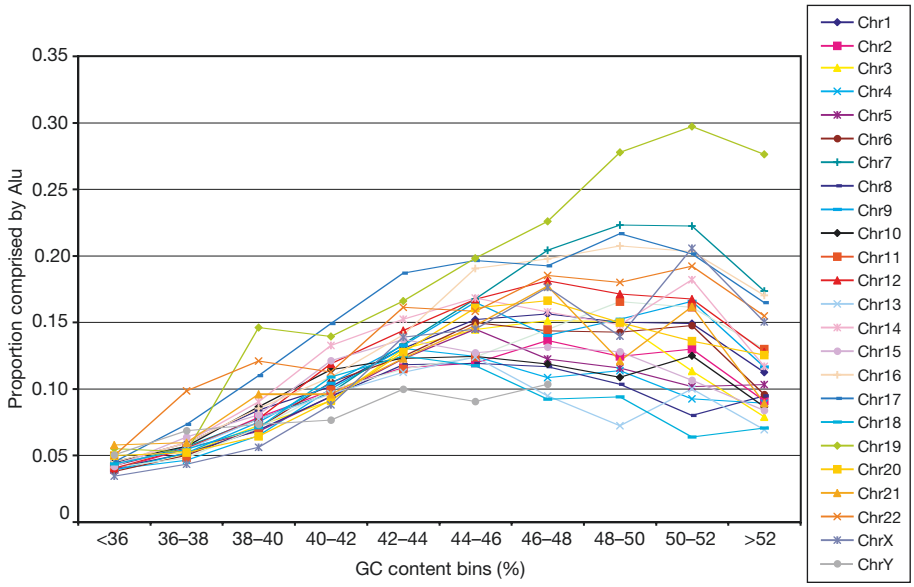

Figure 26 Comparison of the Alu density of each chromosome as a function of local GC content. At higher GC levels, the Alu density varies widely between chromosomes, with chromosome 19 being a particular outlier. In contrast, the LINE1 density pattern is quite uniform for most chromosomes, with the exception of a 1.5 to 2-fold over-representation in AT-rich regions of the X and Y chromosomes (not shown).

© 2001 Macmillan Magazines Ltd

genomes[184–187]. By studying sets of repeat elements belonging to a common cohort, one can directly measure nucleotide substitution rates in different regions of the genome. We find strong evidence that the pattern of neutral substitution differs as a function of local GC content (Fig. 27). Because the results are observed in repetitive elements throughout the genome, the variation in the pattern of nucleotide substitution seems likely to be due to differences in the underlying mutational process rather than to selection.

The effect can be seen most clearly by focusing on the substitution process $\gamma \leftrightarrow \alpha$, where γ denotes GC or CG base pairs and α denotes AT or TA base pairs. If K is the equilibrium constant in the direction of α base pairs (defined by the ratio of the forward and reverse rates), then the equilibrium GC content should be $1/(1+K)$. Two observations emerge.

First, there is a regional bias in substitution patterns. The equilibrium constant varies as a function of local GC content: γ base pairs are more likely to mutate towards α base pairs in AT-rich regions than in GC-rich regions. For the analysis in Fig. 27, the equilibrium constant K is 2.5, 1.9 and 1.2 when the draft genome sequence is partitioned into three bins with average GC content of 37, 43 and 50%, respectively. This bias could be due to a reported tendency for GC-rich regions to replicate earlier in the cell cycle than AT-rich regions and for guanine pools, which are limiting for DNA replication, to become depleted late in the cell cycle, thereby resulting in a small but significant shift in substitution towards α base pairs[186,188]. Another theory proposes that many substitutions are due to differences in DNA repair mechanisms, possibly related to transcriptional activity and thereby to gene density and GC content[185,189,190].

There is also an absolute bias in substitution patterns resulting in directional pressure towards lower GC content throughout the human genome. The genome is not at equilibrium with respect to the pattern of nucleotide substitution: the expected equilibrium GC content corresponding to the values of K above is 29, 35 and 44% for regions with average GC contents of 37, 43 and 50%, respectively. Recent observations on SNPs[190] confirm that the mutation pattern in GC-rich DNA is biased towards α base pairs; it should be possible to perform similar analyses throughout the genome with the availability of 1.4 million SNPs[97,191]. On the basis solely of nucleotide substitution patterns, the GC content would be expected to be about 7% lower throughout the genome.

What accounts for the higher GC content? One possible explanation is that in GC-rich regions, a considerable fraction of the nucleotides is likely to be under functional constraint owing to the high gene density. Selection on coding regions and regulatory CpG islands may maintain the higher-than-predicted GC content. Another is that throughout the rest of the genome, a constant influx of transposable elements tends to increase GC content (Fig. 28). Young repeat elements clearly have a higher GC content than their surrounding regions, except in extremely GC-rich regions. Moreover, repeat elements clearly shift with age towards a lower GC content, closer to that of the neighbourhood in which they reside. Much of the 'non-repeat' DNA in AT-rich regions probably consists of ancient repeats that are not detectable by current methods and that have had more time to approach the local equilibrium value.

The repeats can also be used to study how the mutation process is affected by the immediately adjacent nucleotide. Such 'context effects' will be discussed elsewhere (A. Kas and A. F. A. Smit, unpublished results).

Fast living on chromosome Y. The pattern of interspersed repeats can be used to shed light on the unusual evolutionary history of chromosome Y. Our analysis shows that the genetic material on

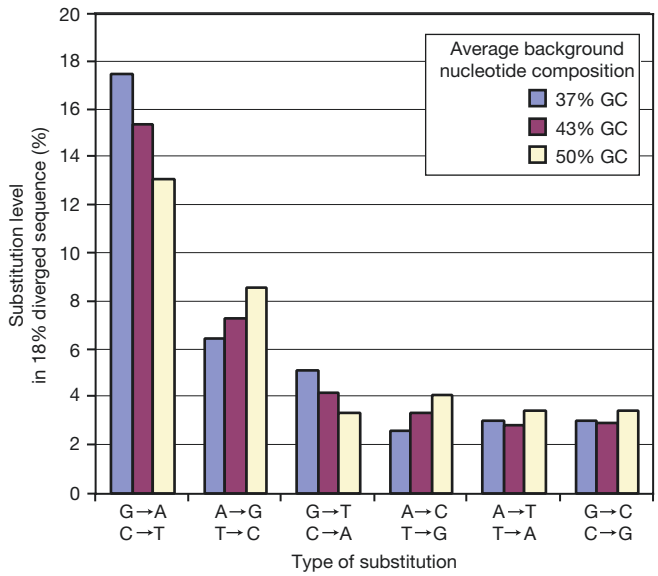

Figure 27 Substitution patterns in interspersed repeats differ as a function of GC content. We collected all copies of five DNA transposons (Tigger1, Tigger2, Charlie3, MER1 and HSMAR2), chosen for their high copy number and well defined consensus sequences. DNA transposons are optimal for the study of neutral substitutions: they do not segregate into subfamilies with diagnostic differences, presumably because they are short-lived and new active families do not evolve in a genome (see text). Duplicates and close paralogues resulting from duplication after transposition were eliminated. The copies were grouped on the basis of GC content of the flanking 1,000 bp on both sides and aligned to the consensus sequence (representing the state of the copy at integration). Recursive efforts using parameters arising from this study did not change the alignments significantly. Alignments were inspected by hand, and obvious misalignments caused by insertions and duplications were eliminated. Substitutions ($n = 80,000$) were counted for each position in the consensus, excluding those in CpG dinucleotides, and a substitution frequency matrix was defined. From the matrices for each repeat (which corresponded to different ages), a single rate matrix was calculated for these bins of GC content (< 40% GC, 40–47% GC and > 47% GC). Data are shown for a repeat with an average divergence (in non-CpG sites) of 18% in 43% GC content (the repeat has slightly higher divergence in AT-rich DNA and lower in GC-rich DNA). From the rate matrix, we calculated log-likelihood matrices with different entropies (divergence levels), which are theoretically optimal for alignments of neutrally diverged copies to their common ancestral state (A. Kas and A. F. A. Smit, unpublished). These matrices are in use by the RepeatMasker program.

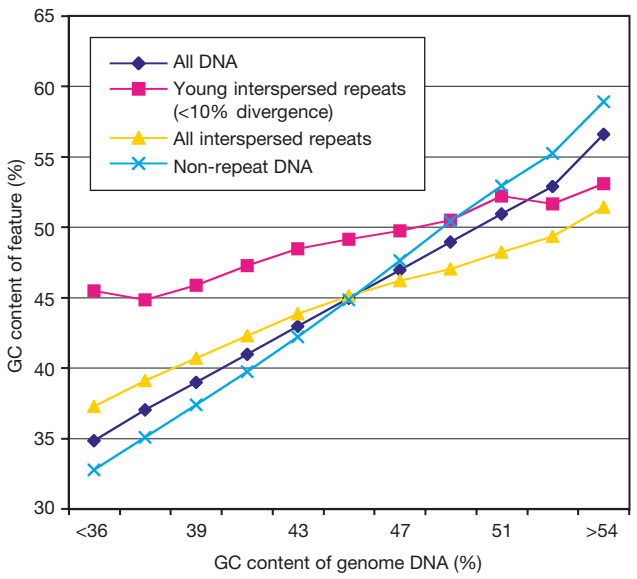

Figure 28 Interspersed repeats tend to diminish the differences between GC bins, despite the fact that GC-rich transposable elements (specifically Alu) accumulate in GC-rich DNA, and AT-rich elements (LINE1) in AT-rich DNA. The GC content of particular components of the sequence (repeats, young repeats and non-repeat sequence) was calculated as a function of overall GC content.

© 2001 Macmillan Magazines Ltd

chromosome Y is unusually young, probably owing to a high tolerance for gain of new material by insertion and loss of old material by deletion. Several lines of evidence support this picture. For example, LINE elements on chromosome Y are on average much younger than those on autosomes (not shown). Similarly, MaLR-family retroposons on chromosome Y are younger than those on autosomes, with the representation of subfamilies showing a strong inverse correlation with the age of the subfamily. Moreover, chromosome Y has a relative over-representation of the younger retroviral class II (ERVK) and a relative under-representation of the primarily older class III (ERVL) compared with other chromosomes. Overall, chromosome Y seems to maintain a youthful appearance by rapid turnover.

Interspersed repeats on chromosome Y can also be used to estimate the relative mutation rates, α_m and α_f, in the male and female germlines. Chromosome Y always resides in males, whereas chromosome X resides in females twice as often as in males. The substitution rates, μ_Y and μ_X, on these two chromosomes should thus be in the ratio $\mu_Y:\mu_X = (\alpha_m):(\alpha_m + 2\alpha_f)/3$, provided that one considers equivalent neutral sequences. Several authors have estimated the mutation rate in the male germline to be fivefold higher than in the female germline, by comparing the rates of evolution of X- and Y-linked genes in humans and primates. However, Page and colleagues[192] have challenged these estimates as too high. They studied a 39-kb region that is apparently devoid of genes and resides within a large segmental duplication from X to Y that occurred 3–4 Myr ago in the human lineage. On the basis of phylogenetic analysis of the sequence on human Y and human, chimp and gorilla X, they obtained a much lower estimate of $\mu_Y:\mu_X = 1.36$, corresponding to $\alpha_m:\alpha_f = 1.7$. They suggested that the other estimates may have been higher because they were based on much longer evolutionary periods or because the genes studied may have been under selection.

Our database of human repeats provides a powerful resource for addressing this question. We identified the repeat elements from recent subfamilies (effectively, birth cohorts dating from the past 50 Myr) and measured the substitution rates for subfamily members on chromosomes X and Y (Fig. 29). There is a clear linear relationship with a slope of $\mu_Y:\mu_X = 1.57$ corresponding to $\alpha_m:\alpha_f = 2.1$. The estimate is in reasonable agreement with that of Page *et al.*, although it is based on much more total sequence (360 kb on Y, 1.6 Mb on X) and a much longer time period. In particular, the discrepancy with earlier reports is not explained by recent changes in the human lineage. Various theories have been proposed for the higher mutation rate in the male germline, including the greater number of cell divisions in the formation of sperm than eggs and different repair mechanisms in sperm and eggs.

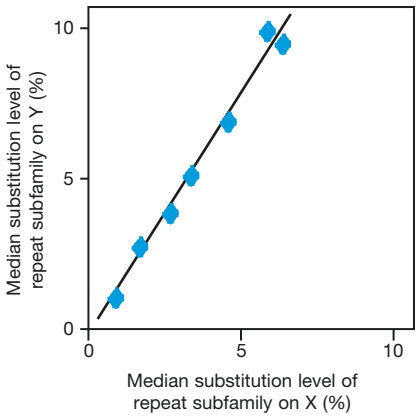

Figure 29 Higher substitution rate on chromosome Y than on chromosome X. We calculated the median substitution level (excluding CpG sites) for copies of the most recent L1 subfamilies (L1Hs–L1PA8) on the X and Y chromosomes. Only the 3′ UTR of the L1 element was considered because its consensus sequence is best established.

Active transposons. We were interested in identifying the youngest retrotransposons in the draft genome sequence. This set should contain the currently active retrotransposons, as well as the insertion sites that are still polymorphic in the human population.

The youngest branch in the phylogenetic tree of human LINE1 elements is called L1Hs (ref. 158); it differs in its 3′ untranslated region (UTR) by 12 diagnostic substitutions from the next oldest subfamily (L1PA2). Within the L1Hs family, there are two subsets referred to as Ta and pre-Ta, defined by a diagnostic trinucleotide[193,194]. All active L1 elements are thought to belong to these two subsets, because they account for all 14 known cases of human disease arising from new L1 transposition (with 13 belonging to the Ta subset and one to the pre-Ta subset)[195,196]. These subsets are also of great interest for population genetics because at least 50% are still segregating as polymorphisms in the human population[194,197]; they provide powerful markers for tracing population history because they represent unique (non-recurrent and non-revertible) genetic events that can be used (along with similarly polymorphic Alus) for reconstructing human migrations.

LINE1 elements that are retrotransposition-competent should consist of a full-length sequence and should have both ORFs intact. Eleven such elements from the Ta subset have been identified, including the likely progenitors of mutagenic insertions into the factor VIII and dystrophin genes[198–202]. A cultured cell retrotransposition assay has revealed that eight of these elements remain retrotransposition-competent[200,202,203].

We searched the draft genome sequence and identified 535 LINEs belonging to the Ta subset and 415 belonging to the pre-Ta subset. These elements provide a large collection of tools for probing human population history. We also identified those consisting of full-length elements with intact ORFs, which are candidate active LINEs. We found 39 such elements belonging to the Ta subset and 22 belonging to the pre-Ta subset; this substantially increases the number in the first category and provides the first known examples in the second category. These elements can now be tested for retrotransposition competence in the cell culture assay. Preliminary analysis resulted in the identification of two of these elements as the likely progenitors of mutagenic insertions into the β-globin and RP2 genes (R. Badge and J. V. Moran, unpublished data). Similar analyses should allow the identification of the progenitors of most, if not all, other known mutagenic L1 insertions.

L1 elements can carry extra DNA if transcription extends through the native transcriptional termination site into flanking genomic DNA. This process, termed L1-mediated transduction, provides a means for the mobilization of DNA sequences around the genome and may be a mechanism for 'exon shuffling'[204]. Twenty-one per cent of the 71 full-length L1s analysed contained non-L1-derived sequences before the 3′ target-site duplication site, in cases in which the site was unambiguously recognizable. The length of the transduced sequence was 30–970 bp, supporting the suggestion that 0.5–1.0% of the human genome may have arisen by LINE-based transduction of 3′ flanking sequences[205,206].

Our analysis also turned up two instances of 5′ transduction (145 bp and 215 bp). Although this possibility had been suggested on the basis of cell culture models[195,203], these are the first documented examples. Such events may arise from transcription initiating in a cellular promoter upstream of the L1 elements. L1 transcription is generally confined to the germline[207,208], but transcription from other promoters could explain a somatic L1 retrotransposition event that resulted in colon cancer[206].

Transposons as a creative force. The primary force for the origin and expansion of most transposons has been selection for their ability to create progeny, and not a selective advantage for the host. However, these selfish pieces of DNA have been responsible for important innovations in many genomes, for example by contributing regulatory elements and even new genes.

Twenty human genes have been recognized as probably derived

© 2001 Macmillan Magazines Ltd

from transposons[142,209]. These include the RAG1 and RAG2 recombinases and the major centromere-binding protein CENPB. We scanned the draft genome sequence and identified another 27 cases, bringing the total to 47 (Table 13; refs 142, 209). All but four are derived from DNA transposons, which give rise to only a small proportion of the interspersed repeats in the genome. Why there are so many DNA transposase-like genes, many of which still contain the critical residues for transposase activity, is a mystery.

To illustrate this concept, we describe the discovery of one of the new examples. We searched the draft genome sequence to identify the autonomous DNA transposon responsible for the distribution of the non-autonomous MER85 element, one of the most recently (40–50 Myr ago) active DNA transposons. Most non-autonomous elements are internal deletion products of a DNA transposon. We identified one instance of a large (1,782 bp) ORF flanked by the 5′ and 3′ halves of a MER85 element. The ORF encodes a novel protein (partially published as pID 6453533) whose closest homologue is the transposase of the piggyBac DNA transposon, which is found in insects and has the same characteristic TTAA target-site duplications[210] as MER85. The ORF is actively transcribed in fetal brain and in cancer cells. That it has not been lost to mutation in 40–50 Myr of evolution (whereas the flanking, noncoding, MER85-like termini show the typical divergence level of such elements) and is actively transcribed provides strong evidence that it has been adopted by the human genome as a gene. Its function is unknown.

LINE1 activity clearly has also had fringe benefits. We mentioned above the possibility of exon reshuffling by cotranscription of neighbouring DNA. The LINE1 machinery can also cause reverse transcription of genic mRNAs, which typically results in nonfunctional processed pseudogenes but can, occasionally, give rise to functional processed genes. There are at least eight human and eight mouse genes for which evidence strongly supports such an origin[211] (see http://www-ifi.uni-muenster.de/exapted-retrogenes/tables.html). Many other intronless genes may have been created in the same way.

Transposons have made other creative contributions to the genome. A few hundred genes, for example, use transcriptional terminators donated by LTR retroposons (data not shown). Other genes employ regulatory elements derived from repeat elements[211].

Simple sequence repeats

Simple sequence repeats (SSRs) are a rather different type of repetitive structure that is common in the human genome—perfect or slightly imperfect tandem repeats of a particular *k*-mer. SSRs with a short repeat unit (n = 1–13 bases) are often termed microsa-

Table 13 Human genes derived from transposable elements

GenBank ID*	Gene name	Related transposon family†	Possible fusion gene§	Newly recognized derivation‖
nID 3150436	BC200	FLAM Alu‡		
pID 2330017	Telomerase	non-LTR retrotransposon		
pID 1196425	HERV-3 env	Retroviridae/HERV-R‡		
pID 4773880	Syncytin	Retroviridae/HERV-W‡		
pID 131827	RAG1 and 2	Tc1-like		
pID 29863	CENP-B	Tc1/Pogo		
EST 2529718		Tc1/Pogo		+
PID 10047247		Tc1/Pogo/Pogo		+
EST 4524463		Tc1/Pogo/Pogo		+
pID 4504807	Jerky	Tc1/Pogo/Tigger		
pID 7513096	JRKL	Tc1/Pogo/Tigger		
EST 5112721		Tc1/Pogo/Tigger		+
EST 11097233		Tc1/Pogo/Tigger		+
EST 6986275	Sancho	Tc1/Pogo/Tigger		
EST 8616450		Tc1/Pogo/Tigger		+
EST 8750408		Tc1/Pogo/Tigger		+
EST 5177004		Tc1/Pogo/Tigger		+
PID 3413884	KIAA0461	Tc1/Pogo/Tc2	+	
PID 7959287	KIAA1513	Tc1/Pogo/Tc2		+
PID 2231380		Tc1/Mariner/Hsmar1‡	+	
EST 10219887		hAT/Hobo	+	+
PID 6581095	Buster1	hAT/Charlie	+	
PID 7243087	Buster2	hAT/Charlie	+	
PID 6581097	Buster3	hAT/Charlie		
PID 7662294	KIAA0766	hAT/Charlie	+	
PID 10439678		hAT/Charlie		+
PID 7243087	KIAA1353	hAT/Charlie		+
PID 7021900		hAT/Charlie/Charlie3‡		+
PID 4263748		hAT/Charlie/Charlie8‡	+	
EST 8161741		hAT/Charlie/Charlie9‡		+
pID 4758872	DAP4,pP52^{rIPK}	hAT/Tip100/Zaphod		
EST 10990063		hAT/Tip100/Zaphod		+
EST 10101591		hAT/Tip100/Zaphod		+
pID 7513011	KIAA0543	hAT/Tip100/Tip100	+	
pID 10439744		hAT/Tip100/Tip100		+
pID 10047247	KIAA1586	hAT/Tip100/Tip100		+
pID 10439762		hAT/Tip100	+	+
EST 10459804		hAT/Tip100		+
pID 4160548	Tramp	hAT/Tam3		+
BAC 3522927		hAT/Tam3		+
pID 3327088	KIAA0637	hAT/Tam3	+	
EST 1928552		hAT/Tam3		+
pID 6453533		piggyBac/MER85‡	+	
EST 3594004		piggyBac/MER85‡		+
BAC 4309921		piggyBac/MER85‡		+
EST 4073914		piggyBac/MER75‡		+
EST 1963278		piggyBac		+

The Table lists 47 human genes, with a likely origin in up to 38 different transposon copies.
* Where available, the GenBank ID numbers are given for proteins, otherwise a representative EST or a clone name is shown. Six groups (two or three genes each) have similarity at the DNA level well beyond that observed between different DNA transposon families in the genome; they are indicated in italics, with all but the initial member of each group indented. This could be explained if the genes were paralogous (derived from a single inserted transposon and subsequently duplicated).
† Classification of the transposon.
‡ Indicates that the transposon from which the gene is derived is precisely known.
§ Proteins probably formed by fusion of a cellular and transposon gene; many have acquired zinc-finger domains.
‖ Not previously reported as being derived from transposable element genes. The remaining genes can be found in refs 142, 209.

© 2001 Macmillan Magazines Ltd

Table 14 SSR content of the human genome

Length of repeat unit	Average bases per Mb	Average number of SSR elements per Mb
1	1,660	36.7
2	5,046	43.1
3	1,013	11.8
4	3,383	32.5
5	2,686	17.6
6	1,376	15.2
7	906	8.4
8	1,139	11.1
9	900	8.6
10	1,576	8.6
11	770	8.7

SSRs were identified by using the computer program Tandem Repeat Finder with the following parameters: match score 2, mismatch score 3, indel 5, minimum alignment 50, maximum repeat length 500, minimum repeat length 1.

tellites, whereas those with longer repeat units (n = 14–500 bases) are often termed minisatellites. With the exception of poly(A) tails from reverse transcribed messages, SSRs are thought to arise by slippage during DNA replication[212,213].

We compiled a catalogue of all SSRs over a given length in the human draft genome sequence, and studied their properties (Table 14). SSRs comprise about 3% of the human genome, with the greatest single contribution coming from dinucleotide repeats (0.5%). (The precise criteria for the number of repeat units and the extent of divergence allowed in an SSR affect the exact census, but not the qualitative conclusions.)

There is approximately one SSR per 2 kb (the number of non-overlapping tandem repeats is 437 per Mb). The catalogue confirms various properties of SSRs that have been inferred from sampling approaches (Table 15). The most frequent dinucleotide repeats are AC and AT (50 and 35% of dinucleotide repeats, respectively), whereas AG repeats (15%) are less frequent and GC repeats (0.1%) are greatly under-represented. The most frequent trinucleotides are AAT and AAC (33% and 21%, respectively), whereas ACC (4.0%), AGC (2.2%), ACT (1.4%) and ACG (0.1%) are relatively rare. Overall, trinucleotide SSRs are much less frequent than dinucleotide SSRs[214].

SSRs have been extremely important in human genetic studies, because they show a high degree of length polymorphism in the human population owing to frequent slippage by DNA polymerase during replication. Genetic markers based on SSRs—particularly $(CA)_n$ repeats—have been the workhorse of most human disease-mapping studies[101,102]. The availability of a comprehensive catalogue of SSRs is thus a boon for human genetic studies.

The SSR catalogue also allowed us to resolve a mystery regarding mammalian genetic maps. Such genetic maps in rat, mouse and human have a deficit of polymorphic $(CA)_n$ repeats on chromosome X[30,101]. There are two possible explanations for this deficit. There may simply be fewer $(CA)_n$ repeats on chromosome X; or $(CA)_n$ repeats may be as dense on chromosome X but less polymorphic in the population. In fact, analysis of the draft genome sequence shows that chromosome X has the same density of $(CA)_n$ repeats per Mb as the autosomes (data not shown). Thus, the deficit of polymorphic markers relative to autosomes results from population genetic forces. Possible explanations include that chromosome X has a smaller effective population size, experiences more frequent selective sweeps reducing diversity (owing to its hemizygosity in males), or has a lower mutation rate (owing to its more frequent passage through the less mutagenic female germline). The availability of the draft genome sequence should provide ways to test these alternative explanations.

Table 15 SSRs by repeat unit

Repeat unit	Number of SSRs per Mb
AC	27.7
AT	19.4
AG	8.2
GC	0.1
AAT	4.1
AAC	2.6
AGG	1.5
AAG	1.4
ATG	0.7
CGG	0.6
ACC	0.4
AGC	0.3
ACT	0.2
ACG	0.0

SSRs were identified as in Table 14.

Segmental duplications

A remarkable feature of the human genome is the segmental duplication of portions of genomic sequence[215–217]. Such duplications involve the transfer of 1–200-kb blocks of genomic sequence to one or more locations in the genome. The locations of both donor and recipient regions of the genome are often not tandemly arranged, suggesting mechanisms other than unequal crossing-over for their origin. They are relatively recent, inasmuch as strong sequence identity is seen in both exons and introns (in contrast to regions that are considered to show evidence of ancient duplications, characterized by similarities only in coding regions). Indeed, many such duplications appear to have arisen in very recent evolutionary time, as judged by high sequence identity and by their absence in closely related species.

Segmental duplications can be divided into two categories. First, interchromosomal duplications are defined as segments that are duplicated among nonhomologous chromosomes. For example, a 9.5-kb genomic segment of the adrenoleukodystrophy locus from Xq28 has been duplicated to regions near the centromeres of chromosomes 2, 10, 16 and 22 (refs 218, 219). Anecdotal observations suggest that many interchromosomal duplications map near the centromeric and telomeric regions of human chromosomes[218–233].

The second category is intrachromosomal duplications, which occur within a particular chromosome or chromosomal arm. This category includes several duplicated segments, also known as low copy repeat sequences, that mediate recurrent chromosomal structural rearrangements associated with genetic disease[215,217]. Examples on chromosome 17 include three copies of a roughly 200-kb repeat separated by around 5 Mb and two copies of a roughly 24-kb repeat separated by 1.5 Mb. The copies are so similar (99% identity) that paralogous recombination events can occur, giving rise to contiguous gene syndromes: Smith–Magenis syndrome and Charcot–Marie–Tooth syndrome 1A, respectively[34,234]. Several other examples are known and are also suspected to be responsible for recurrent microdeletion syndromes (for example, Prader–Willi/Angelman,

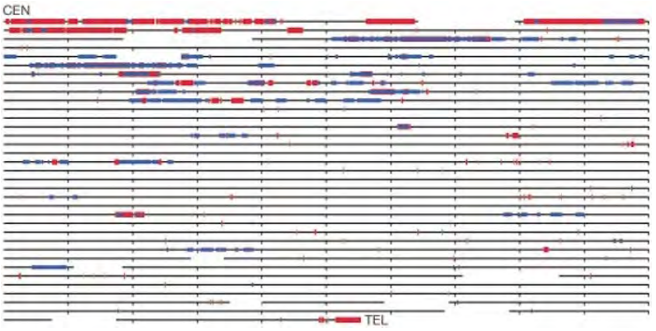

Figure 30 Duplication landscape of chromosome 22. The size and location of intrachromosomal (blue) and interchromosomal (red) duplications are depicted for chromosome 22q, using the PARASIGHT computer program (Bailey and Eichler, unpublished). Each horizontal line represents 1 Mb (ticks, 100-kb intervals). The chromosome sequence is oriented from centromere (top left) to telomere (bottom right). Pairwise alignments with > 90% nucleotide identity and > 1 kb long are shown. Gaps within the chromosomal sequence are of known size and shown as empty space.

© 2001 Macmillan Magazines Ltd

velocardiofacial/DiGeorge and Williams' syndromes[215,235–240]).

Until now, the identification and characterization of segmental duplications have been based on anecdotal reports—for example, finding that certain probes hybridize to multiple chromosomal sites or noticing duplicated sequence at certain recurrent chromosomal breakpoints. The availability of the entire genomic sequence will make it possible to explore the nature of segmental duplications more systematically. This analysis can begin with the current state of the draft genome sequence, although caution is required because some apparent duplications may arise from a failure to merge sequence contigs from overlapping clones. Alternatively, erroneous assembly of closely related sequences from nonoverlapping clones may underestimate the true frequency of such features, particularly among those segments with the highest sequence similarity. Accordingly, we adopted a conservative approach for estimating such duplication from the available draft genome sequence.

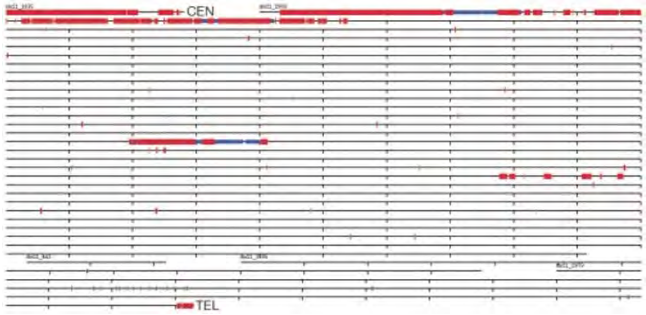

Figure 31 Duplication landscape of chromosome 21. The size and location of intrachromosomal (blue) and interchromosomal (red) duplications are depicted along the sequence of the long arm of chromosome 21. Gaps between finished sequence are denoted by empty space but do not represent actual gap size.

Pericentromeres and subtelomeres. We began by re-evaluating the finished sequences of chromosomes 21 and 22. The initial papers on these chromosomes[93,94] noted some instances of interchromosomal duplication near each centromere. With the ability now to compare these chromosomes to the vast majority of the genome, it is apparent that the regions near the centromeres consist almost entirely of interchromosomal duplicated segments, with little or no unique sequence. Smaller regions of interchromosomal duplication are also observed near the telomeres.

Chromosome 22 contains a region of 1.5 Mb adjacent to the centromere in which 90% of sequence can now be recognized to consist of interchromosomal duplication (Fig. 30). Conversely, 52% of the interchromosomal duplications on chromosome 22 were located in this region, which comprises only 5% of the chromosome. Also, the subtelomeric end consists of a 50-kb region consisting almost entirely of interchromosomal duplications.

Chromosome 21 presents a similar landscape (Fig. 31). The first 1 Mb after the centromere is composed of interchromosomal repeats, as well as the largest (> 200 kb) block of intrachromosomally duplicated material. Again, most interchromosomal duplications on the chromosome map to this region and the most subtelomeric region (30 kb) shows extensive duplication among nonhomologous chromosomes.

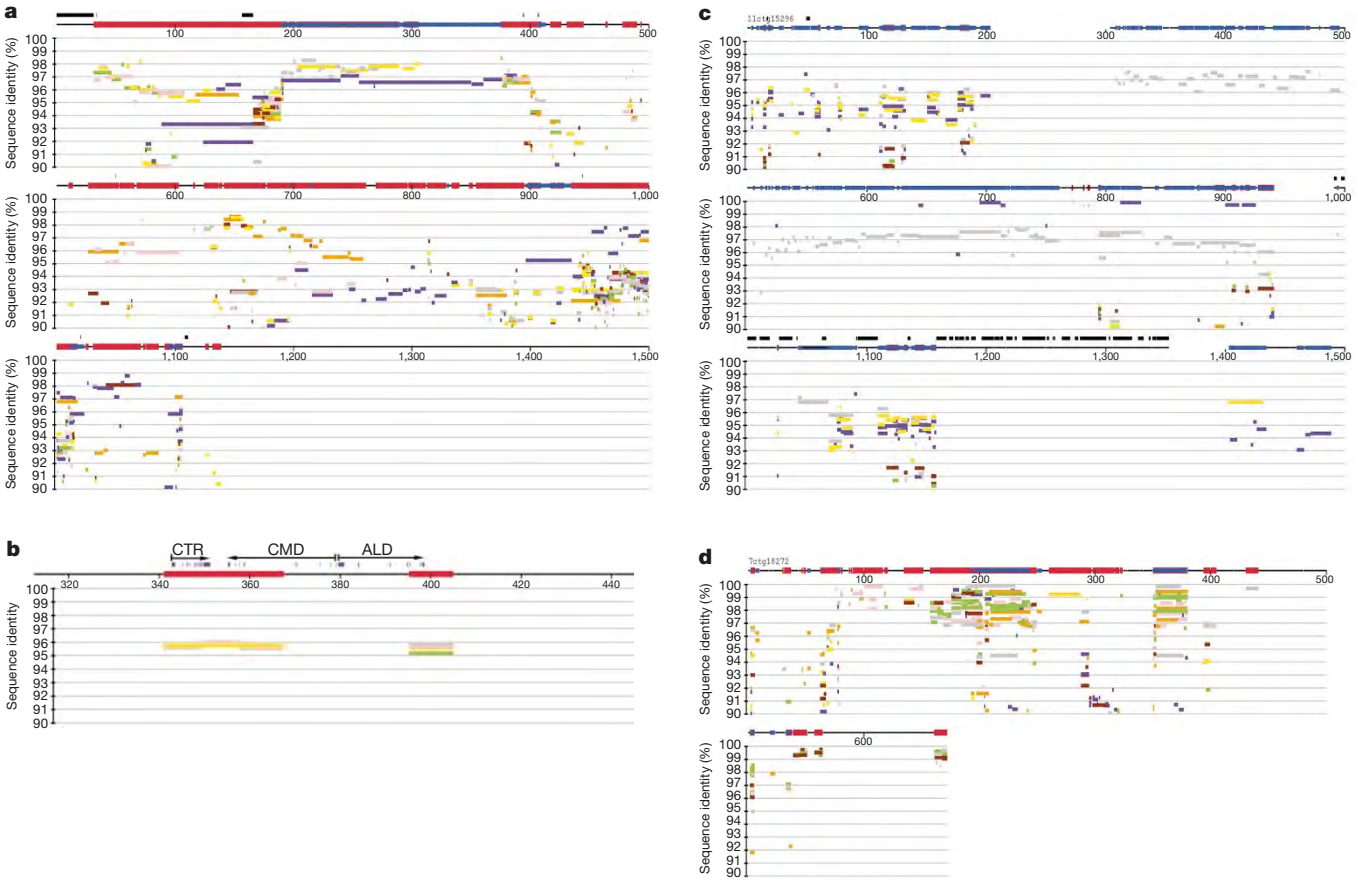

Figure 32 Mosaic patterns of duplications. Panels depict various patterns of duplication within the human genome (PARASIGHT). For each region, a segment of draft genome sequence (100–500 kb) is shown with both interchromosomal (red) and intrachromosomal (blue) duplications displayed along the horizontal line. Below the line, each separate sequence duplication is indicated (with a distinct colour) relative to per cent nucleotide identity for the duplicated segment (*y* axis). Black bars show the relative locations of large blocks of heterochromatic sequences (alpha, gamma and HSAT sequence). **a**, An active pericentromeric region on chromosome 21. **b**, An ancestral region from Xq28 that has contributed various 'genic' segments to pericentromeric regions. **c**, A pericentromeric

© 2001 Macmillan Magazines Ltd

The pericentromeric regions are structurally very complex, as illustrated for chromosome 21 in Fig. 32a. The pericentromeric regions appear to have been bombarded by successive insertions of duplications; the insertion events must be fairly recent because the degree of sequence conservation with the genomic source loci is fairly high (90–100%, with an apparent peak around 96%). Distinct insertions are typically separated by AT-rich or GC-rich minisatellite-like repeats that have been hypothesized to have a functional role in targeting duplications to these regions[233,241].

A single genomic source locus often gives rise to pericentromeric copies on multiple chromosomes, with each having essentially the same breakpoints and the same degree of divergence. An example of such a source locus on Xq28 is shown in Fig. 32b. Phylogenetic analysis has suggested a two-step mechanism for the origin and dispersal of these segments, whereby an initial segmental duplication in the pericentromeric region of one chromosome occurs and is then redistributed as part of a larger cassette to other such regions[242].

A comprehensive analysis for all chromosomes will have to await complete sequencing of the genome, but the evidence from the draft genome sequence indicates that the same picture is likely to be seen throughout the genome. Several papers have analysed finished segments within pericentromeric regions of chromosomes 2 (160 kb), 10 (400 kb) and 16 (300 kb), all of which show extensive interchromosomal segmental duplication[215,219,232,233]. An example from another pericentromeric region on chromosome 11 is shown in Fig. 32c. Interchromosomal duplications in subtelomeric regions also appear to be a fairly general phenomenon, as illustrated by a large tract (~500 kb) of complex duplication on chromosome 7 (Fig. 32d).

The explanation for the clustering of segmental duplications may be that the genome has a damage-control mechanism whereby chromosomal breakage products are preferentially inserted into pericentromeric and, to a lesser extent, subtelomeric regions. The possibility of a specific mechanism for the insertion of these sequences has been suggested on the basis of the unusual sequences found flanking the insertions. Although it is also possible that these regions simply have greater tolerance for large insertions, many large gene-poor 'deserts' have been identified[93] and there is no accumulation of duplicated segments within these regions. Along with the fact that transitions between duplicons (from different regions of the genome) occur at specific sequences, this suggests that active recruitment of duplications to such regions may occur. In any case, the duplicated regions are in general young (with many duplications showing <6% nucleotide divergence from their source loci) and in constant flux, both through additional duplications and by large-scale exchange among similar chromosomal environments. There is evidence of structural polymorphism in the human population, such as the presence or absence of olfactory receptor segments located within the telomeric regions of several human chromosomes[226,227].

Genome-wide analysis of segmental duplications. We also performed a global genome-wide analysis to characterize the amount of segmental duplication in the genome. We 'repeat-masked' the known interspersed repeats in the draft genome sequence and compared the remaining draft genomic sequence with itself in a massive all-by-all BLASTN similarity search. We excluded matches in which the sequence identity was so high that it might reflect artefactual duplications resulting from a failure to overlap sequence contigs correctly in assembling the draft genome sequence. Specifically, we considered only matches with less than 99.5% identity for finished sequence and less than 98% identity for unfinished sequence.

We took several approaches to avoid counting artefactual duplications in the sequence. In the first approach, we studied only finished sequence. We compared the finished sequence with itself, to identify segments of at least 1 kb and 90–99.5% sequence identity. This analysis will underestimate the extent of segmental duplication, because it requires that at least two copies of the segment are present in the finished sequence and because some true duplications have over 99.5% identity.

The finished sequence consists of at least 3.3% segmental duplication (Table 16). Interchromosomal duplication accounts for about 1.5% and intrachromosomal duplication for about 2%, with some overlap (0.2%) between these categories. We analysed the lengths and divergence of the segmental duplications (Fig. 33). The duplications tend to be large (10–50 kb) and highly homologous, especially for the interchromosomal segments. The sequence divergence for the interchromosomal duplications appears to peak between 96.5% and 97.5%. This may indicate that interchromosomal duplications occurred in a punctuated manner. It will be intriguing to investigate whether such genomic upheaval has a role in speciation events.

In a second approach, we compared the entire human draft genome sequence (finished and unfinished) with itself to identify duplications with 90–98% sequence identity (Table 17). The draft genome sequence contains at least 3.6% segmental duplication. The actual proportion will be significantly higher, because we excluded many true matches with more than 98% sequence identity (at least 1.1% of the finished sequence). Although exact measurement must await a finished sequence, the human genome seems likely to contain about 5% segmental duplication, with most of this sequence in large blocks (> 10 kb). Such a high proportion of large duplications clearly distinguishes the human genome from other sequenced genomes, such as the fly and worm (Table 18).

The structure of large highly paralogous regions presents one of the 'serious and unanticipated challenges' to producing a finished sequence of the genome[46]. The absence of unique STS or fingerprint signatures over large genomic distances (~1 Mb) and the high degree of sequence similarity makes the distinction between paralogous sequence variation and allelic polymorphism problematic. Furthermore, the fact that such regions frequently harbour intron–exon structures of genuine unique sequence will complicate efforts to generate a genome-wide SNP map. The data indicate that a modest portion of the human genome may be relatively recalcitrant to genomic-based methods for SNP detection. Owing to their repetitive nature and their location in the genome, segmental

Table 16 Fraction of finished sequence in inter- and intrachromosomal duplications

Chromosome	Intrachromosomal (%)	Interchromosomal (%)	All (%)
1	1.4	0.5	1.9
2	0.1	0.6	0.7
3	0.3	1.1	1.1
4	0.0	1.0	1.0
5	0.6	0.3	0.9
6	0.8	0.4	1.1
7	3.4	1.3	4.1
8	0.3	0.1	0.3
9	0.8	2.9	3.7
10	2.1	0.8	2.9
11	1.2	2.1	2.3
12	1.5	0.3	1.8
13	0.0	0.5	0.5
14	0.6	0.4	1.0
15	3.0	6.9	6.9
16	4.5	2.0	5.8
17	1.6	0.3	1.8
18	0.0	0.7	0.7
19	3.6	0.3	3.8
20	0.2	0.3	0.5
21	1.4	1.6	3.0
22	6.1	2.6	7.5
X	1.8	3.2	5.0
Y	12.1	16.0	27.4
Un	0.0	0.5	0.5
Total	2.0	1.5	3.3

Excludes duplications with identities >99.5% to avoid artefactual duplication due to incomplete merger in the assembly process. Calculation was performed on the finished sequence available in September 2000 and reflects the duplications found within the total amount of finished sequence then. Note that there is some overlap between the interchromosomal and intrachromosomal sets.

© 2001 Macmillan Magazines Ltd

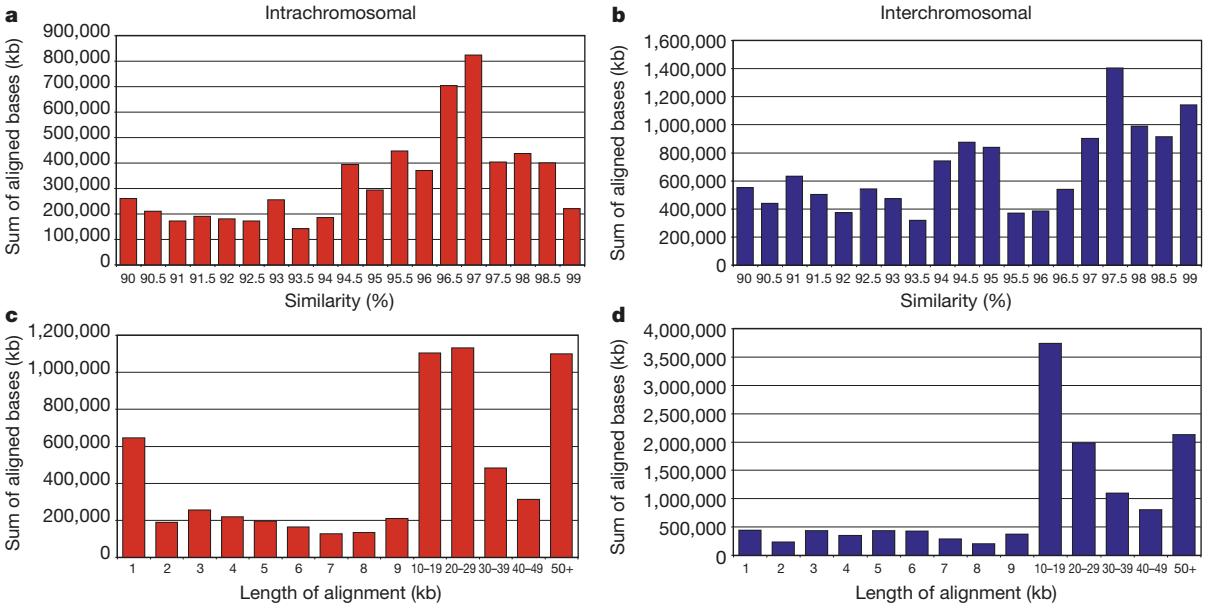

Figure 33 a–d, Sequence properties of segmental duplications. Distributions of length and per cent nucleotide identity for segmental duplications are shown as a function of the number of aligned bp, for the subset of finished genome sequence. Intrachromosomal, red; interchromosomal, blue.

duplications may well be underestimated by the current analysis. An understanding of the biology, pathology and evolution of these duplications will require specialized efforts within these exceptional regions of the human genome. The presence and distribution of such segments may provide evolutionary fodder for processes of exon shuffling and a general increase in protein diversity associated with domain accretion. It will be important to consider both genome-wide duplication events and more restricted punctuated events of genome duplication as forces in the evolution of vertebrate genomes.

Table 17 Fraction of the draft genome sequence in inter- and intrachromosomal duplications

Chromosome	Intrachromosomal (%)	Interchromosomal (%)	All (%)
1	2.1	1.7	3.4
2	1.6	1.6	2.6
3	1.8	1.4	2.7
4	1.5	2.2	3.0
5	1.0	0.9	1.8
6	1.5	1.4	2.7
7	3.6	1.8	4.5
8	1.2	1.5	2.1
9	2.1	2.3	3.8
10	3.3	2.0	4.7
11	2.7	1.4	3.7
12	2.1	1.2	2.8
13	1.7	1.6	3.0
14	0.6	0.6	1.2
15	4.1	4.4	6.7
16	3.4	3.4	5.5
17	4.4	1.7	5.7
18	0.9	1.0	1.9
19	5.4	1.6	6.3
20	0.8	1.4	2.0
21	1.9	4.0	4.8
22	6.8	7.7	11.9
X	1.2	1.1	2.2
Y	10.9	13.1	20.8
NA	2.3	7.8	8.3
UL	11.6	20.8	22.2
Total	2.3	2.0	3.6

Excludes duplications with identities >98% to avoid artefactual duplication due to incomplete merger in the assembly process. Calculation was performed on an earlier version of the draft genome sequence based on data available in July 2000 and reflects the duplications found within the total amount of finished sequence then. Note that there is some overlap between the interchromosomal and intrachromosomal sets.

Gene content of the human genome

Genes (or at least their coding regions) comprise only a tiny fraction of human DNA, but they represent the major biological function of the genome and the main focus of interest by biologists. They are also the most challenging feature to identify in the human genome sequence.

The ultimate goal is to compile a complete list of all human genes and their encoded proteins, to serve as a 'periodic table' for biomedical research[243]. But this is a difficult task. In organisms with small genomes, it is straightforward to identify most genes by the presence of long ORFs. In contrast, human genes tend to have small exons (encoding an average of only 50 codons) separated by long introns (some exceeding 10 kb). This creates a signal-to-noise problem, with the result that computer programs for direct gene prediction have only limited accuracy. Instead, computational prediction of human genes must rely largely on the availability of cDNA sequences or on sequence conservation with genes and proteins from other organisms. This approach is adequate for strongly conserved genes (such as histones or ubiquitin), but may be less sensitive to rapidly evolving genes (including many crucial to speciation, sex determination and fertilization).

Here we describe our efforts to recognize both the RNA genes and protein-coding genes in the human genome. We also study the properties of the predicted human protein set, attempting to discern how the human proteome differs from those of invertebrates such as worm and fly.

Noncoding RNAs

Although biologists often speak of a tight coupling between 'genes

Table 18 Cross-species comparison for large, highly homologous segmental duplications

	Percentage of genome (%)		
	Fly	Worm	Human (finished)*
> 1 kb	1.2	4.25	3.25
> 5 kb	0.37	1.50	2.86
> 10 kb	0.08	0.66	2.52

*This is an underestimate of the total amount of segmental duplication in the human genome because it only reflects duplication detectable with available finished sequence. The proportion of segmental duplications of > 1 kb is probably about 5% (see text).

© 2001 Macmillan Magazines Ltd

and their encoded protein products', it is important to remember that thousands of human genes produce noncoding RNAs (ncRNAs) as their ultimate product[244]. There are several major classes of ncRNA. (1) Transfer RNAs (tRNAs) are the adapters that translate the triplet nucleic acid code of RNA into the amino-acid sequence of proteins; (2) ribosomal RNAs (rRNAs) are also central to the translational machinery, and recent X-ray crystallography results strongly indicate that peptide bond formation is catalysed by rRNA, not protein[245,246]; (3) small nucleolar RNAs (snoRNAs) are required for rRNA processing and base modification in the nucleolus[247,248]; and (4) small nuclear RNAs (snRNAs) are critical components of spliceosomes, the large ribonucleoprotein (RNP) complexes that splice introns out of pre-mRNAs in the nucleus. Humans have both a major, U2 snRNA-dependent spliceosome that splices most introns, and a minor, U12 snRNA-dependent spliceosome that splices a rare class of introns that often have AT/AC dinucleotides at the splice sites instead of the canonical GT/AG splice site consensus[249].

Other ncRNAs include both RNAs of known biochemical function (such as telomerase RNA and the 7SL signal recognition particle RNA) and ncRNAs of enigmatic function (such as the large Xist transcript implicated in X dosage compensation[250], or the small vault RNAs found in the bizarre vault ribonucleoprotein complex[251], which is three times the mass of the ribosome but has unknown function).

ncRNAs do not have translated ORFs, are often small and are not polyadenylated. Accordingly, novel ncRNAs cannot readily be found by computational gene-finding techniques (which search for features such as ORFs) or experimental sequencing of cDNA or EST libraries (most of which are prepared by reverse transcription using a primer complementary to a poly(A) tail). Even if the complete finished sequence of the human genome were available, discovering novel ncRNAs would still be challenging. We can, however, identify genomic sequences that are homologous to known ncRNA genes, using BLASTN or, in some cases, more specialized methods.

It is sometimes difficult to tell whether such homologous genes are orthologues, paralogues or closely related pseudogenes (because inactivating mutations are much less obvious than for protein-coding genes). For tRNA, there is sufficiently detailed information about the cloverleaf secondary structure to allow true genes and pseudogenes to be distinguished with high sensitivity. For many other ncRNAs, there is much less structural information and so we employ an operational criterion of high sequence similarity (> 95% sequence identity and > 95% full length) to distinguish true genes from pseudogenes. These assignments will eventually need to be reconciled with experimental data.

Transfer RNA genes. The classical experimental estimate of the number of human tRNA genes is 1,310 (ref. 252). In the draft genome sequence, we find only 497 human tRNA genes (Tables 19, 20). How do we account for this discrepancy? We believe that the original estimate is likely to have been inflated in two respects. First, it came from a hybridization experiment that probably counted closely related pseudogenes; by analysis of the draft genome sequence, there are in fact 324 tRNA-derived putative pseudogenes (Table 20). Second, the earlier estimate assumed too high a value for the size of the human genome; repeating the calculation using the correct value yields an estimate of about 890 tRNA-related loci, which is in reasonable accord with our count of 821 tRNA genes and pseudogenes in the draft genome sequence.

Table 19 Number of tRNA genes in various organisms

Organism	Number of canonical tRNAs	SeCys tRNA
Human	497	1
Worm	584	1
Fly	284	1
Yeast	273	0
Methanococcus jannaschii	36	1
Escherichia coli	86	1

Number of tRNA genes in each of six genome sequences, according to analysis by the computer program tRNAscan-SE . Canonical tRNAs read one of the standard 61 sense codons; this category excludes pseudogenes, undetermined anticodons, putative supressors and selenocysteine tRNAs. Most organisms have a selenocysteine (SeCys) tRNA species, but some unicellular eukaryotes do not (such as the yeast *S. cerevisiae*).

The human tRNA gene set predicted from the draft genome sequence appears to include most of the known human tRNA species. The draft genome sequence contains 37 of 38 human tRNA species listed in a tRNA database[253], allowing for up to one mismatch. This includes one copy of the known gene for a specialized selenocysteine tRNA, one of several components of a baroque translational mechanism that reads UGA as a selenocysteine codon in certain rare mRNAs that carry a specific *cis*-acting RNA regulatory site (a so-called SECIS element) in their 3′ UTRs. The one tRNA gene in the database not found in the draft genome sequence is DE9990, a tRNAGlu species, which differs in two positions from the most related tRNA gene in the human genome. Possible explanations are that the database version of this tRNA contains two errors, the gene is polymorphic or this is a genuine functional tRNA that is missing from the draft genome sequence. (The database also lists one additional tRNA gene (*DS9994*), but this is apparently a contaminant, most similar to bacterial tRNAs; the parent entry (*Z13399*) was withdrawn from the DNA database, but the tRNA entry has not yet been removed from the tRNA database.) Although the human set appears substantially complete by this test, the tRNA gene numbers in Table 19 should be considered tentative and used with caution. The human and fly (but not the worm) are known to be missing significant amounts of heterochromatic DNA, and additional tRNA genes could be located there.

With this caveat, the results indicate that the human has fewer tRNA genes than the worm, but more than the fly. This may seem surprising, but tRNA gene number in metazoans is thought to be related not to organismal complexity, but more to idiosyncrasies of the demand for tRNA abundance in certain tissues or stages of embryonic development. For example, the frog *Xenopus laevis*, which must load each oocyte with a remarkable 40 ng of tRNA, has thousands of tRNA genes[254].

The degeneracy of the genetic code has allowed an inspired economy of tRNA anticodon usage. Although 61 sense codons need to be decoded, not all 61 different anticodons are present in tRNAs. Rather, tRNAs generally follow stereotyped and conserved wobble rules[255–257]. Wobble reduces the number of required anticodons substantially, and provides a connection between the genetic code and the hybridization stability of modified and unmodified RNA bases. In eukaryotes, the rules proposed by Guthrie and Abelson[256] predict that about 46 tRNA species will be sufficient to read the 61 sense codons (counting the initiator and elongator methionine tRNAs as two species). According to these rules, in the codon's third (wobble) position, U and C are generally decoded by a single tRNA species, whereas A and G are decoded by two separate tRNA species.

In 'two-codon boxes' of the genetic code (where codons ending with U/C encode a different amino acid from those ending with A/G), the U/C wobble position should be decoded by a G at position 34 in the tRNA anticodon. Thus, in the top left of Fig. 34, there is no tRNA with an AAA anticodon for Phe, but the GAA anticodon can recognize both UUU and UUC codons in the mRNA. In 'four-codon boxes' of the genetic code (where U, C, A and G in the wobble position all encode the same amino acid), the U/C wobble position is almost always decoded by I34 (inosine) in the tRNA, where the inosine is produced by post-transcriptional modification of an adenine (A). In the bottom left of Fig. 34, for example, the GUU and GUC codons of the four-codon Val box are decoded by a tRNA with an anticodon of AAC, which is no doubt modified to IAC. Presumably this pattern, which is strikingly conserved in eukaryotes, has to do with the fact that IA base pairs are also possible; thus

© 2001 Macmillan Magazines Ltd

the IAC anticodon for a Val tRNA could recognize GUU, GUC and even GUA codons. Were this same I34 to be utilized in two-codon boxes, however, misreading of the NNA codon would occur, resulting in translational havoc. Eukaryotic glycine tRNAs represent a conserved exception to this last rule; they use a GCC anticodon to decode GGU and GGC, rather than the expected ICC anticodon.

Satisfyingly, the human tRNA set follows these wobble rules almost perfectly (Fig. 34). Only three unexpected tRNA species are found: single genes for a tRNATyr-AUA, tRNAIle-GAU, and tRNAAsn-AUU. Perhaps these are pseudogenes, but they appear to be plausible tRNAs. We also checked the possibility of sequencing errors in their anticodons, but each of these three genes is in a region of high sequence accuracy, with PHRAP quality scores higher than 70 for every base in their anticodons.

As in all other organisms, human protein-coding genes show codon bias—preferential use of one synonymous codon over another[258] (Fig. 34). In less complex organisms, such as yeast or bacteria, highly expressed genes show the strongest codon bias. Cytoplasmic abundance of tRNA species is correlated with both codon bias and overall amino-acid frequency (for example, tRNAs for preferred codons and for more common amino acids are more abundant). This is presumably driven by selective pressure for efficient or accurate translation[259]. In many organisms, tRNA abundance in turn appears to be roughly correlated with tRNA gene copy number, so tRNA gene copy number has been used as a proxy for tRNA abundance[260]. In vertebrates, however, codon bias is not so obviously correlated with gene expression level. Differing codon biases between human genes is more a function of their location in regions of different GC composition[261]. In agreement with the literature, we see only a very rough correlation of human tRNA gene number with either amino-acid frequency or codon bias (Fig. 34). The most obvious outliers in these weak correlations are the strongly preferred CUG leucine codon, with a mere six tRNA-Leu-CAG genes producing a tRNA to decode it, and the relatively rare cysteine UGU and UGC codons, with 30 tRNA genes to decode them.

The tRNA genes are dispersed throughout the human genome. However, this dispersal is nonrandom. tRNA genes have sometimes been seen in clusters at small scales[262,263] but we can now see striking clustering on a genome-wide scale. More than 25% of the tRNA genes (140) are found in a region of only about 4 Mb on chromosome 6. This small region, only about 0.1% of the genome, contains an almost sufficient set of tRNA genes all by itself. The 140 tRNA genes contain a representative for 36 of the 49 anticodons found in the complete set; and of the 21 isoacceptor types, only tRNAs to decode Asn, Cys, Glu and selenocysteine are missing. Many of these tRNA genes, meanwhile, are clustered elsewhere; 18 of the 30 Cys tRNAs are found in a 0.5-Mb stretch of chromosome 7 and many of the Asn and Glu tRNA genes are loosely clustered on chromosome 1. More than half of the tRNA genes (280 out of 497) reside on either chromosome 1 or chromosome 6. Chromosomes 3, 4, 8, 9, 10, 12, 18, 20, 21 and X appear to have fewer than 10 tRNA genes each; and chromosomes 22 and Y have none at all (each has a single pseudogene).

Ribosomal RNA genes. The ribosome, the protein synthetic machine of the cell, is made up of two subunits and contains four rRNA species and many proteins. The large ribosomal subunit contains 28S and 5.8S rRNAs (collectively called 'large subunit' (LSU) rRNA) and also a 5S rRNA. The small ribosomal subunit contains 18S rRNA ('small subunit' (SSU) rRNA). The genes for LSU and SSU rRNA occur in the human genome as a 44-kb tandem repeat unit[264]. There are thought to be about 150–200 copies of this repeat unit arrayed on the short arms of acrocentric chromosomes 13, 14, 15, 21 and 22 (refs 254, 264). There are no true complete

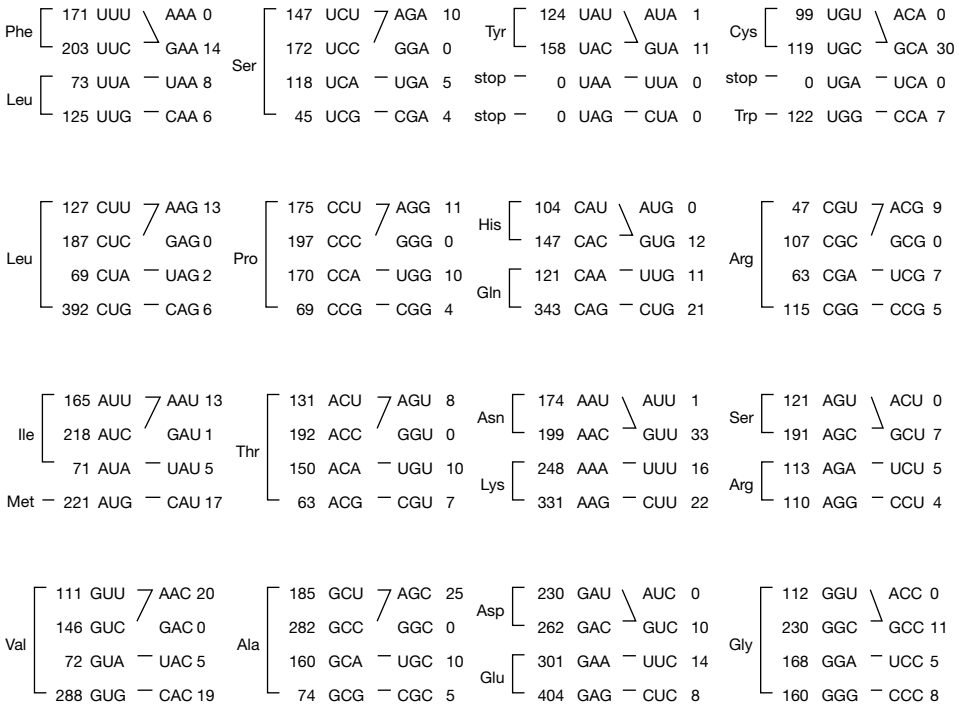

Figure 34 The human genetic code and associated tRNA genes. For each of the 64 codons, we show: the corresponding amino acid; the observed frequency of the codon per 10,000 codons; the codon; predicted wobble pairing to a tRNA anticodon (black lines); an unmodified tRNA anticodon sequence; and the number of tRNA genes found with this anticodon. For example, phenylalanine is encoded by UUU or UUC; UUC is seen more frequently, 203 to 171 occurrences per 10,000 total codons; both codons are expected to be decoded by a single tRNA anticodon type, GAA, using a G/U wobble; and there are 14 tRNA genes found with this anticodon. The modified anticodon sequence in the mature tRNA is not shown, even where post-transcriptional modifications can be confidently predicted (for example, when an A is used to decode a U/C third position, the A is almost certainly an inosine in the mature tRNA). The Figure also does not show the number of distinct tRNA species (such as distinct sequence families) for each anticodon; often there is more than one species for each anticodon.

© 2001 Macmillan Magazines Ltd

copies of the rDNA tandem repeats in the draft genome sequence, owing to the deliberate bias in the initial phase of the sequencing effort against sequencing BAC clones whose restriction fragment fingerprints showed them to contain primarily tandemly repeated sequence. Sequence similarity analysis with the BLASTN computer program does, however, detect hundreds of rDNA-derived sequence fragments dispersed throughout the complete genome, including one 'full-length' copy of an individual 5.8S rRNA gene not associated with a true tandem repeat unit (Table 20).

The 5S rDNA genes also occur in tandem arrays, the largest of which is on chromosome 1 between 1q41.11 and 1q42.13, close to the telomere[265,266]. There are 200–300 true 5S genes in these arrays[265,267]. The number of 5S-related sequences in the genome, including numerous dispersed pseudogenes, is classically cited as 2,000 (refs 252, 254). The long tandem array on chromosome 1 is not yet present in the draft genome sequence because there are no *Eco*RI or *Hin*dIII sites present, and thus it was not cloned in the most heavily utilized BAC libraries (Table 1). We expect to recover it during the finishing stage. We do detect four individual copies of 5S rDNA by our search criteria ($\geq$95% identity and $\geq$95% full length). We also find many more distantly related dispersed sequences (520 at $P \leq 0.001$), which we interpret as probable pseudogenes (Table 20).

Small nucleolar RNA genes. Eukaryotic rRNA is extensively processed and modified in the nucleolus. Much of this activity is directed by numerous snoRNAs. These come in two families: C/D box snoRNAs (mostly involved in guiding site-specific 2′-*O*-ribose methylations of other RNAs) and H/ACA snoRNAs (mostly involved in guiding site-specific pseudouridylations)[247,248]. We compiled a set of 97 known human snoRNA gene sequences; 84 of these (87%) have at least one copy in the draft genome sequence (Table 20), almost all as single-copy genes.

It is thought that all 2′-*O*-ribose methylations and pseudouridylations in eukaryotic rRNA are guided by snoRNAs. There are 105–107 methylations and around 95 pseudouridylations in human rRNA[268]. Only about half of these have been tentatively assigned to known guide snoRNAs. There are also snoRNA-directed modifications on other stable RNAs, such as U6 (ref. 269), and the extent of this is just beginning to be explored. Sequence similarity has so far proven insufficient to recognize all snoRNA genes. We therefore expect that there are many unrecognized snoRNA genes that are not detected by BLAST queries.

Spliceosomal RNAs and other ncRNA genes. We also looked for copies of other known ncRNA genes. We found at least one copy of 21 (95%) of 22 known ncRNAs, including the spliceosomal snRNAs. There were multiple copies for several ncRNAs, as expected; for example, we find 44 dispersed genes for U6 snRNA, and 16 for U1 snRNA (Table 20).

For some of these RNA genes, homogeneous multigene families that occur in tandem arrays are again under-represented owing to the restriction enzymes used in constructing the BAC libraries and, in some instances, the decision to delay the sequencing of BAC clones with low complexity fingerprints indicative of tandemly repeated DNA. The U2 RNA genes are located at the RNU2 locus, a tandem array of 10–20 copies of nearly identical 6.1-kb units at 17q21–q22 (refs 270–272). Similarly, the U3 snoRNA genes (included in the aggregate count of C/D snoRNAs in Table 20) are clustered at the RNU3 locus at 17p11.2, not in a tandem array, but in a complex inverted repeat structure of about 5–10 copies per haploid genome[273]. The U1 RNA genes are clustered with about 30 copies at the RNU1 locus at 1p36.1, but this cluster is thought to be loose and irregularly organized; no two U1 genes have been cloned on the same cosmid[271]. In the draft genome sequence, we see six copies of U2 RNA that meet our criteria for true genes, three of which appear to be in the expected position on chromosome 17. For U3, so far we see one true copy at the correct place on chromosome 17p11.2. For U1, we see 16 true genes, 6 of which are loosely clustered within 0.6 Mb at 1p36.1 and another 6 are elsewhere on chromosome 1. Again, these and other clusters will be a matter for the finishing process.

Table 20 Known non-coding RNA genes in the draft genome sequence

RNA gene*	Number expected†	Number found‡	Number of related genes§	Function
tRNA	1,310	497	324	Protein synthesis
SSU (18S) rRNA	150–200	0	40	Protein synthesis
5.8S rRNA	150–200	1	11	Protein synthesis
LSU (28S) rRNA	150–200	0	181	Protein synthesis
5S rRNA	200–300	4	520	Protein synthesis
U1	~30	16	134	Spliceosome component
U2	10–20	6	94	Spliceosome component
U4	??	4	87	Spliceosome component
U4atac	??	1	20	Component of minor (U11/U12) spliceosome
U5	??	1	31	Spliceosome component
U6	??	44	1,135	Spliceosome component
U6atac	??	4	32	Component of minor (U11/U12) spliceosome
U7	1	1	3	Histone mRNA 3′ processing
U11	1	0	6	Component of minor (U11/U12) spliceosome
U12	1	1	0	Component of minor (U11/U12) spliceosome
SRP (7SL) RNA	4	3	773	Component of signal recognition particle (protein secretion)
RNAse P	1	1	2	tRNA 5′ end processing
RNAse MRP	1	1	6	rRNA processing
Telomerase RNA	1	1	4	Template for addition of telomeres
hY1	1	1	353	Component of Ro RNP, function unknown
hY3	1	25	414	Component of Ro RNP, function unknown
hY4	1	3	115	Component of Ro RNP, function unknown
hY5 (4.5S RNA)	1	1	9	Component of Ro RNP, function unknown
Vault RNAs	3	3	1	Component of 13-MDa vault RNP, function unknown
7SK	1	1	330	Unknown
H19	1	1	2	Unknown
Xist	1	1	0	Initiation of X chromosome inactivation (dosage compensation)
Known C/D snoRNAs	81	69	558	Pre-rRNA processing or site-specific ribose methylation of rRNA
Known H/ACA snoRNAs	16	15	87	Pre-rRNA processing or site-specific pseudouridylation of rRNA

* Known ncRNA genes (or gene families, such as the C/D and H/ACA snoRNA families); reference sequences were extracted from GenBank and used to probe the draft genome sequence.
† Number of genes that were expected in the human genome, based on previous literature (note that earlier experimental techniques probably tend to overestimate copy number, by counting closely related pseudogenes).
‡ The copy number of 'true' full-length genes identified in the draft genome sequence.
§ The copy number of other significantly related copies (pseudogenes, fragments, paralogues) found. Except for the 497 true tRNA genes, all sequence similarities were identified by WashU BLASTN 2.0MP (W. Gish, unpublished; http://blast.wustl.edu), with parameters '-kap wordmask = seg B = 50000 W = 8' and the default +5/–4 DNA scoring matrix. True genes were operationally defined as BLAST hits with $\geq$95% identity over $\geq$95% of the length of the query. Related sequences were operationally defined as all other BLAST hits with *P*-values $\leq$0.001.

© 2001 Macmillan Magazines Ltd

Table 21 Characteristics of human genes

	Median	Mean	Sample (size)
Internal exon	122 bp	145 bp	RefSeq alignments to draft genome sequence, with confirmed intron boundaries (43,317 exons)
Exon number	7	8.8	RefSeq alignments to finished sequence (3,501 genes)
Introns	1,023 bp	3,365 bp	RefSeq alignments to finished sequence (27,238 introns)
3′ UTR	400 bp	770 bp	Confirmed by mRNA or EST on chromosome 22 (689)
5′ UTR	240 bp	300 bp	Confirmed by mRNA or EST on chromosome 22 (463)
Coding sequence	1,100 bp	1,340 bp	Selected RefSeq entries (1,804)
(CDS)	367 aa	447 aa	
Genomic extent	14 kb	27 kb	Selected RefSeq entries (1,804)

Median and mean values for a number of properties of human protein-coding genes. The 1,804 selected RefSeq entries were those that could be unambiguously aligned to finished sequence over their entire length.

Our observations also confirm the striking proliferation of ncRNA-derived pseudogenes (Table 20). There are hundreds or thousands of sequences in the draft genome sequence related to some of the ncRNA genes. The most prolific pseudogene counts generally come from RNA genes transcribed by RNA polymerase III promoters, including U6, the hY RNAs and SRP-RNA. These ncRNA pseudogenes presumably arise through reverse transcription. The frequency of such events gives insight into how ncRNA genes can evolve into SINE retroposons, such as the tRNA-derived SINEs found in many vertebrates and the SRP-RNA-derived Alu elements found in humans.

Protein-coding genes

Identifying the protein-coding genes in the human genome is one of the most important applications of the sequence data, but also one of the most difficult challenges. We describe below our efforts to create an initial human gene and protein index.

Exploring properties of known genes. Before attempting to identify new genes, we explored what could be learned by aligning the cDNA sequences of known genes to the draft genome sequence. Genomic alignments allow one to study exon–intron structure and local GC content, and are valuable for biomedical studies because they connect genes with the genetic and cytogenetic map, link them with regulatory sequences and facilitate the development of polymerase chain reaction (PCR) primers to amplify exons. Until now, genomic alignment was available for only about a quarter of known genes.

The 'known' genes studied were those in the RefSeq database[110], a manually curated collection designed to contain nonredundant representatives of most full-length human mRNA sequences in GenBank (RefSeq intentionally contains some alternative splice forms of the same genes). The version of RefSeq used contained 10,272 mRNAs.

The RefSeq genes were aligned with the draft genome sequence, using both the Spidey (S. Wheelan, personal communication) and Acembly (D. Thierry-Mieg and J. Thierry-Mieg, unpublished; http://www.acedb.org) computer programs. Because this sequence is incomplete and contains errors, not all genes could be fully aligned and some may have been incorrectly aligned. More than 92% of the RefSeq entries could be aligned at high stringency over at least part of their length, and 85% could be aligned over more than half of their length. Some genes (16%) had high stringency alignments to more than one location in the draft genome sequence owing, for example, to paralogues or pseudogenes. In such cases, we considered only the best match. In a few of these cases, the assignment may not be correct because the true matching region has not yet been sequenced. Three per cent of entries appeared to be alternative splice products of the same gene, on the basis of their alignment to the same location in the draft genome sequence. In all, we obtained at least partial genomic alignments for 9,212 distinct known genes and essentially complete alignment for 5,364 of them.

Previous efforts to study human gene structure[116,274,275] have been hampered by limited sample sizes and strong biases in favour of compact genes. Table 21 gives the mean and median values of some basic characteristics of gene structures. Some of the values may be underestimates. In particular, the UTRs given in the RefSeq database are likely to be incomplete; they are considerably shorter, for example, than those derived from careful reconstructions on chromosome 22. Intron sizes were measured only for genes in finished genomic sequence, to mitigate the bias arising from the fact that

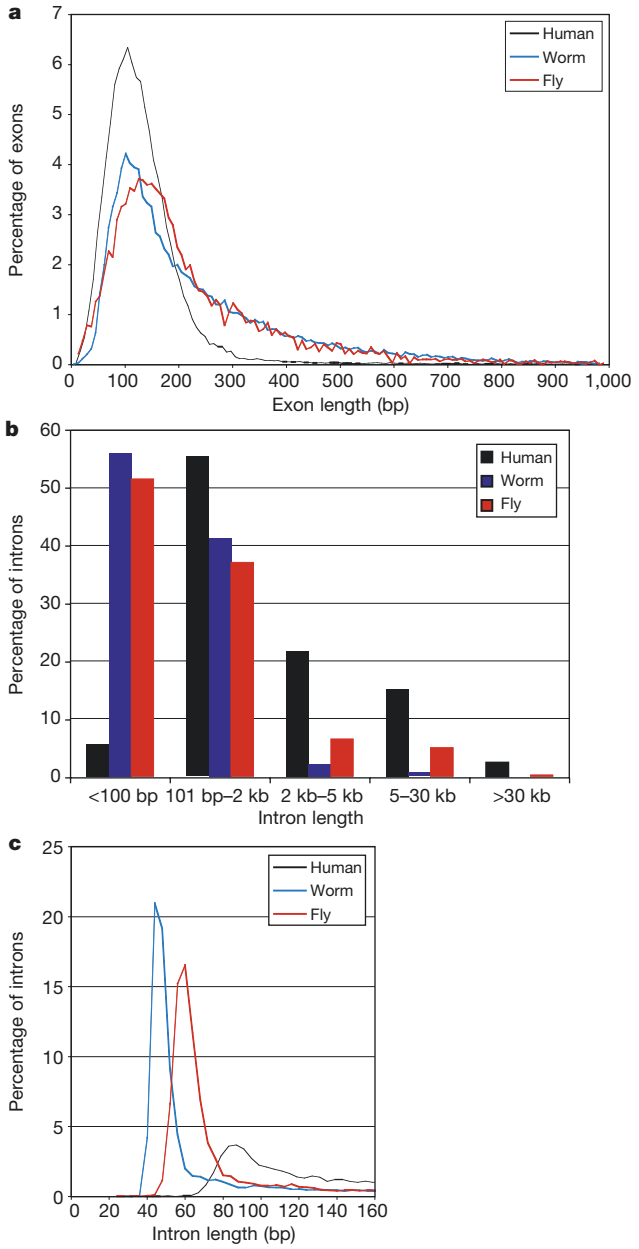

Figure 35 Size distributions of exons, introns and short introns, in sequenced genomes. **a**, Exons; **b**, introns; **c**, short introns (enlarged from **b**). Confirmed exons and introns for the human were taken from RefSeq alignments and for worm and fly from Acembly alignments of ESTs (J. and D. Thierry-Mieg and, for worm, Y. Kohara, unpublished).

© 2001 Macmillan Magazines Ltd

long introns are more likely than short introns to be interrupted by gaps in the draft genome sequence. Nonetheless, there may be some residual bias against long genes and long introns.

There is considerable variation in overall gene size and intron size, with both distributions having very long tails. Many genes are over 100 kb long, the largest known example being the dystrophin gene (DMD) at 2.4 Mb. The variation in the size distribution of coding sequences and exons is less extreme, although there are still some remarkable outliers. The titin gene[276] has the longest currently known coding sequence at 80,780 bp; it also has the largest number of exons (178) and longest single exon (17,106 bp).

It is instructive to compare the properties of human genes with those from worm and fly. For all three organisms, the typical length of a coding sequence is similar (1,311 bp for worm, 1,497 bp for fly and 1,340 bp for human), and most internal exons fall within a common peak between 50 and 200 bp (Fig. 35a). However, the worm and fly exon distributions have a fatter tail, resulting in a larger mean size for internal exons (218 bp for worm versus 145 bp for human). The conservation of preferred exon size across all three species supports suggestions of a conserved exon-based component of the splicing machinery[277]. Intriguingly, the few extremely short human exons show an unusual base composition. In 42 detected human exons of less than 19 bp, the nucleotide frequencies of A, G, T and C are 39, 33, 15 and 12%, respectively, showing a strong purine bias. Purine-rich sequences may enhance splicing[278,279], and it is possible that such sequences are required or strongly selected for to ensure correct splicing of very short exons. Previous studies have shown that short exons require intronic, but not exonic, splicing enhancers[280].

In contrast to the exons, the intron size distributions differ substantially among the three species (Fig. 35b, c). The worm and fly each have a reasonably tight distribution, with most introns near the preferred minimum intron length (47 bp for worm, 59 bp for fly) and an extended tail (overall average length of 267 bp for worm and 487 bp for fly). Intron size is much more variable in humans, with a peak at 87 bp but a very long tail resulting in a mean of more than 3,300 bp. The variation in intron size results in great variation in gene size.

The variation in gene size and intron size can partly be explained by the fact that GC-rich regions tend to be gene-dense with many compact genes, whereas AT-rich regions tend to be gene-poor with many sprawling genes containing large introns. The correlation of gene density with GC content is shown in Fig. 36a, b; the relative density increases more than tenfold as GC content increases from

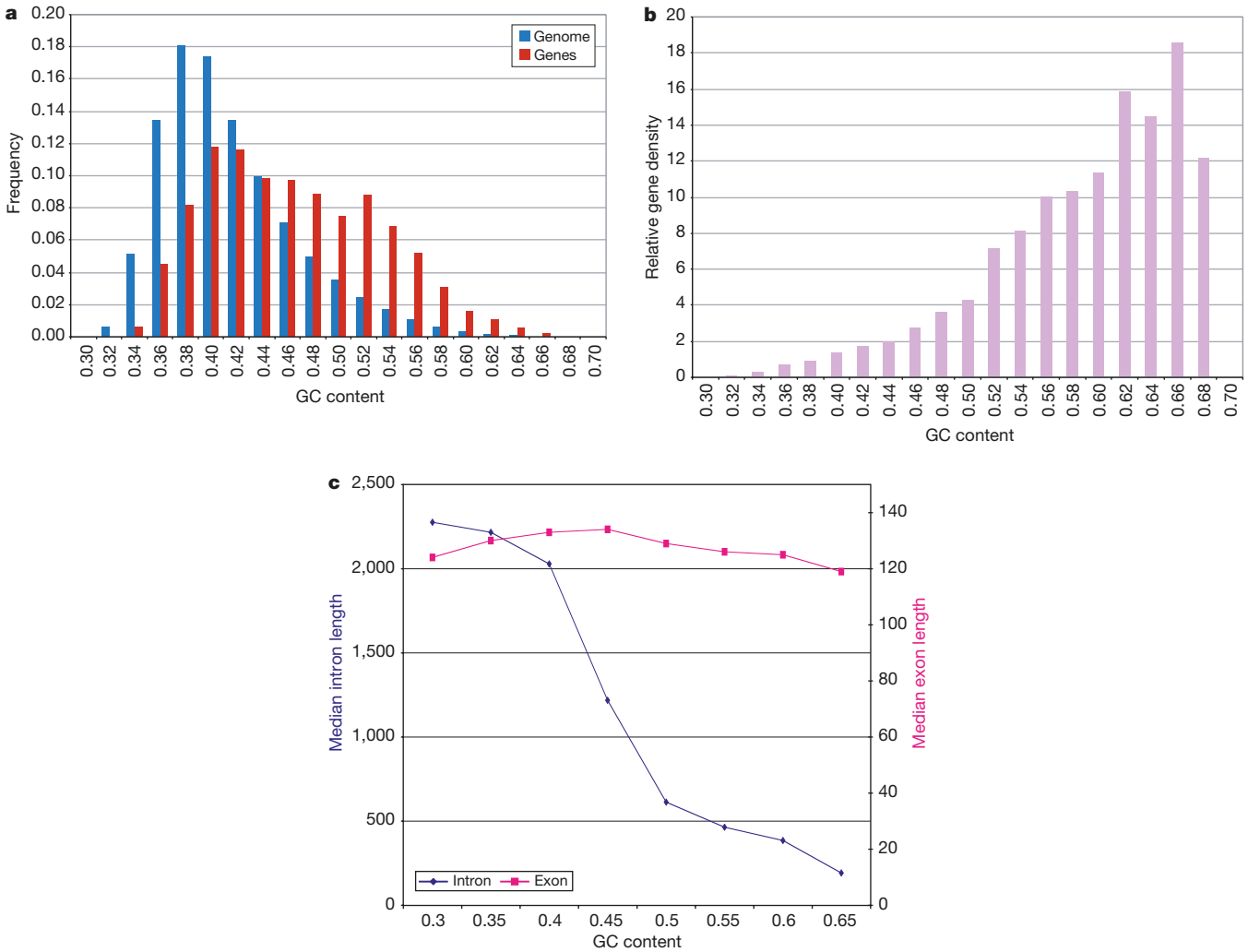

Figure 36 GC content. **a**, Distribution of GC content in genes and in the genome. For 9,315 known genes mapped to the draft genome sequence, the local GC content was calculated in a window covering either the whole alignment or 20,000 bp centred around the midpoint of the alignment, whichever was larger. Ns in the sequence were not counted. GC content for the genome was calculated for adjacent nonoverlapping 20,000-bp windows across the sequence. Both the gene and genome distributions have been normalized to sum to one. **b**, Gene density as a function of GC content, obtained by taking the ratio of the data in **a**. Values are less accurate at higher GC levels because the denominator is small. **c**, Dependence of mean exon and intron lengths on GC content. For exons and introns, the local GC content was derived from alignments to finished sequence only, and were calculated from windows covering the feature or 10,000 bp centred on the feature, whichever was larger.

© 2001 Macmillan Magazines Ltd

30% to 50%. The correlation appears to be due primarily to intron size, which drops markedly with increasing GC content (Fig. 36c). In contrast, coding properties such as exon length (Fig. 36c) or exon number (data not shown) vary little. Intergenic distance is also probably lower in high-GC areas, although this is hard to prove directly until all genes have been identified.

The large number of confirmed human introns allows us to analyse variant splice sites, confirming and extending recent reports[281]. Intron positions were confirmed by applying a stringent criterion that EST or mRNA sequence show an exact match of 8 bp in the flanking exonic sequence on each side. Of 53,295 confirmed introns, 98.12% use the canonical dinucleotides GT at the 5′ splice site and AG at the 3′ site (GT–AG pattern). Another 0.76% use the related GC–AG. About 0.10% use AT–AC, which is a rare alternative pattern primarily recognized by the variant U12 splicing machinery[282]. The remaining 1% belong to 177 types, some of which undoubtedly reflect sequencing or alignment errors.

Finally, we looked at alternative splicing of human genes. Alternative splicing can allow many proteins to be produced from a single gene and can be used for complex gene regulation. It appears to be prevalent in humans, with lower estimates of about 35% of human genes being subject to alternative splicing[283–285]. These studies may have underestimated the prevalence of alternative splicing, because they examined only EST alignments covering only a portion of a gene.

To investigate the prevalence of alternative splicing, we analysed reconstructed mRNA transcripts covering the entire coding regions of genes on chromosome 22 (omitting small genes with coding regions of less than 240 bp). Potential transcripts identified by alignments of ESTs and cDNAs to genomic sequence were verified by human inspection. We found 642 transcripts, covering 245 genes (average of 2.6 distinct transcripts per gene). Two or more alternatively spliced transcripts were found for 145 (59%) of these genes. A similar analysis for the gene-rich chromosome 19 gave 1,859 transcripts, corresponding to 544 genes (average 3.2 distinct transcripts per gene). Because we are sampling only a subset of all transcripts, the true extent of alternative splicing is likely to be greater. These figures are considerably higher than those for worm, in which analysis reveals alternative splicing for 22% of genes for which ESTs have been found, with an average of 1.34 (12,816/9,516) splice variants per gene. (The apparently higher extent of alternative splicing seen in human than in worm was not an artefact resulting from much deeper coverage of human genes by ESTs and mRNAs. Although there are many times more ESTs available for human than worm, these ESTs tend to have shorter average length (because many were the product of early sequencing efforts) and many match no human genes. We calculated the actual coverage per bp used in the analysis of the human and worm genes; the coverage is only modestly higher (about 50%) for the human, with a strong bias towards 3′ UTRs which tend to show much less alternative splicing. We also repeated the analysis using equal coverage for the two organisms and confirmed that higher levels of alternative splicing were still seen in human.)

Seventy per cent of alternative splice forms found in the genes on chromosomes 19 and 22 affect the coding sequence, rather than merely changing the 3′ or 5′ UTR. (This estimate may be affected by the incomplete representation of UTRs in the RefSeq database and in the transcripts studied.) Alternative splicing of the terminal exon was seen for 20% of 6,105 mRNAs that were aligned to the draft genome sequence and correspond to confirmed 3′ EST clusters. In addition to alternative splicing, we found evidence of the terminal exon employing alternative polyadenylation sites (separated by >100 bp) in 24% of cases.

Towards a complete index of human genes. We next focused on creating an initial index of human genes and proteins. This index is quite incomplete, owing to the difficulty of gene identification in human DNA and the imperfect state of the draft genome sequence. Nonetheless, it is valuable for experimental studies and provides important insights into the nature of human genes and proteins.

The challenge of identifying genes from genomic sequence varies greatly among organisms. Gene identification is almost trivial in bacteria and yeast, because the absence of introns in bacteria and their paucity in yeast means that most genes can be readily recognized by *ab initio* analysis as unusually long ORFs. It is not as simple, but still relatively straightforward, to identify genes in animals with small genomes and small introns, such as worm and fly. A major factor is the high signal-to-noise ratio—coding sequences comprise a large proportion of the genome and a large proportion of each gene (about 50% for worm and fly), and exons are relatively large.

Gene identification is more difficult in human DNA. The signal-to-noise ratio is lower: coding sequences comprise only a few per cent of the genome and an average of about 5% of each gene; internal exons are smaller than in worms; and genes appear to have more alternative splicing. The challenge is underscored by the work on human chromosomes 21 and 22. Even with the availability of finished sequence and intensive experimental work, the gene content remains uncertain, with upper and lower estimates differing by as much as 30%. The initial report of the finished sequence of chromosome 22 (ref. 94) identified 247 previously known genes, 298 predicted genes confirmed by sequence homology or ESTs and 325 *ab initio* predictions without additional support. Many of the confirmed predictions represented partial genes. In the past year, 440 additional exons (10%) have been added to existing gene annotations by the chromosome 22 annotation group, although the number of confirmed genes has increased by only 17 and some previously identified gene predictions have been merged[286].

Before discussing the gene predictions for the human genome, it is useful to consider background issues, including previous estimates of the number of human genes, lessons learned from worms and flies and the representativeness of currently 'known' human genes.

Previous estimates of human gene number. Although direct enumeration of human genes is only now becoming possible with the advent of the draft genome sequence, there have been many attempts in the past quarter of a century to estimate the number of genes indirectly. Early estimates based on reassociation kinetics estimated the mRNA complexity of typical vertebrate tissues to be 10,000–20,000, and were extrapolated to suggest around 40,000 for the entire genome[287]. In the mid-1980s, Gilbert suggested that there might be about 100,000 genes, based on the approximate ratio of the size of a typical gene ($\sim 3\times10^4$ bp) to the size of the genome (3×10^9 bp). Although this was intended only as a back-of-the-envelope estimate, the pleasing roundness of the figure seems to have led to it being widely quoted and adopted in many textbooks. (W. Gilbert, personal communication; ref. 288). An estimate of 70,000–80,000 genes was made by extrapolating from the number of CpG islands and the frequency of their association with known genes[129].

As human sequence information has accumulated, it has been possible to derive estimates on the basis of sampling techniques[289]. Such studies have sought to extrapolate from various types of data, including ESTs, mRNAs from known genes, cross-species genome comparisons and analysis of finished chromosomes. Estimates based on ESTs[290] have varied widely, from 35,000 (ref. 130) to 120,000 genes[291]. Some of the discrepancy lies in differing estimates of the amount of contaminating genomic sequence in the EST collection and the extent to which multiple distinct ESTs correspond to a single gene. The most rigorous analyses[130] exclude as spurious any ESTs that appear only once in the data set and carefully calibrate sensitivity and specificity. Such calculations consistently produce low estimates, in the region of 35,000.

Comparison of whole-genome shotgun sequence from the pufferfish *T. nigroviridis* with the human genome[292] can be used to estimate the density of exons (detected as conserved sequences

© 2001 Macmillan Magazines Ltd

between fish and human). These analyses also suggest around 30,000 human genes.

Extrapolations have also been made from the gene counts for chromosomes 21 and 22 (refs 93, 94), adjusted for differences in gene densities on these chromosomes, as inferred from EST mapping. These estimates are between 30,500 and 35,500, depending on the precise assumptions used[286].

Insights from invertebrates. The worm and fly genomes contain a large proportion of novel genes (around 50% of worm genes and 30% of fly genes), in the sense of showing no significant similarity to organisms outside their phylum[293–295]. Such genes may have been present in the original eukaryotic ancestor, but were subsequently lost from the lineages of the other eukaryotes for which sequence is available; they may be rapidly diverging genes, so that it is difficult to recognize homologues solely on the basis of sequence; they may represent true innovations developed within the lineage; or they may represent acquisitions by horizontal transfer. Whatever their origin, these genes tend to have different biological properties from highly conserved genes. In particular, they tend to have low expression levels as assayed both by direct studies and by a paucity of corresponding ESTs, and are less likely to produce a visible phenotype in loss-of-function genetic experiments[294,296].

Gene prediction. Current gene prediction methods employ combinations of three basic approaches: direct evidence of transcription provided by ESTs or mRNAs[297–299]; indirect evidence based on sequence similarity to previously identified genes and proteins[300,301]; and *ab initio* recognition of groups of exons on the basis of hidden Markov models (HMMs) that combine statistical information about splice sites, coding bias and exon and intron lengths (for example, Genscan[275], Genie[302,303] and FGENES[304]).

The first approach relies on direct experimental data, but is subject to artefacts arising from contaminating ESTs derived from unspliced mRNAs, genomic DNA contamination and nongenic transcription (for example, from the promoter of a transposable element). The first two problems can be mitigated by comparing transcripts with the genomic sequence and using only those that show clear evidence of splicing. This solution, however, tends to discard evidence from genes with long terminal exons or single exons. The second approach tends correctly to identify gene-derived sequences, although some of these may be pseudogenes. However, it obviously cannot identify truly novel genes that have no sequence similarity to known genes. The third approach would suffice alone if one could accurately define the features used by cells for gene recognition, but our current understanding is insufficient to do so. The sensitivity and specificity of *ab initio* predictions are greatly affected by the signal-to-noise ratio. Such methods are more accurate in the fly and worm than in human. In fly, *ab initio* methods can correctly predict around 90% of individual exons and can correctly predict all coding exons of a gene in about 40% of cases[303]. For human, the comparable figures are only about 70% and 20%, respectively[94,305]. These estimates may be optimistic, owing to the design of the tests used.

In any collection of gene predictions, we can expect to see various errors. Some gene predictions may represent partial genes, because of inability to detect some portions of a gene (incomplete sensitivity) or to connect all the components of a gene (fragmentation); some may be gene fusions; and others may be spurious predictions (incomplete specificity) resulting from chance matches or pseudogenes.

Creating an initial gene index. We set out to create an initial integrated gene index (IGI) and an associated integrated protein index (IPI) for the human genome. We describe the results obtained from a version of the draft genome sequence based on the sequence data available in July 2000, to allow time for detailed analysis of the gene and protein content. The additional sequence data that has since become available will affect the results quantitatively, but are unlikely to change the conclusions qualitatively.

We began with predictions produced by the Ensembl system[306]. Ensembl starts with *ab initio* predictions produced by Genscan[275] and then attempts to confirm them by virtue of similarity to proteins, mRNAs, ESTs and protein motifs (contained in the Pfam database[307]) from any organism. In particular, it confirms introns if they are bridged by matches and exons if they are flanked by confirmed introns. It then attempts to extend protein matches using the GeneWise computer program[308]. Because it requires confirmatory evidence to support each gene component, it frequently produces partial gene predictions. In addition, when there is evidence of alternative splicing, it reports multiple overlapping transcripts. In total, Ensembl produced 35,500 gene predictions with 44,860 transcripts.

To reduce fragmentation, we next merged Ensembl-based gene predictions with overlapping gene predictions from another program, Genie[302]. Genie starts with mRNA or EST matches and employs an HMM to extend these matches by using *ab initio* statistical approaches. To avoid fragmentation, it attempts to link information from 5′ and 3′ ESTs from the same cDNA clone and thereby to produce a complete coding sequence from an initial ATG to a stop codon. As a result, it may generate complete genes more accurately than Ensembl in cases where there is extensive EST support. (Genie also generates potential alternative transcripts, but we used only the longest transcript in each group.) We merged 15,437 Ensembl predictions into 9,526 clusters, and the longest transcript in each cluster (from either Genie or Ensembl) was taken as the representative.

Next, we merged these results with known genes contained in the RefSeq (version of 29 September 2000), SWISSPROT (release 39.6 of 30 August 2000) and TrEMBL databases (TrEMBL release 14.17 of 1 October 2000, TrEMBL_new of 1 October 2000). Incorporating these sequences gave rise to overlapping sequences because of alternative splice forms and partial sequences. To construct a nonredundant set, we selected the longest sequence from each overlapping set by using direct protein comparison and by mapping the gene predictions back onto the genome to construct the overlapping sets. This may occasionally remove some close paralogues in the event that the correct genomic location has not yet been sequenced, but this number is expected to be small.

Finally, we searched the set to eliminate any genes derived from contaminating bacterial sequences, recognized by virtue of near identity to known bacterial plasmids, transposons and chromosomal genes. Although most instances of such contamination had been removed in the assembly process, a few cases had slipped through and were removed at this stage.

The process resulted in version 1 of the IGI (IGI.1). The composition of the corresponding IPI.1 protein set, obtained by translating IGI.1, is given in Table 22. There are 31,778 protein predictions, with 14,882 from known genes, 4,057 predictions from Ensembl merged with Genie and 12,839 predictions from Ensembl alone. The average lengths are 469 amino acids for the known proteins, 443 amino acids for protein predictions from the Ensembl–Genie merge, and 187 amino acids for those from Ensembl alone. (The smaller average size for the predictions from Ensembl alone reflects its tendency to predict partial genes where there is supporting evidence for only part of the gene; the remainder of the gene will often not be predicted at all, rather than included as part of another prediction. Accordingly, the smaller size cannot be used to estimate the rate of fragmentation in such predictions.)

The set corresponds to fewer than 31,000 actual genes, because some genes are fragmented into more than one partial prediction and some predictions may be spurious or correspond to pseudogenes. As discussed below, our best estimate is that IGI.1 includes about 24,500 true genes.

Evaluation of IGI/IPI. We used several approaches to evaluate the sensitivity, specificity and fragmentation of the IGI/IPI set.

Comparison with 'new' known genes. One approach was to examine

© 2001 Macmillan Magazines Ltd

Table 22 Properties of the IGI/IPI human protein set

Source	Number	Average length (amino acids)	Matches to nonhuman proteins	Matches to RIKEN mouse cDNA set	Matches to RIKEN mouse cDNA set but not to nonhuman proteins
RefSeq/SwissProt/TrEMBL	14,882	469	12,708 (85%)	11,599 (78%)	776 (36%)
Ensembl–Genie	4,057	443	2,989 (74%)	3,016 (74%)	498 (47%)
Ensembl	12,839	187	81,126 (63%)	7,372 (57%)	1,449 (31%)
Total	31,778	352	23,813 (75%)	219,873 (69%)	2,723 (34%)

The matches to nonhuman proteins were obtained by using Smith-Waterman sequence alignment with an *E*-value threshold of 10^{-3} and the matches to the RIKEN mouse cDNAs by using TBLASTN with an *E*-value threshold of 10^{-6}. The last column shows that a significant number of the IGI members that do not have nonhuman protein matches do match sequences in the RIKEN mouse cDNA set, suggesting that both the IGI and the RIKEN sets contain a significant number of novel proteins.

newly discovered genes arising from independent work that were not used in our gene prediction effort. We identified 31 such genes: 22 recent entries to RefSeq and 9 from the Sanger Centre's gene identification program on chromosome X. Of these, 28 were contained in the draft genome sequence and 19 were represented in the IGI/IPI. This suggests that the gene prediction process has a sensitivity of about 68% (19/28) for the detection of novel genes in the draft genome sequence and that the current IGI contains about 61% (19/31) of novel genes in the human genome. On average, 79% of each gene was detected. The extent of fragmentation could also be estimated: 14 of the genes corresponded to a single prediction in the IGI/IPI, three genes corresponded to two predictions, one gene to three predictions and one gene to four predictions. This corresponds to a fragmentation rate of about 1.4 gene predictions per true gene.

Comparison with RIKEN mouse cDNAs. In a less direct but larger-scale approach, we compared the IGI gene set to a set of mouse cDNAs sequenced by the Genome Exploration Group of the RIKEN Genomic Sciences Center[309]. This set of 15,294 cDNAs, subjected to full-insert sequencing, was enriched for novel genes by selecting cDNAs with novel 3′ ends from a collection of nearly one million ESTs from diverse tissues and developmental timepoints. We determined the proportion of the RIKEN cDNAs that showed sequence similarity to the draft genome sequence and the proportion that showed sequence similarity to the IGI/IPI. Around 81% of the genes in the RIKEN mouse set showed sequence similarity to the human genome sequence, whereas 69% showed sequence similarity to the IGI/IPI. This suggests a sensitivity of 85% (69/81). This is higher than the sensitivity estimate above, perhaps because some of the matches may be due to paralogues rather than orthologues. It is consistent with the IGI/IPI representing a substantial fraction of the human proteome.

Conversely, 69% (22,013/31,898) of the IGI matches the RIKEN cDNA set. Table 22 shows the breakdown of these matches among the different components of the IGI. This is lower than the proportion of matches among known proteins, although this is expected because known proteins tend to be more highly conserved (see above) and because the predictions are on average shorter than known proteins. Table 22 also shows the numbers of matches to the RIKEN cDNAs among IGI members that do not match known proteins. The results indicate that both the IGI and the RIKEN set contain a significant number of genes that are novel in the sense of not having known protein homologues.

Comparison with genes on chromosome 22. We also compared the IGI/IPI with the gene annotations on chromosome 22, to assess the proportion of gene predictions corresponding to pseudogenes and to estimate the rate of overprediction. We compared 477 IGI gene predictions to 539 confirmed genes and 133 pseudogenes on chromosome 22 (with the immunoglobulin lambda locus excluded owing to its highly atypical gene structure). Of these, 43 hit 36 annotated pseudogenes. This suggests that 9% of the IGI predictions may correspond to pseudogenes and also suggests a fragmentation rate of 1.2 gene predictions per gene. Of the remaining hits, 63 did not overlap with any current annotations. This would suggest a rate of spurious predictions of about 13% (63/477), although the true rate is likely to be much lower because many of these may correspond to unannotated portions of existing gene predictions or to currently unannotated genes (of which there are estimated to be about 100 on this chromosome[94]).

Chromosomal distribution. Finally, we examined the chromosomal distribution of the IGI gene set. The average density of gene predictions is 11.1 per Mb across the genome, with the extremes being chromosome 19 at 26.8 per Mb and chromosome Y at 6.4 per Mb. It is likely that a significant number of the predictions on chromosome Y are pseudogenes (this chromosome is known to be rich in pseudogenes) and thus that the density for chromosome Y is an overestimate. The density of both genes and Alus on chromosome 19 is much higher than expected, even accounting for the high GC content of the chromosome; this supports the idea that Alu density is more closely correlated with gene density than with GC content itself.

Summary. We are clearly still some way from having a complete set of human genes. The current IGI contains significant numbers of partial genes, fragmented and fused genes, pseudogenes and spurious predictions, and it also lacks significant numbers of true genes. This reflects the current state of gene prediction methods in vertebrates even in finished sequence, as well as the additional challenges related to the current state of the draft genome sequence. Nonetheless, the gene predictions provide a valuable starting point for a wide range of biological studies and will be rapidly refined in the coming year.

The analysis above allows us to estimate the number of distinct genes in the IGI, as well as the number of genes in the human genome. The IGI set contains about 15,000 known genes and about 17,000 gene predictions. Assuming that the gene predictions are subject to a rate of overprediction (spurious predictions and pseudogenes) of 20% and a rate of fragmentation of 1.4, the IGI would be estimated to contain about 24,500 actual human genes. Assuming that the gene predictions contain about 60% of previously unknown human genes, the total number of genes in the human genome would be estimated to be about 31,000. This is consistent with most recent estimates based on sampling, which suggest a gene number of 30,000–35,000. If there are 30,000–35,000 genes, with an average coding length of about 1,400 bp and average genomic extent of about 30 kb, then about 1.5% of the human genome would consist of coding sequence and one-third of the genome would be transcribed in genes.

The IGI/IPI was constructed primarily on the basis of gene predictions from Ensembl. However, we also generated an expanded set (IGI+) by including additional predictions from two other gene prediction programs, Genie and GenomeScan (C. Burge, personal communication). These predictions were not included in the core IGI set, because of the concern that each additional set will provide diminishing returns in identifying true genes while contributing its own false positives (increased sensitivity at the expense of specificity). Genie produced an additional 2,837 gene predictions not overlapping the IGI, and GenomeScan produced 6,534 such gene predictions. If all of these gene predictions were included in the IGI, the number of the 31 new 'known' genes (see above) contained in the IGI would rise from 19 to 24. This would amount to an increase of about 26% in sensitivity, at the expense of increasing the number of predicted genes (excluding knowns) by 55%. Allowing a higher

© 2001 Macmillan Magazines Ltd

overprediction rate of 30% for gene predictions in this expanded set, the analysis above suggests that IGI+ set contains about 28,000 true genes and yields an estimate of about 32,000 human genes. We are investigating ways to filter the expanded set, to produce an IGI with the advantage of the increased sensitivity resulting from combining multiple gene prediction programs without the corresponding loss of specificity. Meanwhile, the IGI+ set can be used by researchers searching for genes that cannot be found in the IGI.

Some classes of genes may have been missed by all of the gene-finding methods. Genes could be missed if they are expressed at low levels or in rare tissues (being absent or very under-represented in EST and mRNA databases) and have sequences that evolve rapidly (being hard to detect by protein homology and genome comparison). Both the worm and fly gene sets contain a substantial number of such genes[293,294]. Single-exon genes encoding small proteins may also have been missed, because EST evidence that supports them cannot be distinguished from genomic contamination in the EST dataset and because homology may be hard to detect for small proteins[310].

The human thus appears to have only about twice as many genes as worm or fly. However, human genes differ in important respects from those in worm and fly. They are spread out over much larger regions of genomic DNA, and they are used to construct more alternative transcripts. This may result in perhaps five times as many primary protein products in the human as in the worm or fly.

The predicted gene and protein sets described here are clearly far from final. Nonetheless, they provide a valuable starting point for experimental and computational research. The predictions will improve progressively as the sequence is finished, as further confirmatory evidence becomes available (particularly from other vertebrate genome sequences, such as those of mouse and *T. nigroviridis*), and as computational methods improve. We intend to create and release updated versions of the IGI and IPI regularly, until they converge to a final accurate list of every human gene. The gene predictions will be linked to RefSeq, HUGO and SWISSPROT identifiers where available, and tracking identifiers between versions will be included, so that individual genes under study can be traced forwards as the human sequence is completed.

Comparative proteome analysis

Knowledge of the human proteome will provide unprecedented opportunities for studies of human gene function. Often clues will be provided by sequence similarity with proteins of known function in model organisms. Such initial observations must then be followed up by detailed studies to establish the actual function of these molecules in humans.

For example, 35 proteins are known to be involved in the vacuolar protein-sorting machinery in yeast. Human genes encoding homologues can be found in the draft human sequence for 34 of these yeast proteins, but precise relationships are not always clear. In nine cases there appears to be a single clear human orthologue (a gene that arose as a consequence of speciation); in 12 cases there are matches to a family of human paralogues (genes that arose owing to intra-genome duplication); and in 13 cases there are matches to specific protein domains[311–314]. Hundreds of similar stories emerge from the draft sequence, but each merits a detailed interpretation in context. To treat these subjects properly, there will be many following studies, the first of which appear in accompanying papers[315–323].

Here, we aim to take a more global perspective on the content of the human proteome by comparing it with the proteomes of yeast, worm, fly and mustard weed. Such comparisons shed useful light on the commonalities and differences among these eukaryotes[294,324,325]. The analysis is necessarily preliminary, because of the imperfect nature of the human sequence, uncertainties in the gene and protein sets for all of the multicellular organisms considered and our incomplete knowledge of protein structures. Nonetheless, some general patterns emerge. These include insights into fundamental mechanisms that create functional diversity, including invention of protein domains, expansion of protein and domain families, evolution of new protein architectures and horizontal transfer of genes. Other mechanisms, such as alternative splicing, post-translational modification and complex regulatory networks, are also crucial in generating diversity but are much harder to discern from the primary sequence. We will not attempt to consider the effects of alternative splicing on proteins; we will consider only a single splice form from each gene in the various organisms, even when multiple splice forms are known.

Functional and evolutionary classification. We began by classifying the human proteome on the basis of functional categories and evolutionary conservation. We used the InterPro annotation protocol to identify conserved biochemical and cellular processes. InterPro is a tool for combining sequence-pattern information from four databases. The first two databases (PRINTS[326] and Prosite[327]) primarily contain information about motifs corresponding to specific family subtypes, such as type II receptor tyrosine kinases (RTK-II) in particular or tyrosine kinases in general. The second two databases (Pfam[307] and Prosite Profile[327]) contain information (in the form of profiles or HMMs) about families of structural domains—for example, protein kinase domains. InterPro integrates the motif and domain assignments into a hierarchical classification system; so a protein might be classified at the most detailed level as being an RTK-II, at a more general level as being a kinase specific for tyrosine, and at a still more general level as being a protein kinase. The complete hierarchy of InterPro entries is described at http://www.ebi.ac.uk/interpro/. We collapsed the InterPro entries into 12 broad categories, each reflecting a set of cellular functions.

The InterPro families are partly the product of human judgement and reflect the current state of biological and evolutionary knowledge. The system is a valuable way to gain insight into large collections of proteins, but not all proteins can be classified at present. The proportions of the yeast, worm, fly and mustard weed protein sets that are assigned to at least one InterPro family is, for each organism, about 50% (Table 23; refs 307, 326, 327).

About 40% of the predicted human proteins in the IPI could be assigned to InterPro entries and functional categories. On the basis of these assignments, we could compare organisms according to the number of proteins in each category (Fig. 37). Compared with the two invertebrates, humans appear to have many proteins involved in cytoskeleton, defence and immunity, and transcription and translation. These expansions are clearly related to aspects of vertebrate physiology. Humans also have many more proteins that are classified as falling into more than one functional category (426 in human versus 80 in worm and 57 in fly, data not shown). Interestingly, 32% of these are transmembrane receptors.

We obtained further insight into the evolutionary conservation of proteins by comparing each sequence to the complete nonredundant database of protein sequences maintained at NCBI, using the BLASTP computer program[328] and then breaking down the matches according to organismal taxonomy (Fig. 38). Overall, 74% of the proteins had significant matches to known proteins.

Such classifications are based on the presence of clearly detectable homologues in existing databases. Many of these genes have surely evolved from genes that were present in common ancestors but have since diverged substantially. Indeed, one can detect more distant relationships by using sensitive computer programs that can recognize weakly conserved features. Using PSI-BLAST, we can recognize probable nonvertebrate homologues for about 45% of the 'vertebrate-specific' set. Nonetheless, the classification is useful for gaining insights into the commonalities and differences among the proteomes of different organisms.

Probable horizontal transfer. An interesting category is a set of 223 proteins that have significant similarity to proteins from bacteria, but no comparable similarity to proteins from yeast, worm, fly and

© 2001 Macmillan Magazines Ltd

Table 23 Properties of genome and proteome in essentially completed eukaryotic proteomes

	Human	Fly	Worm	Yeast	Mustard weed
Number of identified genes	~32,000*	13,338	18,266	6,144	25,706
% with InterPro matches	51	56	50	50	52
Number of annotated domain families	1,262	1,035	1,014	851	1,010
Number of InterPro entries per gene	0.53	0.84	0.63	0.6	0.62
Number of distinct domain architectures	1,695	1,036	1,018	310	–
Percentage of 1-1-1-1	1.40	4.20	3.10	9.20	–
% Signal sequences	20	20	24	11	–
% Transmembrane proteins	20	25	28	15	–
% Repeat-containing	10	11	9	5	–
% Coiled-coil	11	13	10	9	–

The numbers of distinct architectures were calculated using SMART[339] and the percentages of repeat-containing proteins were estimated using Prospero[452] and a *P*-value threshold of 10^{-5}. The protein sets used in the analysis were taken from http://www.ebi.ac.uk/proteome/ for yeast, worm and fly. The proteins from mustard weed were taken from the TAIR website (http:// www.arabidopsis.org/) on 5 September 2000. The protein set was searched against the InterPro database (http://www.ebi.ac.uk/interpro/) using the InterProscan software. Comparison of protein sequences with the InterPro database allows prediction of protein families, domain and repeat families and sequence motifs. The searches used Pfam release 5.2[307], Prints release 26.1[326], Prosite release 16[327] and Prosite preliminary profiles. InterPro analysis results are available as Supplementary Information. The fraction of 1-1-1-1 is the percentage of the genome that falls into orthologous groups composed of only one member each in human, fly, worm and yeast.
*The gene number for the human is still uncertain (see text). Table is based on 31,778 known genes and gene predictions.

mustard weed, or indeed from any other (nonvertebrate) eukaryote. These sequences should not represent bacterial contamination in the draft human sequence, because we filtered the sequence to eliminate sequences that were essentially identical to known bacterial plasmid, transposon or chromosomal DNA (such as the host strains for the large-insert clones). To investigate whether these were genuine human sequences, we designed PCR primers for 35 of these genes and confirmed that most could be readily detected directly in human genomic DNA (Table 24). Orthologues of many of these genes have also been detected in other vertebrates (Table 24).

A more detailed computational analysis indicated that at least 113 of these genes are widespread among bacteria, but, among eukaryotes, appear to be present only in vertebrates. It is possible that the genes encoding these proteins were present in both early prokaryotes and eukaryotes, but were lost in each of the lineages of yeast, worm, fly, mustard weed and, possibly, from other nonvertebrate eukaryote lineages. A more parsimonious explanation is that these genes entered the vertebrate (or prevertebrate) lineage by horizontal transfer from bacteria. Many of these genes contain introns, which presumably were acquired after the putative horizontal transfer event. Similar observations indicating probable lineage-specific horizontal gene transfers, as well as intron insertion in the acquired genes, have been made in the worm genome[329].

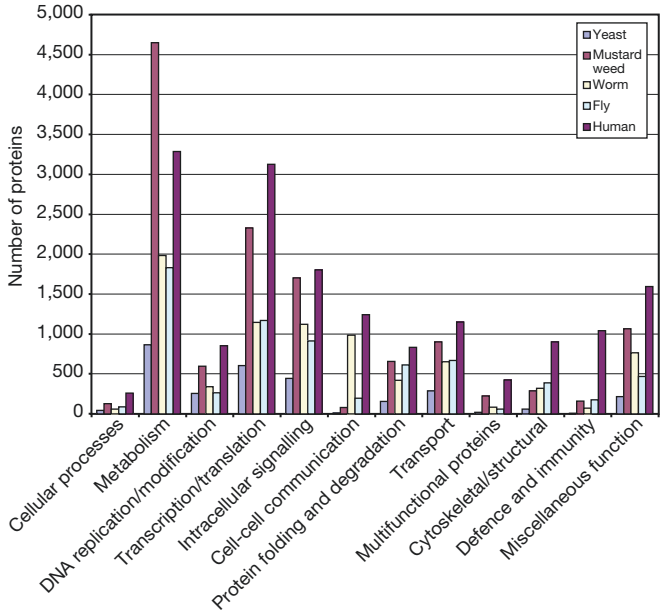

Figure 37 Functional categories in eukaryotic proteomes. The classification categories were derived from functional classification systems, including the top-level biological function category of the Gene Ontology project (GO; see http://www.geneontology.org).

We cannot formally exclude the possibility that gene transfer occurred in the opposite direction—that is, that the genes were invented in the vertebrate lineage and then transferred to bacteria. However, we consider this less likely. Under this scenario, the broad distribution of these genes among bacteria would require extensive horizontal dissemination after their initial acquisition. In addition, the functional repertoire of these genes, which largely encode intracellular enzymes (Table 24), is uncharacteristic of vertebrate-specific evolutionary innovations (which appear to be primarily extracellular proteins; see below).

We did not identify a strongly preferred bacterial source for the putative horizontally transferred genes, indicating the likelihood of multiple independent gene transfers from different bacteria (Table 24). Notably, several of the probable recent acquisitions have established (or likely) roles in metabolism of xenobiotics or stress response. These include several hydrolases of different specificities, including epoxide hydrolase, and several dehydrogenases (Table 24). Of particular interest is the presence of two paralogues of monoamine oxidase (MAO), an enzyme of the mitochondrial outer membrane that is central in the metabolism of neuromediators and is a target of important psychiatric drugs[330–333]. This example shows that at least some of the genes thought to be horizontally transferred into the vertebrate lineage appear to be involved in important physiological functions and so probably have been fixed and maintained during evolution because

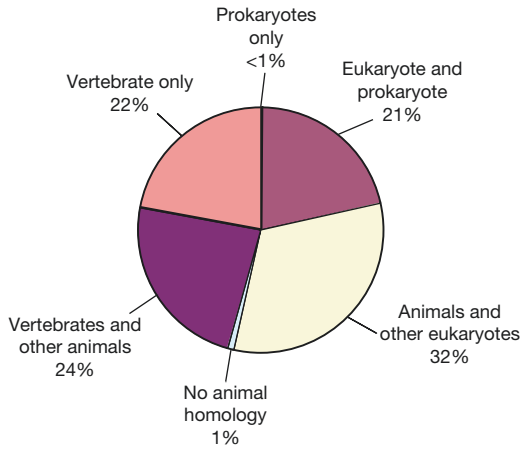

Figure 38 Distribution of the homologues of the predicted human proteins. For each protein, a homologue to a phylogenetic lineage was considered present if a search of the NCBI nonredundant protein sequence database, using the gapped BLASTP program, gave a random expectation (*E*) value of ≤ 0.001. Additional searches for probable homologues with lower sequence conservation were performed using the PSI-BLAST program, run for three iterations using the same cut-off for inclusion of sequences into the profile[328].

© 2001 Macmillan Magazines Ltd

of the increased selective advantage(s) they provide.

Genes shared with fly, worm and yeast. IPI.1 contains apparent homologues of 61% of the fly proteome, 43% of the worm proteome and 46% of the yeast proteome. We next considered the groups of proteins containing likely orthologues and paralogues (genes that arose from intragenome duplication) in human, fly, worm and yeast.

Briefly, we performed all-against-all sequence comparison[334] for the combined protein sets of human, yeast, fly and worm. Pairs of sequences that were one another's best matches in their respective genomes were considered to be potential orthologues. These were then used to identify orthologous groups across three organisms[335]. Recent species-specific paralogues were defined by using the all-against-all sequence comparison to cluster the protein set for each organism. For each sequence found in an orthologous group, the recent paralogues were defined to be the largest species-specific cluster including it. The set of paralogues may be inflated by unrecognized splice variants and by fragmentation.

We identified 1,308 groups of proteins, each containing at least one predicted orthologue in each species and many containing additional paralogues. The 1,308 groups contained 3,129 human proteins, 1,445 fly proteins, 1,503 worm proteins and 1,441 yeast proteins. These 1,308 groups represent a conserved core of proteins that are mostly responsible for the basic 'housekeeping' functions of the cell, including metabolism, DNA replication and repair, and translation.

In 564 of the 1,308 groups, one orthologue (and no additional paralogues) could be unambiguously assigned for each of human, fly, worm and yeast. These groups will be referred to as 1-1-1-1 groups. More than half (305) of these groups could be assigned to the functional categories shown in Fig. 37. Within these functional categories, the numbers of groups containing single orthologues in each of the four proteomes was: 19 for cellular processes, 66 for metabolism, 31 for DNA replication and modification, 106 for transcription/translation, 13 for intracellular signalling, 24 for protein folding and degradation, 38 for transport, 5 for

Table 24 Probable vertebrate-specific acquisitions of bacterial genes

Human protein (accession)	Predicted function	Known orthologues in other vertebrates	Bacterial homologues		Human origin confirmed by PCR
			Range	Best hit	
AAG01853.1	Formiminotransferase cyclodeaminase	Pig, rat, chicken	*Thermotoga*, *Thermoplasma*, *Methylobacter*	*Thermotoga maritima*	Yes
CAB81772.1 AAB59448.1 AAA36608.1 AAC41747.1	Na/glucose cotransporter	Rodents, ungulates	Most bacteria	*Vibrio parahaemolyticus*	Yes (CAB81772, AAC41747.1) NT* (AAB59448.1, AAA36608.1)
BAA1143.21	Epoxide hydrolase (α/β-hydrolase)	Mouse, *Danio*, fugu fish	Most bacteria	*Pseudomonas aeruginosa*	Yes
CAB59628.1	Protein-methionine-*S*-oxide reductase	Cow	Most bacteria	*Synechocystis sp.*	Yes
BAA91273.1	Hypertension-associated protein SA/ acetate-CoA ligase	Mouse, rat, cow	Most bacteria	*Bacillus halodurans*	NT*
CAA75608.1	Glucose-6-phosphate transporter/ glycogen storage disease type 1b protein	Mouse, rat	Most bacteria	*Chlamydophila pneumoniae*	Yes
AAA59548.1 AAB27229.1	Monoamine oxidase	Cow, rat, salmon	Most bacteria	*Mycobacterium tuberculosis*	Yes
AAF12736.1 AAA51565.1	Acyl-CoA dehydrogenase, mitochondrial protein	Mouse, rat, pig	Most bacteria	*P. aeruginosa*	Yes
IGI_M1_ctg19153_147	Aldose-1-epimerase	Pig (also found in plants)	*Streptomyces*, *Bacillus*	*Streptomyces coelicolor*	Yes
BAA92632.1	Predicted carboxylase (C-terminal domain, N-terminal domain unique)	None	*Streptomyces, Rhizobium, Bacillus*	*S. coelicolor*	Yes
BAA34458.1	Uncharacterized protein	None	Gamma-proteobacteria	*Escherichia coli*	Yes
AAF24044.1	Uncharacterized protein	None	Most bacteria	*T. maritima*	Yes
BAA34458.1	β-Lactamase superfamily hydrolase	None	Most bacteria	*Synechocystis* sp.	Yes
BAA91839.1	Oxidoreductase (Rossmann fold) fused to a six-transmembrane protein	None (several human paralogues of both parts)	*Actinomycetes*, *Leptospira*; more distant homologues in other bacteria	*S. coelicolor*	Yes
BAA92073.1	Oxidoreductase (Rossmann fold)	None	*Synechocystis, Pseudomonas*	*Synechocystis* sp.	Yes
BAA92133.1	α/β-hydrolase	None	*Rickettsia*; more distant homologues in other bacteria	*Rickettsia prowazekii*	Yes
BAA91174.1	ADP-ribosylglycohydrolase	None	*Streptomyces*, *Aquifex*, *Archaeoglobus* (archaeon), *E. coli*	*S. coelicolor*	Yes
AAA60043.1	Thymidine phosporylase/endothelial cell growth factor	None	Most bacteria	*Bacillus stearothermophilus*	Yes
BAA86552.1	Ribosomal protein S6-glutamic acid ligase	None	Most bacteria and archaea	*Haemophilus influenzae*	Yes
IGI_M1_ctg12741_7	Ribosomal protein S6-glutamic acid ligase (paralogue of the above)	None	Most bacteria and archaea	*H. influenzae*	Yes
IGI_M1_ctg13238_61	Hydratase	None	*Synechocystis*, *Sphingomonas*	*Synechocystis* sp.	Yes
IGI_M1_ctg13305_116	Homologue of histone macro-2A C-terminal domain, predicted phosphatase	None (several human paralogues, RNA viruses)	*Thermotoga*, *Alcaligenes*, *E. coli*, more distant homologues in other bacteria	*T. maritima*	Yes
IGI_M1_ctg14420_10	Sugar transporter	None	Most bacteria	*Synechocystis* sp.	Yes
IGI_M1_ctg16010_18	Predicted metal-binding protein	None	Most bacteria	*Borrelia burgdorferi*	Yes
IGI_M1_ctg16227_58	Pseudouridine synthase	None	Most bacteria	*Zymomonas mobilis*	Yes
IGI_M1_ctg25107_24	Surfactin synthetase domain	None	Gram-positive bacteria, *Actinomycetes*, *Cyanobacteria*	*Bacillus subtilis*	Yes

*NT, not tested.

Representative genes confirmed by PCR to be present in the human genome. The similarity to a bacterial homologue was considered to be 'significantly' greater than that to eukaryotic homologues if the difference in alignment scores returned by BLASTP was greater than 30 bits (~9 orders of magnitude in terms of *E*-value). A complete, classified and annotated list of probable vertebrate-specific horizontal gene transfers detected in this analysis is available as Supplementary Information. cDNA sequences for each protein were searched, using the SSAHA algorithm, against the draft genome sequence. Primers were designed and PCR was performed using three human genomic samples and a random BAC clone. The predicted genes were considered to be present in the human genome if a band of the expected size was found in all three human samples but not in the control clone.

© 2001 Macmillan Magazines Ltd

multifunctional proteins and 3 for cytoskeletal/structural. No such groups were found for defence and immunity or cell–cell communication.

The 1-1-1-1 groups probably represent key functions that have not undergone duplication and elaboration in the various lineages. They include many anabolic enzymes responsible for such functions as respiratory chain and nucleotide biosynthesis. In contrast, there are few catabolic enzymes. As anabolic pathways branch less frequently than catabolic pathways, this indicates that alternative routes and displacements are more frequent in catabolic reactions. If proteins from the single-celled yeast are excluded from the analysis, there are 1,195 1-1-1 groups. The additional groups include many examples of more complex signalling proteins, such as receptor-type and src-like tyrosine kinases, likely to have arisen early in the metazoan lineage. The fact that this set comprises only a small proportion of the proteome of each of the animals indicates that, apart from a modest conserved core, there has been extensive elaboration and innovation within the protein complement.

Most proteins do not show simple 1-1-1 orthologous relationships across the three animals. To illustrate this, we investigated the nuclear hormone receptor family. In the human proteome, this family consists of 60 different 'classical' members, each with a zinc finger and a ligand-binding domain. In comparison, the fly proteome has 19 and the worm proteome has 220. As shown in Fig. 39, few simple orthologous relationships can be derived among these homologues. And, where potential subgroups of orthologues and paralogues could be identified, it was apparent that the functions of the subgroup members could differ significantly. For example, the fly receptor for the fly-specific hormone ecdysone and the human retinoic acid receptors cluster together on the basis of sequence similarity. Such examples underscore that the assignment of functional similarity on the basis of sequence similarities among these three organisms is not trivial in most cases.

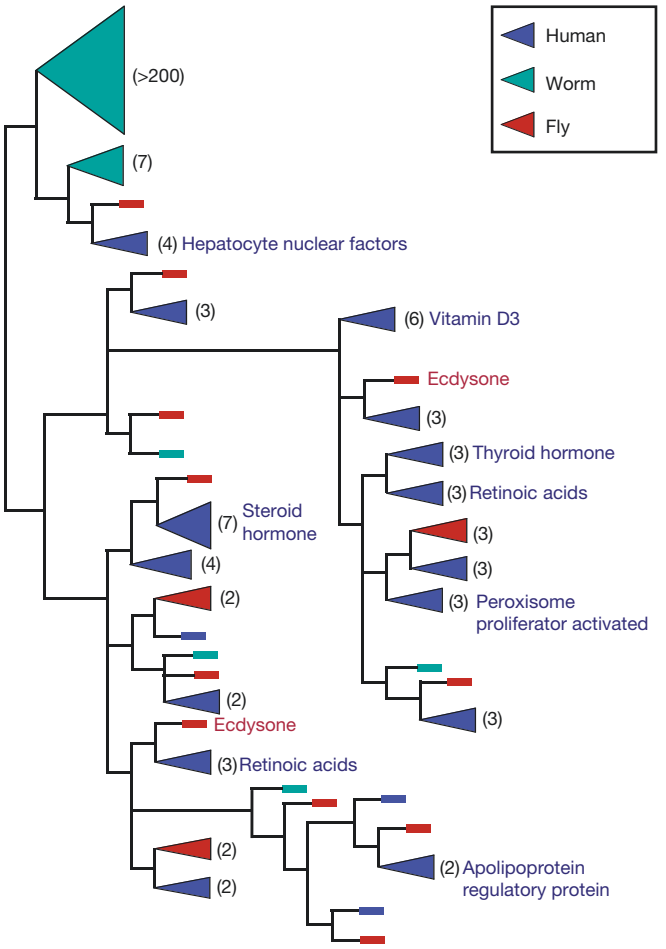

Figure 39 Simplified cladogram (relationship tree) of the 'many-to-many' relationships of classical nuclear receptors. Triangles indicate expansion within one lineage; bars represent single members. Numbers in parentheses indicate the number of paralogues in each group.

New vertebrate domains and proteins. We then explored how the proteome of vertebrates (as represented by the human) differs from those of the other species considered. The 1,262 InterPro families were scanned to identify those that contain only vertebrate proteins. Only 94 (7%) of the families were 'vertebrate-specific'. These represent 70 protein families and 24 domain families. Only one of the 94 families represents enzymes, which is consistent with the ancient origins of most enzymes[336]. The single vertebrate-specific enzyme family identified was the pancreatic or eosinophil-associated ribonucleases. These enzymes evolved rapidly, possibly to combat vertebrate pathogens[337].

The relatively small proportion of vertebrate-specific multicopy families suggests that few new protein domains have been invented in the vertebrate lineage, and that most protein domains trace at least as far back as a common animal ancestor. This conclusion must be tempered by the fact that the InterPro classification system is incomplete; additional vertebrate-specific families undoubtedly exist that have not yet been recognized in the InterPro system.

The 94 vertebrate-specific families appear to reflect important physiological differences between vertebrates and other eukaryotes. Defence and immunity proteins (23 families) and proteins that function in the nervous system (17 families) are particularly enriched in this set. These data indicate the recent emergence or rapid divergence of these proteins.

Representative human proteins were previously known for nearly all of the vertebrate-specific families. This was not surprising, given the anthropocentrism of biological research. However, the analysis did identify the first mammalian proteins belonging to two of these families. Both of these families were originally defined in fish. The first is the family of polar fish antifreeze III proteins. We found a human sialic acid synthase containing a domain homologous to polar fish antifreeze III protein (BAA91818.1). This finding suggests that fish created the antifreeze function by adaptation of this domain. We also found a human protein (CAB60269.1) homologous to the ependymin found in teleost fish. Ependymins are major glycoproteins of fish brains that have been claimed to be involved in long-term memory formation[338]. The function of the mammalian ependymin homologue will need to be elucidated.

New architectures from old domains. Whereas there appears to be only modest invention at the level of new vertebrate protein domains, there appears to be substantial innovation in the creation of new vertebrate proteins. This innovation is evident at the level of domain architecture, defined as the linear arrangement of domains within a polypeptide. New architectures can be created by shuffling, adding or deleting domains, resulting in new proteins from old parts.

We quantified the number of distinct protein architectures found in yeast, worm, fly and human by using the SMART annotation resource[339] (Fig. 40). The human proteome set contained 1.8 times as many protein architectures as worm or fly and 5.8 times as many as yeast. This difference is most prominent in the recent evolution of novel extracellular and transmembrane architectures in the human lineage. Human extracellular proteins show the greatest innovation: the human has 2.3 times as many extracellular architectures as fly and 2.0 times as many as worm. The larger number of human architectures does not simply reflect differences in the number of domains known in these organisms; the result remains qualitatively the same even if the number of architectures in each organism is normalized by dividing by the total number of domains (not shown). (We also checked that the larger number of human

© 2001 Macmillan Magazines Ltd

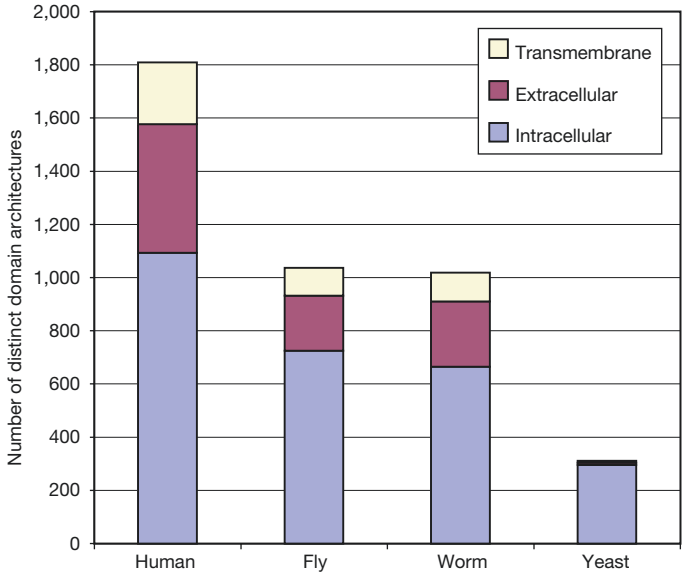

Figure 40 Number of distinct domain architectures in the four eukaryotic genomes, predicted using SMART[339]. The number of architectures is split into three cellular environments: intracellular, extracellular and membrane-associated. The increase in architectures for the human, relative to the other lineages, is seen when these numbers are normalized with respect to the numbers of domains predicted in each phylum. To avoid artefactual results from the relatively low detection rate for some repeat types, tandem occurrences of tetratricopeptide, armadillo, EF-hand, leucine-rich, WD40 or ankyrin repeats or C2H2-type zinc fingers were treated as single occurrences.

architectures could not be an artefact resulting from erroneous gene predictions. Three-quarters of the architectures can be found in known genes, which already yields an increase of about 50% over worm and fly. We expect the final number of human architectures to grow as the complete gene set is identified.)

A related measure of proteome complexity can be obtained by considering an individual domain and counting the number of different domain types with which it co-occurs. For example, the trypsin-like serine protease domain (number 12 in Fig. 41) co-occurs with 18 domain types in human (including proteins involved in the mammalian complement system, blood coagulation, and fibrinolytic and related systems). By contrast, the trypsin-like serine protease domain occurs with only eight other domains in fly, five in worm and one in yeast. Similar results for 27 common domains are shown in Fig. 41. In general, there are more different co-occurring domains in the human proteome than in the other proteomes.

One mechanism by which architectures evolve is through the fusion of additional domains, often at one or both ends of the proteins. Such 'domain accretion'[340] is seen in many human proteins when compared with proteins from other eukaryotes. The effect is illustrated by several chromatin-associated proteins (Fig. 42). In these examples, the domain architectures of human proteins differ from those found in yeast, worm and fly proteins only by the addition of domains at their termini.

Among chromatin-associated proteins and transcription factors, a significant proportion of domain architectures is shared between the vertebrate and fly, but not with worm (Fig. 43a). The trend was even more prominent in architectures of proteins involved in another key cellular process, programmed cell death (Fig. 43b). These examples might seem to bear upon the unresolved issue of the evolutionary branching order of worms, flies and humans, suggesting that worms branched off first. However, there were other cases in which worms and humans shared architectures not present in fly. A global analysis of shared architectures could not conclusively distinguish between the two models, given the possibility of lineage-specific loss of architectures. Comparison of protein architectures may help to resolve the evolutionary issue, but it will require more detailed analyses of many protein families.

New physiology from old proteins. An important aspect of

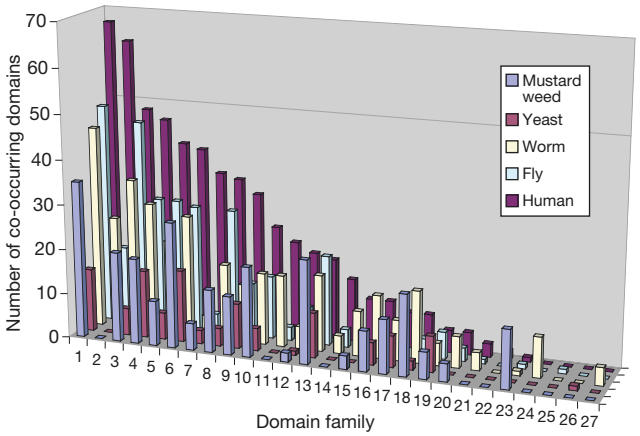

Figure 41 Number of different Pfam domain types that co-occur in the same protein, for each of the 10 most common domain families in each of the five eukaryotic proteomes. Because some common domain families are shared, there are 27 families rather than 50. The data are ranked according to decreasing numbers of human co-occurring Pfam domains. The domain families are: (1) eukaryotic protein kinase [IPR000719]; (2) immunoglobulin domain [IPR003006]; (3) ankyrin repeat [IPR002110]; (4) RING finger [IPR001841]; (5) C2H2-type zinc finger [IPR000822]; (6) ATP/GTP-binding P-loop [IPR001687]; (7) reverse transcriptase (RNA-dependent DNA polymerase) [IPR000477]; (8) leucine-rich repeat [IPR001611]; (9) G-proteinβ WD-40 repeats [IPR001680]; (10) RNA-binding region RNP-1 (RNA recognition motif) [IPR000504]; (11) C-type lectin domain [IPR001304]; (12) serine proteases, trypsin family [IPR001254]; (13) helicase C-terminal domain [IPR001650]; (14) collagen triple helix repeat [IPR000087]; (15) rhodopsin-like GPCR superfamily [IPR000276]; (16) esterase/lipase/thioesterase [IPR000379]; (17) Myb DNA-binding domain [IPR001005]; (18) F-box domain [IPR001810]; (19) ATP-binding transport protein, 2nd P-loop motif [IPR001051]; (20) homeobox domain [IPR001356]; (21) C4-type steroid receptor zinc finger [IPR001628]; (22) sugar transporter [IPR001066]; (23) PPR repeats [IPR002885]; (24) seven-helix G-protein-coupled receptor, worm (probably olfactory) family [IPR000168]; (25) cytochrome P450 enzyme [IPR001128]; (26) fungal transcriptional regulatory protein, N terminus [IPR001138]; (27) domain of unknown function DUF38 [IPR002900].

© 2001 Macmillan Magazines Ltd

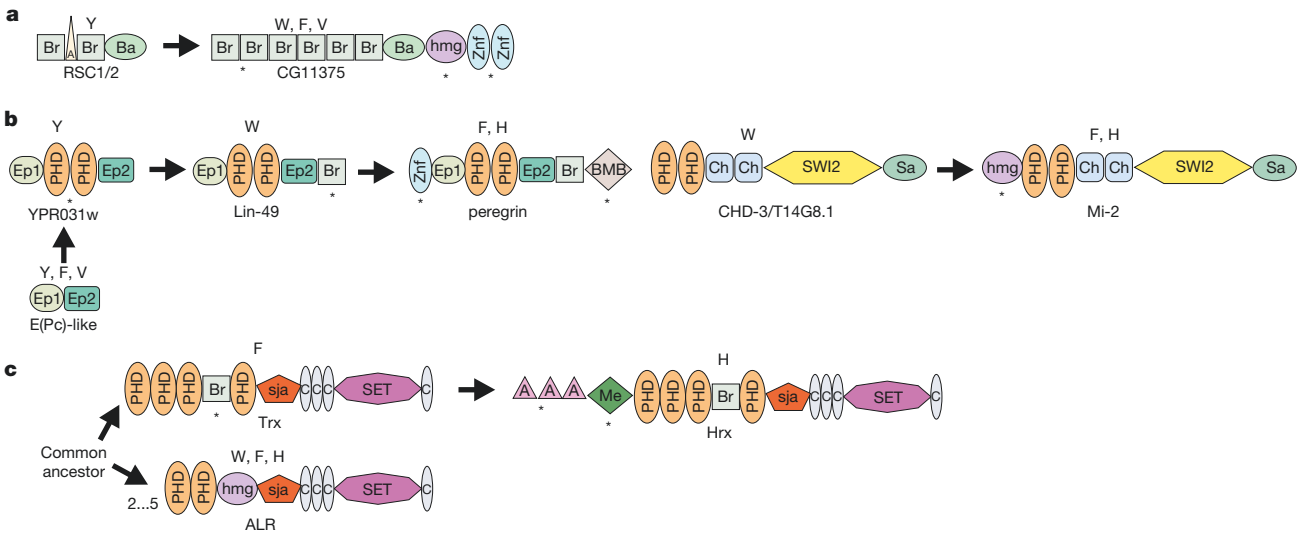

Figure 42 Examples of domain accretion in chromatin proteins. Domain accretion in various lineages before the animal divergence, in the apparent coelomate lineage and the vertebrate lineage are shown using schematic representations of domain architectures (not to scale). Asterisks, mobile domains that have participated in the accretion. Species in which a domain architecture has been identified are indicated above the diagram (Y, yeast; W, worm; F, fly; V, vertebrate). Protein names are below the diagrams. The domains are SET, a chromatin protein methyltransferase domain; SWI2, a superfamily II helicase/ATPase domain; Sa, sant domain; Br, bromo domain; Ch, chromodomain; C, a cysteine triad motif associated with the Msl-2 and SET domains; A, AT hook motif; EP1/EP2, enhancer of polycomb domains 1 and 2; Znf, zinc finger; sja, SET-JOR-associated domain (L. Aravind, unpublished); Me, DNA methylase/Hrx-associated DNA binding zinc finger; Ba, bromo-associated homology motif. **a**–**c**, Different examples of accretion.

vertebrate innovation lies in the expansion of protein families. Table 25 shows the most prevalent protein domains and protein families in humans, together with their relative ranks in the other species. About 60% of families are more numerous in the human than in any of the other four organisms. This shows that gene duplication has been a major evolutionary force during vertebrate evolution. A comparison of relative expansions in human versus fly is shown in Fig. 44.

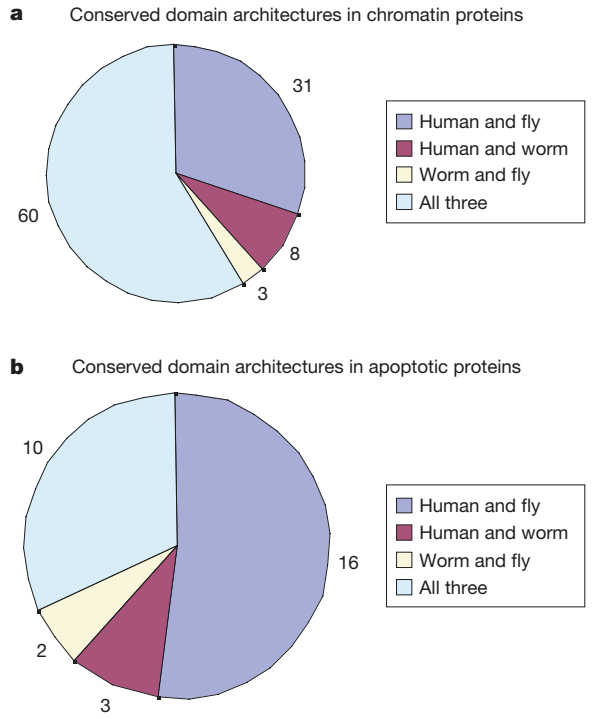

Figure 43 Conservation of architectures between animal species. The pie charts illustrate the shared domain architectures of apparent orthologues that are conserved in at least two of the three sequenced animal genomes. If an architecture was detected in fungi or plants, as well as two of the animal lineages, it was omitted as ancient and its absence in the third animal lineage attributed to gene loss. **a**, Chromatin-associated proteins. **b**, Components of the programmed cell death system.

Many of the families that are expanded in human relative to fly and worm are involved in distinctive aspects of vertebrate physiology. An example is the family of immunoglobulin (IG) domains, first identified in antibodies thirty years ago. Classic (as opposed to divergent) IG domains are completely absent from the yeast and mustard weed proteomes and, although prokaryotic homologues exist, they have probably been transferred horizontally from metazoans[341]. Most IG superfamily proteins in invertebrates are cell-surface proteins. In vertebrates, the IG repertoire includes immune functions such as those of antibodies, MHC proteins, antibody receptors and many lymphocyte cell-surface proteins. The large expansion of IG domains in vertebrates shows the versatility of a single family in evoking rapid and effective response to infection.

Two prominent families are involved in the control of development. The human genome contains 30 fibroblast growth factors (FGFs), as opposed to two FGFs each in the fly and worm. It contains 42 transforming growth factor-βs (TGFβs) compared with nine and six in the fly and worm, respectively. These growth factors are involved in organogenesis, such as that of the liver and the lung. A fly FGF protein, branchless, is involved in developing respiratory organs (tracheae) in embryos[342]. Thus, developmental triggers of morphogenesis in vertebrates have evolved from related but simpler systems in invertebrates[343].

Another example is the family of intermediate filament proteins, with 127 family members. This expansion is almost entirely due to 111 keratins, which are chordate-specific intermediate filament proteins that form filaments in epithelia. The large number of human keratins suggests multiple cellular structural support roles for the many specialized epithelia of vertebrates.

Finally, the olfactory receptor genes comprise a huge gene family of about 1,000 genes and pseudogenes[344,345]. The number of olfactory receptors testifies to the importance of the sense of smell in vertebrates. A total of 906 olfactory receptor genes and pseudogenes could be identified in the draft genome sequence, two-thirds of which were not previously annotated. About 80% are found in about two dozen clusters ranging from 6 to 138 genes and encompassing about 30 Mb (~1%) of the human genome. Despite the importance of smell among our vertebrate ancestors, hominids

© 2001 Macmillan Magazines Ltd

appear to have considerably less interest in this sense. About 60% of the olfactory receptors in the draft genome sequence have disrupted ORFs and appear to be pseudogenes, consistent with recent reports[344,346] suggesting massive functional gene loss in the last 10 Myr[347,348]. Interestingly, there appears to be a much higher proportion of intact genes among class I than class II olfactory receptors, suggesting functional importance.

Vertebrates are not unique in employing gene family expansion. For many domain types, expansions appear to have occurred independently in each of the major eukaryotic lineages. A good example is the classical C2H2 family of zinc finger domains, which have expanded independently in the yeast, worm, fly and human lineages (Fig. 45). These independent expansions have resulted in numerous C2H2 zinc finger domain-containing proteins that are specific to each lineage. In flies, the important components of the C2H2 zinc finger expansion are architectures in which it is combined with the POZ domain and the C4DM domain (a metal-binding domain found only in fly). In humans, the most prevalent expansions are combinations of the C2H2 zinc finger with POZ (independent of the one in insects) and the vertebrate-specific KRAB and SCAN domains.

The homeodomain is similarly expanded in all animals and is present in both architectures that are conserved and lineage-specific architectures (Fig. 45). This indicates that the ancestral animal probably encoded a significant number of homeodomain proteins, but subsequent evolution involved multiple, independent expansions and domain shuffling after lineages diverged. Thus, the most prevalent transcription factor families are different in worm, fly and human (Fig. 45). This has major biological implications because transcription factors are critical in animal development and differentiation. The emergence of major variations in the developmental body plans that accompanied the early radiation of the animals[349] could have been driven by lineage-specific proliferation of such transcription factors. Beyond these large expansions of protein families, protein components of particular functional systems such as the cell death signalling system show a general increase in diversity and numbers in the vertebrates relative to other animals. For example, there are greater numbers of and more novel architectures in cell death regulatory proteins such as BCL-2, TNFR and NFκB from vertebrates.

Conclusion. Five lines of evidence point to an increase in the complexity of the proteome from the single-celled yeast to the multicellular invertebrates and to vertebrates such as the human. Specifically, the human contains greater numbers of genes, domain and protein families, paralogues, multidomain proteins with multiple functions, and domain architectures. According to these measures, the relatively greater complexity of the human proteome is a consequence not simply of its larger size, but also of large-scale protein innovation.

An important question is the extent to which the greater phenotypic complexity of vertebrates can be explained simply by two- or threefold increases in proteome complexity. The real explanation may lie in combinatorial amplification of these modest differences, by mechanisms that include alternative splicing, post-translational modification and cellular regulatory networks. The potential numbers of different proteins and protein–protein interactions are vast, and their actual numbers cannot readily be discerned from the genome sequence. Elucidating such system-level properties presents one of the great challenges for modern biology.

Table 25 The most populous InterPro families in the human proteome and other species

	Human		Fly		Worm		Yeast		Mustard weed		
InterPro ID	No. of genes	Rank	No. of genes	Rank	No. of genes	Rank	No. of genes	Rank	No. of genes	Rank	
IPR003006	765	(1)	140	(9)	64	(34)	0	(na)	0	(na)	Immunoglobulin domain
PR000822	706	(2)	357	(1)	151	(10)	48	(7)	115	(20)	C2H2 zinc finger
IPR000719	575	(3)	319	(2)	437	(2)	121	(1)	1049	(1)	Eukaryotic protein kinase
IPR000276	569	(4)	97	(14)	358	(3)	0	(na)	16	(84)	Rhodopsin-like GPCR superfamily
IPR001687	433	(5)	198	(4)	183	(7)	97	(2)	331	(5)	P-loop motif
IPR000477	350	(6)	10	(65)	50	(41)	6	(36)	80	(35)	Reverse transcriptase (RNA-dependent DNA polymerase)
IPR000504	300	(7)	157	(6)	96	(21)	54	(6)	255	(8)	rrm domain
IPR001680	277	(8)	162	(5)	102	(19)	91	(3)	210	(10)	G-protein β WD-40 repeats
IPR002110	276	(9)	105	(13)	107	(17)	19	(23)	120	(18)	Ankyrin repeat
IPR001356	267	(10)	148	(7)	109	(15)	9	(33)	118	(19)	Homeobox domain
IPR001849	252	(11)	77	(22)	71	(31)	27	(17)	27	(73)	PH domain
IPR002048	242	(12)	111	(12)	81	(25)	15	(27)	167	(12)	EF-hand family
IPR000561	222	(13)	81	(20)	113	(14)	0	(na)	17	(83)	EGF-like domain
IPR001452	215	(14)	72	(23)	62	(35)	25	(18)	3	(97)	SH3 domain
IPR001841	210	(15)	114	(11)	126	(12)	35	(12)	379	(4)	RING finger
IPR001611	188	(16)	115	(10)	54	(38)	7	(35)	392	(2)	Leucine-rich repeat
IPR001909	171	(17)	0	(na)	0	(na)	0	(na)	0	(na)	KRAB box
IPR001777	165	(18)	63	(27)	51	(40)	2	(40)	4	(96)	Fibronectin type III domain
IPR001478	162	(19)	70	(24)	66	(33)	2	(40)	15	(85)	PDZ domain
IPR001650	155	(20)	87	(17)	78	(27)	79	(4)	148	(13)	Helicase C-terminal domain
IPR001440	150	(21)	86	(18)	46	(43)	36	(11)	125	(17)	TPR repeat
IPR002216	133	(22)	65	(26)	99	(20)	2	(40)	31	(69)	Ion transport protein
IPR001092	131	(23)	84	(19)	41	(46)	7	(35)	106	(24)	Helix–loop–helix DNA-binding domain
IPR000008	123	(24)	43	(34)	36	(49)	9	(33)	82	(34)	C2 domain
IPR001664	119	(25)	4	(71)	22	(63)	1	(41)	2	(98)	SH2 domain
IPR001254	118	(26)	210	(3)	12	(73)	1	(41)	15	(85)	Serine protease, trypsin family
IPR002126	114	(27)	19	(56)	16	(69)	0	(na)	0	(na)	Cadherin domain
IPR000210	113	(28)	78	(21)	117	(13)	1	(41)	54	(50)	BTB/POZ domain
IPR000387	112	(29)	35	(40)	108	(16)	12	(30)	21	(79)	Tyrosine-specific protein phosphatase and dual specificity protein phosphatase family
IPR000087	106	(30)	18	(57)	169	(9)	0	(na)	5	(95)	Collagen triple helix repeat
IPR000379	94	(31)	141	(8)	134	(11)	40	(10)	194	(11)	Esterase/lipase/thioesterase
IPR000910	89	(32)	38	(38)	18	(67)	8	(34)	18	(82)	HMG1/2 (high mobility group) box
IPR000130	87	(33)	56	(29)	92	(22)	8	(34)	12	(88)	Neutral zinc metallopeptidase
IPR001965	84	(34)	37	(39)	24	(61)	16	(26)	71	(39)	PHD-finger
IPR000636	83	(35)	32	(43)	24	(61)	1	(41)	14	(86)	Cation channels (non-ligand gated)
IPR001781	81	(36)	38	(38)	36	(49)	4	(38)	8	(92)	LIM domain
IPR002035	81	(36)	8	(67)	45	(44)	3	(39)	17	(83)	VWA domain
IPR001715	80	(37)	33	(42)	30	(55)	3	(39)	18	(82)	Calponin homology domain
IPR000198	77	(38)	20	(55)	20	(65)	10	(32)	9	(91)	RhoGAP domain

Forty most populous Interpro families found in the human proteome compared with equivalent numbers from other species. na, not applicable (used when there are no proteins in an organism in that family).

© 2001 Macmillan Magazines Ltd

Segmental history of the human genome

In bacteria, genomic segments often convey important information about function: genes located close to one another often encode proteins in a common pathway and are regulated in a common operon. In mammals, genes found close to each other only rarely have common functions, but they are still interesting because they have a common history. In fact, the study of genomic segments can shed light on biological events as long as 500 Myr ago and as recently as 20,000 years ago.

Conserved segments between human and mouse

Humans and mice shared a common ancestor about 100 Myr ago. Despite the 200 Myr of evolutionary distance between the species, a significant fraction of genes show synteny between the two, being preserved within conserved segments. Genes tightly linked in one mammalian species tend to be linked in others. In fact, conserved segments have been observed in even more distant species: humans show conserved segments with fish[350,351] and even with invertebrates such as fly and worm[352]. In general, the likelihood that a syntenic relationship will be disrupted correlates with the physical distance between the loci and the evolutionary distance between the species.

Studying conserved segments between human and mouse has several uses. First, conservation of gene order has been used to identify likely orthologues between the species, particularly when investigating disease phenotypes. Second, the study of conserved segments among genomes helps us to deduce evolutionary ancestry.

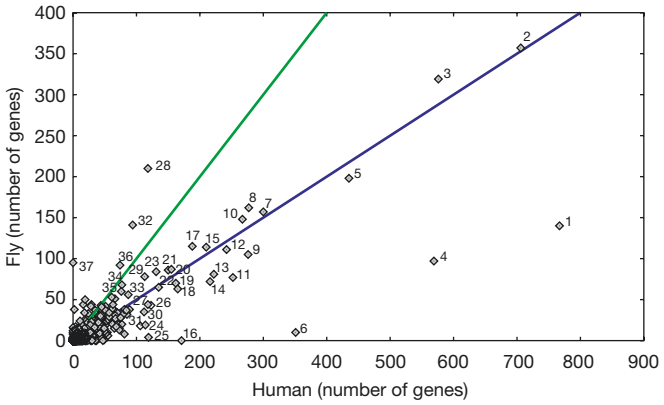

Figure 44 Relative expansions of protein families between human and fly. These data have not been normalized for proteomic size differences. Blue line, equality between normalized family sizes in the two organisms. Green line, equality between unnormalized family sizes. Numbered InterPro entries: (1) immunoglobulin domain [IPR003006]; (2) zinc finger, C2H2 type [IPR000822]; (3) eukaryotic protein kinase [IPR000719]; (4) rhodopsin-like GPCR superfamily [IPR000276]; (5) ATP/GTP-binding site motif A (P-loop) [IPR001687]; (6) reverse transcriptase (RNA-dependent DNA polymerase) [IPR000477]; (7) RNA-binding region RNP-1 (RNA recognition motif) [IPR000504]; (8) G-proteinβ WD-40 repeats [IPR001680]; (9) ankyrin repeat [IPR002110]; (10) homeobox domain [IPR001356]; (11) PH domain [IPR001849]; (12) EF-hand family [IPR002048]; (13) EGF-like domain [IPR000561]; (14) Src homology 3 (SH3) domain [IPR001452]; (15) RING finger [IPR001841]; (16) KRAB box [IPR001909]; (17) leucine-rich repeat [IPR001611]; (18) fibronectin type III domain [IPR001777]; (19) PDZ domain (also known as DHR or GLGF) [IPR001478]; (20) TPR repeat [IPR001440]; (21) helicase C-terminal domain [IPR001650]; (22) ion transport protein [IPR002216]; (23) helix–loop–helix DNA-binding domain [IPR001092]; (24) cadherin domain [IPR002126]; (25) intermediate filament proteins [IPR001664]; (26) C2 domain [IPR000008]; (27) Src homology 2 (SH2) domain [IPR000980]; (28) serine proteases, trypsin family [IPR001254]; (29) BTB/POZ domain [IPR000210]; (30) tyrosine-specific protein phosphatase and dual specificity protein phosphatase family [IPR000387]; (31) collagen triple helix repeat [IPR000087]; (32) esterase/lipase/thioesterase [IPR000379]; (33) neutral zinc metallopeptidases, zinc-binding region [IPR000130]; (34) ATP-binding transport protein, 2nd P-loop motif [IPR001051]; (35) ABC transporters family [IPR001617]; (36) cytochrome P450 enzyme [IPR001128]; (37) insect cuticle protein [IPR000618].

And third, detailed comparative maps may assist in the assembly of the mouse sequence, using the human sequence as a scaffold.

Two types of linkage conservation are commonly described[353]. 'Conserved synteny' indicates that at least two genes that reside on a common chromosome in one species are also located on a common chromosome in the other species. Syntenic loci are said to lie in a 'conserved segment' when not only the chromosomal position but the linear order of the loci has been preserved, without interruption by other chromosomal rearrangements.

An initial survey of homologous loci in human and mouse[354] suggested that the total number of conserved segments would be about 180. Subsequent estimates based on increasingly detailed comparative maps have remained close to this projection[353,355,356] (http://www.informatics.jax.org). The distribution of segment lengths has corresponded reasonably well to the truncated negative exponential curve predicted by the random breakage model[357].

The availability of a draft human genome sequence allows the first global human–mouse comparison in which human physical distances can be measured in Mb, rather than cM or orthologous gene counts. We identified likely orthologues by reciprocal comparison of the human and mouse mRNAs in the LocusLink database, using megaBLAST. For each orthologous pair, we mapped the location of the human gene in the draft genome sequence and then checked the location of the mouse gene in the Mouse Genome Informatics database (http://www.informatics.jax.org). Using a conservative threshold, we identified 3,920 orthologous pairs in which the human gene could be mapped on the draft genome sequence with high confidence. Of these, 2,998 corresponding mouse genes had a known position in the mouse genome. We then searched for definitive conserved segments, defined as human regions containing orthologues of at least two genes from the same mouse chromosome region (<15 cM) without interruption by segments from other chromosomes.

We identified 183 definitive conserved segments (Fig. 46). The average segment length was 15.4 Mb, with the largest segment being 90.5 Mb and the smallest 24 kb. There were also 141 'singletons', segments that contained only a single locus; these are not counted in the statistics. Although some of these could be short conserved segments, they could also reflect incorrect choices of orthologues or problems with the human or mouse maps. Because of this conservative approach, the observed number of definitive segments is likely be lower than the correct total. One piece of evidence for this conclusion comes from a more detailed analysis on human chromosome 7 (ref. 358), which identified 20 conserved segments, of which three were singletons. Our analysis revealed only 13 definitive segments on this chromosome, with nine singletons.

The frequency of observing a particular gene count in a conserved segment is plotted on a logarithmic scale in Fig. 47. If chromosomal breaks occur in a random fashion (as has been proposed) and differences in gene density are ignored, a roughly straight line should result. There is a clear excess for $n = 1$, suggesting that 50% or more of the singletons are indeed artefactual. Thus, we estimate that true number of conserved segments is around 190–230, in good agreement with the original Nadeau–Taylor prediction[354].

Figure 48 shows a plot of the frequency of lengths of conserved segments, where the x-axis scale is shown in Mb. As before, there is a fair amount of scatter in the data for the larger segments (where the numbers are small), but the trend appears to be consistent with a random breakage model.

We attempted to ascertain whether the breakpoint regions have any special characteristics. This analysis was complicated by imprecision in the positioning of these breaks, which will tend to blur any relationships. With 2,998 orthologues, the average interval within which a break is known to have occurred is about 1.1 Mb. We compared the aggregate features of these breakpoint intervals with the genome as a whole. The mean gene density was lower in breakpoint regions than in the conserved segments (13.8 versus

© 2001 Macmillan Magazines Ltd

18.6 per Mb). This suggests that breakpoints may be more likely to occur or to undergo fixation in gene-poor intervals than in gene-rich intervals. The occurrence of breakpoints may be promoted by homologous recombination among repeated sequences[359]. When the sequence of the mouse genome is finished, this analysis can be revisited more precisely.

A number of examples of extended conserved segments and syntenies are apparent in Fig. 46. As has been noted, almost all human genes on chromosome 17 are found on mouse chromosome 11, with two members of the placental lactogen family from mouse 13 inserted. Apart from two singleton loci, human chromosome 20 appears to be entirely orthologous to mouse chromosome 2, apparently in a single segment. The largest apparently contiguous conserved segment in the human genome is on chromosome 4, including roughly 90.5 Mb of human DNA that is orthologous to mouse chromosome 5. This analysis also allows us to infer the likely location of thousands of mouse genes for which the human orthologue has been located in the draft genome sequence but the mouse locus has not yet been mapped.

With about 200 conserved segments between mouse and human and about 100 Myr of evolution from their common ancestor[360], we obtain an estimated rate of about 1.0 chromosomal rearrangement being fixed per Myr. However, there is good evidence that the rate of chromosomal rearrangement (like the rate of nucleotide substitutions; see above) differs between the two species. Among mammals, rodents may show unusually rapid chromosome alteration. By comparison, very few rearrangements have been observed among primates, and studies of a broader array of mammalian orders, including cats, cows, sheep and pigs, suggest an average rate of chromosome alteration of only about 0.2 rearrangements per Myr in these lineages[361]. Additional evidence that rodents are outliers comes from a recent analysis of synteny between the human and zebrafish genomes. From a study of 523 orthologues, it was possible to project 418 conserved segments[350]. Assuming 400 Myr since a common vertebrate ancestor of zebrafish and humans[362], we obtain an estimate of 0.52 rearrangements per Myr. Recent estimates of rearrangement rates in plants have suggested bimodality, with some pairs showing rates of 0.15–0.41 rearrangements per Myr, and others showing higher rates of 1.1–1.3 rearrangements per Myr[363]. With additional detailed genome maps of multiple species, it should be possible to determine whether this particular molecular clock is truly operating at a different rate in various branches of the evolutionary tree, and whether variations in that rate are bimodal or continuous. It should also be possible to reconstruct the karyotypes of common ancestors.

Ancient duplicated segments in the human genome

Another approach to genomic history is to study segmental duplications within the human genome. Earlier, we discussed examples of recent duplications of genomic segments to pericentromeric and subtelomeric regions. Most of these events appear to be evolutionary dead-ends resulting in nonfunctional pseudogenes; however, segmental duplication is also an important mode of evolutionary innovation: a duplication permits one copy of each gene to drift and potentially to acquire a new function.

Segmental duplications can occur through unequal crossing over to create gene families in specific chromosomal regions. This mechanism can create both small families, such as the five related genes of the β-globin cluster on chromosome 11, and large ones, such as the olfactory receptor gene clusters, which together contain nearly 1,000 genes and pseudogenes.

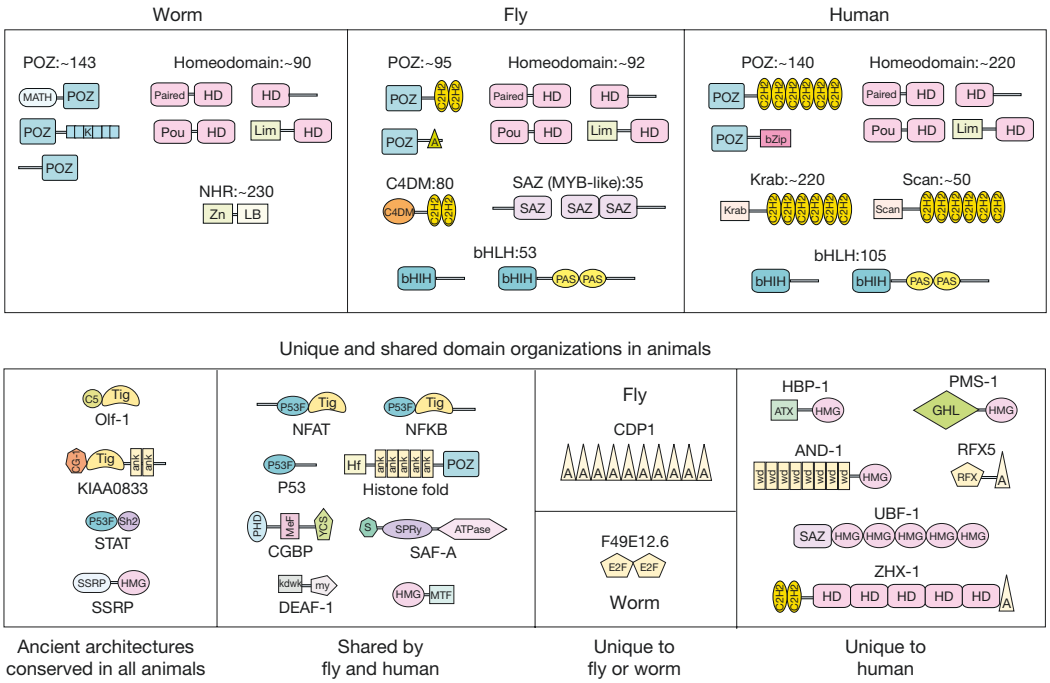

Figure 45 Lineage-specific expansions of domains and architectures of transcription factors. Top, specific families of transcription factors that have been expanded in each of the proteomes. Approximate numbers of domains identified in each of the (nearly) complete proteomes representing the lineages are shown next to the domains, and some of the most common architectures are shown. Some are shared by different animal lineages; others are lineage-specific. Bottom, samples of architectures from transcription factors that are shared by all animals (ancient architectures), shared by fly and human and unique to each lineage. Domains: K, kelch; HD, homeodomain; Zn, zinc-binding domain; LB, ligand-binding domain; C4DM, novel Zn cluster with four cysteines, probably involved in protein–protein interactions (L. Aravind, unpublished); MATH, meprin-associated TRAF domain; CG-1, novel domain in KIAA0909-like transcription factors (L. Aravind, unpublished); MTF, myelin transcription factor domain; SAZ, specialized Myb-like helix-turn-helix (HTH) domain found in Stonewall, ADF-1 and Zeste (L. Aravind, unpublished); A, AT-hook motif; E2F, winged HTH DNA-binding domain; GHL, gyraseB-histidine kinase-MutL ATPase domain; ATX, ATaXin domain; RFX, RFX winged HTH DNA binding domain; My, MYND domain; KDWK, KDWK DNA-binding domain; POZ, Pox zinc finger domain; S, SAP domain; P53F, P53 fold domain; HF, histone fold; ANK, ankyrin repeat; TIG, transcription factor Ig domain; SSRP, structure-specific recognition protein domain; C5, 5-cysteine metal binding domain; C2H2, classic zinc finger domain; WD, WD40 repeats.

© 2001 Macmillan Magazines Ltd

The most extreme mechanism is whole-genome duplication (WGD), through a polyploidization event in which a diploid organism becomes tetraploid. Such events are classified as autopolyploidy or allopolyploidy, depending on whether they involve hybridization between members of the same species or different species. Polyploidization is common in the plant kingdom, with many known examples among wild and domesticated crop species. Alfalfa (*Medicago sativa*) is a naturally occurring autotetraploid[364], and *Nicotiana tabacum*, some species of cotton (*Gossypium*) and several of the common brassicas are allotetraploids containing pairs of 'homeologous' chromosome pairs.

In principle, WGD provides the raw material for great bursts of innovation by allowing the duplication and divergence of entire pathways. Ohno[365] suggested that WGD has played a key role in evolution. There is evidence for an ancient WGD event in the ancestry of yeast and several independent such events in the ancestry of mustard weed[366–369]. Such ancient WGD events can be hard to detect because only a minority of the duplicated loci may be retained, with the result that the genes in duplicated segments cannot be aligned in a one-to-one correspondence but rather require many gaps. In addition, duplicated segments may be subsequently rearranged. For example, the ancient duplication in the yeast genome appears to have been followed by loss of more than 90% of the newly duplicated genes[366].

One of the most controversial hypotheses about vertebrate evolution is the proposal that two WGD events occurred early in the vertebrate lineage, around the time of jawed fishes some 500 Myr ago. Some authors[370–373] have seen support for this theory in the fact that many human genes occur in sets of four homologues—most notably the four extensive HOX gene clusters on chromosomes 2, 7, 12 and 17, whose duplication dates to around the correct time. However, other authors have disputed this interpretation[374], suggesting that these cases may reflect unrelated duplications of specific regions rather than successive WGD.

We analysed the draft genome sequence for evidence that might bear on this question. The analysis provides many interesting observations, but no convincing evidence of ancient WGD. We looked for evidence of pairs of chromosomal regions containing many homologous genes. Although we found many pairs containing a few homologous genes, the human genome does not appear to contain any pairs of regions where the density of duplicated genes approaches the densities seen in yeast or mustard weed[366–369].

We also examined human proteins in the IPI for which the orthologues among fly or worm proteins occur in the ratios 2:1:1, 3:1:1, 4:1:1 and so on (Fig. 49). The number of such families falls smoothly, with no peak at four and some instances of five or more homologues. Although this does not rule out two rounds of WGD followed by extensive gene loss and some unrelated gene duplication, it provides no support for the theory. More probatively, if two successive rounds of genome duplication occurred, phylogenetic analysis of the proteins having 4:1:1 ratios between human, fly and worm would be expected to show more trees with the topology (A,B)(C,D) for the human sequences than (A,(B,(C,D)))[375]. However, of 57 sets studied carefully, only 24% of the trees constructed from the 4:1:1 set have the former topology; this is not significantly different from what would be expected under the hypothesis of random sequential duplication of individual loci.

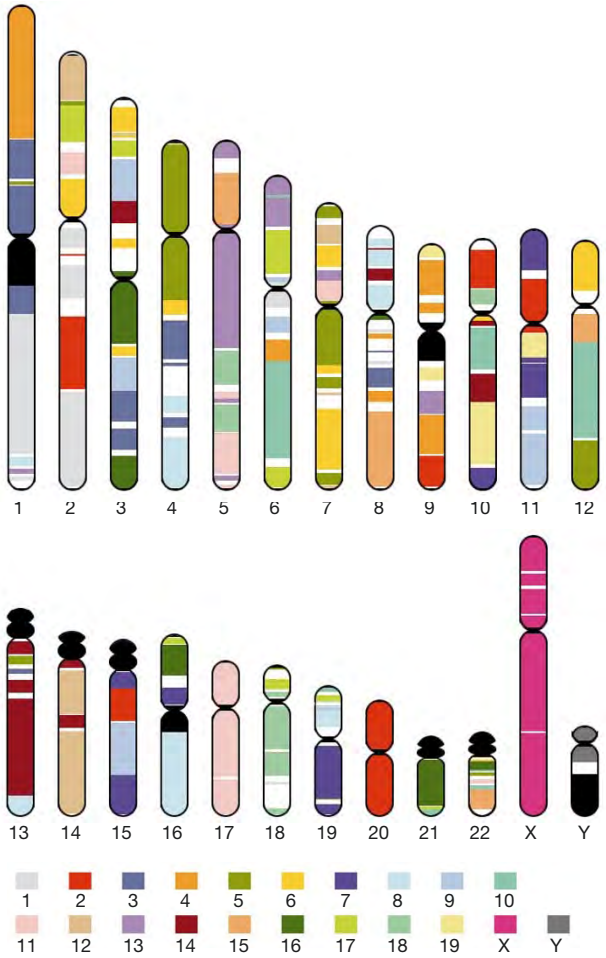

Figure 46 Conserved segments in the human and mouse genome. Human chromosomes, with segments containing at least two genes whose order is conserved in the mouse genome as colour blocks. Each colour corresponds to a particular mouse chromosome. Centromeres, subcentromeric heterochromatin of chromosomes 1, 9 and 16, and the repetitive short arms of 13, 14, 15, 21 and 22 are in black.

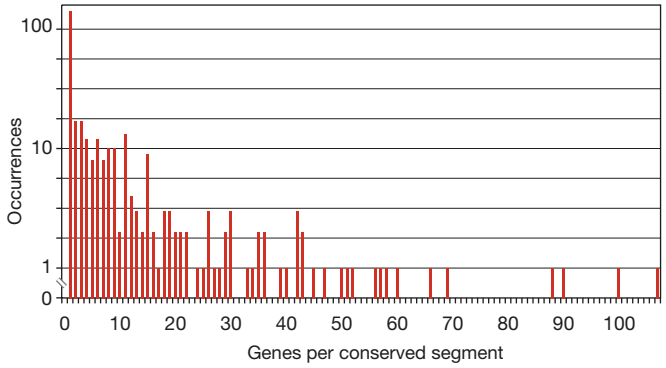

Figure 47 Distribution of number of genes per conserved segment between human and mouse genomes.

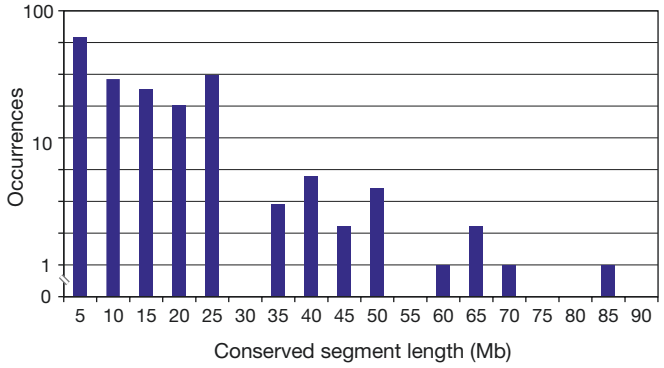

Figure 48 Distribution of lengths (in 5-Mb bins) of conserved segments between human and mouse genomes, omitting singletons.

© 2001 Macmillan Magazines Ltd

We also searched for sets of four chromosomes where there are multiple genes with homologues on each of the four. The strongest example was chromosomes 2, 7, 12 and 17, containing the HOX clusters as well as additional genes. These four chromosomes appear to have an excess of quadruplicated genes. The genes are not all clustered in a single region; this may reflect intrachromosomal rearrangement since the duplication of these genes, or it may indicate that they result from several independent events. Of the genes with homologues on chromosomes 2, 12 and 17, many of those missing on chromosome 7 are clustered on chromosome 3, suggesting a translocation. Several additional examples of groups of four chromosomes were found, although they were connected by fewer homologous genes.

Although the analyses are sensitive to the imperfect quality of the gene predictions, our results so far are insufficient to settle whether two rounds of WGD occurred around 500 Myr ago. It may be possible to resolve the issue by systematically estimating the time of each of the many gene duplication events on the basis of sequence divergence, although this is beyond the scope of this report. Another approach to determining whether a widespread duplication occurred at a particular time in vertebrate evolution would be to sequence the genomes of organisms whose lineages diverged from vertebrates at appropriate times, such as amphioxus.

Recent history from human polymorphism

The recent history of genomic segments can be probed by studying the properties of SNPs segregating in the current human population. The sequence information generated in the course of this project has yielded a huge collection of SNPs. These SNPs were extracted in two ways: by comparing overlapping large-insert clones derived from distinct haplotypes (either different individuals or different chromosomes within an individual) and by comparing random reads from whole-genome shotgun libraries derived from multiple individuals. The analysis confirms an average heterozygosity rate in the human population of about 1 in 1,300 bp (ref. 97).

More than 1.42 million SNPs have been assembled into a genome-wide map and are analysed in detail in an accompanying paper[97]. SNP density is also displayed across the genome in Fig. 9. The SNPs have an average spacing of 1.9 kb and 63% of 5-kb intervals contain a SNP. These polymorphisms are of immediate utility for medical genetic studies. Whereas investigators studying a gene previously had to expend considerable effort to discover polymorphisms across the region of interest, the current collection now provides then with about 15 SNPs for gene loci of average size.

The density of SNPs (adjusted for ascertainment—that is, polymorphisms per base screened) varies considerably across the genome[97] and sheds light on the unique properties and history of each genomic region. The average heterozygosity at a locus will tend to increase in proportion to the local mutation rate and the 'age' of the locus (which can be defined as the average number of generations since the most recent common ancestor of two randomly chosen copies in the population). For example, positive selection can cause a locus to be unusually 'young' and balancing selection can cause it to be unusually 'old'. An extreme example is the HLA region, in which a high SNP density is observed, reflecting the fact that diverse HLA haplotypes have been maintained for many millions of years by balancing selection and greatly predate the origin of the human species.

SNPs can also be used to study linkage disequilibrium in the human genome[376]. Linkage disequilibrium refers to the persistence of ancestral haplotypes—that is, genomic segments carrying particular combinations of alleles descended from a common ancestor. It can provide a powerful tool for mapping disease genes[377,378] and for probing population history[379–381]. There has been considerably controversy concerning the typical distance over which linkage disequilibrium extends in the human genome[382–387]. With the collection of SNPs now available, it should be possible to resolve this important issue.

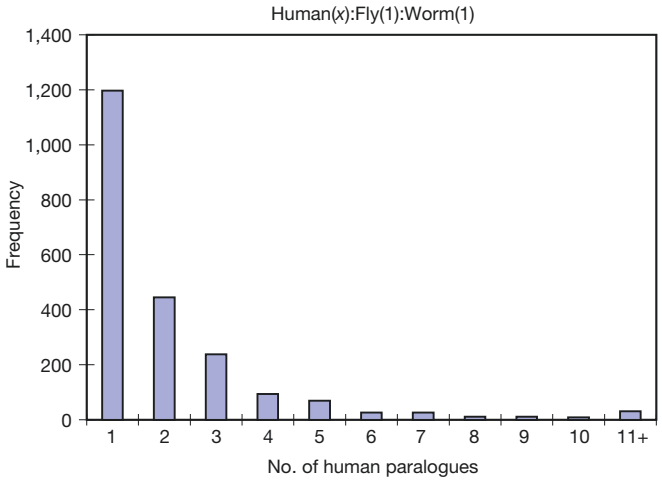

Figure 49 Number of human paralogues of genes having single orthologues in worm and fly.

Applications to medicine and biology

In most research papers, the authors can only speculate about future applications of the work. Because the genome sequence has been released on a daily basis over the past four years, however, we can already cite many direct applications. We focus on a handful of applications chosen primarily from medical research.

Disease genes

A key application of human genome research has been the ability to find disease genes of unknown biochemical function by positional cloning[388]. This method involves mapping the chromosomal region containing the gene by linkage analysis in affected families and then scouring the region to find the gene itself. Positional cloning is powerful, but it has also been extremely tedious. When the approach was first proposed in the early 1980s[9], a researcher wishing to perform positional cloning had to generate genetic markers to trace inheritance; perform chromosomal walking to obtain genomic DNA covering the region; and analyse a region of around 1 Mb by either direct sequencing or indirect gene identification methods. The first two barriers were eliminated with the development in the mid-1990s of comprehensive genetic and physical maps of the human chromosomes, under the auspices of the Human Genome Project. The remaining barrier, however, has continued to be formidable.

All that is changing with the availability of the human draft genome sequence. The human genomic sequence in public databases allows rapid identification *in silico* of candidate genes, followed by mutation screening of relevant candidates, aided by information on gene structure. For a mendelian disorder, a gene search can now often be carried out in a matter of months with only a modestly sized team.

At least 30 disease genes[55,389–422] (Table 26) have been positionally cloned in research efforts that depended directly on the publicly available genome sequence. As most of the human sequence has only arrived in the past twelve months, it is likely that many similar discoveries are not yet published. In addition, there are many cases in which the genome sequence played a supporting role, such as providing candidate microsatellite markers for finer genetic linkage analysis.

The genome sequence has also helped to reveal the mechanisms leading to some common chromosomal deletion syndromes. In several instances, recurrent deletions have been found to result from homologous recombination and unequal crossing over between large, nearly identical intrachromosomal duplications. Examples

© 2001 Macmillan Magazines Ltd

include the DiGeorge/velocardiofacial syndrome region on chromosome 22 (ref. 238) and the Williams–Beuren syndrome recurrent deletion on chromosome 7 (ref. 239).

The availability of the genome sequence also allows rapid identification of paralogues of disease genes, which is valuable for two reasons. First, mutations in a paralogous gene may give rise to a related genetic disease. A good example, discovered through use of the genome sequence, is achromatopsia (complete colour blindness). The *CNGA3* gene, encoding the α-subunit of the cone photoreceptor cyclic GMP-gated channel, had been shown to harbour mutations in some families with achromatopsia. Computational searching of the genome sequences revealed the paralogous gene encoding the corresponding β-subunit, *CNGB3* (which had not been apparent from EST databases). The *CNGB3* gene was rapidly shown to be the cause of achromatopsia in other families[407,408]. Another example is provided by the presenilin-1 and presenilin-2 genes, in which mutations can cause early-onset Alzheimer's disease[423,424]. Second, the paralogue may provide an opportunity for therapeutic intervention, as exemplified by attempts to reactivate the fetally expressed haemoglobin genes in individuals with sickle cell disease or β-thalassaemia, caused by mutations in the β-globin gene[425].

We undertook a systematic search for paralogues of 971 known human disease genes with entries in both the Online Mendelian Inheritance in Man (OMIM) database (http://www.ncbi.nlm.nih.gov/Omim/) and either the SwissProt or TrEMBL protein databases. We identified 286 potential paralogues (with the requirement of a match of at least 50 amino acids with identity greater than 70% but less than 90% if on the same chromosome, and less than 95% if on a different chromosome). Although this analysis may have identified some pseudogenes, 89% of the matches showed homology over more than one exon in the new target sequence, suggesting that many are functional. This analysis shows the potential for rapid identification of disease gene paralogues *in silico*.

Drug targets

Over the past century, the pharmaceutical industry has largely depended upon a limited set of drug targets to develop new therapies. A recent compendium[426,427] lists 483 drug targets as accounting for virtually all drugs on the market. Knowing the complete set of human genes and proteins will greatly expand the search for suitable drug targets. Although only a minority of human genes may be drug targets, it has been predicted that the number will exceed several thousand, and this prospect has led to a massive expansion of genomic research in pharmaceutical research and development. A few examples will illustrate the point.

(1) The neurotransmitter serotonin (5-HT) mediates rapid excitatory responses through ligand-gated channels. The previously identified 5-HT_{3A} receptor gene produces functional receptors, but with a much smaller conductance than observed *in vivo*. Cross-hybridization experiments and analysis of ESTs failed to reveal any other homologues of the known receptor. Recently, however, by searching the human draft genome sequence at low stringency, a putative homologue was identified within a PAC clone from the long arm of chromosome 11 (ref. 428). The homologue was shown to be expressed in the amygdala, caudate and hippocampus, and a full-length cDNA was subsequently obtained. The gene, which codes for a serotonin receptor, was named 5-HT_{3B}. When assembled in a heterodimer with 5-HT_{3A}, it was shown to account for the large-conductance neuronal serotonin channel. Given the central role of the serotonin pathway in mood disorders and schizophrenia, the discovery of a major new therapeutic target is of considerable interest.

(2) The contractile and inflammatory actions of the cysteinyl leukotrienes, formerly known as the slow reacting substance of anaphylaxis (SRS-A), are mediated through specific receptors. The second such receptor, $CysLT_2$, was identified using the combination of a rat EST and the human genome sequence. This led to the cloning of a gene with 38% amino-acid identity to the only other receptor that had previously been identified[429]. This new receptor, which shows high-affinity binding to several leukotrienes, maps to a region of chromosome 13 that is linked to atopic asthma. The gene is expressed in airway smooth muscles and in the heart. As the leukotriene pathway has been a significant target for the development of drugs against asthma, the discovery of a new receptor has obvious and important consequences.

(3) Abundant deposition of β-amyloid in senile plaques is the hallmark of Alzheimer's disease. β-Amyloid is generated by proteolytic processing of the amyloid precursor protein (APP). One of the enzymes involved is the β-site APP-cleaving enzyme (BACE), which is a transmembrane aspartyl protease. Computational searching of the public human draft genome sequence recently identified a new sequence homologous to BACE, encoding a protein now named BACE2[430,431]. BACE2, which has 52% amino-acid sequence identity to BACE, contains two active protease sites and maps to the obligatory Down's syndrome region of chromosome 21, as does APP. This raises the question of whether the extra copies of both BACE2 and APP may contribute to accelerated deposition of β-amyloid in the brains of Down's syndrome patients. The development of antagonists to BACE and BACE2 represents a promising approach to preventing Alzheimer's disease.

Given these examples, we undertook a systematic effort to identify paralogues of the classic drug target proteins in the draft genome sequence. The target list[427] was used to identify 603 entries in the SwissProt database with unique accession numbers. These were then searched against the current genome sequence database, using the requirement that a match should have 70–100% identity to at least 50 amino acids. Matches to named proteins were ignored, as we assumed that these represented known homologues.

We found 18 putative novel paralogues (Table 27), including apparent dopamine receptors, purinergic receptors and insulin-like growth factor receptors. In six cases, the novel paralogue matches at least one EST, adding confidence that this search process can identify novel functional genes. For the remaining 12 putative paralogues without an EST match, all have long ORFs and all but

Table 26 Disease genes positionally cloned using the draft genome sequence

Locus	Disorder	Reference(s)
BRCA2	Breast cancer susceptibility	55
AIRE	Autoimmune polyglandular syndrome type 1 (APS1 or APECED)	389
PEX1	Peroxisome biogenesis disorder	390, 391
PDS	Pendred syndrome	392
XLP	X-linked lymphoproliferative disease	393
DFNA5	Nonsyndromic deafness	394
ATP2A2	Darier's disease	395
SEDL	X-linked spondyloepiphyseal dysplasia tarda	396
WISP3	Progressive pseudorheumatoid dysplasia	397
CCM1	Cerebral cavernous malformations	398, 399
COL11A2/DFNA13	Nonsyndromic deafness	400
LGMD 2G	Limb-girdle muscular dystrophy	401
EVC	Ellis-Van Creveld syndrome, Weyer's acrodental dysostosis	402
ACTN4	Familial focal segmental glomerulosclerosis	403
SCN1A	Generalized epilepsy with febrile seizures plus type 2	404
AASS	Familial hyperlysinaemia	405
NDRG1	Hereditary motor and sensory neuropathy-Lom	406
CNGB3	Total colour-blindness	407, 408
MUL	Mulibrey nanism	409
USH1C	Usher type 1C	410, 411
MYH9	May-Hegglin anomaly	412, 413
PRKAR1A	Carney's complex	414
MYH9	Nonsyndromic hereditary deafness DFNA17	415
SCA10	Spinocerebellar ataxia type 10	416
OPA1	Optic atrophy	417
XLCSNB	X-linked congenital stationary night blindness	418
FGF23	Hypophosphataemic rickets	419
GAN	Giant axonal neuropathy	420
AAAS	Triple-A syndrome	421
HSPG2	Schwartz-Jampel syndrome	422

© 2001 Macmillan Magazines Ltd

one show similarity spanning multiple exons separated by introns, so these are not processed pseudogenes. They are likely to represent interesting new candidate drug targets.

Basic biology

Although the examples above reflect medical applications, there are also many similar applications to basic physiology and cell biology. To cite one satisfying example, the publicly available sequence was used to solve a mystery that had vexed investigators for several decades: the molecular basis of bitter taste[432]. Humans and other animals are polymorphic for response to certain bitter tastes. Recently, investigators mapped this trait in both humans and mice and then searched the relevant region of the human draft genome sequence for G-protein coupled receptors. These studies led, in quick succession, to the discovery of a new family of such proteins, the demonstration that they are expressed almost exclusively in taste buds, and the experimental confirmation that the receptors in cultured cells respond to specific bitter substances[433–435].

The next steps

Considerable progress has been made in human sequencing, but much remains to be done to produce a finished sequence. Even more work will be required to extract the full information contained in the sequence. Many of the key next steps are already underway.

Finishing the human sequence

The human sequence will serve as a foundation for biomedical research in the years ahead, and it is thus crucial that the remaining gaps be filled and ambiguities be resolved as quickly as possible. This will involve a three-step program.

The first stage involves producing finished sequence from clones spanning the current physical map, which covers more than 96% of the euchromatic regions of the genome. About 1 Gb of finished sequence is already completed. Almost all of the remaining clones are already sequenced to at least draft coverage, and the rest have been selected for sequencing. All clones are expected to reach 'full shotgun' coverage (8–10-fold redundancy) by about mid-2001 and finished form (99.99% accuracy) not long thereafter, using established and increasingly automated protocols.

The next stage will be to screen additional libraries to close gaps between clone contigs. Directed probing of additional large-insert clone libraries should close many of the remaining gaps. Unclosed gaps will be sized by FISH techniques or other methods. Two chromosomes, 22 and 21, have already been assembled in this 'essentially complete' form in this manner[93,94], and chromosomes 20, Y, 19, 14 and 7 are likely to reach this status in the next few months. All chromosomes should be essentially completed by 2003, if not sooner.

Finally, techniques must be developed to close recalcitrant gaps. Several hundred such gaps in the euchromatic sequence will probably remain in the genome after exhaustive screening of existing large-insert libraries. New methodologies will be needed to recover sequence from these segments, and to define biological reasons for their lack of representation in standard libraries. Ideally, it would be desirable to obtain complete sequence from all heterochromatic regions, such as centromeres and ribosomal gene clusters, although most of this sequence will consist of highly polymorphic tandem repeats containing few protein-coding genes.

Developing the IGI and IPI

The draft genome sequence has provided an initial look at the human gene content, but many ambiguities remain. A high priority will be to refine the IGI and IPI to the point where they accurately reflect every gene and every alternatively spliced form. Several steps are needed to reach this ambitious goal.

Finishing the human sequence will assist in this effort, but the experiences gained on chromosomes 21 and 22 show that sequence alone is not enough to allow complete gene identification. One powerful approach is cross-species sequence comparison with related organisms at suitable evolutionary distances. The sequence coverage from the pufferfish *T. nigroviridis* has already proven valuable in identifying potential exons[292]; this work is expected to continue from its current state of onefold coverage to reach at least fivefold coverage later this year. The genome sequence of the laboratory mouse will provide a particularly powerful tool for exon identification, as sequence similarity is expected to identify 95–97% of the exons, as well as a significant number of regulatory domains[436–438]. A public-private consortium is speeding this effort, by producing freely accessible whole-genome shotgun coverage that can be readily used for cross-species comparison[439]. More than onefold coverage from the C57BL/6J strain has already been completed and threefold is expected within the next few months. In the slightly longer term, a program is under way to produce a finished sequence of the laboratory mouse.

Another important step is to obtain a comprehensive collection of full-length human cDNAs, both as sequences and as actual clones. The Mammalian Gene Collection project has been underway for a year[18] and expects to produce 10,000–15,000 human full-length cDNAs over the coming year, which will be available without restrictions on use. The Genome Exploration Group of the RIKEN Genomic Sciences Center is similarly developing a collection of cDNA clones from mouse[309], which is a valuable complement

Table 27 New paralogues of common drug targets identified by searching the draft human genome sequence

Drug target	HGM symbol	Drug target SwissProt accession	Chromosome	Novel match IGI number	Chromosome containing paralogue	Per cent identity	dbEST GenBank accession
Aquaporin 7	AQP7	O14520	9	IGI_M1_ctg15869_11	2	92.3	AW593324
Arachidonate 12-lipoxygenase	ALOX12	P18054	17	IGI_M1_ctg17216_23	17	70.1	
Calcitonin	CALCA	P01258	11	IGI_M1_ctg14138_20	12	93.6	
Calcium channel, voltage-dependent, γ-subunit	CACNG2	Q9Y698	22	IGI_M1_ctg17137_10	19	70.7	
DNA polymerase-δ, small subunit	POLD2	P49005	7	IGI_M1_ctg12903_29	5	86.8	
Dopamine receptor, D1-α	DRD1	P21728	5	IGI_M1_ctg25203_33	16	70.7	
Dopamine receptor, D1-β	DRD5	P21918	4	IGI_M1_ctg17190_14	1	88.0	AI148329
Eukaryotic translation elongation factor, 1δ	EEF1D	P29692	2	IGI_M1_ctg16401_37	17	77.6	BE719683
FKBP, tacrolimus binding protein, FK506 binding protein	FKBP1B	Q16645	2	IGI_M1_ctg14291_56	6	79.4	
Glutamic acid decarboxylase	GAD1	Q99259	2	IGI_M1_ctg12341_103	18	70.5	
Glycine receptor, α1	GLRA1	P23415	5	IGI_M1_ctg16547_14	X	85.5	
Heparan *N*-deacetylase/*N*-sulphotransferase	NDST1	P52848	5	IGI_M1_ctg13263_18	4	81.5	
Insulin-like growth factor-1 receptor	IGF1R	P08069	15	IGI_M1_ctg18444_3	19	71.8	
Na,K-ATPase, α-subunit	ATP1A1	P05023	1	IGI_M1_ctg14877_54	1	83	
Purinergic receptor 7 (P2X), ligand-gated ion channel	P2RX7	Q99572	12	IGI_M1_ctg15140_15	12	80.3	H84353
Tubulin, ε-chain	TUBE*	Q9UJT0	6	IGI_M1_ctg13826_4	5	78.5	AA970498
Tubulin, χ-chain	TUBG1	P23258	17	IGI_M1_ctg12599_5	7	84.0	
Voltage-gated potassium channel, KV3.3	KCNC3	Q14003	19	IGI_M1_ctg13492_5	12	80.1	H49142

* HGM symbol unknown.

© 2001 Macmillan Magazines Ltd

because of the availability of tissues from all developmental time points. A challenge will be to define the gene-specific patterns of alternative splicing, which may affect half of human genes. Existing collections of ESTs and cDNAs may allow identification of the most abundant of these isoforms, but systematic exploration of this problem may require exhaustive analysis of cDNA libraries from multiple tissues or perhaps high-throughput reverse transcription–PCR studies. Deep understanding of gene function will probably require knowledge of the structure, tissue distribution and abundance of these alternative forms.

Large-scale identification of regulatory regions

The one-dimensional script of the human genome, shared by essentially all cells in all tissues, contains sufficient information to provide for differentiation of hundreds of different cell types, and the ability to respond to a vast array of internal and external influences. Much of this plasticity results from the carefully orchestrated symphony of transcriptional regulation. Although much has been learned about the *cis*-acting regulatory motifs of some specific genes, the regulatory signals for most genes remain uncharacterized. Comparative genomics of multiple vertebrates offers the best hope for large-scale identification of such regulatory sites[440]. Previous studies of sequence alignment of regulatory domains of orthologous genes in multiple species has shown a remarkable correlation between sequence conservation, dubbed 'phylogenetic footprints'[441], and the presence of binding motifs for transcription factors. This approach could be particularly powerful if combined with expression array technologies that identify cohorts of genes that are coordinately regulated, implicating a common set of *cis*-acting regulatory sequences[442–445]. It will also be of considerable interest to study epigenetic modifications such as cytosine methylation on a genome-wide scale, and to determine their biological consequences[446,447]. Towards this end, a pilot Human Epigenome Project has been launched[448,449].

Sequencing of additional large genomes

More generally, comparative genomics allows biologists to peruse evolution's laboratory notebook—to identify conserved functional features and recognize new innovations in specific lineages. Determination of the genome sequence of many organisms is very desirable. Already, projects are underway to sequence the genomes of the mouse, rat, zebrafish and the pufferfishes *T. nigroviridis* and *Takifugu rubripes*. Plans are also under consideration for sequencing additional primates and other organisms that will help define key developments along the vertebrate and nonvertebrate lineages.

To realize the full promise of comparative genomics, however, it needs to become simple and inexpensive to sequence the genome of any organism. Sequencing costs have dropped 100-fold over the last 10 years, corresponding to a roughly twofold decrease every 18 months. This rate is similar to 'Moore's law' concerning improvements in semiconductor manufacture. In both sequencing and semiconductors, such improvement does not happen automatically, but requires aggressive technological innovation fuelled by major investment. Improvements are needed to move current dideoxy sequencing to smaller volumes and more rapid sequencing times, based upon advances such as microchannel technology. More revolutionary methods, such as mass spectrometry, single-molecule sequencing and nanopore approaches[76], have not yet been fully developed, but hold great promise and deserve strong encouragement.

Completing the catalogue of human variation

The human draft genome sequence has already allowed the identification of more than 1.4 million SNPs, comprising a substantial proportion of all common human variation. This program should be extended to obtain a nearly complete catalogue of common variants and to identify the common ancestral haplotypes present in the population. In principle, these genetic tools should make it possible to perform association studies and linkage disequilibrium studies[376] to identify the genes that confer even relatively modest risk for common diseases. Launching such an intense era of human molecular epidemiology will also require major advances in the cost efficiency of genotyping technology, in the collection of carefully phenotyped patient cohorts and in statistical methods for relating large-scale SNP data to disease phenotype.

From sequence to function

The scientific program outlined above focuses on how the genome sequence can be mined for biological information. In addition, the sequence will serve as a foundation for a broad range of functional genomic tools to help biologists to probe function in a more systematic manner. These will need to include improved techniques and databases for the global analysis of: RNA and protein expression, protein localization, protein–protein interactions and chemical inhibition of pathways. New computational techniques will be needed to use such information to model cellular circuitry. A full discussion of these important directions is beyond the scope of this paper.

Concluding thoughts

The Human Genome Project is but the latest increment in a remarkable scientific program whose origins stretch back a hundred years to the rediscovery of Mendel's laws and whose end is nowhere in sight. In a sense, it provides a capstone for efforts in the past century to discover genetic information and a foundation for efforts in the coming century to understand it.

We find it humbling to gaze upon the human sequence now coming into focus. In principle, the string of genetic bits holds long-sought secrets of human development, physiology and medicine. In practice, our ability to transform such information into understanding remains woefully inadequate. This paper simply records some initial observations and attempts to frame issues for future study. Fulfilling the true promise of the Human Genome Project will be the work of tens of thousands of scientists around the world, in both academia and industry. It is for this reason that our highest priority has been to ensure that genome data are available rapidly, freely and without restriction.

The scientific work will have profound long-term consequences for medicine, leading to the elucidation of the underlying molecular mechanisms of disease and thereby facilitating the design in many cases of rational diagnostics and therapeutics targeted at those mechanisms. But the science is only part of the challenge. We must also involve society at large in the work ahead. We must set realistic expectations that the most important benefits will not be reaped overnight. Moreover, understanding and wisdom will be required to ensure that these benefits are implemented broadly and equitably. To that end, serious attention must be paid to the many ethical, legal and social implications (ELSI) raised by the accelerated pace of genetic discovery. This paper has focused on the scientific achievements of the human genome sequencing efforts. This is not the place to engage in a lengthy discussion of the ELSI issues, which have also been a major research focus of the Human Genome Project, but these issues are of comparable importance and could appropriately fill a paper of equal length.

Finally, it is has not escaped our notice that the more we learn about the human genome, the more there is to explore.

"We shall not cease from exploration. And the end of all our exploring will be to arrive where we started, and know the place for the first time."—T. S. Eliot[450] □

Received 7 December 2000; accepted 9 January 2001.

1. Correns, C. Untersuchungen über die Xenien bei Zea mays. *Berichte der Deutsche Botanische Gesellschaft* **17,** 410–418 (1899).
2. De Vries, H. Sur la loie de disjonction des hybrides. *Comptes Rendue Hebdemodaires, Acad. Sci. Paris* **130,** 845–847 (1900).
3. von Tschermack, E. Uber Künstliche Kreuzung bei Pisum sativum. *Berichte der Deutsche Botanische Gesellschaft* **18,** 232–239. (1900).
4. Sanger, F. *et al.* Nucleotide sequence of bacteriophage Φ X174 DNA. *Nature* **265,** 687–695 (1977).
5. Sanger, F. *et al.* The nucleotide sequence of bacteriophage ΦX174. *J Mol Biol* **125,** 225–246 (1978).

© 2001 Macmillan Magazines Ltd

6. Sanger, F., Coulson, A. R., Hong, G. F., Hill, D. F. & Petersen, G. B. Nucleotide-sequence of bacteriophage Lambda DNA. *J. Mol. Biol.* **162,** 729–773 (1982).
7. Fiers, W. *et al.* Complete nucleotide sequence of SV40 DNA. *Nature* **273,** 113–120 (1978).
8. Anderson, S. *et al.* Sequence and organization of the human mitochondrial genome. *Nature* **290,** 457–465 (1981).
9. Botstein, D., White, R. L., Skolnick, M. & Davis, R. W. Construction of a genetic linkage map in man using restriction fragment length polymorphisms. *Am. J. Hum. Genet.* **32,** 314–331 (1980).
10. Olson, M. V. *et al.* Random-clone strategy for genomic restriction mapping in yeast. *Proc. Natl Acad. Sci. USA* **83,** 7826–7830 (1986).
11. Coulson, A., Sulston, J., Brenner, S. & Karn, J. Toward a physical map of the genome of the nematode *Caenorhabditis elegans*. *Proc. Natl Acad. Sci. USA* **83,** 7821–7825 (1986).
12. Putney, S. D., Herlihy, W. C. & Schimmel, P. A new troponin T and cDNA clones for 13 different muscle proteins, found by shotgun sequencing. *Nature* **302,** 718–721 (1983).
13. Milner, R. J. & Sutcliffe, J. G. Gene expression in rat brain. *Nucleic Acids Res.* **11,** 5497–5520 (1983).
14. Adams, M. D. *et al.* Complementary DNA sequencing: expressed sequence tags and human genome project. *Science* **252,** 1651–1656 (1991).
15. Adams, M. D. *et al.* Initial assessment of human gene diversity and expression patterns based upon 83 million nucleotides of cDNA sequence. *Nature* **377,** 3–174 (1995).
16. Okubo, K. *et al.* Large scale cDNA sequencing for analysis of quantitative and qualitative aspects of gene expression. *Nature Genet.* **2,** 173–179 (1992).
17. Hillier, L. D. *et al.* Generation and analysis of 280,000 human expressed sequence tags. *Genome Res.* **6,** 807–828 (1996).
18. Strausberg, R. L., Feingold, E. A., Klausner, R. D. & Collins, F. S. The mammalian gene collection. *Science* **286,** 455–457 (1999).
19. Berry, R. *et al.* Gene-based sequence-tagged-sites (STSs) as the basis for a human gene map. *Nature Genet.* **10,** 415–423 (1995).
20. Houlgatte, R. *et al.* The Genexpress Index: a resource for gene discovery and the genic map of the human genome. *Genome Res.* **5,** 272–304 (1995).
21. Sinsheimer, R. L. The Santa Cruz Workshop—May 1985. *Genomics* **5,** 954–956 (1989).
22. Palca, J. Human genome—Department of Energy on the map. *Nature* **321,** 371 (1986).
23. National Research Council *Mapping and Sequencing the Human Genome* (National Academy Press, Washington DC, 1988).
24. Bishop, J. E. & Waldholz, M. *Genome* (Simon and Schuster, New York, 1990).
25. Kevles, D. J. & Hood, L. (eds) *The Code of Codes: Scientific and Social Issues in the Human Genome Project* (Harvard Univ. Press, Cambridge, Massachusetts, 1992).
26. Cook-Deegan, R. *The Gene Wars: Science, Politics, and the Human Genome* (W. W. Norton & Co., New York, London, 1994).
27. Donis-Keller, H. *et al.* A genetic linkage map of the human genome. *Cell* **51,** 319–337 (1987).
28. Gyapay, G. *et al.* The 1993–94 Genethon human genetic linkage map. *Nature Genet.* **7,** 246–339 (1994).
29. Hudson, T. J. *et al.* An STS-based map of the human genome. *Science* **270,** 1945–1954 (1995).
30. Dietrich, W. F. *et al.* A comprehensive genetic map of the mouse genome. *Nature* **380,** 149–152 (1996).
31. Nusbaum, C. *et al.* A YAC-based physical map of the mouse genome. *Nature Genet.* **22,** 388–393 (1999).
32. Oliver, S. G. *et al.* The complete DNA sequence of yeast chromosome III. *Nature* **357,** 38–46 (1992).
33. Wilson, R. *et al.* 2.2 Mb of contiguous nucleotide sequence from chromosome III of *C. elegans*. *Nature* **368,** 32–38 (1994).
34. Chen, E. Y. *et al.* The human growth hormone locus: nucleotide sequence, biology, and evolution. *Genomics* **4,** 479–497 (1989).
35. McCombie, W. R. *et al.* Expressed genes, Alu repeats and polymorphisms in cosmids sequenced from chromosome 4p16.3. *Nature Genet.* **1,** 348–353 (1992).
36. Martin-Gallardo, A. *et al.* Automated DNA sequencing and analysis of 106 kilobases from human chromosome 19q13.3. *Nature Genet.* **1,** 34–39 (1992).
37. Edwards, A. *et al.* Automated DNA sequencing of the human HPRT locus. *Genomics* **6,** 593–608 (1990).
38. Marshall, E. A strategy for sequencing the genome 5 years early. *Science* **267,** 783–784 (1995).
39. Project to sequence human genome moves on to the starting blocks. *Nature* **375,** 93–94 (1995).
40. Shizuya, H. *et al.* Cloning and stable maintenance of 300-kilobase-pair fragments of human DNA in *Escherichia coli* using an F-factor-based vector. *Proc. Natl Acad. Sci. USA* **89,** 8794–8797 (1992).
41. Burke, D. T., Carle, G. F. & Olson, M. V. Cloning of large segments of exogenous DNA into yeast by means of artificial chromosome vectors. *Science* **236,** 806–812 (1987).
42. Marshall, E. A second private genome project. *Science* **281,** 1121 (1998).
43. Marshall, E. NIH to produce a 'working draft' of the genome by 2001. *Science* **281,** 1774–1775 (1998).
44. Pennisi, E. Academic sequencers challenge Celera in a sprint to the finish. *Science* **283,** 1822–1823 (1999).
45. Bouck, J., Miller, W., Gorrell, J. H., Muzny, D. & Gibbs, R. A. Analysis of the quality and utility of random shotgun sequencing at low redundancies. *Genome Res.* **8,** 1074–1084 (1998).
46. Collins, F. S. *et al.* New goals for the U. S. Human Genome Project: 1998–2003. *Science* **282,** 682–689 (1998).
47. Sanger, F. & Coulson, A. R. A rapid method for determining sequences in DNA by primed synthesis with DNA polymerase. *J. Mol. Biol.* **94,** 441–448 (1975).
48. Maxam, A. M. & Gilbert, W. A new method for sequencing DNA. *Proc. Natl Acad. Sci. USA* **74,** 560–564 (1977).
49. Anderson, S. Shotgun DNA sequencing using cloned DNase I-generated fragments. *Nucleic Acids Res.* **9,** 3015–3027 (1981).
50. Gardner, R. C. *et al.* The complete nucleotide sequence of an infectious clone of cauliflower mosaic virus by M13mp7 shotgun sequencing. *Nucleic Acids Res.* **9,** 2871–2888 (1981).
51. Deininger, P. L. Random subcloning of sonicated DNA: application to shotgun DNA sequence analysis. *Anal. Biochem.* **129,** 216–223 (1983).
52. Chissoe, S. L. *et al.* Sequence and analysis of the human ABL gene, the BCR gene, and regions involved in the Philadelphia chromosomal translocation. *Genomics* **27,** 67–82 (1995).
53. Rowen, L., Koop, B. F. & Hood, L. The complete 685-kilobase DNA sequence of the human beta T cell receptor locus. *Science* **272,** 1755–1762 (1996).
54. Koop, B. F. *et al.* Organization, structure, and function of 95 kb of DNA spanning the murine T-cell receptor C alpha/C delta region. *Genomics* **13,** 1209–1230 (1992).
55. Wooster, R. *et al.* Identification of the breast cancer susceptibility gene BRCA2. *Nature* **378,** 789–792 (1995).
56. Fleischmann, R. D. *et al.* Whole-genome random sequencing and assembly of *Haemophilus influenzae* Rd. *Science* **269,** 496–512 (1995).
57. Lander, E. S. & Waterman, M. S. Genomic mapping by fingerprinting random clones: a mathematical analysis. *Genomics* **2,** 231–239 (1988).
58. Weber, J. L. & Myers, E. W. Human whole-genome shotgun sequencing. *Genome Res.* **7,** 401–409 (1997).
59. Green, P. Against a whole-genome shotgun. *Genome Res.* **7,** 410–417 (1997).
60. Venter, J. C. *et al.* Shotgun sequencing of the human genome. *Science* **280,** 1540–1542 (1998).
61. Venter, J. C. *et al.* The sequence of the human genome. *Science* **291,** 1304–1351 (2001).
62. Smith, L. M. *et al.* Fluorescence detection in automated DNA sequence analysis. *Nature* **321,** 674–679 (1986).
63. Ju, J. Y., Ruan, C. C., Fuller, C. W., Glazer, A. N. & Mathies, R. A. Fluorescence energy-transfer dye-labeled primers for DNA sequencing and analysis. *Proc. Natl Acad. Sci. USA* **92,** 4347–4351 (1995).
64. Lee, L. G. *et al.* New energy transfer dyes for DNA sequencing. *Nucleic Acids Res.* **25,** 2816–2822 (1997).
65. Rosenblum, B. B. *et al.* New dye-labeled terminators for improved DNA sequencing patterns. *Nucleic Acids Res.* **25,** 4500–4504 (1997).
66. Metzker, M. L., Lu, J. & Gibbs, R. A. Electrophoretically uniform fluorescent dyes for automated DNA sequencing. *Science* **271,** 1420–1422 (1996).
67. Prober, J. M. *et al.* A system for rapid DNA sequencing with fluorescent chain-terminating dideoxynucleotides. *Science* **238,** 336–341 (1987).
68. Reeve, M. A. & Fuller, C. W. A novel thermostable polymerase for DNA sequencing. *Nature* **376,** 796–797 (1995).
69. Tabor, S. & Richardson, C. C. Selective inactivation of the exonuclease activity of bacteriophage T7 DNA polymerase by in vitro mutagenesis. *J. Biol. Chem.* **264,** 6447–6458 (1989).
70. Tabor, S. & Richardson, C. C. DNA sequence analysis with a modified bacteriophage T7 DNA polymerase—effect of pyrophosphorolysis and metal ions. *J. Biol. Chem.* **265,** 8322–8328 (1990).
71. Murray, V. Improved double-stranded DNA sequencing using the linear polymerase chain reaction. *Nucleic Acids Res.* **17,** 8889 (1989).
72. Guttman, A., Cohen, A. S., Heiger, D. N. & Karger, B. L. Analytical and micropreparative ultrahigh resolution of oligonucleotides by polyacrylamide-gel high-performance capillary electrophoresis. *Anal. Chem.* **62,** 137–141 (1990).
73. Luckey, J. A. *et al.* High-speed DNA sequencing by capillary electrophoresis. *Nucleic Acids Res.* **18,** 4417–4421 (1990).
74. Swerdlow, H., Wu, S., Harke, H. & Dovichi, N. J. Capillary gel-electrophoresis for DNA sequencing—laser-induced fluorescence detection with the sheath flow cuvette. *J. Chromatogr.* **516,** 61–67 (1990).
75. Meldrum, D. Automation for genomics, part one: preparation for sequencing. *Genome Res.* **10,** 1081–1092 (2000).
76. Meldrum, D. Automation for genomics, part two: sequencers, microarrays, and future trends. *Genome Res.* **10,** 1288–1303 (2000).
77. Ewing, B. & Green, P. Base-calling of automated sequencer traces using phred. II. Error probabilities. *Genome Res.* **8,** 186–194 (1998).
78. Ewing, B., Hillier, L., Wendl, M. C. & Green, P. Base-calling of automated sequencer traces using phred. I. Accuracy assessment. *Genome Res.* **8,** 175–185 (1998).
79. Bentley, D. R. Genomic sequence information should be released immediately and freely in the public domain. *Science* **274,** 533–534 (1996).
80. Guyer, M. Statement on the rapid release of genomic DNA sequence. *Genome Res.* **8,** 413 (1998).
81. Dietrich, W. *et al.* A genetic map of the mouse suitable for typing intraspecific crosses. *Genetics* **131,** 423–447 (1992).
82. Kim, U. J. *et al.* Construction and characterization of a human bacterial artificial chromosome library. *Genomics* **34,** 213–218 (1996).
83. Osoegawa, K. *et al.* Bacterial artificial chromosome libraries for mouse sequencing and functional analysis. *Genome Res.* **10,** 116–128 (2000).
84. Marra, M. A. *et al.* High throughput fingerprint analysis of large-insert clones. *Genome Res.* **7,** 1072–1084 (1997).
85. Marra, M. *et al.* A map for sequence analysis of the *Arabidopsis thaliana* genome. *Nature Genet.* **22,** 265–270 (1999).
86. The International Human Genome Mapping Consortium. A physical map of the human genome. *Nature* **409,** 934–941 (2001).
87. Zhao, S. *et al.* Human BAC ends quality assessment and sequence analyses. *Genomics* **63,** 321–332 (2000).
88. Mahairas, G. G. *et al.* Sequence-tagged connectors: A sequence approach to mapping and scanning the human genome. *Proc. Natl Acad. Sci. USA* **96,** 9739–9744 (1999).
89. Tilford, C. A. *et al.* A physical map of the human Y chromosome. *Nature* **409,** 943–945 (2001).
90. Bentley, D. R. *et al.* The physical maps for sequencing human chromosomes 1, 6, 9, 10, 13, 20 and X. *Nature* **409,** 942–943 (2001).
91. Montgomery, K. T. *et al.* A high-resolution map of human chromosome 12. *Nature* **409,** 945–946 (2001).
92. Brüls, T. *et al.* A physical map of human chromosome 14. *Nature* **409,** 947–948 (2001).
93. Hattori, M. *et al.* The DNA sequence of human chromosome 21. *Nature* **405,** 311–319 (2000).
94. Dunham, I. *et al.* The DNA sequence of human chromosome 22. *Nature* **402,** 489–495 (1999).
95. Cox, D. *et al.* Radiation hybrid map of the human genome. *Science* (in the press).
96. Osoegawa, K. *et al.* An improved approach for construction of bacterial artificial chromosome libraries. *Genomics* **52,** 1–8 (1998).
97. The International SNP Map Working Group. A map of human genome sequence variation containing 1.42 million single nucleotide polymorphisms. *Nature* **409,** 928–933 (2001).
98. Collins, F. S., Brooks, L. D. & Chakravarti, A. A DNA polymorphism discovery resource for research on human genetic variation. *Genome Res.* **8,** 1229–1231 (1998).
99. Stewart, E. A. *et al.* An STS-based radiation hybrid map of the human genome. *Genome Res.* **7,** 422–433 (1997).
100. Deloukas, P. *et al.* A physical map of 30,000 human genes. *Science* **282,** 744–746 (1998).
101. Dib, C. *et al.* A comprehensive genetic map of the human genome based on 5,264 microsatellites.

© 2001 Macmillan Magazines Ltd

Nature **380,** 152–154 (1996).
102. Broman, K. W., Murray, J. C., Sheffield, V. C., White, R. L. & Weber, J. L. Comprehensive human genetic maps: individual and sex-specific variation in recombination. *Am. J. Hum. Genet.* **63,** 861–869 (1998).
103. The BAC Resource Consortium. Integration of cytogenetic landmarks into the draft sequence of the human genome. *Nature* **409,** 953–958 (2001).
104. Kent, W. J. & Haussler, D. GigAssembler: an algorithm for the initial assembly of the human working draft . Technical Report UCSC-CRL-00-17 (Univ. California at Santa Cruz, Santa Cruz, California, 2001).
105. Morton, N. E. Parameters of the human genome. *Proc. Natl Acad. Sci. USA* **88,** 7474–7476 (1991).
106. Podugolnikova, O. A. & Blumina, M. G. Heterochromatic regions on chromosomes 1, 9, 16, and Y in children with some disturbances occurring during embryo development. *Hum. Genet.* **63,** 183–188 (1983).
107. Lundgren, R., Berger, R. & Kristoffersson, U. Constitutive heterochromatin C-band polymorphism in prostatic cancer. *Cancer Genet. Cytogenet.* **51,** 57–62 (1991).
108. Lee, C., Wevrick, R., Fisher, R. B., Ferguson-Smith, M. A. & Lin, C. C. Human centromeric DNAs. *Hum. Genet.* **100,** 291–304 (1997).
109. Riethman, H. C. *et al.* Integration of telomere sequences with the draft human genome sequence. *Nature* **409,** 953–958 (2001).
110. Pruit, K. D. & Maglott, D. R. RefSeq and LocusLink: NCBI gene-centered resources. *Nucleic Acids Res.* **29,** 137–140 (2001).
111. Wolfsberg, T. G., McEntyre, J. & Schuler, G. D. Guide to the draft human genome. *Nature* **409,** 824–826 (2001).
112. Hurst, L. D. & Eyre-Walker, A. Evolutionary genomics: reading the bands. *Bioessays* **22,** 105–107 (2000).
113. Saccone, S. *et al.* Correlations between isochores and chromosomal bands in the human genome. *Proc. Natl Acad. Sci. USA* **90,** 11929–11933 (1993).
114. Zoubak, S., Clay, O. & Bernardi, G. The gene distribution of the human genome. *Gene* **174,** 95–102 (1996).
115. Gardiner, K. Base composition and gene distribution: critical patterns in mammalian genome organization. *Trends Genet.* **12,** 519–524 (1996).
116. Duret, L., Mouchiroud, D. & Gautier, C. Statistical analysis of vertebrate sequences reveals that long genes are scarce in GC-rich isochores. *J. Mol. Evol.* **40,** 308–317 (1995).
117. Saccone, S., De Sario, A., Della Valle, G. & Bernardi, G. The highest gene concentrations in the human genome are in telomeric bands of metaphase chromosomes. *Proc. Natl Acad. Sci. USA* **89,** 4913–4917 (1992).
118. Bernardi, G. *et al.* The mosaic genome of warm-blooded vertebrates. *Science* **228,** 953–958 (1985).
119. Bernardi, G. Isochores and the evolutionary genomics of vertebrates. *Gene* **241,** 3–17 (2000).
120. Fickett, J. W., Torney, D. C. & Wolf, D. R. Base compositional structure of genomes. *Genomics* **13,** 1056–1064 (1992).
121. Churchill, G. A. Stochastic models for heterogeneous DNA sequences. *Bull. Math. Biol.* **51,** 79–94 (1989).
122. Bird, A., Taggart, M., Frommer, M., Miller, O. J. & Macleod, D. A fraction of the mouse genome that is derived from islands of nonmethylated, CpG-rich DNA. *Cell* **40,** 91–99 (1985).
123. Bird, A. P. CpG islands as gene markers in the vertebrate nucleus. *Trends Genet.* **3,** 342–347 (1987).
124. Chan, M. F., Liang, G. & Jones, P. A. Relationship between transcription and DNA methylation. *Curr. Top. Microbiol. Immunol.* **249,** 75–86 (2000).
125. Holliday, R. & Pugh, J. E. DNA modification mechanisms and gene activity during development. *Science* **187,** 226–232 (1975).
126. Larsen, F., Gundersen, G., Lopez, R. & Prydz, H. CpG islands as gene markers in the human genome. *Genomics* **13,** 1095–1107 (1992).
127. Tazi, J. & Bird, A. Alternative chromatin structure at CpG islands. *Cell* **60,** 909–920 (1990).
128. Gardiner-Garden, M. & Frommer, M. CpG islands in vertebrate genomes. *J. Mol. Biol.* **196,** 261–282 (1987).
129. Antequera, F. & Bird, A. Number of CpG islands and genes in human and mouse. *Proc. Natl Acad. Sci. USA* **90,** 11995–11999 (1993).
130. Ewing, B. & Green, P. Analysis of expressed sequence tags indicates 35,000 human genes. *Nature Genet.* **25,** 232–234 (2000).
131. Yu, A. Comparison of human genetic and sequence-based physical maps. *Nature* **409,** 951–953 (2001).
132. Kaback, D. B., Guacci, V., Barber, D. & Mahon, J. W. Chromosome size-dependent control of meiotic recombination. *Science* **256,** 228–232 (1992).
133. Riles, L. *et al.* Physical maps of the 6 smallest chromosomes of *Saccharomyces cerevisiae* at a resolution of 2.6-kilobase pairs. *Genetics* **134,** 81–150 (1993).
134. Lynn, A. *et al.* Patterns of meiotic recombination on the long arm of human chromosome 21. *Genome Res.* **10,** 1319–1332 (2000).
135. Laurie, D. A. & Hulten, M. A. Further studies on bivalent chiasma frequency in human males with normal karyotypes. *Ann. Hum. Genet.* **49,** 189–201 (1985).
136. Roeder, G. S. Meiotic chromosomes: it takes two to tango. *Genes Dev.* **11,** 2600–2621 (1997).
137. Wu, T.-C. & Lichten, M. Meiosis-induced double-strand break sites determined by yeast chromatin structure. *Science* **263,** 515–518 (1994).
138. Gerton, J. L. *et al.* Global mapping of meiotic recombination hotspots and coldspots in the yeast *Saccharomyces cerevisiae*. *Proc. Natl Acad. Sci. USA* **97,** 11383–11390 (2000).
139. Li, W. -H. *Molecular Evolution* (Sinauer, Sunderland, Massachusetts, 1997).
140. Gregory, T. R. & Hebert, P. D. The modulation of DNA content: proximate causes and ultimate consequences. *Genome Res.* **9,** 317–324 (1999).
141. Hartl, D. L. Molecular melodies in high and low C. *Nature Rev. Genet.* **1,** 145–149 (2000).
142. Smit, A. F. Interspersed repeats and other mementos of transposable elements in mammalian genomes. *Curr. Opin. Genet. Dev.* **9,** 657–663 (1999).
143. Prak, E. L. & Haig, H. K. Jr Mobile elements and the human genome. *Nature Rev. Genet.* **1,** 134–144 (2000).
144. Okada, N., Hamada, M., Ogiwara, I. & Ohshima, K. SINEs and LINEs share common 3′ sequences: a review. *Gene* **205,** 229–243 (1997).
145. Esnault, C., Maestre, J. & Heidmann, T. Human LINE retrotransposons generate processed pseudogenes. *Nature Genet.* **24,** 363–367 (2000).
146. Wei, W. *et al.* Human L1 retrotransposition: cis-preference vs. trans-complementation. *Mol. Cell. Biol.* **21,** 1429–1439 (2001)
147. Malik, H. S., Henikoff, S. & Eickbush, T. H. Poised for contagion: evolutionary origins of the infectious abilities of invertebrate retroviruses. *Genome Res.* **10,** 1307–1318 (2000).
148. Smit, A. F. The origin of interspersed repeats in the human genome. *Curr. Opin. Genet. Dev.* **6,** 743–748 (1996).
149. Clark, J. B. & Tidwell, M. G. A phylogenetic perspective on P transposable element evolution in Drosophila. *Proc. Natl Acad. Sci. USA* **94,** 11428–11433 (1997).
150. Haring, E., Hagemann, S. & Pinsker, W. Ancient and recent horizontal invasions of Drosophilids by P elements. *J. Mol. Evol.* **51,** 577–586 (2000).
151. Koga, A. *et al.* Evidence for recent invasion of the medaka fish genome by the Tol2 transposable element. *Genetics* **155,** 273–281 (2000).
152. Robertson, H. M. & Lampe, D. J. Recent horizontal transfer of a mariner transposable element among and between Diptera and Neuroptera. *Mol. Biol. Evol.* **12,** 850–862 (1995).
153. Simmons, G. M. Horizontal transfer of hobo transposable elements within the *Drosophila melanogaster* species complex: evidence from DNA sequencing. *Mol. Biol. Evol.* **9,** 1050–1060 (1992).
154. Malik, H. S., Burke, W. D. & Eickbush, T. H. The age and evolution of non-LTR retrotransposable elements. *Mol. Biol. Evol.* **16,** 793–805 (1999).
155. Kordis, D. & Gubensek, F. Bov-B long interspersed repeated DNA (LINE) sequences are present in *Vipera ammodytes* phospholipase A2 genes and in genomes of Viperidae snakes. *Eur. J. Biochem.* **246,** 772–779 (1997).
156. Jurka, J. Repbase update: a database and an electronic journal of repetitive elements. *Trends Genet.* **16,** 418–420 (2000).
157. Sarich, V. M. & Wilson, A. C. Generation time and genome evolution in primates. *Science* **179,** 1144–1147 (1973).
158. Smit, A. F., Toth, G., Riggs, A. D., & Jurka, J. Ancestral, mammalian-wide subfamilies of LINE-1 repetitive sequences. *J. Mol. Biol.* **246,** 401–417 (1995).
159. Lim, J. K. & Simmons, M. J. Gross chromosome rearrangements mediated by transposable elements in *Drosophila melanogaster*. *Bioessays* **16,** 269–275 (1994).
160. Caceres, M., Ranz, J. M., Barbadilla, A., Long, M. & Ruiz, A. Generation of a widespread Drosophila inversion by a transposable element. *Science* **285,** 415–418 (1999).
161. Gray, Y. H. It takes two transposons to tango: transposable-element-mediated chromosomal rearrangements. *Trends Genet.* **16,** 461–468 (2000).
162. Zhang, J. & Peterson, T. Genome rearrangements by nonlinear transposons in maize. *Genetics* **153,** 1403–1410 (1999).
163. Smit, A. F. Identification of a new, abundant superfamily of mammalian LTR-transposons. *Nucleic Acids Res.* **21,** 1863–1872 (1993).
164. Cordonnier, A., Casella, J. F. & Heidmann, T. Isolation of novel human endogenous retrovirus-like elements with foamy virus-related pol sequence. *J. Virol.* **69,** 5890–5897 (1995).
165. Medstrand, P. & Mager, D. L. Human-specific integrations of the HERV-K endogenous retrovirus family. *J. Virol.* **72,** 9782–9787 (1998).
166. Myers, E. W. *et al.* A whole-genome assembly of Drosophila. *Science* **287,** 2196–2204 (2000).
167. Petrov, D. A., Lozovskaya, E. R. & Hartl, D. L. High intrinsic rate of DNA loss in *Drosophila*. *Nature* **384,** 346–349 (1996).
168. Li, W. H., Ellsworth, D. L., Krushkal, J., Chang, B. H. & Hewett-Emmett, D. Rates of nucleotide substitution in primates and rodents and the generation-time effect hypothesis. *Mol. Phylogenet. Evol.* **5,** 182–187 (1996).
169. Goodman, M. *et al.* Toward a phylogenetic classification of primates based on DNA evidence complemented by fossil evidence. *Mol. Phylogenet. Evol.* **9,** 585–598 (1998).
170. Kazazian, H. H. Jr & Moran, J. V. The impact of L1 retrotransposons on the human genome. *Nature Genet.* **19,** 19–24 (1998).
171. Malik, H. S. & Eickbush, T. H. NeSL-1, an ancient lineage of site-specific non-LTR retrotransposons from *Caenorhabditis elegans*. *Genetics* **154,** 193–203 (2000).
172. Casavant, N. C. *et al.* The end of the LINE?: lack of recent L1 activity in a group of South American rodents. *Genetics* **154,** 1809–1817 (2000).
173. Meunier-Rotival, M., Soriano, P., Cuny, G., Strauss, F. & Bernardi, G. Sequence organization and genomic distribution of the major family of interspersed repeats of mouse DNA. *Proc. Natl Acad. Sci. USA* **79,** 355–359 (1982).
174. Soriano, P., Meunier-Rotival, M. & Bernardi, G. The distribution of interspersed repeats is nonuniform and conserved in the mouse and human genomes. *Proc. Natl Acad. Sci. USA* **80,** 1816–1820 (1983).
175. Goldman, M. A., Holmquist, G. P., Gray, M. C., Caston, L. A. & Nag, A. Replication timing of genes and middle repetitive sequences. *Science* **224,** 686–692 (1984).
176. Manuelidis, L. & Ward, D. C. Chromosomal and nuclear distribution of the *Hin*dIII 1.9-kb human DNA repeat segment. *Chromosoma* **91,** 28–38 (1984).
177. Feng, Q., Moran, J. V., Kazazian, H. H. Jr & Boeke, J. D. Human L1 retrotransposon encodes a conserved endonuclease required for retrotransposition. *Cell* **87,** 905–916 (1996).
178. Jurka, J. Sequence patterns indicate an enzymatic involvement in integration of mammalian retroposons. *Proc. Natl Acad. Sci. USA* **94,** 1872–1877 (1997).
179. Arcot, S. S. *et al.* High-resolution cartography of recently integrated human chromosome 19-specific Alu fossils. *J. Mol. Biol.* **281,** 843–856 (1998).
180. Schmid, C. W. Does SINE evolution preclude Alu function? *Nucleic Acids Res.* **26,** 4541–4550 (1998).
181. Chu, W. M., Ballard, R., Carpick, B. W., Williams, B. R. & Schmid, C. W. Potential Alu function: regulation of the activity of double-stranded RNA-activated kinase PKR. *Mol. Cell. Biol.* **18,** 58–68 (1998).
182. Li, T., Spearow, J., Rubin, C. M. & Schmid, C. W. Physiological stresses increase mouse short interspersed element (SINE) RNA expression in vivo. *Gene* **239,** 367–372 (1999).
183. Liu, W. M., Chu, W. M., Choudary, P. V. & Schmid, C. W. Cell stress and translational inhibitors transiently increase the abundance of mammalian SINE transcripts. *Nucleic Acids Res.* **23,** 1758–1765 (1995).
184. Filipski, J. Correlation between molecular clock ticking, codon usage fidelity of DNA repair, chromosome banding and chromatin compactness in germline cells. *FEBS Lett.* **217,** 184–186 (1987).
185. Sueoka, N. Directional mutation pressure and neutral molecular evolution. *Proc. Natl Acad. Sci.*

© 2001 Macmillan Magazines Ltd

USA **85,** 2653–2657 (1988).
186. Wolfe, K. H., Sharp, P. M. & Li, W. H. Mutation rates differ among regions of the mammalian genome. *Nature* **337,** 283–285 (1989).
187. Bains, W. Local sequence dependence of rate of base replacement in mammals. *Mutat. Res.* **267,** 43–54 (1992).
188. Mathews, C. K. & Ji, J. DNA precursor asymmetries, replication fidelity, and variable genome evolution. *Bioessays* **14,** 295–301 (1992).
189. Holmquist, G. P. & Filipski, J. Organization of mutations along the genome: a prime determinant of genome evolution. *Trends Ecol. Evol.* **9,** 65–68 (1994).
190. Eyre-Walker, A. Evidence of selection on silent site base composition in mammals: potential implications for the evolution of isochores and junk DNA. *Genetics* **152,** 675–683 (1999).
191. The International SNP Map Working Group. An SNP map of the human genome generated by reduced representation shotgun sequencing. *Nature* **407,** 513–516 (2000).
192. Bohossian, H. B., Skaletsky, H. & Page, D. C. Unexpectedly similar rates of nucleotide substitution found in male and female hominids. *Nature* **406,** 622–625 (2000).
193. Skowronski, J., Fanning, T. G. & Singer, M. F. Unit-length LINE-1 transcripts in human teratocarcinoma cells. *Mol. Cell. Biol.* **8,** 1385–1397 (1988).
194. Boissinot, S., Chevret, P. & Furano, A. V. L1 (LINE-1) retrotransposon evolution and amplification in recent human history. *Mol. Biol. Evol.* **17,** 915–928 (2000).
195. Moran, J. V. Human L1 retrotransposition: insights and peculiarities learned from a cultured cell retrotransposition assay. *Genetica* **107,** 39–51 (1999).
196. Kazazian, H. H. Jr *et al.* Haemophilia A resulting from *de novo* insertion of L1 sequences represents a novel mechanism for mutation in man. *Nature* **332,** 164–166 (1988).
197. Sheen, F.-m. *et al.* Reading between the LINEs: Human genomic variation introduced by LINE-1 retrotransposition. *Genome Res.* **10,** 1496–1508 (2000).
198. Dombroski, B. A., Mathias, S. L., Nanthakumar, E., Scott, A. F. & Kazazian, H. H. Jr Isolation of an active human transposable element. *Science* **254,** 1805–1808 (1991).
199. Holmes, S. E., Dombroski, B. A., Krebs, C. M., Boehm, C. D. & Kazazian, H. H. Jr A new retrotransposable human L1 element from the LRE2 locus on chromosome 1q produces a chimaeric insertion. *Nature Genet.* **7,** 143–148 (1994).
200. Sassaman, D. M. *et al.* Many human L1 elements are capable of retrotransposition. *Nature Genet.* **16,** 37–43 (1997).
201. Dombroski, B. A., Scott, A. F. & Kazazian, H. H. Jr Two additional potential retrotransposons isolated from a human L1 subfamily that contains an active retrotransposable element. *Proc. Natl Acad. Sci. USA* **90,** 6513–6517 (1993).
202. Kimberland, M. L. *et al.* Full-length human L1 insertions retain the capacity for high frequency retrotransposition in cultured cells. *Hum. Mol. Genet.* **8,** 1557–1560 (1999).
203. Moran, J. V. *et al.* High frequency retrotransposition in cultured mammalian cells. *Cell* **87,** 917–927 (1996).
204. Moran, J. V., DeBerardinis, R. J. & Kazazian, H. H. Jr Exon shuffling by L1 retrotransposition. *Science* **283,** 1530–1534 (1999).
205. Pickeral, O. K., Makalowski, W., Boguski, M. S. & Boeke, J. D. Frequent human genomic DNA transduction driven by LINE-1 retrotransposition. *Genome Res.* **10,** 411–415 (2000).
206. Miki, Y. *et al.* Disruption of the APC gene by a retrotransposal insertion of L1 sequence in a colon cancer. *Cancer Res.* **52,** 643–645 (1992).
207. Branciforte, D. & Martin, S. L. Developmental and cell type specificity of LINE-1 expression in mouse testis: implications for transposition. *Mol. Cell. Biol.* **14,** 2584–2592 (1994).
208. Trelogan, S. A. & Martin, S. L. Tightly regulated, developmentally specific expression of the first open reading frame from LINE-1 during mouse embryogenesis. *Proc. Natl Acad. Sci. USA* **92,** 1520–1524 (1995).
209. Jurka, J. & Kapitonov, V. V. Sectorial mutagenesis by transposable elements. *Genetica* **107,** 239–248 (1999).
210. Fraser, M. J., Ciszczon, T., Elick, T. & Bauser, C. Precise excision of TTAA-specific lepidopteran transposons piggyBac (IFP2) and tagalong (TFP3) from the baculovirus genome in cell lines from two species of Lepidoptera. *Insect Mol. Biol.* **5,** 141–151 (1996).
211. Brosius, J. Genomes were forged by massive bombardments with retroelements and retrosequences. *Genetica* **107,** 209–238 (1999).
212. Kruglyak, S., Durrett, R. T., Schug, M. D. & Aquadro, C. F. Equilibrium distribution of microsatellite repeat length resulting from a balance between slippage events and point mutations. *Proc. Natl Acad. Sci. USA* **95,** 10774–10778 (1998).
213. Toth, G., Gaspari, Z. & Jurka, J. Microsatellites in different eukaryotic genomes: survey and analysis. *Genome Res.* **10,** 967–981 (2000).
214. Ellegren, H. Heterogeneous mutation processes in human microsatellite DNA sequences. *Nature Genet.* **24,** 400–402 (2000).
215. Ji, Y., Eichler, E. E., Schwartz, S. & Nicholls, R. D. Structure of chromosomal duplicons and their role in mediating human genomic disorders. *Genome Res.* **10,** 597–610 (2000).
216. Eichler, E. E. Masquerading repeats: paralogous pitfalls of the human genome. *Genome Res.* **8,** 758–762 (1998).
217. Mazzarella, R. & D. Schlessinger, D. Pathological consequences of sequence duplications in the human genome. *Genome Res.* **8,** 1007–1021 (1998).
218. Eichler, E. E. *et al.* Interchromosomal duplications of the adrenoleukodystrophy locus: a phenomenon of pericentromeric plasticity. *Hum. Mol. Genet.* **6,** 991–1002 (1997).
219. Horvath, J. E., Schwartz, S. & Eichler, E. E. The mosaic structure of human pericentromeric DNA: a strategy for characterizing complex regions of the human genome. *Genome Res.* **10,** 839–852 (2000).
220. Brand-Arpon, V. *et al.* A genomic region encompassing a cluster of olfactory receptor genes and a myosin light chain kinase (MYLK) gene is duplicated on human chromosome regions 3q13-q21 and 3p13. *Genomics* **56,** 98–110 (1999).
221. Arnold, N., Wienberg, J., Ermert, K. & Zachau, H. G. Comparative mapping of DNA probes derived from the V kappa immunoglobulin gene regions on human and great ape chromosomes by fluorescence in situ hybridization. *Genomics* **26,** 147–150 (1995).
222. Eichler, E. E. *et al.* Duplication of a gene-rich cluster between 16p11.1 and Xq28: a novel pericentromeric-directed mechanism for paralogous genome evolution. *Hum. Mol. Genet.* **5,** 899–912 (1996).
223. Potier, M. *et al.* Two sequence-ready contigs spanning the two copies of a 200-kb duplication on human 21q: partial sequence and polymorphisms. *Genomics* **51,** 417–426 (1998).
224. Regnier, V. *et al.* Emergence and scattering of multiple neurofibromatosis (NF1)-related sequences during hominoid evolution suggest a process of pericentromeric interchromosomal transposition. *Hum. Mol. Genet.* **6,** 9–16 (1997).
225. Ritchie, R. J., Mattei, M. G. & Lalande, M. A large polymorphic repeat in the pericentromeric region of human chromosome 15q contains three partial gene duplications. *Hum. Mol. Genet.* **7,** 1253–1260 (1998).
226. Trask, B. J. *et al.* Members of the olfactory receptor gene family are contained in large blocks of DNA duplicated polymorphically near the ends of human chromosomes. *Hum. Mol. Genet.* **7,** 13–26 (1998).
227. Trask, B. J. *et al.* Large multi-chromosomal duplications encompass many members of the olfactory receptor gene family in the human genome. *Hum. Mol. Genet.* **7,** 2007–2020 (1998).
228. van Deutekom, J. C. *et al.* Identification of the first gene (FRG1) from the FSHD region on human chromosome 4q35. *Hum. Mol. Genet.* **5,** 581–590 (1996).
229. Zachau, H. G. The immunoglobulin kappa locus—or—what has been learned from looking closely at one-tenth of a percent of the human genome. *Gene* **135,** 167–173 (1993).
230. Zimonjic, D. B., Kelley, M. J., Rubin, J. S., Aaronson, S. A. & Popescu, N. C. Fluorescence in situ hybridization analysis of keratinocyte growth factor gene amplification and dispersion in evolution of great apes and humans. *Proc. Natl Acad. Sci. USA* **94,** 11461–11465 (1997).
231. van Geel, M. *et al.* The FSHD region on human chromosome 4q35 contains potential coding regions among pseudogenes and a high density of repeat elements. *Genomics* **61,** 55–65 (1999).
232. Horvath, J. E. *et al.* Molecular structure and evolution of an alpha satellite/non-alpha satellite junction at 16p11. *Hum. Mol. Genet.* **9,** 113–123 (2000).
233. Guy, J. *et al.* Genomic sequence and transcriptional profile of the boundary between pericentromeric satellites and genes on human chromosome arm 10q. *Hum. Mol. Genet.* **9,** 2029–2042 (2000).
234. Reiter, L. T., Murakami, T., Koeuth, T., Gibbs, R. A. & Lupski, J. R. The human COX10 gene is disrupted during homologous recombination between the 24 kb proximal and distal CMT1A-REPs. *Hum. Mol. Genet.* **6,** 1595–1603 (1997).
235. Amos-Landgraf, J. M. *et al.* Chromosome breakage in the Prader-Willi and Angelman syndromes involves recombination between large, transcribed repeats at proximal and distal breakpoints. *Am. J. Hum. Genet.* **65,** 370–386 (1999).
236. Christian, S. L., Fantes, J. A., Mewborn, S. K., Huang, B. & Ledbetter, D. H. Large genomic duplicons map to sites of instability in the Prader-Willi/Angelman syndrome chromosome region (15q11-q13). *Hum. Mol. Genet.* **8,** 1025–1037 (1999).
237. Edelmann, L., Pandita, R. K. & Morrow, B. E. Low-copy repeats mediate the common 3-Mb deletion in patients with velo-cardio-facial syndrome. *Am. J. Hum. Genet.* **64,** 1076–1086 (1999).
238. Shaikh, T. H. *et al.* Chromosome 22-specific low copy repeats and the 22q11.2 deletion syndrome: genomic organization and deletion endpoint analysis. *Hum. Mol. Genet.* **9,** 489–501 (2000).
239. Francke, U. Williams-Beuren syndrome: genes and mechanisms. *Hum. Mol. Genet.* **8,** 1947–1954 (1999).
240. Peoples, R. *et al.* A physical map, including a BAC/PAC clone contig, of the Williams-Beuren syndrome-deletion region at 7q11.23. *Am. J. Hum. Genet.* **66,** 47–68 (2000).
241. Eichler, E. E., Archidiacono, N. & Rocchi, M. CAGGG repeats and the pericentromeric duplication of the hominoid genome. *Genome Res.* **9,** 1048–1058 (1999).
242. O'Keefe, C. & Eichler, E. in *Comparative Genomics: Empirical and Analytical Approaches to Gene Order Dynamics, Map Alignment and the Evolution of Gene Families* (eds Sankoff, D. & Nadeau, J.) 29–46 (Kluwer Academic, Dordrecht, 2000).
243. Lander, E. S. The new genomics: Global views of biology. *Science* **274,** 536–539 (1996).
244. Eddy, S. R. Noncoding RNA genes. *Curr. Op. Genet. Dev.* **9,** 695–699 (1999).
245. Ban, N., Nissen, P., Hansen, J., Moore, P. B. & Steitz, T. A. The complete atomic structure of the large ribosomal subunit at 2.4 angstrom resolution. *Science* **289,** 905–920 (2000).
246. Nissen, P., Hansen, J., Ban, N., Moore, P. B. & Steitz, T. A. The structural basis of ribosome activity in peptide bond synthesis. *Science* **289,** 920–930 (2000).
247. Weinstein, L. B. & Steitz, J. A. Guided tours: from precursor snoRNA to functional snoRNP. *Curr. Opin. Cell Biol.* **11,** 378–384 (1999).
248. Bachellerie, J.-P. & Cavaille, J. in *Modification and Editing of RNA* (ed. Benne, H. G. a. R.) 255–272 (ASM, Washington DC, 1998).
249. Burge, C. & Sharp, P. A. Classification of introns: U2-type or U12-type. *Cell* **91,** 875–879 (1997).
250. Brown, C. J. *et al.* The Human Xist gene—analysis of a 17 kb inactive X-specific RNA that contains conserved repeats and is highly localized within the nucleus. *Cell* **71,** 527–542 (1992).
251. Kickhoefer, V. A., Vasu, S. K. & Rome, L. H. Vaults are the answer, what is the question? *Trends Cell Biol.* **6,** 174–178 (1996).
252. Hatlen, L. & Attardi, G. Proportion of the HeLa cell genome complementary to the transfer RNA and 5S RNA. *J. Mol. Biol.* **56,** 535–553 (1971).
253. Sprinzl, M., Horn, C., Brown, M., Ioudovitch, A. & Steinberg, S. Compilation of tRNA sequences and sequences of tRNA genes. *Nucleic Acids Res.* **26,** 148–153 (1998).
254. Long, E. O. & Dawid, I. B. Repeated genes in eukaryotes. *Annu. Rev. Biochem.* **49,** 727–764 (1980).
255. Crick, F. H. Codon–anticodon pairing: the wobble hypothesis. *J. Mol. Biol.* **19,** 548–555 (1966).
256. Guthrie, C. & Abelson, J. in *The Molecular Biology of the Yeast Saccharomyces: Metabolism and Gene Expression* (eds Strathern, J. & Broach J.) 487–528 (Cold Spring Harbor Laboratory Press, Cold Spring Harbor, New York, 1982).
257. Soll, D. & RajBhandary, U. (eds) *tRNA: Structure, Biosynthesis, and Function* (ASM, Washington DC, 1995).
258. Ikemura, T. Codon usage and tRNA content in unicellular and multicellular organisms. *Mol. Biol. Evol.* **2,** 13–34 (1985).
259. Bulmer, M. Coevolution of codon usage and transfer-RNA abundance. *Nature* **325,** 728–730 (1987).
260. Duret, L. tRNA gene number and codon usage in the *C. elegans* genome are co-adapted for optimal translation of highly expressed genes. *Trends Genet.* **16,** 287–289 (2000).
261. Sharp, P. M. & Matassi, G. Codon usage and genome evolution. *Curr. Opin. Genet. Dev.* **4,** 851–860 (1994).
262. Buckland, R. A. A primate transfer-RNA gene cluster and the evolution of human chromosome 1. *Cytogenet. Cell Genet.* **61,** 1–4 (1992).
263. Gonos, E. S. & Goddard, J. P. Human tRNA-Glu genes: their copy number and organization. *FEBS Lett.* **276,** 138–142 (1990).
264. Sylvester, J. E. *et al.* The human ribosomal RNA genes: structure and organization of the complete repeating unit. *Hum. Genet.* **73,** 193–198 (1986).

© 2001 Macmillan Magazines Ltd

265. Sorensen, P. D. & Frederiksen, S. Characterization of human 5S ribosomal RNA genes. *Nucleic Acids Res.* **19,** 4147–4151 (1991).
266. Timofeeva, M. *et al.* [Organization of a 5S ribosomal RNA gene cluster in the human genome]. *Mol. Biol. (Mosk.)* **27,** 861–868 (1993).
267. Little, R. D. & Braaten, D. C. Genomic organization of human 5S rDNA and sequence of one tandem repeat. *Genomics* **4,** 376–383 (1989).
268. Maden, B. E. H. The numerous modified nucleotides in eukaryotic ribosomal RNA. *Prog. Nucleic Acid Res. Mol. Biol.* **39,** 241–303 (1990).
269. Tycowski, K. T., You, Z. H., Graham, P. J. & Steitz, J. A. Modification of U6 spliceosomal RNA is guided by other small RNAs. *Mol. Cell* **2,** 629–638 (1998).
270. Pavelitz, T., Liao, D. Q. & Weiner, A. M. Concerted evolution of the tandem array encoding primate U2 snRNA (the RNU2 locus) is accompanied by dramatic remodeling of the junctions with flanking chromosomal sequences. *EMBO J.* **18,** 3783–3792 (1999).
271. Lindgren, V., Ares, A., Weiner, A. M. & Francke, U. Human genes for U2 small nuclear RNA map to a major adenovirus 12 modification site on chromosome 17. *Nature* **314,** 115–116 (1985).
272. Van Arsdell, S. W. & Weiner, A. M. Human genes for U2 small nuclear RNA are tandemly repeated. *Mol. Cell. Biol.* **4,** 492–499 (1984).
273. Gao, L. I., Frey, M. R. & Matera, A. G. Human genes encoding U3 snRNA associate with coiled bodies in interphase cells and are clustered on chromosome 17p11. 2 in a complex inverted repeat structure. *Nucleic Acids Res.* **25,** 4740–4747 (1997).
274. Hawkins, J. D. A survey on intron and exon lengths. *Nucleic Acids Res.* **16,** 9893–9908 (1988).
275. Burge, C. & Karlin, S. Prediction of complete gene structures in human genomic DNA. *J. Mol. Biol.* **268,** 78–94 (1997).
276. Labeit, S. & Kolmerer, B. Titins: giant proteins in charge of muscle ultrastructure and elasticity. *Science* **270,** 293–296 (1995).
277. Sterner, D. A., Carlo, T. & Berget, S. M. Architectural limits on split genes. *Proc. Natl Acad. Sci. USA* **93,** 15081–15085 (1996).
278. Sun, Q., Mayeda, A., Hampson, R. K., Krainer, A. R. & Rottman, F. M. General splicing factor SF2/ASF promotes alternative splicing by binding to an exonic splicing enhancer. *Genes Dev.* **7,** 2598–2608 (1993).
279. Tanaka, K., Watakabe, A. & Shimura, Y. Polypurine sequences within a downstream exon function as a splicing enhancer. *Mol. Cell. Biol.* **14,** 1347–1354 (1994).
280. Carlo, T., Sterner, D. A. & Berget, S. M. An intron splicing enhancer containing a G-rich repeat facilitates inclusion of a vertebrate micro-exon. *RNA* **2,** 342–353 (1996).
281. Burset, M., Seledtsov, I. A. & Solovyev, V. V. Analysis of canonical and non-canonical splice sites in mammalian genomes. *Nucleic Acids Res.* **28,** 4364–4375 (2000).
282. Burge, C. B., Padgett, R. A. & Sharp, P. A. Evolutionary fates and origins of U12-type introns. *Mol. Cell* **2,** 773–785 (1998).
283. Mironov, A. A., Fickett, J. W. & Gelfand, M. S. Frequent alternative splicing of human genes. *Genome Res.* **9,** 1288–1293 (1999).
284. Hanke, J. *et al.* Alternative splicing of human genes: more the rule than the exception? *Trends Genet.* **15,** 389–390 (1999).
285. Brett, D. *et al.* EST comparison indicates 38% of human mRNAs contain possible alternative splice forms. *FEBS Lett.* **474,** 83–86 (2000).
286. Dunham, I. The gene guessing game. *Yeast* **17,** 218–224 (2000).
287. Lewin, B. *Gene Expression* (Wiley, New York, 1980).
288. Lewin, B. *Genes IV* 466–481 (Oxford Univ. Press, Oxford, 1990).
289. Smaglik, P. Researchers take a gamble on the human genome. *Nature* **405,** 264 (2000).
290. Fields, C., Adams, M. D., White, O. & Venter, J. C. How many genes in the human genome? *Nature Genet.* **7,** 345–346 (1994).
291. Liang, F. *et al.* Gene index analysis of the human genome estimates approximately 120,000 genes. *Nature Genet.* **25,** 239–240 (2000).
292. Roest Crollius, H. *et al.* Estimate of human gene number provided by genome-wide analysis using *Tetraodon nigroviridis* DNA sequence. *Nature Genet.* **25,** 235–238 (2000).
293. The C. elegans Sequencing Consortium. Genome sequence of the nematode *C. elegans*: A platform for investigating biology. *Science* **282,** 2012–2018 (1998).
294. Rubin, G. M. *et al.* Comparative genomics of the eukaryotes. *Science* **287,** 2204–2215 (2000).
295. Green, P. *et al.* Ancient conserved regions in new gene sequences and the protein databases. *Science* **259,** 1711–1716 (1993).
296. Fraser, A. G. *et al.* Functional genomic analysis of *C. elegans* chromosome I by systematic RNA interference. *Nature* **408,** 325–330 (2000).
297. Mott, R. EST_GENOME: a program to align spliced DNA sequences to unspliced genomic DNA. *Comput. Appl. Biosci.* **13,** 477–478 (1997).
298. Florea, L., Hartzell, G., Zhang, Z., Rubin, G. M. & Miller, W. A computer program for aligning a cDNA sequence with a genomic DNA sequence. *Genome Res.* **8,** 967–974 (1998).
299. Bailey, L. C. Jr, Searls, D. B. & Overton, G. C. Analysis of EST-driven gene annotation in human genomic sequence. *Genome Res.* **8,** 362–376 (1998).
300. Birney, E., Thompson, J. D. & Gibson, T. J. PairWise and SearchWise: finding the optimal alignment in a simultaneous comparison of a protein profile against all DNA translation frames. *Nucleic Acids Res.* **24,** 2730–2739 (1996).
301. Gelfand, M. S., Mironov, A. A. & Pevzner, P. A. Gene recognition via spliced sequence alignment. *Proc. Natl Acad. Sci. USA* **93,** 9061–9066 (1996).
302. Kulp, D., Haussler, D., Reese, M. G. & Eeckman, F. H. A generalized hidden Markov model for the recognition of human genes in DNA. *ISMB* **4,** 134–142 (1996).
303. Reese, M. G., Kulp, D., Tammana, H. & Haussler, D. Genie—gene finding in *Drosophila melanogaster. Genome Res.* **10,** 529–538 (2000).
304. Solovyev, V. & Salamov, A. The Gene-Finder computer tools for analysis of human and model organisms genome sequences. *ISMB* **5,** 294–302 (1997).
305. Guigo, R., Agarwal, P., Abril, J. F., Burset, M. & Fickett, J. W. An assessment of gene prediction accuracy in large DNA sequences. *Genome Res.* **10,** 1631–1642 (2000).
306. Hubbard, T. & Birney, E. Open annotation offers a democratic solution to genome sequencing. *Nature* **403,** 825 (2000).
307. Bateman, A. *et al.* The Pfam protein families database. *Nucleic Acids Res.* **28,** 263–266 (2000).
308. Birney, E. & Durbin, R. Using GeneWise in the Drosophila annotation experiment. *Genome Res.* **10,** 547–548 (2000).
309. The RIKEN Genome Exploration Research Group Phase II Team and the FANTOM Consortium. Functional annotation of a full-length mouse cDNA collection. *Nature* **409,** 685–690 (2001).
310. Basrai, M. A., Hieter, P. & Boeke, J. D. Small open reading frames: beautiful needles in the haystack. *Genome Res.* **7,** 768–771 (1997).
311. Janin, J. & Chothia, C. Domains in proteins: definitions, location, and structural principles. *Methods Enzymol.* **115,** 420–430 (1985).
312. Ponting, C. P., Schultz, J., Copley, R. R., Andrade, M. A. & Bork, P. Evolution of domain families. *Adv. Protein Chem.* **54,** 185–244 (2000).
313. Doolittle, R. F. The multiplicity of domains in proteins. *Annu. Rev. Biochem.* **64,** 287–314 (1995).
314. Bateman, A. & Birney, E. Searching databases to find protein domain organization. *Adv. Protein Chem.* **54,** 137–157 (2000).
315. Futreal, P. A. *et al.* Cancer and genomics. *Nature* **409,** 850–852 (2001).
316. Nestler, E. J. & Landsman, D. Learning about addiction from the human draft genome. *Nature* **409,** 834–835 (2001).
317. Tupler, R., Perini, G. & Green, M. R. Expressing the human genome. *Nature* **409,** 832–835 (2001).
318. Fahrer, A. M., Bazan, J. F., Papathanasiou, P., Nelms, K. A. & Goodnow, C. C. A genomic view of immunology. *Nature* **409,** 836–838 (2001).
319. Li, W. -H., Gu, Z., Wang, H. & Nekrutenko, A. Evolutionary analyses of the human genome. *Nature* **409,** 847–849 (2001).
320. Bock, J. B., Matern, H. T., Peden, A. A. & Scheller, R. H. A genomic perspective on membrane compartment organization. *Nature* **409,** 839–841 (2001).
321. Pollard, T. D. Genomics, the cytoskeleton and motility. *Nature* **409,** 842–843 (2001).
322. Murray, A. W. & Marks, D. Can sequencing shed light on cell cycling? *Nature* **409,** 844–846 (2001).
323. Clayton, J. D., Kyriacou, C. P. & Reppert, S. M. Keeping time with the human genome. *Nature* **409,** 829–831 (2001).
324. Chervitz, S. A. *et al.* Comparison of the complete protein sets of worm and yeast: orthology and divergence. *Science* **282,** 2022–2028 (1998).
325. Aravind, L. & Subramanian, G. Origin of multicellular eukaryotes—insights from proteome comparisons. *Curr. Opin. Genet. Dev.* **9,** 688–694 (1999).
326. Attwood, T. K. *et al.* PRINTS-S: the database formerly known as PRINTS. *Nucleic Acids Res.* **28,** 225–227 (2000).
327. Hofmann, K., Bucher, P., Falquet, L. & Bairoch, A. The PROSITE database, its status in 1999. *Nucleic Acids Res.* **27,** 215–219 (1999).
328. Altschul, S. F. *et al.* Gapped BLAST and PSI-BLAST: a new generation of protein database search programs. *Nucleic Acids Res.* **25,** 3389–3402 (1997).
329. Wolf, Y. I., Kondrashov, F. A. & Koonin, E. V. No footprints of primordial introns in a eukaryotic genome. *Trends Genet.* **16,** 333–334 (2000).
330. Brunner, H. G., Nelen, M., Breakefield, X. O., Ropers, H. H. & van Oost, B. B. A. Abnormal behavior associated with a point mutation in the structural gene for monoamine oxidase A. *Science* **262,** 578–580 (1993).
331. Cases, O. *et al.* Aggressive behavior and altered amounts of brain serotonin and norepinephrine in mice lacking MAOA. *Science* **268,** 1763–1766 (1995).
332. Brunner, H. G. *et al.* X-linked borderline mental retardation with prominent behavioral disturbance: phenotype, genetic localization, and evidence for disturbed monoamine metabolism. *Am. J. Hum. Genet.* **52,** 1032–1039 (1993).
333. Deckert, J. *et al.* Excess of high activity monoamine oxidase A gene promoter alleles in female patients with panic disorder. *Hum. Mol. Genet.* **8,** 621–624 (1999).
334. Smith, T. F. & Waterman, M. S. Identification of common molecular subsequences. *J. Mol. Biol.* **147,** 195–197 (1981).
335. Tatusov, R. L., Koonin, E. V. & Lipman, D. J. A genomic perspective on protein families. *Science* **278,** 631–637 (1997).
336. Ponting, C. P., Aravind, L., Schultz, J., Bork, P. & Koonin, E. V. Eukaryotic signalling domain homologues in archaea and bacteria. Ancient ancestry and horizontal gene transfer. *J. Mol. Biol.* **289,** 729–745 (1999).
337. Zhang, J., Dyer, K. D. & Rosenberg, H. F. Evolution of the rodent eosinophil-associated Rnase gene family by rapid gene sorting and positive selection. *Proc. Natl Acad. Sci. USA* **97,** 4701–4706 (2000).
338. Shashoua, V. E. Ependymin, a brain extracellular glycoprotein, and CNS plasticity. *Ann. NY Acad. Sci.* **627,** 94–114 (1991).
339. Schultz, J., Copley, R. R., Doerks, T., Ponting, C. P. & Bork, P. SMART: a web-based tool for the study of genetically mobile domains. *Nucleic Acids Res.* **28,** 231–234 (2000).
340. Koonin, E. V., Aravind, L. & Kondrashov, A. S. The impact of comparative genomics on our understanding of evolution. *Cell* **101,** 573–576 (2000).
341. Bateman, A., Eddy, S. R. & Chothia, C. Members of the immunoglobulin superfamily in bacteria. *Protein Sci.* **5,** 1939–1941 (1996).
342. Sutherland, D., Samakovlis, C. & Krasnow, M. A. Branchless encodes a Drosophila FGF homolog that controls tracheal cell migration and the pattern of branching. *Cell* **87,** 1091–1101 (1996).
343. Warburton, D. *et al.* The molecular basis of lung morphogenesis. *Mech. Dev.* **92,** 55–81 (2000).
344. Fuchs, T., Glusman, G., Horn-Saban, S., Lancet, D. & Pilpel, Y. The human olfactory subgenome: from sequence to structure to evolution. *Hum. Genet.* **108,** 1–13 (2001).
345. Glusman, G. *et al.* The olfactory receptor gene family: data mining, classification and nomenclature. *Mamm. Genome* **11,** 1016–1023 (2000).
346. Rouquier, S. *et al.* Distribution of olfactory receptor genes in the human genome. *Nature Genet.* **18,** 243–250 (1998).
347. Sharon, D. *et al.* Primate evolution of an olfactory receptor cluster: Diversification by gene conversion and recent emergence of a pseudogene. *Genomics* **61,** 24–36 (1999).
348. Gilad, Y. *et al.* Dichotomy of single-nucleotide polymorphism haplotypes in olfactory receptor genes and pseudogenes. *Nature Genet.* **26,** 221–224 (2000).
349. Gearhart, J. & Kirschner, M. *Cells, Embryos, and Evolution* (Blackwell Science, Malden, Massachusetts, 1997).
350. Barbazuk, W. B. *et al.* The syntenic relationship of the zebrafish and human genomes. *Genome Res.* **10,** 1351–1358 (2000).
351. McLysaght, A., Enright, A. J., Skrabanek, L. & Wolfe, K. H. Estimation of synteny conservation and genome compaction between pufferfish (Fugu) and human. *Yeast* **17,** 22–36 (2000).
352. Trachtulec, Z. *et al.* Linkage of TATA-binding protein and proteasome subunit C5 genes in mice and humans reveals synteny conserved between mammals and invertebrates. *Genomics* **44,** 1–7 (1997).

© 2001 Macmillan Magazines Ltd

353. Nadeau, J. H. Maps of linkage and synteny homologies between mouse and man. *Trends Genet.* **5,** 82–86 (1989).
354. Nadeau, J. H. & Taylor, B. A. Lengths of chromosomal segments conserved since divergence of man and mouse. *Proc. Natl Acad. Sci. USA* **81,** 814–818 (1984).
355. Copeland, N. G. *et al.* A genetic linkage map of the mouse: current applications and future prospects. *Science* **262,** 57–66 (1993).
356. DeBry, R. W. & Seldin, M. F. Human/mouse homology relationships. *Genomics* **33,** 337–351 (1996).
357. Nadeau, J. H. & Sankoff, D. The lengths of undiscovered conserved segments in comparative maps. *Mamm. Genome* **9,** 491–495 (1998).
358. Thomas, J. W. *et al.* Comparative genome mapping in the sequence-based era: early experience with human chromosome 7. *Genome Res.* **10,** 624–633 (2000).
359. Pletcher, M. T. *et al.* Chromosome evolution: The junction of mammalian chromosomes in the formation of mouse chromosome 10. *Genome Res.* **10,** 1463–1467 (2000).
360. Novacek, M. J. Mammalian phylogeny: shaking the tree. *Nature* **356,** 121–125 (1992).
361. O'Brien, S. J. *et al.* Genome maps 10. Comparative genomics. Mammalian radiations. Wall chart. *Science* **286,** 463–478 (1999).
362. Romer, A. S. *Vertebrate Paleontology* (Univ. Chicago Press, Chicago and New York, 1966).
363. Paterson, A. H. *et al.* Toward a unified genetic map of higher plants, transcending the monocot-dicot divergence. *Nature Genet.* **14,** 380–382 (1996).
364. Jenczewski, E., Prosperi, J. M. & Ronfort, J. Differentiation between natural and cultivated populations of *Medicago sativa* (Leguminosae) from Spain: analysis with random amplified polymorphic DNA (RAPD) markers and comparison to allozymes. *Mol. Ecol.* **8,** 1317–1330 (1999).
365. Ohno, S. *Evolution by Gene Duplication* (George Allen and Unwin, London, 1970).
366. Wolfe, K. H. & Shields, D. C. Molecular evidence for an ancient duplication of the entire yeast genome. *Nature* **387,** 708–713 (1997).
367. Blanc, G., Barakat, A., Guyot, R., Cooke, R. & Delseny, M. Extensive duplication and reshuffling in the arabidopsis genome. *Plant Cell* **12,** 1093–1102 (2000).
368. Paterson, A. H. *et al.* Comparative genomics of plant chromosomes. *Plant Cell* **12,** 1523–1540 (2000).
369. Vision, T., Brown, D. & Tanksley, S. The origins of genome duplications in *Arabidopsis*. *Science* **290,** 2114–2117 (2000).
370. Sidow, A. & Bowman, B. H. Molecular phylogeny. *Curr. Opin. Genet. Dev.* **1,** 451–456 (1991).
371. Sidow, A. & Thomas, W. K. A molecular evolutionary framework for eukaryotic model organisms. *Curr. Biol.* **4,** 596–603 (1994).
372. Sidow, A. Gen(om)e duplications in the evolution of early vertebrates. *Curr. Opin. Genet. Dev.* **6,** 715–722 (1996).
373. Spring, J. Vertebrate evolution by interspecific hybridisation—are we polyploid? *FEBS Lett.* **400,** 2–8 (1997).
374. Skrabanek, L. & Wolfe, K. H. Eukaryote genome duplication—where's the evidence? *Curr. Opin. Genet. Dev.* **8,** 694–700 (1998).
375. Hughes, A. L. Phylogenies of developmentally important proteins do not support the hypothesis of two rounds of genome duplication early in vertebrate history. *J. Mol. Evol.* **48,** 565–576 (1999).
376. Lander, E. S. & Schork, N. J. Genetic dissection of complex traits. *Science* **265,** 2037–2048 (1994).
377. Horikawa, Y. *et al.* Genetic variability in the gene encoding calpain-10 is associated with type 2 diabetes mellitus. *Nature Genet.* **26,** 163–175 (2000).
378. Hastbacka, J. *et al.* The diastrophic dysplasia gene encodes a novel sulfate transporter: positional cloning by fine-structure linkage disequilibrium mapping. *Cell* **78,** 1073–1087 (1994).
379. Tischkoff, S. A. *et al.* Global patterns of linkage disequilibrium at the CD4 locus and modern human origins. *Science* **271,** 1380–1387 (1996).
380. Kidd, J. R. *et al.* Haplotypes and linkage disequilibrium at the phenylalanine hydroxylase locus PAH, in a global representation of populations. *Am. J. Hum. Genet.* **63,** 1882–1899 (2000).
381. Mateu, E. *et al.* Worldwide genetic analysis of the CFTR region. *Am. J. Hum. Genet.* **68,** 103–117 (2001).
382. Abecasis, G. R. *et al.* Extent and distribution of linkage disequilibrium in three genomic regions. *Am. J. Hum. Genet.* **68,** 191–197 (2001).
383. Taillon-Miller, P. *et al.* Juxtaposed regions of extensive and minimal linkage disequilibrium in Xq25 and Xq28. *Nature Genet.* **25,** 324–328 (2000).
384. Martin, E. R. *et al.* SNPing away at complex diseases: analysis of single-nucleotide polymorphisms around APOE in Alzheimer disease. *Am. J. Hum. Genet.* **67,** 383–394 (2000).
385. Collins, A., Lonjou, C. & Morton, N. E. Genetic epidemiology of single-nucleotide polymorphisms. *Proc. Natl Acad. Sci. USA* **96,** 15173–15177 (1999).
386. Dunning, A. M. *et al.* The extent of linkage disequilibrium in four populations with distinct demographic histories. *Am. J. Hum. Genet.* **67,** 1544–1554 (2000).
387. Rieder, M. J., Taylor, S. L., Clark, A. G. & Nickerson, D. A. Sequence variation in the human angiotensin converting enzyme. *Nature Genet.* **22,** 59–62 (1999).
388. Collins, F. S. Positional cloning moves from perditional to traditional. *Nature Genet.* **9,** 347–350 (1995).
389. Nagamine, K. *et al.* Positional cloning of the APECED gene. *Nature Genet.* **17,** 393–398 (1997).
390. Reuber, B. E. *et al.* Mutations in PEX1 are the most common cause of peroxisome biogenesis disorders. *Nature Genet.* **17,** 445–448 (1997).
391. Portsteffen, H. *et al.* Human PEX1 is mutated in complementation group 1 of the peroxisome biogenesis disorders. *Nature Genet.* **17,** 449–452 (1997).
392. Everett, L. A. *et al.* Pendred syndrome is caused by mutations in a putative sulphate transporter gene (PDS). *Nature Genet.* **17,** 411–422 (1997).
393. Coffey, A. J. *et al.* Host response to EBV infection in X-linked lymphoproliferative disease results from mutations in an SH2-domain encoding gene. *Nature Genet.* **20,** 129–135 (1998).
394. Van Laer, L. *et al.* Nonsyndromic hearing impairment is associated with a mutation in DFNA5. *Nature Genet.* **20,** 194–197 (1998).
395. Sakuntabhai, A. *et al.* Mutations in ATP2A2, encoding a Ca2+ pump, cause Darier disease. *Nature Genet.* **21,** 271–277 (1999).
396. Gedeon, A. K. *et al.* Identification of the gene (SEDL) causing X-linked spondyloepiphyseal dysplasia tarda. *Nature Genet.* **22,** 400–404 (1999).
397. Hurvitz, J. R. *et al.* Mutations in the CCN gene family member WISP3 cause progressive pseudorheumatoid dysplasia. *Nature Genet.* **23,** 94–98 (1999).
398. Laberge-le Couteulx, S. *et al.* Truncating mutations in CCM1, encoding KRIT1, cause hereditary cavernous angiomas. *Nature Genet.* **23,** 189–193 (1999).
399. Sahoo, T. *et al.* Mutations in the gene encoding KRIT1, a Krev-1/rap1a binding protein, cause cerebral cavernous malformations (CCM1). *Hum. Mol. Genet.* **8,** 2325–2333 (1999).
400. McGuirt, W. T. *et al.* Mutations in COL11A2 cause non-syndromic hearing loss (DFNA13). *Nature Genet.* **23,** 413–419 (1999).
401. Moreira, E. S. *et al.* Limb-girdle muscular dystrophy type 2G is caused by mutations in the gene encoding the sarcomeric protein telethonin. *Nature Genet.* **24,** 163–166 (2000).
402. Ruiz-Perez, V. L. *et al.* Mutations in a new gene in Ellis-van Creveld syndrome and Weyers acrodental dysostosis. *Nature Genet.* **24,** 283–286 (2000).
403. Kaplan, J. M. *et al.* Mutations in ACTN4, encoding alpha-actinin-4, cause familial focal segmental glomerulosclerosis. *Nature Genet.* **24,** 251–256 (2000).
404. Escayg, A. *et al.* Mutations of SCN1A, encoding a neuronal sodium channel, in two families with GEFS+2. *Nature Genet.* **24,** 343–345 (2000).
405. Sacksteder, K. A. *et al.* Identification of the alpha-aminoadipic semialdehyde synthase gene, which is defective in familial hyperlysinemia. *Am. J. Hum. Genet.* **66,** 1736–1743 (2000).
406. Kalaydjieva, L. *et al.* N-myc downstream-regulated gene 1 is mutated in hereditary motor and sensory neuropathy-Lom. *Am. J. Hum. Genet.* **67,** 47–58 (2000).
407. Sundin, O. H. *et al.* Genetic basis of total colourblindness among the Pingelapese islanders. *Nature Genet.* **25,** 289–293 (2000).
408. Kohl, S. *et al.* Mutations in the CNGB3 gene encoding the beta-subunit of the cone photoreceptor cGMP-gated channel are responsible for achromatopsia (ACHM3) linked to chromosome 8q21. *Hum. Mol. Genet.* **9,** 2107–2116 (2000).
409. Avela, K. *et al.* Gene encoding a new RING-B-box-coiled-coil protein is mutated in mulibrey nanism. *Nature Genet.* **25,** 298–301 (2000).
410. Verpy, E. *et al.* A defect in harmonin, a PDZ domain-containing protein expressed in the inner ear sensory hair cells, underlies usher syndrome type 1C. *Nature Genet.* **26,** 51–55 (2000).
411. Bitner-Glindzicz, M. *et al.* A recessive contiguous gene deletion causing infantile hyperinsulinism, enteropathy and deafness identifies the usher type 1C gene. *Nature Genet.* **26,** 56–60 (2000).
412. The May-Hegglin/Fetchner Syndrome Consortium. Mutations in MYH9 result in the May-Hegglin anomaly, and Fechtner and Sebastian syndromes. *Nature Genet.* **26,** 103–105 (2000).
413. Kelley, M. J., Jawien, W., Ortel, T. L. & Korczak, J. F. Mutation of MYH9, encoding non-muscle myosin heavy chain A, in May-Hegglin anomaly. *Nature Genet.* **26,** 106–108 (2000).
414. Kirschner, L. S. *et al.* Mutations of the gene encoding the protein kinase A type I-α regulatory subunit in patients with the Carney complex. *Nature Genet.* **26,** 89–92 (2000).
415. Lalwani, A. K. *et al.* Human nonsyndromic hereditary deafness DFNA17 is due to a mutation in non-muscle myosin MYH9. *Am. J. Hum. Genet.* **67,** 1121–1128 (2000).
416. Matsuura, T. *et al.* Large expansion of the ATTCT pentanucleotide repeat in spinocerebellar ataxia type 10. *Nature Genet.* **26,** 191–194 (2000).
417. Delettre, C. *et al.* Nuclear gene OPA1, encoding a mitochondrial dynamin-related protein, is mutated in dominant optic atrophy. *Nature Genet.* **26,** 207–210 (2000).
418. Pusch, C. M. *et al.* The complete form of X-linked congenital stationary night blindness is caused by mutations in a gene encoding a leucine-rich repeat protein. *Nature Genet.* **26,** 324–327 (2000).
419. The ADHR Consortium. Autosomal dominant hypophosphataemic rickets is associated with mutations in FGF23. *Nature Genet.* **26,** 345–348 (2000).
420. Bomont, P. *et al.* The gene encoding gigaxonin, a new member of the cytoskeletal BTB/kelch repeat family, is mutated in giant axonal neuropathy. *Nature Genet.* **26,** 370–374 (2000).
421. Tullio-Pelet, A. *et al.* Mutant WD-repeat protein in triple-A syndrome. *Nature Genet.* **26,** 332–335 (2000).
422. Nicole, S. *et al.* Perlecan, the major proteoglycan of basement membranes, is altered in patients with Schwartz-Jampel syndrome (chondrodystrophic myotonia). *Nature Genet.* **26,** 480–483 (2000).
423. Rogaev, E. I. *et al.* Familial Alzheimer's disease in kindreds with missense mutations in a gene on chromosome 1 related to the Alzheimer's disease type 3 gene. *Nature* **376,** 775–778 (1995).
424. Sherrington, R. *et al.* Cloning of a gene bearing missense mutations in early-onset familial Alzheimer's disease. *Nature* **375,** 754–760 (1995).
425. Olivieri, N. F. & Weatherall, D. J. The therapeutic reactivation of fetal haemoglobin. *Hum. Mol. Genet.* **7,** 1655–1658 (1998).
426. Drews, J. Research & development. Basic science and pharmaceutical innovation. *Nature Biotechnol.* **17,** 406 (1999).
427. Drews, J. Drug discovery: a historical perspective. *Science* **287,** 1960–1964 (2000).
428. Davies, P. A. *et al.* The 5-HT3B subunit is a major determinant of serotonin-receptor function. *Nature* **397,** 359–363 (1999).
429. Heise, C. E. *et al.* Characterization of the human cysteinyl leukotriene 2 receptor. *J. Biol. Chem.* **275,** 30531–30536 (2000).
430. Fan, W. *et al.* BACE maps to chromosome 11 and a BACE homolog, BACE2, reside in the obligate Down Syndrome region of chromosome 21. *Science* **286,** 1255a (1999).
431. Saunders, A. J., Kim, T. -W. & Tanzi, R. E. BACE maps to chromosome 11 and a BACE homolog, BACE2, reside in the obligate Down Syndrome region of chromosome 21. *Science* **286,** 1255a (1999).
432. Firestein, S. The good taste of genomics. *Nature* **404,** 552–553 (2000).
433. Matsunami, H., Montmayeur, J. P. & Buck, L. B. A family of candidate taste receptors in human and mouse. *Nature* **404,** 601–604 (2000).
434. Adler, E. *et al.* A novel family of mammalian taste receptors. *Cell* **100,** 693–702 (2000).
435. Chandrashekar, J. *et al.* T2Rs function as bitter taste receptors. *Cell* **100,** 703–711 (2000).
436. Hardison, R. C. Conserved non-coding sequences are reliable guides to regulatory elements. *Trends Genet.* **16,** 369–372 (2000).
437. Onyango, P. *et al.* Sequence and comparative analysis of the mouse 1-megabase region orthologous to the human 11p15 imprinted domain. *Genome Res.* **10,** 1697–1710 (2000).
438. Bouck, J. B., Metzker, M. L. & Gibbs, R. A. Shotgun sample sequence comparisons between mouse and human genomes. *Nature Genet.* **25,** 31–33 (2000).
439. Marshall, E. Public-private project to deliver mouse genome in 6 months. *Science* **290,** 242–243 (2000).
440. Wasserman, W. W., Palumbo, M., Thompson, W., Fickett, J. W. & Lawrence, C. E. Human-mouse genome comparisons to locate regulatory sites. *Nature Genet.* **26,** 225–228 (2000).
441. Tagle, D. A. *et al.* Embryonic epsilon and gamma globin genes of a prosimian primate (*Galago crassicaudatus*). Nucleotide and amino acid sequences, developmental regulation and phylogenetic footprints. *J. Mol. Biol.* **203,** 439–455 (1988).
442. McGuire, A. M., Hughes, J. D. & Church, G. M. Conservation of DNA regulatory motifs and discovery of new motifs in microbial genomes. *Genome Res.* **10,** 744–757 (2000).

© 2001 Macmillan Magazines Ltd

443. Roth, F. P., Hughes, J. D., Estep, P. W. & Church, G. M. Finding DNA regulatory motifs within unaligned noncoding sequences clustered by whole-genome mRNA quantitation. *Nature Biotechnol.* **16,** 939–945 (1998).
444. Cheng, Y. & Church, G. M. Biclustering of expression data. *ISMB* **8,** 93–103 (2000).
445. Cohen, B. A., Mitra, R. D., Hughes, J. D. & Church, G. M. A computational analysis of whole-genome expression data reveals chromosomal domains of gene expression. *Nature Genet.* **26,** 183–186 (2000).
446. Feil, R. & Khosla, S. Genomic imprinting in mammals: an interplay between chromatin and DNA methylation? *Trends Genet.* **15,** 431–434 (1999).
447. Robertson, K. D. & Wolffe, A. P. DNA methylation in health and disease. *Nature Rev. Genet.* **1,** 11–19 (2000).
448. Beck, S., Olek, A. & Walter, J. From genomics to epigenomics: a loftier view of life. *Nature Biotechnol.* **17,** 1144–1144 (1999).
449. Hagmann, M. Mapping a subtext in our genetic book. *Science* **288,** 945–946 (2000).
450. Eliot, T. S. in *T. S. Eliot. Collected Poems 1909–1962* (Harcourt Brace, New York, 1963).
451. Soderland, C., Longden, I. & Mott, R. FPC: a system for building contigs from restriction fingerprinted clones. *Comput. Appl. Biosci.* **13,** 523–535 (1997).
452. Mott, R. & Tribe, R. Approximate statistics of gapped alignments. *J. Comp. Biol.* **6,** 91–112 (1999).

Supplementary Information is available on *Nature*'s World-Wide Web site (http://www.nature.com) or as paper copy from the London editorial office of *Nature*.

Acknowledgements

Beyond the authors, many people contributed to the success of this work. E. Jordan provided helpful advice throughout the sequencing effort. We thank D. Leja and J. Shehadeh for their expert assistance on the artwork in this paper, especially the foldout figure; K. Jegalian for editorial assistance; J. Schloss, E. Green and M. Seldin for comments on an earlier version of the manuscript; P. Green and F. Ouelette for critiques of the submitted version; C. Caulcott, A. Iglesias, S. Renfrey, B. Skene and J. Stewart of the Wellcome Trust, P. Whittington and T. Dougans of NHGRI and M. Meugnier of Genoscope for staff support for meetings of the international consortium; and the University of Pennsylvania for facilities for a meeting of the genome analysis group.

We thank Compaq Computer Corporations's High Performance Technical Computing Group for providing a Compaq Biocluster (a 27 node configuration of AlphaServer ES40s, containing 108 CPUs, serving as compute nodes and a file server with one terabyte of secondary storage) to assist in the annotation and analysis. Compaq provided the systems and implementation services to set up and manage the cluster for continuous use by members of the sequencing consortium. Platform Computing Ltd. provided its LSF scheduling and loadsharing software without license fee.

In addition to the data produced by the members of the International Human Genome Sequencing Consortium, the draft genome sequence includes published and unpublished human genomic sequence data from many other groups, all of whom gave permission to include their unpublished data. Four of the groups that contributed particularly significant amounts of data were: M. Adams *et al.* of the Institute for Genomic Research; E. Chen *et al.* of the Center for Genetic Medicine and Applied Biosystems; S.-F. Tsai of National Yang-Ming University, Institute of Genetics, Taipei, Taiwan, Republic of China; and Y. Nakamura, K. Koyama *et al.* of the Institute of Medical Science, University of Tokyo, Human Genome Center, Laboratory of Molecular Medicine, Minato-ku, Tokyo, Japan. Many other groups provided smaller numbers of database entries. We thank them all; a full list of the contributors of unpublished sequence is available as Supplementary Information.

This work was supported in part by the National Human Genome Research Institute of the US NIH; The Wellcome Trust; the US Department of Energy, Office of Biological and Environmental Research, Human Genome Program; the UK MRC; the Human Genome Sequencing Project from the Science and Technology Agency (STA) Japan; the Ministry of Education, Science, Sport and Culture, Japan; the French Ministry of Research; the Federal German Ministry of Education, Research and Technology (BMBF) through Projektträger DLR, in the framework of the German Human Genome Project; BEO, Projektträger Biologie, Energie, Umwelt des BMBF und BMWT; the Max-Planck-Society; DFG—Deutsche Forschungsgemeinschaft; TMWFK, Thüringer Ministerium für Wissenschaft, Forschung und Kunst; EC BIOMED2—European Commission, Directorate Science, Research and Development; Chinese Academy of Sciences (CAS), Ministry of Science and Technology (MOST), National Natural Science Foundation of China (NSFC); US National Science Foundation EPSCoR and The SNP Consortium Ltd. Additional support for members of the Genome Analysis group came, in part, from an ARCS Foundation Scholarship to T.S.F., a Burroughs Wellcome Foundation grant to C.B.B. and P.A.S., a DFG grant to P.B., DOE grants to D.H., E.E.E. and T.S.F., an EU grant to P.B., a Marie-Curie Fellowship to L.C., an NIH-NHGRI grant to S.R.E., an NIH grant to E.E.E., an NIH SBIR to D.K., an NSF grant to D.H., a Swiss National Science Foundation grant to L.C., the David and Lucille Packard Foundation, the Howard Hughes Medical Institute, the University of California at Santa Cruz and the W. M. Keck Foundation.

Correspondence and requests for materials should be addressed to E. S. Lander (e-mail: lander@genome.wi.mit.edu), R. H. Waterston (e-mail: bwaterst@watson.wustl.edu), J. Sulston (e-mail: jes@sanger.ac.uk) or F. S. Collins (e-mail: fc23a@nih.gov).

Affiliations for authors: 1, Whitehead Institute for Biomedical Research, Center for Genome Research, Nine Cambridge Center, Cambridge, Massachusetts 02142, USA; 2, The Sanger Centre, The Wellcome Trust Genome Campus, Hinxton, Cambridgeshire CB10 1RQ, United Kingdom; 3, Washington University Genome Sequencing Center, Box 8501, 4444 Forest Park Avenue, St. Louis, Missouri 63108, USA; 4, US DOE Joint Genome Institute, 2800 Mitchell Drive, Walnut Creek, California 94598, USA; 5, Baylor College of Medicine Human Genome Sequencing Center, Department of Molecular and Human Genetics, One Baylor Plaza, Houston, Texas 77030, USA; 6, Department of Cellular and Structural Biology, The University of Texas Health Science Center at San Antonio, 7703 Floyd Curl Drive, San Antonio, Texas 78229-3900, USA; 7, Department of Molecular Genetics, Albert Einstein College of Medicine, 1635 Poplar Street, Bronx, New York 10461, USA; 8, Baylor College of Medicine Human Genome Sequencing Center and the Department of Microbiology & Molecular Genetics, University of Texas Medical School, PO Box 20708, Houston, Texas 77225, USA; 9, RIKEN Genomic Sciences Center, 1-7-22 Suehiro-cho, Tsurumi-ku Yokohama-city, Kanagawa 230-0045, Japan; 10, Genoscope and CNRS UMR-8030, 2 Rue Gaston Cremieux, CP 5706, 91057 Evry Cedex, France; 11, GTC Sequencing Center, Genome Therapeutics Corporation, 100 Beaver Street, Waltham, Massachusetts 02453-8443, USA; 12, Department of Genome Analysis, Institute of Molecular Biotechnology, Beutenbergstrasse 11, D-07745 Jena, Germany; 13, Beijing Genomics Institute/Human Genome Center, Institute of Genetics, Chinese Academy of Sciences, Beijing 100101, China; 14, Southern China National Human Genome Research Center, Shanghai 201203, China; 15, Northern China National Human Genome Research Center, Beijing 100176, China; 16, Multimegabase Sequencing Center, The Institute for Systems Biology, 4225 Roosevelt Way, NE Suite 200, Seattle, Washington 98105, USA; 17, Stanford Genome Technology Center, 855 California Avenue, Palo Alto, California 94304, USA; 18, Stanford Human Genome Center and Department of Genetics, Stanford University School of Medicine, Stanford, California 94305-5120, USA; 19, University of Washington Genome Center, 225 Fluke Hall on Mason Road, Seattle, Washington 98195, USA; 20, Department of Molecular Biology, Keio University School of Medicine, 35 Shinanomachi, Shinjuku-ku, Tokyo 160-8582, Japan; 21, University of Texas Southwestern Medical Center at Dallas, 6000 Harry Hines Blvd., Dallas, Texas 75235-8591, USA; 22, University of Oklahoma's Advanced Center for Genome Technology, Dept. of Chemistry and Biochemistry, University of Oklahoma, 620 Parrington Oval, Rm 311, Norman, Oklahoma 73019, USA; 23, Max Planck Institute for Molecular Genetics, Ihnestrasse 73, 14195 Berlin, Germany; 24, Cold Spring Harbor Laboratory, Lita Annenberg Hazen Genome Center, 1 Bungtown Road, Cold Spring Harbor, New York 11724, USA; 25, GBF - German Research Centre for Biotechnology, Mascheroder Weg 1, D-38124 Braunschweig, Germany; 26, National Center for Biotechnology Information, National Library of Medicine, National Institutes of Health, Bldg. 38A, 8600 Rockville Pike, Bethesda, Maryland 20894, USA; 27, Department of Genetics, Case Western Reserve School of Medicine and University Hospitals of Cleveland, BRB 720, 10900 Euclid Ave., Cleveland, Ohio 44106, USA; 28, EMBL European Bioinformatics Institute, Wellcome Trust Genome Campus, Hinxton, Cambridge CB10 1SD, United Kingdom; 29, Max Delbrück Center for Molecular Medicine, Robert-Rossle-Strasse 10, 13125 Berlin-Buch, Germany; 30, EMBL, Meyerhofstrasse 1, 69012 Heidelberg, Germany; 31, Dept. of Biology, Massachusetts Institute of Technology, 77 Massachusetts Ave., Cambridge, Massachusetts 02139-4307, USA; 32, Howard Hughes Medical Institute, Dept. of Genetics, Washington University School of Medicine, Saint Louis, Missouri 63110, USA; 33, Dept. of Computer Science, University of California at Santa Cruz, Santa Cruz, California 95064, USA; 34, Affymetrix, Inc., 2612 8th St, Berkeley, California 94710, USA; 35, Genome Exploration Research Group, Genomic Sciences Center, RIKEN Yokohama Institute, 1-7-22 Suehiro-cho, Tsurumi-ku, Yokohama, Kanagawa 230-0045, Japan; 36, Howard Hughes Medical Institute, Department of Computer Science, University of California at Santa Cruz, California 95064, USA; 37, University of Dublin, Trinity College, Department of Genetics, Smurfit Institute, Dublin 2, Ireland; 38, Cambridge Research Laboratory, Compaq Computer Corporation and MIT Genome Center, 1 Cambridge Center, Cambridge, Massachusetts 02142, USA; 39, Dept. of Mathematics, University of California at Santa Cruz, Santa Cruz, California 95064, USA; 40, Dept. of Biology, University of California at Santa Cruz, Santa Cruz, California 95064, USA; 41, Crown Human Genetics Center and Department of Molecular Genetics, The Weizmann Institute of Science, Rehovot 71600, Israel; 42, Dept. of Genetics, Stanford University School of Medicine, Stanford, California 94305, USA; 43, The University of Michigan Medical School, Departments of Human Genetics and Internal Medicine, Ann Arbor, Michigan

 © 2001 Macmillan Magazines Ltd

48109, USA; 44, MRC Functional Genetics Unit, Department of Human Anatomy and Genetics, University of Oxford, South Parks Road, Oxford OX1 3QX, UK; 45, Institute for Systems Biology, 4225 Roosevelt Way NE, Seattle, WA 98105, USA; 46, National Human Genome Research Institute, US National Institutes of Health, 31 Center Drive, Bethesda, Maryland 20892, USA; 47, Office of Science, US Department of Energy, 19901 Germantown Road, Germantown, Maryland 20874, USA; 48, The Wellcome Trust, 183 Euston Road, London, NW1 2BE, UK.

† Present addresses: Genome Sequencing Project, Egea Biosciences, Inc., 4178 Sorrento Valley Blvd., Suite F, San Diego, CA 92121, USA (G.A.E.); INRA, Station d'Amélioration des Plantes, 63039 Clermont-Ferrand Cedex 2, France (L.C.).

DNA sequence databases

GenBank, National Center for Biotechnology Information, National Library of Medicine, National Institutes of Health, Bldg. 38A, 8600 Rockville Pike, Bethesda, Maryland 20894, USA

EMBL, European Bioinformatics Institute, Wellcome Trust Genome Campus, Hinxton, Cambridge CB10 1SD, UK

DNA Data Bank of Japan, Center for Information Biology, National Institute of Genetics, 1111 Yata, Mishima-shi, Shizuoka-ken 411-8540, Japan

© 2001 Macmillan Magazines Ltd

Supplementary Information for Initial Sequencing and Analysis of the Human Genome.

International Human Genome Sequencing Consortium.

Methods and additional notes

Section: Generating the draft genome sequence (p. 864)

Subsection: Clone selection (p. 865)

Page 866 col. 2, para.3 "Fingerprint data were reviewed ….bias against rearranged clones).

Seed clones were picked from the growing contigs as follows: We began by identifying fingerprint clone contigs that had been localized to targeted locations and that did not contain any clones that had previously been selected for sequencing. Contigs were localized using mapping data from a variety of sources that could be attached to the fingerprinted clones, including STS/hybridization data from McPherson and colleagues[86], FISH data from several sources (C. McPherson et al., ref. 103), STS/PCR mapping data from several sources[92,95,103], electronic PCR data (http://www.ncbi.nlm.nih.gov/STS/) matching the BAC end sequences with mapped STSs and others. Beginning with the largest available clone in a valid contig (clones >250 kb were excluded to avoid artifacts), the FPC program[451] evaluated the fingerprints of all of the clones in the contig to determine largest clone for which all (but 2) of the individual bands in the restriction fragment pattern were common to or shared with (confirmed; having a band of equivalent size ±3%) with bands in the patterns of flanking clones (again, ignoring >250 kb flanking clones >250 kb). (Since the restriction enzyme used to produce the clone inserts is different than the enzyme used to produce the fingerprints, two bands may arise from the insert-vector junction, which are not found in the genome or in flanking clones.) Selected clones were then checked for excessive overlap with previously selected or sequenced clones and with each other. The allowable overlap at this stage was varied to suit the demands of the project.

Clones (walking clones) extending from seed or other selected clones were selected as follows: In the early phases of the effort, clones were not necessarily correctly ordered within a fingerprint clone contig and indeed not all of the available clones had necessarily been incorporated into the contig. Starting with a previously selected (seed) clone, the FPC program compared the restriction fragment pattern of that clone with the patterns of all of the clones in the fingerprint database that overlapped with the seed clone. It then iteratively analyzed the clones identified in the first round of analysis to identify the additional clones that overlapped with those. In this way, a set of overlapping clones was identified and the clones in the set were ordered based on their overlap statistics. After ordering, all of the valid clones were identified (valid clones were defined as those with all but three of their bands confirmed by clones within 4 clones on either side). Any clone that also had outside evidence of overlap, e.g. through BAC end sequence matches or shared

STS/hybridization data was selected for further evaluation. In cases with more than one clone with such outside evidence, the clone with the lowest overlap statistic (i.e., the one that was least redundant) was selected (in the case of ties, the largest clone was favored). Where there was no outside evidence, a clone was picked based on evaluation of the overlaps. The candidate clone was the first one that was found to have the minimal overlap with the seed clone (initially <20% overlap, rising to 30% in later phases of the mapping effort; the percentage overlap was estimated by dividing the sum of the sizes of the common bands by the size of the smaller of the two clones). To be picked, the clone also had to be bridged to the seed clone by a third, intermediate clone that confidently ($<1e^{-4}$) overlapped both the seed clone and the candidate clone. The candidate clone was then further evaluated for fingerprint overlap with previously selected or sequenced clones.

Once clones were ordered within fingerprint clone contigs, a similar algorithm that exploited the known clone order was used to pick the walking clones. This algorithm was also adapted to pick a spanning/walking clone for complex contigs with 2 or more clones in the sequencing pipeline, using the fingerprint map as a guide.

Subsection: Sequencing (p. 867)

Page 868, left-hand column, line 20: “By examining … 500 bp.”

The sizes of the gaps between adjacent initial sequence contigs in draft clones were measured using alignments of the initial sequence contigs from individual draft clones to contigs of size ≥ 40 kb from overlapping clones, usually finished clones. 10,999 gaps were examined. 1,726 gaps larger than 6,000 bp were discarded as probable artefacts due to misassemblies or incorrect alignments. The mean size of the gaps between the initial sequence contigs in draft clones was 554 bases. When the cutoff for discarding gaps was lowered to 3000 bp or raised to 12,000 bp, the mean gap size decreased to about 400 bp (estimated from 9,801 gaps) and increased to about 800 bp (estimated from 11,972 gaps) accordingly, indicating that there is still considerable uncertainty in the mean value. The 554 bp estimate for the mean gap size was used, along with the number of initial sequence contigs (Table 7) and the total number of bases in the initial sequence contigs (data not shown) to estimate the percentage of the draft clones that were covered by the initial sequence contigs. It was thus determined that, on average, about 96% of the draft clones was covered; assuming a mean gap size between 400 and 800 bp, the range in coverage is about 94-97%.

This comment also pertains to page 874, left-hand column, line 57: “Assuming that the sequence gaps … gaps within the draft sequenced clones”

Subsection: Assembly of the draft genome (p. 868)

Page 868, right-hand column, l. 47, "To eliminate such problems, sequenced clones were associated with the fingerprint clone contigs in the physical map…"

An FPC match statistic better than $1e^{-7}$ for the sequenced clone against the fpc fingerprint database was considered significant, based on empirical evidence. This match level was the weakest value used for placement when there was other confirmatory evidence to support the placement. In the absence of additional supportive data, a match score of better than $1e^{-9}$ was required for placement. In general, only the best match was used. Other confirmatory evidence included BAC end matches; the BAC end sequences were obtained from NCBI (dbGSS; http://www.ncbi.nlm.nih.gov/dbGSS/index.html). Only BAC end sequences with 15 or fewer matches to the genomic sequence were used to eliminate repetitive sequences. Additional information used to place clones included BAC paired-end sequence matches, shared STS matches, and "believed" sequence overlap relationships determined by investigators at the NCBI and at UC-Santa Cruz. In instances in which the data led to conflicting placements, the data were weighted based on estimates of reliability. In some cases, if there was conflicting placement data or only weak data for placement and, according to GigAssembler, the sequenced clone failed to overlap any clones in the assembly at their original placement positions, a placement was attempted at secondary sites suggested by the placement data.

Page 869, left-hand column, line 48 "Of these 942 contigs with sequenced clones… "

In general, merges between fingerprint clone contigs were based primarily on evaluation of the fingerprint data. Information about the STS map location of the fingerprint contigs was used to prevent spurious merges, to break spurious contigs and to suggest possible merges that had not been previously recognized. In addition, 62 contigs were merged on the basis of sequence overlap information, supported by STS map positions.

Subsection: Quality assessment (p. 871)
Sub-subsection: Alignment of the fingerprint clone contigs (p. 873)

Page 873, right-hand column, line 28: "The positions of most of the STSs… about 1.7% differed from one or more of them."

We localized the STS markers from seven different physical maps (the Genethon[101] and Marshfield (http://research.marshfieldclinic.org/genetics/) genetic maps, the GeneMap99[100], the G3 and Stanford TNG radiation hybrid maps (http://www-shgc.stanford.edu/Mapping/Marker/STSindex.html), and the Whitehead YAC and radiation hybrid map[29]) on the draft genome sequence using e-PCR, allowing one mismatch per primer and the default distance constraints between primers (50 bp deviation from expected size of product). Only those markers that were uniquely placed on the draft sequence were considered. There were 62,239 such markers. Of these, 1,095, or 1.7%, were mapped by ePCR to a chromosome of the draft sequence that was different from the chromosome indicated by the information from a genetic or radiation hybrid map.

Subsection: representation of random raw sequences (p. 874)

Page 875, left-hand column, line 9: "We compared the raw sequences … using the BLAST computer program."

> We processed whole genome shotgun reads from four independently constructed libraries as follows. All reads with fewer than 300 bases of PHRED quality 20 or greater were removed. The remaining reads were then trimmed for vector and for quality, looking at the 5' end for the first window with at least 15 continuous non-vector bases of >PHRED20 and at the 3' end, starting from the left cutoff, for 12 contiguous non-vector bases with <PHRED20 scores. Only trimmed reads that had >95% of their trimmed bases with PHRED>20 and a length of >250 bases were kept. The reads after trimming were composed of 40% GC base pairs. Reads were masked for repeats using the RepeatMasker program (A.F.A. Smit & P. Green, http://repeatmasker.genome.washington.edu/cgi-bin/RM2_req.pl) and for low entropy data using the nseg option of BLAST (W. Gish, unpublished; http://blast.wustl.edu)Reads were retained and used only if there were at least 100 consecutive bases of PHRED quality 20 or greater and 100 consecutive unmasked bases.
>
> Based on a test data set of random reads from finished projects, the following BLAST parameters were found to match 100% of the reads without false matches: -filter seg S=170 S2=150 W=13 gapW=4 gapS2=150 M=5 N=-11 Q=11 R=11. The set of masked trimmed reads was compared to the 7 October 7 2000 freeze of the HTGS data set, to all of Genbank and to the TSC SNP database using BLASTN 2.0MP (W. Gish, unpublished; http://blast.wustl.edu). The highest scoring match was aligned against the read using CROSSMATCH, demanding alignment of the full trimmed read at ≥97% identity for genomic sequence and with appropriate topological constraints for the SNP reads. Typically 1-2% of the matches were eliminated by this step.

Page 875, left-hand column, line 30: "We found that 88% of the bases of these cDNAs could be aligned ..."

> We aligned the RefSeq cDNA sequences to the draft genome using the psLayout program[104] and gathered statistics on the percentage of cDNA bases that aligned at various percent identity thresholds.
>
> The distal 200 bases of each cDNA were not included in the computation of the percentage of aligning bases because alignments in these regions are less reliable. If any cDNA aligned in more than one way, each cDNA base involved in any alignment was counted only once. At a threshold of 98% identity for the alignments, we found that 87.9% of the cDNA bases aligned somewhere in the draft genome. When the threshold was increased to 99% identity, the percentage of aligning bases fell to 85.83%, and when the threshold was decreased to 97% identity, it rose to 88.5%. Further decreases in the threshold all the way down to 90% identity only

increased the percentage of aligning bases one more percentage point, so the value of approximately 88% aligning bases, achieved by requiring 98% identity, represents a knee in the curve.

Section: Broad genomic landscape (p. 875)

page 876, right-hand column, line 9: "In addition, the human cytogenetic map ..."

The locations of the cytogenetically mapped clones on the draft genome sequence can be viewed at http://genome.ucsc.edu/goldenPath/mapPlots . Further information about the individual clones can be obtained at http://www.ncbi.nlm.nih.gov/genome/cyto/ and http://www.ncbi.nlm.nih.gov/genome/guide. Here, as well as on the browser at http://genome.ucsc.edu and http://www.ensembl.org/ , they can be viewed in the context of other genome annotation.

Subsection: Long-range variation in GC content (p. 876)

Page 877, left-hand column, line 30 "About three-quarters of the genome-wide variance… consistent with a homogeneous distribution"

All 3,312 windows of length 300 kb that had at least eight gap-free 20 kb subwindows and did not contain more than 50% simple repeats were extracted from the draft genome sequence. The average sample variance of the GC content of the subwindows of a window was 7.3%. The sample variance of all subwindows genome-wide (N = 36,562) was 27.4%. Hence, the variance of GC content within the 20 kb subwindows of a 300 kb window accounts for approximately one quarter of the overall variance of the GC content among all 20 kb subwindows in this sample. The average sample standard deviation of the GC content of the subwindows of a window was 2.4%.

Page 877, left-hand column, line 34: "In fact, the hypothesis … draft genome sequence."

For each of the 3,312 windows of length 300 kb, we tested the hypothesis that its 20 kb subwindows were sampled from a homogeneous GC distribution. The distribution was defined to have mean m equal to the GC-content in the combined subwindows of the 300 kb window, and the bases were taken as independent. Under this distribution, the GC-content of a 20 kb subwindow would have mean m and variance $s^2 = m(100-m)/20000$. For m = 41%, the typical value, this gives $s^2 = 0.121\%$, which is about 0.017 times the average sample variance of 7.3%. For each window, the variance s^2 and the sample variance $\hat{s}^2$ were determined, along with the value $c^2 = (n-1)\,\hat{s}^2/s^2$, where n is the number of subwindows of the window. Under the hypothesis of homogeneity, the statistic c^2 should have an approximately chi-square distribution with n-1 degrees of freedom. However, for every one of the 3,312 windows, $c^2 > 31.5$, which rejects the hypothesis of homogeneity with p-value >> 0.995.

Another way to test the hypothesis of homogeneity is to look in each 300 kb window for one 20 kb subwindow whose GC content differs significantly from the mean m for that window. In these tests, all 300 kb windows with less than 50% simple repeats and less than 25% gaps were tested (N = 10,596). Under the assumptions above, if X is the GC content of a subwindow, then D = (X-m)/sqrt[m(100-m)/20000] should have an approximately normal distribution. However, in all but four windows there is a subwindow with |D| > 3.0, i.e the GC content of the subwindow is more than 3.0 standard deviations from the mean of the window. The p-value for such a deviation is 0.0026. Considering that there are 15 possible subwindows, this gives an overall p-value of 0.039, i.e. the hypothesis of homogeneity is rejected with a p-value greater than 0.96.

The above analysis was repeated using 5 kb subwindows of 300 kb windows, and the hypothesis of homogeneity was rejected for all windows with p-value greater than 0.96, and with greater confidence for those windows tested with the chi-square test. Similar results were also obtained for 5 kb subwindows of 100 kb windows: all but thirteen windows were rejected with p-value greater than approximately 0.95, and all but three were rejected from those examined with the chi-square test. Since any region of 200 kb must contain one of the regions of 100 kb we tested for homogeneity, this indicates that there are few if any regions of 200 kb in the genome with homogeneous GC content.

Page 877, right-hand column, line 25: “Estimated band locations …”

Bands were assigned by a dynamic programming algorithm that attempted to maximize the number of cytogenetically mapped clones that lie within the range of possible sub-bands predicted from FISH, with special emphasis on high-resolution FISH-mapped clones provided by investigators at the National Cancer Institute[103]. The band positions were optimized subject to the constraint that the bands must appear in the known order along the draft genome sequence. Slight penalties for band size deviation from the standard fractional sizes were also imposed, so that in the absence of any FISH-mapped clones at all in a particular region, and given that there are no constraints from surrounding regions, the program would produce sub-bands corresponding to the standard fractional band lengths.

Section: Repeat content of the human genome (p. 879)

Subsection: Distribution of GC content (p. 884)

Concerning the subdivision of the draft genome sequence into 50 kb pieces of similar GC level. The same results will be obtained however the sequence is subdivided, as long as the fragments are around 50 kb long. Specifically, however, for the analyses shown in Figures 22 to 26, the draft genome sequence was subdivided in fragments of 40-60 kb (averaging 50 kb) overlappong by 1 kb. These fragments were created on the fly by the RepeatMasker program, and for each a

repeat analysis was done. The repeat information files were grouped by the GC level of the fragment, and processed according to need.

For the analyses shown in Figures 23 and 25, the number of repeat copies was compared. The number of individual insertions per megabase of DNA of a particular GC level was extracted from the RepeatMasker output (RepeatMasker provides information on which fragments originated from the same inserted transposable element). The Y axis is the ratio of the frequency of Alu (fig 23) or LINE1 (fig 25) over the average frequency of these elements in the genome.

Subsection: Segmental Duplications (p. 889)

Our assessment of low copy repeats (genomic duplications) within the draft genome sequence involved a global analysis of all non-overlapping sequence. The analysis using a combination of DNA sequence analysis software and a suite of perlscripts developed for paralogy detection (J. A. Bailey and E. E. Eichler, *in preparation*). The basic methodology included: repeatmasking (RepeatMasker v.4/20) of all reference sequences for common repeats, the removal and splicing of such repeat segments, global BLAST analysis of the segments for the identification of non-overlapping high-scoring segments, using relaxed affine gapping parameters which allowed large gaps up to 1 kb to be traversed (parameters: -G 180 –E 1 –q –80 –r 30 -z 3000000000 –Y 3000000000 –e 1e-10 –F F)), the reintroduction of common repeat elements into each pairwise alignment followed by optimal global alignment of the segments using the program ALIGN (E.W. Myers and W. Miller, CABIOS (1989) 4:11-17). To detect internal duplications within each query segment, a modified version of BLASTZ (W. Miller, unpublished) was used with similar relaxed gap parameters (B=2 M=30 I=-80 V=-80 O=180 E=1 W=14 Y=1400). Alignment statistics were generated (program:ALIGN_SCORER), and alignments that equaled or exceeded the threshold of 1000 bases aligned with over 90% similarity (i.e. gaps excluded) were analyzed. Generation of global alignments also acted as a safeguard against false positives from BLAST analysis. In cases of extremely large gaps (>1kb, alignments were fractured. Such cases were detected and merged for gaps up to 20 kb.

Subsection: Pericentromeres and telomeres (p. 890)

Chromosome 22 (May 2000, Sanger Centre) and Chromosome 21 (Sept., NCBI) were analyzed for large duplications as described. For interchromosomal duplications, the chromosome was analyzed versus the NT accession contigs (NCBI) and versus all remaining HTGS accessions (draft and finished) for interchromosomal duplications. A final global alignment threshold, >90%; >=1000 bases, was used. Due to unassembled allelic overlaps, sequences containing highly similar alignments (>99.5% NT; >99.0% HTGS) were excluded as probable allelic overlaps. The duplicated sequence for chromosome 21 and chromosome 22 were graphically viewed using the program PARASIGHT (J. A. Bailey and E.E. Eichler, *in preparation*).

Subsection: Genome-wide analysis of segmental duplications. (p. 891)

Finished sequence included all assembled sequence from NCBI within the NT dataset (version of 5 September 2000). A global alignment threshold (>90%; ±1000 bases) was used for comparisons between finished sequence. Further selection limited alignments for analyses to those less than 99.5% identity, as those greater than that were likely to represent unassembled allelic overlaps.

The 15 July 2000 version of the draft genome sequence was used as the basis for the duplication analysis of the entire human draft. A final global alignment threshold (>90%, ±1000 bases and <98%) defined the limits of detection for duplicated sequence. Sequence alignments (>98%) appear to represent mainly missed allelic overlaps many of which were subsequently merged in later releases of the assembly (e.g. 7 October 2000). Final validation of duplicated segments >98% within the working draft will require finished sequence data and/or experimental validation.

Section: Gene content of the human genome (p. 892)

Subsection: Noncoding RNAs (p. 892)

To identify transfer RNA genes, we used tRNAscan-SE version 1.21 [T.M. Lowe, S.R. Eddy. tRNAscan-SE: a program for improved detection of transfer RNA genes in genomic sequence. *Nucleic Acids Res*. **25**,955-964 (1997)] to analyze the 7 October 7 2000 version of the draft genome sequence. tRNAscan-SE predicted 504 tRNA genes and 144 tRNA-derived pseudogenes. Three of the predicted genes had a non-canonical anticodon loop length, preventing tRNAscan-SE from unambiguously identifying the anticodon; although there are many possible explanations for them, for our current purposes we classified these as probable pseudogenes. After manual examination of the tRNAs with unlikely anticodons, four more of the predicted genes were also classified as probable pseudogenes: a putative UAA suppressor, a putative UAG suppressor, and two putative UGA-reading selenocysteine tRNAs. The remaining gene predictions were not examined manually. We know that a small number of the 497 "true" tRNA genes are likely to be pseudogenes or parts of tRNA-derived repetitive sequence elements because tRNAscan-SE's ability to separate pseudogenes from true genes is not perfect. Because tRNAscan-SE models tRNA consensus secondary structure, it is not a reliable detector of divergent tRNA pseudogenes. To more accurately estimate the number of tRNA-derived pseudogenes, all 648 sequences detected by tRNAscan-SE were used as WU-BLASTN queries (see below), and another 173 significantly related sequences were detected, bringing the estimated pseudogene count to 324.

To identify all ncRNA homologues other than tRNA genes, we performed sequence similarity searches using WashU BLASTN 2.0MP (W. Gishl, unpublished; http://blast.wustl.edu) on the 7 October 2000 genome assembly, with parameters "-kap wordmask=seg B=50000 W=8" and the default DNA scoring matrix. True genes were operationally defined as BLAST hits with ≥95% identity over ≥95% the length of the query. Related sequences (e.g. pseudogenes) were operationally defined as all

other BLAST hits with P-values <= 0.001. To reconcile our tRNA gene count of 497 with the larger number of 1310 generally found in textbook references, we reexamined the primary data in a classic paper by Hatlen and Attardi[252]. The textbook estimate of 1310 human tRNA genes was based on their observation that purified and labelled human 4S RNA (e.g. the tRNA population) hybridizes to HeLa genomic DNA and saturates at a fraction of about 1.1×10^{-5} of the genome. The molecular weight of the human genome was thought at that time to be 3.1×10^{12} (about 4.7 billion bases). Recalculation using the current estimated genome size of 3.2 billion bases [T.R. Tiersch, R.W. Chandler, S.S. Wachtel, S. Elias. Reference standards for flow cytometry and application in comparative studies of nuclear DNA content. *Cytometry* **10**, 706-710 (1989); this paper] gives an estimate of 890 tRNA-complementary loci instead of 1310. Hatlen and Attardi also noted, but at the time could not explain, a puzzling length heterogeneity in their hybridized genomic loci. We believe that they were observing the tRNA pseudogene population, many of which are truncated copies of tRNA genes; therefore we believe their hybridization-based estimate of ~890 loci included tRNA pseudogenes (of which we count 324 in the genome) in addition to the true tRNA genes (of which we count 497 in the genome).

Subsection: Protein-coding genes (p. 896)

Sub-subsection: Exploring properties of known genes (p. 896)

Known genes were aligned with Spidey (S. Wheelan et al., manuscript in preparation) and Acembly (D. Thierry-Mieg and J. Thierry-Mieg, unpublished; http://www.acedb.org/), which in both cases align the cDNA to the genome while allowing for introns. The results from the two programs were in broad agreement. 5,364 RefSeq entroess (from a 1 September 2000) release were used as a source of the cDNAs. The alignments of the cDNAs to the genome could be classified by the proportion of the cDNA that aligned to the genome and by the percentage of identical nucleotides between the cDNA and the genomic sequence. In most cases, there was an unambiguous location for a cDNA. However, some proportion at each level of coverage had more than one site with high identity matches; in these cases, one of the locations was arbitrarily chosen.

Sub-subsection: Towards a complete index of human genes (p. 898)

Creating an initial gene index (p. 899)

Ensembl: Ensembl aims to predict coding sequences of true genes with high confidence, by only predicting coding sequence regions which have confirming evidence across their entire length. The sources of confirmation are cDNA, EST and protein-based similarity. The Genscan computer program was run across the individual fragments of the genome and the resulting peptides were used to search vertebrate mRNA sources (extracted from the EMBL databank; http://www.ebi.ac.uk/index.html), EST (vertebrate dbEST; ftp://ncbi.nlm.nih.gov/genbank) and a non-redundant protein database (SWIR; http://www.ebi.ac.uk/swissprot/). Protein hits of greater than 200 bits similarity were then further processed by using the GeneWise

program with the similar protein against the assembled draft genome sequence (the 17 July 2000 version). A final gene-building method was then used to merge all the resulting information, being Genscan predictions with confirming similarity at a number of exons and the GeneWise gene predictions. The method only accepted a join between two exons if consistent similarity evidence was found on each exon with the following thresholds: (a) all GeneWise predictions were accepted, although redundant GeneWise predictions were discarded; and (b) for exons predicted by Genscan, a single protein or cDNA similarity of at least 100 bits or higher, or at least two EST hits of 100 bits or higher. This final process allows for alternative splicing, although modeling alternative splicing has not been optimised. Ensembl produced 35,500 gene predictions with 44,860 transcripts.

Merge procedure to produce a final protein set: To generate a single protein set for further analysis we merged the known protein sequences from RefSeq (version of 29Sept2000), SWISSPROT (Release 39.6 of 30th Aug 200), TREMBL (TrEMBL Release 14.17 of 1 Oct 2000) and TREMBL_NEW (1 Oct 2000) with the gene predictions. The later protein analysis required a non-redundant protein set where genes were represented as a single protein sequence; in the case of alternative splicing, a single, representative protein sequence was required. We are aware of the obvious limitations of this representation of the human proteome, but accommodating alternative splicing in the downstream analysis was very complex.

The genome prediction data set was prepared as follows: the Ensembl and Genie predictions were merged by examining overlap of coding exons in genomic coordinates. Two gene predictions were merged if a single coding exon on the same strand overlapped. From this set of merged predictions, we used only the Ensembl+Genie and the Ensembl-only predictions. In cases where there was more than one prediction, or for Ensembl genes, more than one transcript, we chose the longest protein sequence from each merged unit to represent the gene. The protein level merge then occurred by comparing the union of all the data sources in an all-vs-all FASTA comparison using default parameters. Two protein sequences were merged if the match covered at least 95% of the shorter sequence, and identity was ≥ 95%, which takes into account both nearly identical protein sequences and also nearly identical fragments.

Special attention was needed to prevent overrepresentation of alternative splice forms. Firstly we expanded the Swissprot and Trembl databases to represent known splice variants in the protein merge, but only took a single protein (the canonical database sequence) for the final protein set. An additional cull for alternative splice forms which remained as separate proteins was produced by taking the corresponding DNA sequences of the known proteins (RefSeq, SWISSPROT, TREMBL and TREMBL_NEW) and matching back to the genome using the SSAHA program without requiring a valid gene structure alignment. If the DNA derived from two protein sequences matched at over 28 base pairs at the same location, the longest protein sequence was used. Finally, clear bacterial contamination (proteins which had an almost identical match to a bacterial protein) were removed.

Quality Control on the protein set: We took 31 genes which we could confirm as being unavailable at the time of the gene builds (22 from RefSeq, 9 from the Sanger Centre gene identification program on chromosome X). 3 of the 31 sequences could not be found in the genome assembly. Using the wublastp program (http://blast.wustl.edu) with default parameters, we matched the 31 sequences to the IPI.1 set and visually inspected the alignments. 19 sequences showed a clear match to an IPI protein; 14 hit a single IPI protein, 3 hit 2 IPI proteins, 1 hit 3 IPI proteins and 1 hit 4 IPI proteins.

RIKEN mouse cDNAs. We took a random sample (1,000) of known genes, Ensembl-Genie genes and Ensembl-only genes and matched them to the Riken cDNA set of 15,294 cDNAs using the TBLASTN program (http://www.ncbi.nlm.nih.gov/BLAST/) with default parameters, at the $1e^{-6}$ E-value significance level.

The IPI and IGI can be found at http://www.ensembl.org/IPI/.

Additional information for Table 23 (p. 902). All of the tables of Interpro are accessible through http://www.sanger.ac.uk/Users/agb/Ensembl.

Section: Segmental history of the human genome (p. 908)

Subsection: Conserved segments between human and mouse (p. 908)

Putatively orthologous sequences were determined in two ways. Curated orthologues determined at the Jackson Laboratory (www.informatics.jax.org) were obtained by FTP. In addition, orthologues were calculated at the NCBI using the program megaBLAST [Z. Zhang et al., *J. Comput. Biol.* **7**, 203-214 (2000)]. In order to calculate orthologues, non-EST mRNA sequences found in LocusLink (http://www.ncbi.nlm.nih.gov:80/LocusLink/) were obtained for both human and mouse. The megaBLAST analysis was performed first using the mouse sequence as the query and the human sequence as the database. A second analysis was performed in which the human sequence was the query and the mouse sequence was the database. Reciprocal best hits were retained as putative orthologues.

mRNA sequences were aligned to the draft genome sequence (7 October 2000 version) using the mRNA alignment tool Spidey (S. Wheelan et al., manuscript in preparation). Only mRNAs that could be aligned with high confidence (>90% of the mRNA, including the entire coding sequence, had to align, the worst exon had to have a pc_id >95%, and at least one exon had to have a pc_id >98%), and where more than 50% of the mRNA was found, were kept. If an mRNA aligned to more than one contig, efforts were made to determine the most likely location. Alignments that were in conflict with LocusLink map locations were disregarded.

Segments in the conserved synteny map were determined as follows. A segment had to contain at least 2 genes from the same area of the mouse genome. In addition to the mouse genes having to be on the same chromosome, the genes had

to be on the same part of the chromosome (note the 7 breakpoints on the X chromosome). A cutoff of 15 cM was chosen, so if two mouse genes were from the same chromosome, but >15 cM apart, then a breakpoint was made. A large cutoff was made because the MGD genetic map is an integrated map, and thus the margin of confidence is large.

Section: Applications to medicine and biology

Subsections: Disease genes (p. 911) and Drug targets (p. 912)

971 OMIM loci which had links to the SwissProt or Sptrembl databases were used to define a non-exhaustive set of disease genes. For protein targets of pharmaceutical interest, the list published by Drews[427] was manually mapped to protein database identifiers wherever possible, resulting in a list of 603 drug target proteins. These were matched using wublastp with default parameters [S.F. Altschul et al. Basic local alignment search tool. *J Mol Biol* **215**,403-10 (1990] to the genome protein database IPI.1. The results were filtered to focus primarily on potential paralogues. Thus, distant similarity of only a single domain was rejected. Highly similar proteins, which might arise from artificial duplications in genome assembly, were also rejected. After experimenting with a number of criteria, the following heuristic was used: for cases on the same chromosome, matches with 70% to 90% identity over at least 50 amino acids were accepted, whereas for matches on different chromosomes, matches with 70% to 95% identity over at least 50 amino acids were required. A number of these putative paralogues were then examined by eye to see whether the similarity differences were spread evenly throughout the protein, rather than concentrating between high similarity and weak similarity. The putative paralogues were also compared against other forms of data (e.g., EST databases) to verify the gene prediction.

Full Author List

Genome Sequencing Centers. The centers are listed in order of total genomic sequence contributed.

Whitehead Institute for Biomedical Research, Center for Genome Research, *Nine Cambridge Center, Cambridge, MA 02142, USA*: Emmanuel Adekoya, Mostafa Ait-Zahra, Nicole Allen, Mechele Anderson, Scott Anderson, Faina Anufriev, Jeff Armbruster, Kifle Ayele, Jodi Baker, Jennifer Baldwin, Nicole Barna, Vertilda Bastien, Serafim Batzoglou, Reem Beckerly, Felicienne Beda, John Bernard, Bruce Birren, Bruce Birren, Brendan Blumensteil, Leonid Boguslavsky, Boris Boukghalter, Adam Brown, Greg Burkett, Jody Camarata, Amy Campopiano, Herman Carneiro, Zhuan Chen, Yama Choephal, Mary Colangelo, Sonya Collins, Alville Collymore, Patrick Cooke, Christopher Davis, Tenzin Dawoe, Kurt DeArellano, Keri Devon, Ken Dewar, J. Sebastian Diaz, Sheila Dodge, Elizabeth Donelan, Kunsang Dorjee, Michael Doyle, Antionise Dube, Alan Dupes, Matt Endrizzi, Abderrahim Farina, Susan Faro, Diallo Ferguson, Pat Ferriera, Heather Fischer, William FitzHugh, Ken Flaherty, Karen Foley, Roel Funke, Diane Gage, James Galagan, Stephanie Gardyna, Diane Gilbert, Samir Ginde, Antonio Gomes, Mary Goyette, Joseph Graham, Leslie Graham, Edward Grandbois, Nerline Grand-Pierre, George Grant, Dave Gregoire, Roth Guerrero, Birhane Hagos, Katrina Harris, David Hart, Beah Hatcher, Andrew Heaford, Lloyd Horton, Catherine Hosage-Norman, John Howland, Bill Hulme, Ilian Iliev, Robin Johnson, Charlein Jones, Marie Joseph, Mathew Judd, Lisa Kann, Aysen Karatas, Damian Kelley, Merrilee Kelly, Dawa Lama, Jenny Lamazares, Eric S. Lander, Thomas Landers, Addie Lane, Keri LaRocque, Heidi LeBlanc, Jean-Pierre Leger, Jessica Lehoczky, Rosie LeVine, Doreen Lewis, Tammy Lewis, Charlien Lieu, Lauren Linton, Grace Liu, Xiaohong Liu, Kim Locke, Yeshi Lokyitsang, Pen Macdonald, Rogelio Martinez, Kebede Maru, Megan McCarthy, Paul McEwan, Tina McGhee, Brian McGing, Aisling McGurk, Kevin McKernan, Jacque McLaughlin, Robert McPheeters, James Meldrim, Louis Meneus, Jill Mesirov, Tanya Mihova, Cher Miranda, Val Mlenga, Michelle Modeski, Geoff Montello, William Morris, Jenn Morrow, Leon Mulrain, Thomas Murphy, Josef Mychaleckyj, Jerome Naylor, Christian Newes, Tsering Ngodup, Cindy Nguyen, Thu Nguyen, Chou Dolma Norbu, Nyima Norbu, Chad Nusbaum, Tara O'Connor, Paula O'Donnell, Yousef Okaf, Dominic O'Neil, Jon O'Shea, Sahal Osman, Matt Paresi, Boris Pavlin, K.M. Peterson, Pema Phunkang, Nadia Pierre, Victor Pollara, Christina Raymond, Melanie Rieback, Beckie Riley, Cecil Rise, Peter Rogov, Joe Roman, Magaly Roman, Mark Rosetti, Deborah Rothman, Alice Roy, Karen Roycroft, Ralph Santos, Steven Schauer, Rebecca Schupbach, Steven Seaman, Andrew Sheridan, Cherylyn Smith, Carrie Sougnez, Thomas Speece, Brian Spencer, Nicole Stange-Thomann, Nikola Stojanovic, Casey Stone, Nathaniel Strauss, Aravind Subramanian, Jessica Talamas, Pierre Tchuinga, Mark Temelko, Pema Tenzin, Senait Tesfaye, Joumathe Theodore, Andrea Tirrell, Imani Torruella-Miller, Tee Trac, Mary Travers, Niki Travis, James Trigilio, Elsa Tsao, Helen Vassiliev, Rose Veil, Andy Vo, Alan Wagner, Jamie Walsh, Tsering Wangdi, Jamey Wierzbowski, Bennet Wilson, Xaioyun Wu, Dudley Wyman, Wen Juan Ye, Shane Yeager, Rahel Retta Yeshitela, Geneva Young, Joanne Zainoun, Andrew Zimmer and Michael C. Zody

The Sanger Centre, *The Wellcome Trust Genome Campus, Hinxton, Cambridgeshire CB10 1RQ, United Kingdom*: Zahra Abdellah, Alireza Ahmadi, Shahana Ahmed, Matthew Aimable, Rachael Ainscough, Jeff Almeida, Andrew Ambler, Karen Ambrose, Kerrie Ambrose, Daniel Andrews, Neil Andrews, Hazel Arbery, Beth Archer, Gareth Ash, Kevin Ashcroft, Jennifer Ashurst, Robert Ashwell, Deborah Atkin, Andrea Atkinson, John Attwood, Keith Aubin, Terry Avis, Anne Babbage, Joanne Bacon, Claire Bagguley, Jonathan Bailey, Andrew Baker, Simon Bardill, Darren Barker, Karen Barlow, Laurent Baron, Anika Barrett, Rebecca Bartlett, David Basham, Victoria Basham, Alex Bateman, Karen Bates, Caroline Baynes, Lisa Beard, Susan Beard, David Beare, Alastair Beasley, Oliver Beasley, Stephan Beck, Emma Bell, Damian Bellerby, Tristram Bellerby, Richard Bemrose, James Bennett, David Bentley, Mary Berks, Michael Berks, Graeme Bethel, Christine Bird, Ewan Birney, Helen Bissell, Suzanne Blackburne-Maze, Sarah Blakey, Ralph Bonnett, Richard Border, Nicola Brady, Jason Bray, Sarah Bray-Allen, Anne Bridgeman, Jonathan Brook, Shane Brooking, Andrew Brown, Clive Brown, Jacqui Brown, Margaret Brown, Mary Brown, Richard Bruskiewich, Jackie Bryant, David Buck, Veronica Buckle, Claire Budd, Jill Burberry, Deborah Burford, Joanne Burgess, Wayne Burrill, Christine Burrows, John Burton, Phil Butcher, Adam Butler, Murray Cairns, Bruno Canning, Carol Carder, Paul Carder, Nigel Carter, Tamara Cavanna, Ka Chan, Joanna Chapman, Rachel Charles, Tom Chothia, Connie Chui, Michele Clamp, Anthea Clark, Graham Clark, Kevin Clark, Sarah Clark, Sue Clark, Betty Clarke, Eddie Clarke, Kay Clarke, Chris Clee, Sheila Clegg, Karen Clifford, Julia Coates, Victoria Cobley, Alison Coffey, Penelope Coggill, Lotte Cole, Rachael Collier, Simon Collings, John Collins, Philip Collins, Richard Connor, Jennie Conquer, Donald Conroy, Doug

Constance, Leanna Cook, Jonathan Cooper, Rachel Cooper, Robert Cooper, Teresa Copsey, Nicole Corby, Linda Cornell, Ruth Cornell, Amanda Cottage, Alan Coulson, Gez Coville, Anthony Cox, Tony Cox, Robert Coxhill, Matthew Craig, Tom Crane, Matt Crawley, Victor Crew, James Cuff, Karl Culley, Auli Cummings, Kirsti Cummings, Paul Cummings, Adam Curran, Valery Curwen, Jeffrey Cutts, Rachael Daniels, Lucy Davidson, Jonathon Davies, Joy Davies, Nicholas Davies, Robert Davies, John Davis, Elisabeth Dawson, Rebecca Deadman, Peter Dean, Simon Dear, Frances Dearden, Marcos Delgado, Panos Deloukas, Janet Dennis, Pawandeep Dhami, Catherine Dibling, Ruth Dobbs, Richard Dobson, Catherine Dockree, Daniel Doddington, Steven Dodsworth, Norman Doggett, Andrew Dunham, Ian Dunham, Anne Dunn, Matthew Dunn, Richard Durbin , Jillian Durham, Ruth Dwyer, Mark Earthrowl, Timothy Eastham, Carol Edwards, Karen Edwards, Andrew Ellington, Matthew Ellwood, Becky Emberson, Helen Errington, Gareth Evans, John Evans, Katie Evans, Richard Evans, Theresa Feltwell , Stephen Fennell, Robert Finn, Tina Flack, Kerry Fleming, Jonathan Flint, Mark Flint, Yvonne Floyd, Simon Footman, John Fowler, Deborah Frame, Matthew Francis, Stephen Francis, John Frankland, Audrey Fraser, David Fraser, Lisa French, Daniel Frost, Jackie Frost, Lorna Frost, Carole Frost , Liam Fuller, Kathryn Fullerton, Alison Gardner, Patrick Garner, Jane Garnett, Leigh Gatland, Lindsay Gatland, Jilur Ghori, Ben Gibbs, Diane Gibson, James Gilbert, Lisa Gilby, Christopher Gillson, Matthew Gorton, Darren Grafham, Michael Grant, Susan Grant, Iain Gray, Lisa Green, James Greenhalgh, Joe Greenhill, Philippa Gregg, Simon Gregory, Coline Griffiths, Ed Griffiths, Mark Griffiths, Ian Guthrie, Rhian Gwilliam, Rebekah Hall, Karen Halls, Gretta Hall-Tamlyn, John Hamlett, Sian Hammond, Julie Hancock, Adam Harding, Joanne Harley, David Harper, Georgina Harper, Grant Harradence, Charlene-Lou Harrison, Ruth Harrison, Daniel Hassan, Natalie Hawkins, Kellie Hawley, Kerry Hayes, Paul Heath, Rosemary Heathcott, Cathy Hembry, Tim Herd, Stephen Hewitt, Douglas Higgs, Guy Hillyard, Russell Hinkins, Sara-jane Ho, David Hodgson, Michael Hoffs, Jane Holden, Janet Holdgate, Ele Holloway, Ian Holmes, Sarah Holmes, Simon Holroyd, Alison Hooper, Lucy Hopewell, Ben Hopkins, Gary Hornett, Geoff Hornsby, Tony Hornsby, Sharon Horsley, Roger Horton, Philip Howard, Philip Howden, Gareth Howell, Timothy Hubbard, Elizabeth Huckle, Jaime Hughes, Jennifer Hughes, Louisa Hull, Holger Hummerich, Sean Humphray, Matthew Humphries, Adrienne Hunt, Paul Hunt, Sarah Hunt, David Hyde, Michael Ince, Judith Isherwood, Janet Izatt, Monica Izmajlowicz, Niclas Jareborg, Bijay Jassal, Grant Jeffery, Kim Jeffery, Colin Jeffrey, Kerstin Jekosch, Lee Jenkins, Tina Johansen, Cheryl Johnson, Christopher Johnson, David Johnson, Keith Jolley, Abigail Jones, Claire Jones, Juliet Jones, Matthew Jones, Michael Jones, Steven Jones, Shirin Joseph, Ann Joy, Linsey Joy, Victoria Joy, Gillian Joyce, Mark Jubb, Kanchi Karunaratne, Michael Kay, Danielle Kaye, Lyndal Kearney, Simon Kelley, Joanna Kershaw, Ross Kettleborough, Cathy Kidd, Peter Kierstan, Andrew Kimberley, Andrew King, Simon Kingsley, Gillian Klingle, Andrew Knights, Anders Krogh, Philip Laidlaw, Michael Laing, Gavin Laird, Christine Lambart, Ralph Lamble, Cordelia Langford, Timun Lau, Stephanie Lawlor, Sampsa Leather, Minna Lehvaslaiho, Steven Leonard, Daniel Leongamornlert, Margaret Leversha, Julia Lightning, Sarah Lindsay, Matthew Line, Sally Linsdell, Peter Little, Christine Lloyd, David Lloyd, Victoria Lock, William Lock, Anne Lodziak, Ian Longden, Howard Loraine, Rachel Lord, Jamie Lovell, Georgina Lye, Neil Marriott, Anna Marrone, Paul Marsden, Victoria Marsh, Matthew Martin, Sancha Martin, Gareth Maslen, Debbie Mason, Lucy Matthews, Paul Matthews, Madalynne Maynard, Owen McCann, Joseph McClay, Craig McCollum, Louise McConnachie, Bill McDonald, Louise McDonald, Jennifer McDowall, Carole McKeown, Stuart McLaren, Kirsten McLay, James McLean, John McMurdo, Amanda McMurray, Des McMurray, Natalie McWilliams, Nalini Mehta, Noel Menuge, Simon Mercer, Asab Miah, Gos Micklem, Simon Miles, Sarah Milne, Dippica Mistry, Shailesh Mistry, Jake Mitchell, Jeff Mitchell, Maryam Mohammadi, Christophe Molina, Paul Mooney, Madeline Moore, Andrea Moreland, Beverley Mortimore, Richard Mott, Jim Mullikin, Brian Munday, Elaine Munday, Andy Mungall, Clare Murnane, Kerry Murrell, Alison Myers, David Negus, David Niblett, Jonathan Nicholson, Tim Nickerson, Sukhjit Nijjar, Zemin Ning, James Nisbet, Christopher Odell, Daniel O'Donovan, Francess Ogbighele, Tom Oinn, Hayley Oliver, Karen Oliver, Helena Orbell, Anthony Osborn, Joan Osborne, Emma Overton-Larty, Christopher Parkin, Kim Parkin, Ginny Parry-Brown, Dina Patel, Ritesh Patel, Alexandra Pearce, Danita Pearson, Anna Peck, Richard Peck, John Peden, Chantal Percy, Andrew Perito, Isabelle Perrault, Anna Peters, Roger Pettett, Ben Phillimore, Kim Phillips, Samantha Phillips, Darren Platt, Emma Playford, Bob Plumb, Matthew Pocock, Keith Porter, Christopher Potter, Simon Potter, Don Powell, Radhika Prathalingham, Michael Quail, Chris Quince, Matloob Qureshi, Helen Ramsay, Yvonne Ramsey, Sally Ranby, Richard Rance, Vikki Rand, Joanne Ratford, Lewis Ratford, Daniel Read, Donald Redhead, Christine Rees, Mary Reid, Astrid Reinhardt, Alex Rice, Catherine Rice, Peter Rice, Suzzanne Richard, Susan Richardson, Kerry Ridler, Lyn Riethoven, Melanie Robinson, Rebecca Rochford, Jane Rogers, Lisa Rogers, Hugh Ross, Mark Ross, Angela Rule, James Rule, Ben Russell, Jayne Rutter, Kamal Safdar, Natalie Salter, Javier Santoyo-Lopez, David Saunders, Carol Scott, Deborah Scott, Ian Scott, Fiona Seager, Margaret Searle, Paul Searle, Harminder Sehra, Jason Shardelow, Greg Sharp, Teresa Shaw, Charles Shaw-Smith, Jennifer Shearing, Karen Sheppard, Richard Sheppard, Elizabeth Sheridan, Ratna Shownkeen, Richard Silk, Matthew Sims, Sarah Sims, Shanthi Sivadasan, Carl Skuce, Luc Smink, Andrew Smith, Laura Smith, Lorraine Smith, Michelle Smith, Russell Smith, Stephanie Smith, Hannah Sneath, Cari Soderlund, Victor Solovyev, Erik Sonnhammer, Elizabeth Sotheran, Lee Spraggon, Janet Squares, Suzanna Squares, Michael Stables,

James Stalker, Steve Stamford, Melanie Stammers, Helen Steingruber, Yvonne Stephens, Charles Steward, Aengus Stewart, Michael Stewart, Mo Stock, Lisa Stoppard, Philip Storey, Carol Strachan, Greg Strachan, Claire Stribling, John Sturdy, John Sulston, Chris Swainson, Mark Swann, Neil Sycamore, Matthew Tagney, Steven Tan, Elizabeth Tarling, Amy Taylor, Gillian Taylor, Kate Taylor, Ruth Taylor, Ruth Taylor, Sam Taylor, Susan Taylor, Louise Tee, Julieanne Tester, Andrew Theaker, Craig Thomas, Daniel Thomas, Karen Thomas, Ruth Thomas, Roselin Thommai, Andrea Thorpe, Karen Thorpe, Glen Threadgold, Emma Tinsley, Alan Tracey, Jonathan Travers, Anthony Tromans, Ben Tubby, Cristina Tufarelli, Kathryn Turney, Darren Upson, Mark Vaudin, Ramya Viknaraja, Wendy Vine, Paul Voak, Sarah Walker, Melanie Wall, Justine Wallis, Michelle Wallis, Graham Warren, Georgina Warry, Andy Watson, Anthony Webb, Jeannette Webb, Alan Wells, Sarah Wells, Robert Welton, Paul West, Tony West, Angela Wheatley, Carl Wheatley, Gideon Wheeler, Hayley Whitaker, Adam White, Amelia White, Brian White, Johnathon White, Simon White, Matthew Whiteley, Adam Whittaker, Pamela Whittaker, Sara Widaa, Anna Wild, Jane Wilkinson, Paul Wilkinson, David Willey, Andy Williams, Bill Williams, Leanne Williams, Sophie Williams, Helen Williamson, Tamsin Wilmer, Laurens Wilming, Brian Wilson, Gareth Wilson, Margaret Wilson, Nyree Wilson, Siobhan Wilson, Wendy Wilson, Philip Window, Jenny Winster, James Witt, Fred Wobus, Emma Wood, Joe Wood, Sharon Woodeson, Rebecca Woodhouse, Richard Wooster, Matthew Wray, Paul Wray, Charmain Wright, Kathrine Wright, Julia Wyatt, Jane Xie, Louise Young, Sheila Young, Ruth Younger and Shenru Zhao

Washington University Genome Sequencing Center, *Box 8501, 4444 Forest Park Avenue, St. Louis, MO 63108, USA*: Sabiha Abbas, Amanda Abbott, Jane Abu-Threideh, Ranjeet Ahluwalia, Ella Alexander, Muhammad Alhawagri, Johar Ali, Jason Allen, Mark Ames, Stephanie Andrews, Susanna Angell, Paul Antonacci, Lucinda Antonacci-Fulton, Bessie Antoniou, Jon Armstrong, Clint Arnett, Vanessa Atkins, Kevin Austin, Cindi Bailey, Damon Baisden, Brad Barbazuk, Myrtle Barrett, Lilla Bartko, Chris Bauer, Henry Bauer, Dana Baum, Catherine Beck, Michael C Becker, Joseph Bedell, Kirk Behymer, Sean Behymer, Edward Belter, Gary Bemis, Dan Bentley, Amy Berghoff, Kelly Bernard, Zachary Bevins, Lauren Bielicki, Thomas Biewald, Linda Blackwood, Russell Blaine, Donald Blair, Mary Blanchard, Mary Blandford, Darin Blasiar, Jennifer Bolandis, Stephen Bolla, Traci Bollinger, Jeffrey Bong, Judith Boren-Prydydasz, Sherell Bourne, Kyle Bova, Elizabeth Boyer, Kourtney Bradford, Stephanie Brennan, Michelle Broy, Delali Buatsi, Christina Budnicki, Meghan Burkett, Jennifer Burkhart, Carrie Buss, Jessica Butler, Drucilla Caldwell, Rose Caldwell, Marco Cardenas, Kelly Carpenter, Jason Carter, Tim Carter, Todd Carter, Darren Casimere, Angela Chapman, Brandi Chiapelli, Asif T. Chinwalla, Stephanie L. Chissoe, William Christy, Matthew Cissell, Brenda Clark, Mari Jo Clark, Kathleen Clarke, Sandra W. Clifton, Jim Cloud, Brian Coblitz, Molly Cofman, Megan Connell, Joshua Conyers, Lisa L. Cook, Mark Cook, Matthew Cooper, Veronica Coppedge, Matthew Cordes, Holland Cordum, Marc Cotton, Laura Courtney, William Courtney, Krista Creason, JyeMon Crockett, Kevin Crouse, Taquillia Crum, Michael Dante, Ruth Davenport, Michelle David, Sharon Davidson, Teresa Davidson, Shanoa Davis, Andrew Delehaunty, Kim D. Delehaunty, Sandy Dempsey, Anu Desai, Jasna Despot, Monica Dickes, Kelly Dickinson, Nicole Dietrich, George Dignan, Richard Dixon, Amy Doebber, Nicholas Doerr, Mark Donoho, Margaret Dotson, Jennifer Doucette, Kristy Drone, Feiyu Du, Hui Du, Zijin Du, Chad Dubbelde, Grant Duckels, Sean Eddy, Scott Edinger, Jennifer Edwards, Tonya Ehlmann, James Eldred, Amy Elkin, Glendoria Elliott, Efrem Exum, Amanda Falk, Kimberly Farrow, Anthony Favello, Jacquelyn Fedele, Ginger Fewell, David Ficenec, Tanya Fiedler, Lisa Flagg, Alison Fleming, Nat Florence, Jason Fries, William Fronick, Johanna Fryman, Dan Fuhrmann, Lucinda A. Fulton, Robert S. Fulton, Diane Gaige, Tony Gaige, Joseph Garrett, Stacie Gattung, Cynthia Geisel, Steve Geisel, Alicia Gibson, Edward Gibson, Candi Giddings, Barbara Gillam, Yekaterina Gincherman, Warren R. Gish, Evening Glaser, Danielle Glossip, Jennifer Godfrey, Deepa Goela, Norma Goins, Judith Gotway, Ernest Goyea-Gbadebo, Laura Granderson, Tina Graves, Serena Gregory, Satbir Grewal, Justin Griffin, Heather Grover, Gary Gualberto, Christopher Gund, William Haakenson, Krista Haglund, Priscilla Hale, Shane Hale, Terri Hall, Zeyad Hamdan, Chalet Hannah, Richard Harkins, Gwen Harmon, Mark Harper, Anthony Harris, Michelle Harrison, Rob Hart, Kevin Haub, James Hawkins, Clay Hawryszko, Chuck Heidbrink, Kandis Hendrix, John Henkhaus, Karensa Henley, Carleena Henry, Nathaniel Hershberger, Joshua Heyen, Matthew Hickenbotham, Patrick Hill, Travis Hillen, LaDeana W. Hillier, Kurt Hinds, Jennifer Hodges, Erik Hoefgen, Leonard Holbrook, Holly Hollingsworth, Paul Holloway, Michael Holman, Andrea Holmes, Melisa Hotic, Shunfang Hou, Sean Houshmandi, Cristi Howell, Denise Hoyt, Carla Hubbard, Latonya Isaiah, Amber Isak, Ann Jacobs, Sara Jaeger, Cami Jeliti, Emily Jentes, Arthur Johnson, Douglas L. Johnson, Brenda Jones, Kimberly Jones, Rodney Jones, Corinne Joshu, Kelie Kang, Paula Kassos, Kimberly Keen, Jennifer Kellen, Sara Kennedy, Norma Keppler, Melissa Ketterman, Kyung Kim, Susan Kitchell, Darla Klebe, Bill Klinke, John Kloss, Laurie Knight, Michael Koch, Jeremy Kock, Sara Kohlberg, Ian Korf, Davorka Kovcic, Jeffry Kraemer, Jason B. Kramer, Pawel Krasucki, Piotr Krasucki, Rebecca Krauss, Colin Kremitzki, Scott Kruchowski, Tamara Kucaba, Michelle Lacy, Thomas Lakanen, Elizabeth Lamar, Kelly Lane, Yvonne Langston, John P. Latreille, Daniel Layman, Thomas Le, Thuy-Tien Pham Le, Tri-Tin Le, John J Ledwith, Nahmjee Lee, Lynn Lehnert, Sarah Lennox, Shawn Leonard, Kimberly Lesley, Leana Levin, Andrew Levy, Shannon Lewis, Lili Li, Todd

Littlejohn, Nichole Long, Paul Lowery, Sandra Luxen, Terrie Lynch, Jason Maas, Jill MacDonald, Len Maggi, Maggie Maher, Pamela Marchetto, Elaine R. Mardis, Christopher Markovic, Catherine Marquis-Homeyer, Marco A. Marra, Gabor Marth, John C. Martin, Joseph Martin, Scott Martinka, Rachel Maupin, Kristi Maxeiner, Ryan McAdow, Maria Mcarther, Cynthia McCabe, Quentin McCray, Bradley McDill, Ken McDonald, Ramonna McDonald, Treasa McDonald, Dana McDonough, Rebecca McGrane, Shirley McKinney, Michael McLellan, Rebecca McMahon, John D. McPherson, Yvonne McQuerrey, Kelly Mead, Brian Meininger, Brian Merry, Rick Meyer, Chandra Meyers, Kevin Miller, Nancy Miller, Walt Miller, Tracy L. Miner, Brian Minges, Patrick J. Minx, Sheela Mishra, Deborah Moeller, Lisa Mohd Nor, Kenneth Moire, Bradley Moore, Todd Moore, Richard Morales, Nancy Mudd, Garrett Mullen, Molly Mullen, Elizabeth Mulvaney, Jennifer Murray, Matthew Myers, Amy Nash, William Nash, Joanne Nelson, Christine Nguyen, Nham Nhan, Candace Nicol, Laura Niemann, Laurie Nothaker, Tonia Nwagbo, Ben Oberkfell, Darren O'Brien, David O'Brien, Temitope Odunfa-Jones, Maja Kisic Okuka, Michael O'Malley, Suzanne Owens, Philip Ozersky, Sarah Page, Dimitrios Panussis, Kimberley Pape, Christina Parker, Adele Pauley, Edward Paulson, Julie Peak, Charlene Pearman, Dale Peluso, Kymberlie H. Pepin, Denise Peterson, Janine Pettiford, Brent Pfeiffer, Amy Phillips, Guy Pierce, Carol Pikula, Amy Podhrasky, Craig Pohl, Tracy Ponce, Sarah Puro, Christi Ralph, Jennifer Randall, James Randolph, Jerry Reed, Amy Reily, David Reiniesch, Linda Reitz, John Reskusich, Carrie Rhine, Lorrie Rice, Mark Richards, Jamie Richey, Joanne Rieff, Julie Riley, Ellen Ritchey, Judy Robertson, Kerry Robinson, Susan Rock, Tracy Rohlfing, Christine Rose, Ellen Ryan, Jennifer Ryan, Joseph Ryan, Sarah Ryno, Laura Sammons, Brent Sandberg, Thomas Sandbothe, Nathan Sander, Lisa Sapetti, Samuel Sasso, Mark Schaller, Carrie Schaus, Debra Scheer, Paul Scheet, Emilie Scherger, Luke Schneider, Brian Schultz, Kelsi Scott, Sacha Scott, Doug Scronce, Ryan Seim, Mandeep Sekhon, Shawn Shafer, Neha Shah, Sharhonda Shahid, Karina Shapiro, Proteon Shelby, Kimberly Shih, Michael Slaughter, Joanne Small, Aimee Smith, Angela Smith, Elyse Smith, Jana Smith, Nikki Smith, Reene Smith, Beth Smoker, Jacquelyn Snider, Lisa Spalding, John Spieth, Paula Steele, Laurita Stellyes, Nathan Stitziel, Tamberlyn Stoneking, Cynthia Strong, Joe Strong, Catrina Strowmatt, Eric Stuebe, Jessica Stumpf, Regina Suk, Hui Sun, Carrie Sutterer, Gary Swift, Sameer Talcherkar, Patra Thipkhosithkun, Johannah Thompson, Aye Mon Tin-Wollam, Chad Tomlinson, Mark Tonn, Lee Trani, Evanne Trevaskis, Susan Tucci, Bradley Twyman, Karen Underwood, Melanie Ureta, Phillip Valencia, Andrew Van Brunt, Christa Veath, Joelle Veizer, Caryn Wagner-McPherson, Jason Waligorski, Christopher Walker, Rebecca Walker, Timothy Wall, John Wallis, Pamela Wamsley, Robert H. Waterston, Phenicia Wedgeworth, Andrew Weihe, Michael C. Wendl, Nancy Wheeler, Shirley White, Nichole Whitworth, Donald Williams, Amy Williamson, Richard K. Wilson, Kellie Winchester, Mark Winkelmann, Jeffrey Woessner, Patricia Wohldmann, Jacob Wolff, Cliff Wollam, Kimberly Woods, J. Patrick Woolley, Ronald Worthington, Xiaoyun Wu, Kristine Wylie, Todd Wylie, Mark Yandell, Shiaw-Pyng Yang, Raymond Yeh, Martin Yoakum, Senait Zerazion, Xiao Zheng, Hui Jun Zhu and Michael Zidanic

US DOE Joint Genome Institute, *2800 Mitchell Drive, Walnut Creek, CA 94598, USA*: Anne Abrajano, Andrea Aerts, Dana Alcivare, Michael Altherr, Gina Amico-Keller, Janice Andora, C.H. Andredesz, Tim Andriese, Tim Andriese, Lennie Arcaina, Teresita Arcaina, Ruby Archuleta, Andre Arellano, Nancy Armstrong, Linda Ashworth, Christina Attix, Anita Avery, Aaron Avila, Julie Avila, Hummy Badri, Michele Bakis, Joe Balch, Michael Banda, Keith Beall, Don Beaton, Don Beaton, John Bercovitz, Ann Bergmann, Tony Beugelsdijk, Tory Bobo, John Boehm, Marnel Bondoc, M.P. Bonner, Eric Bowen, Wade Brannon, Elbert Branscomb, Amy Brower, Nancy Brown, Rita Brown, David Bruce, Robert Bruce, Eric Brunkhorst, Jennifer Bryant, Judy Buckingham, Karolyn Burkhart-Schultz, B. Bursell, Mira Bussod, Connie Campbell, Evelyn Campbell, Mary Campbell, Chenier Caoile, Heliodoro Cardenas, Mario Cepeda, Patrick Chain, Sandra Chaparro, Leslie Chasteen, Xian Chen, Jan-Fang Cheng, S.G. Chin , Corey Chinn, Mari Christensen, Alex Chung, Robert Cifelli, Lynne Clark, Jackie Cofield, Judith Cohn, Rick Colayco, Alex Copeland, Rebecca Cordray, Earl Cornell, Lisa Corsetti, Terrence Critchlow, Paul Critz, Linda Danganan, Willow Dean, Larry Deaven, Kerry Deere, Paramvir Dehal, Zuoming Deng, John Chris Detter, Sara Detter, J.M. Dias, Victoria Dias, Mark Dickson, Richard DiGennaro, Karen Dilts, M. Dimitrijevic-Bussod, Kami Dixon, Long Do, Norman Doggett, Suzanne Duarte, Christopher Elkin, Anne Marie Erler, Joe Fawcett, James Fey, Marie Fink, Kathe Fischer, Laurice Fischer, J. Patrick Fitch, Dave Flowers, Peg Folta, Dea Fotopulos, Matt Fourcade, Ken Frankel, Marvin Frazier, Jane Fridlyand, Stuart Gammon, Anca Georgescu, Amy Geotina, Isaias Gil, Tijana Glavina, Kristen Golvineaux, Sheryl Goodman, Lynn Goodwin, Laurie Gordon, Kristine Gould, Bruce Gray, Lance Green, Jeff Griffith, Jane Grimwood, Matt Groza, Hannibal Guarin, Kate Gunning, Chi Ha, Catherine Halsey, Sha Hammond, Cliff Han, Trevor Hawkins, Nina Henderson, Wendell Hom, Roya Hosseini, Zhenping Huang, Hillary Hughes-Hull, David Humphries, Matt Hupman, Jacqulene Hurshman, Kent Hutchings, Doug Hyatt, Joe Jaklevic, Karren Jamaca, Teresa Janecki, Jamie Jett, Phil Jewett, Lingxia Jiang, Jian Jin, Myma Jones, Eugine Jung, Kristen Kadner, Hitesh Kapur, Lisa Kegg, SuSu Khine, Joomyeoung Kim, Heather Kimball-Rojeski, William Kimmerly, Cynthia Ko, Art Kobayashi, William Kolbe, Kristina Kommander, Marie Krawczyk, Brent Kronmiller, V. Anne Krysiak, Carol Kuhn, Jane Lamerdin, Jane Lamerdin, Miriam Land, Frank Larimer, Frank Larimer, Bernadette Lato, Joon Ho Lee, Michael Lee, Karl Lehmann, Tina Leyba, Kenneth Lindo, Karla Lindquist, Albert Linkowski, Kathy Litton, S.Y. Liu,

Crystal Llewellyn-Silva, Rebecca Lobb, Jessica Logan, John Longmire, Jose Luis Lopez, Yunian Lou, Stephen Lowry, X. Lu , Susan Lucas, Migdad Machrus, Madison Macht, Ramki Madabhushi, Ryan Mahnke, Mary Maltbie, Marissa Mariano, Lisa Marie Marieiro, Christopher Martin, Joel Martin, Michele Martinez, Paula McCready, Phil McGurn, Kim McMurry, Catherine Medina, Kristen Meier, Linda Meincke, Jon Menke, Julianne Meyne, Trini Miguel, Christie Miller, Tammy Milligan, Sheri Miner, Virginia Montgomery, Daniel Moy, Mark Mundt, Chris Munk, Richard Mural, Rick Myers, Rick Myers, Mohandas Narla, David Nelson, Jennifer Neunkirch, April Newman, Hoa Nguyen, Lisa Nguyen, Quan Nguyen, Matt Nolan, Pier Oddone, Jason Olivas, Anne Olsen, David Ow, Morey Parang, Beverly Parson-Quintana, Bipin Patel, Shripa Patel, Yi Peng, Ze Peng, Karl Petermann, Bill Petitt, Joyce Pfeiffer, Hoan Phan, Sam Pitluck, Lee Pittson, Ingrid Plajzer-Frick, Martin Pollard, Patricia Poundstone, Eunice Prakash, Paul Predki, Jennifer Primus, Lyle Probst, Emily Prusso, Glenda Quan, Lucia Ramirez, Michele Ramirez, David Randolph, Irmengaard Rapier, Warren Regala, Charles Reiter, X. Ren , Paul Richardson, Darrell Ricke, Donna Robinson, Juan Rodriguez, George Sakaldasis, Christina Sanders, Richard Sarmiento, Elizabeth Saunders, Denise Schmoyer, Jeremy Schmutz, Damian Scott, Duncan Scott, Manesh Shah, Jin Shang, Maria Shin, Jeff Shreve, Julie Simoni, John Sims, Linda Sindelar, Evan Skowronski, Tom Slezak, Joel Smith, Jay Snoddy, Gregory Stanley, Stephanie Stilwagen, Lisa Stubbs, Janet Stultz, Sandhya Subramanian, Rob Sutherland, Kristina Tacey, Tracy Takenaka, Tootie Tatum, Astrid Terry, Judy Tesmer, James Thiel, Paulette Thomas, Linda Thompson, Sue Thompson, Wendy Thompson, Grace Tong, David Torney, Mary Tran, Margie Trankiem, Stephan Trong, Ming Yu Tsai, Heidi Turner, James Turner, Jeanne Turturice, Edward Uberbacher, Chun Un, Quyen Ung, Ryan Van Luchene, Michele Vargas, Steffan Vartanian, N.P. Velasco, Olivia Velasquez, Carolyn Vertuca, V.S. Viswanathan, Jeanette Wagner, Mark Wagner, Wei Wan, Mei Wang, Edward Wehri, Richard Weidenbach, Sarah Wenning, Sara Wentz, Catherine White, Jennifer White, Scott White, Al Williams, David Wilson, Brenda Winleblech-Kelly, J.R. Wollard, Lawreen Woo , John Woolley, Tracy Wright, Melissa Wycoff-Montegro, Joan Yang, Mimi Yeh, Charles Yu, Brian Yumae and D.W. Zimmerman

Baylor College of Medicine Human Genome Sequencing Center, *Department of Molecular and Human Genetics, One Baylor Plaza, Houston, TX 77030, USA*: Charles Adams, Babajide Adio-Oduola, Carlana Allen, Heather Allen, Harshinie Amaratunge, Andrew Arenson*, Michael Bailey*, Tarsha Banks, Joseph Barbaria, Kesha Bimage, Benedict Bodota*, David Bonnin, John Bouck, Anissa Brooks*, Eric Brown*, M. Jennifer Brown, Nathaniel Bryant, Christian Buhay, Paula Burch, Carrie Burkett, Kevin Burrell, Tamika Carron, Kelvin Carter, Sandra Cavazos, Joseph Chacko, Dean Chavez, Guan Chen, Mike Chen, Rui Chen, Zhijian Chen, Constantine Christopoulos, Kerstin Clerc-Blankenburg, Raynard Cockrell, Caroline Cox, Marcus Coyle, Stephanie Dathorne, Robert David*, Mary Louise Davila, Clay Davis, Latarsha Davy-Carroll, Oliver Delgado, Amanda Denn , Denise DeShazo*, Yan Ding, Huyen Dinh, Karen Douthwaite, Heather Draper, Shannon Dugan-Rocha, K. James Durbin, Christopher Earnhardt, Darren Edgar, Carlana Allen, Christian Elhaj, Michael Escotto, Thomas Falls, Nicole Flagg, Jennifer Forcum-Tansey, Priscilla Foster, J. Patrick Frantz*, Abdul Gabisi, Angela Garcia, Dawn K. Garcia[1], Toni Garner, Richard A. Gibbs, Rachel Gill, J. Harley Gorrell*, Lora Leigh Gorrell*, Whitney Guevara, Preethi Gunaratne, Keelan Hamilton, Vincent Hanak, Keith Harris*, Paul Havlak, Alicia Hawes, Judith Hernandez, Omar Hernandez, Anne Hodgson, Marilyn Hogues, Barbara Hollins, Farah Homsi, Hailey Hosak*, Xuanlin Hou*, James Huber, Jennifer Hume, LaRonda Jackson, Yu Jia*, Bennie Johnson, Rudy Johnson, Angela Jolivet, Margaret Jones*, Sary Joudah*, Steven Kaminsky*, James Kelly*, Susan Kelly, Elinor Karlsson*, Umer Khan, LaQuisha King, Natasha Kondejewski*, Christie Kovar, Jasmina Kratovic*, Raju Kucherlapati[2], Belita Leal, LaKeshia Lewis, Lora Lewis, Zhangwan Li, Jane Li, Olivier Lichtarge, Jing Liu, Wen Liu, LaQuinta Logan*, Orlando Logan*, Hermela Loulseged, Ryan Lozado, Jing Lu*, Alice Lucier, Raymond Lucier*, Thang Ly*, Jie Ma, Manjula Maheshwari, Patricia Mapua, Ryan Martin, Ashley Martindale, Carlos Martinez*, Evangelina Martinez, Elizabeth Massey, Samantha Mawhiney, Michael McLeod, Michael Meador, Gangwu Mei*, Iracema Mercado, Michael Metzker, George Miner, Teresa Mitchell, Wei Mo*, Khatera Mohabbat, Baize Montgomery, Kate Montgomery[2], Margaret Morgan, Sidney Morris, Maragaret Moser*, Donna Muzny, Sally Nash*, Susan Naylor[1], Dearl Neal, Angela Nelson*, David Nelson, Natalee Newton, Ahn Nguyen*, Bao-Viet Nguyen, Natalie Nguyen, Ngoc Nguyen, Elizabeth Nickerson, Stanley Nwokenkwo, Maryann Oguh, Geoffrey Okwuonu, Gayatri Oswal*, Rodolfo Oviedo, Araceli Pace, Bridgette Parish*, Seth Paxton*, Brett Payton, Lesette Perez, Leonard Peters, Adam Pickens, Natasha Pieper, Eltrick Primus, Ling-Ling Pu, Miyo Quiles,Juana Quiroz, Danell Reiter*, Yanru Ren, C. Michelle Rives, Alberto Rojas, San Juana Ruiz, Glenford Savery, Steve Scherer, Graham Scott, Hua Shen, Margarita Simon*, Ida Sisson, Erica Sodergren, Titilola Sonaike, Linda Savage*, Anastasia Sparks, Hailey Stanley, Heather Stone*, Angelica Sutton, Amanda Svatek, Leah Anne Svetz, Paul Tabor, Kavitha Tamerisa, Christina Taylor, Tineace Taylor, Nicole Thomas, Shereen Thomas, Kirsten Timms*, Ly Thanh Tran, Kamran Usmani, Lydia Vasquez, Virginia Vera, Deborah Villalon, Donna Villasana, Quyen Vo*, Davian Walker, Randy Wall, Jie Wang, Suzhen Wang, Stephanie Ward-Moore, Ramiah Warren, Surah Watlington*, Mary Watrous*, George Weinstock[3], David Wheeler, Gabrielle Williams, Angela Williamson, Regina Wleczyk, Steven Wooden, Kim Worley, Glenda Wrensford*, Jialing Zhou, Xiaojun Zhou*, Sara Zorrilla.

* Denotes past employees who made significant contributions to the project.

[1] Department of Cellular and Structural Biology
University of Texas Health Science Center at San Antonio
7703 Floyd Curl Drive
San Antonio, Texas 78229-3900
USA

[2] Department of Molecular Genetics
Albert Einstein College of Medicine
1635 Poplar Street
Bronx, New York 10461
USA

[3] Department of Microbiology & Molecular Genetics
University of Texas Health Science Center at Houston
6431 Fannin Street
Houston, Texas 77030
USA

RIKEN Genomic Sciences Center, *1-7-22 Suehiro-cho, Tsurumi-ku Yokohama-city, Kanagawa 230-0045, Japan:* Tomoyuki Aizu, Rie Arai, Yui Asahi, Fumiwo Ejima, Mitsuru Fujioka, Asao Fujiyama, Kyoko Fukano, Rintaro Fukawa, Qun Gu, Masahira Hattori, Matsumi Hirose, Minami Horishima, Kazuo Ishii, Hinako Ishizaki, Emi Isozaki, Noriko Ito, Takehiko Itoh, Chiharu Kawagoe, Kayo Kobayashi, Yoshikazu Kobayashi, Noriko Kodaka, Mai Kondo, Yuka Matsumura, Yuko Mitani, Hiroko Morita, Ayuko Motoyama, Shunsuke Nagao, Saori Nakagawa, Konomi Nakamura, Chikako Nakano, Aki Nishida, Yuko Odama, Nobuhiro Omori, Yoko Ono, Kenshiro Oshima, Yumie Oyama, Ritsuko Ozawa, Hong-seog Park, Ryoko Sakai, Yoshiyuki Sakaki, Hiroko Seki, Hidetsugu Shimizu, Jiuqin Sun, Takashi Tahara, Toshihisa Takagi, Sumiyo Takiguchi, Maho Tanaka, Ryoko Tanaka, Todd Taylor, Yoriko Terada, Miwako Tochigi, Naoko Tomioka, Yasushi Totoki, Atsushi Toyoda, Yumi Tsukamoto, Shiho Tsukuni, Rina Tsuzuki, Nozomi Uyama, Hiromi Wada, Hidemi Watanabe, Tetsushi Yada, Kaoru Yakushiji, Noriko Yamamoto, Yasue Yamashita, Shuji Yokoyama, Miho Yonezawa and Satoru Yoshida

Genoscope and CNRS UMR-8030, *2 Rue Gaston Cremieux, CP 5706, 91057 Evry Cedex, France***:** Francois Artiguenave, Nathalie Barbe, Marielle Besnard, Didier Boscus, Stephanie Briez, Philippe Brottier, Thomas Bruls, Laurence Cattolico, Nathalie Cha, Corinne Da Silva, Ivan Dubois, Michel Gouyvenoux, Gabor Gyapay, Roland Heilig, Stephanie Leclerc, Michael Levy, Ghislaine Magdelenat, Eric Pelletier, Jean-Louis Petit, Catherine Robert, William Saurin, Benoit Vacherie, Virginie Vico, Jean Weissenbach and Patrick Wincker

GTC Sequencing Center, Genome Therapeutics Corporation, *100 Beaver Street, Waltham, MA 02453-8443, USA***:** Michele Bakis, Romina Bashirzadeh, John Battles, Michael Bodnaruk, Gary Breton, Jim Brown, Carole Butler, Patrick Cahill, Anne Caron, Patricia Daggett, Thomas Dorman, Lynn Doucette-Stamm, JoAnn Dubois, Natasha Edwards, Johnny Ezedi, Shaun Flynn, Laura Freeman, Rene Gibson, David Gleeson, Gary Gryan, Becky Herman, Joseph Hitti, Tay Ho, Keri Holtham, Khanh Huynh, Christopher Hynds, Michael Johnson, Paul Joseph, Rachel Kadel-Garcia, Veena Kamath, Arnold Kana, Kristian Keane, Katrina Kopcewiez, Andrew Lach, Anna Lee, Hong Mei Lee, Randy Little, Wendy Lumm, Deepika Madan, Rodolfo Magararu, Jen-I Mao, Luba Mitnik-Gankin, Maribel Munoz, Minh Nguyen, William Nielson, Shashi Prabhakar, Jonathan Prescott-Roy, Dayong Qiu, Bruce Reinemann, Sean Robinson, Mike Roche, Dawn Rossetti, Marc Rubenfield, Olga Russakovskaya, Johnathan Segal, Douglas R. Smith, Phillip Snell, Mathew Stroika, G. Andre Turenne, Jennifer Walsh, Ying Wang, Keith Weinstock, Gerald Wheaton, Michael Wierbonies, Laipeng Wong, Qinxue Xu, Huiren Yang, Effie Zafiropoulos and Eileen Zhang

Department of Genome Analysis, Institute of Molecular Biotechnology, *Beutenbergstrasse 11, D-07745 Jena, Germany***:** Cornelia Baumgart, Ines Baumgart, Karin Blechschmidt, Elisabeth Boehm, Christin Brunnckow, Nicole Creutzburg, Monika Dette, Bernd Drescher, Petra Eißmann, Susanne Fabisch, Beate Fischer, Silke Foerste, Petra Galgoczy, Sabine Gallert, Gernot Glöckner, Yvonne Görlich, Claudia Grosser, Jana Hamann, Ivonne Heintze, Niels Jahn, Erika Kantowski, Heike Klabunde, Sindy Kluge, Dorothee Lagemann, Sabine Landmann, Rüdiger Lehmann,

Denise Lenk, Hella Ludewig, Elke Meier, Uwe Menzel, Evelyn Michaelis, Kati Möckel, Katja Mortag, Oliver Müller, Gabriele Nordsiek, Gerald Nyakatura, Birgit Pawelka, Uta Petz, Uwe Pick, Matthias Platzer, Carola Pohlmann, Andreas Polley, Bettina Raguschke, Norman Rahnis, Kathrin Reichwald, André Rosenthal, Silke Rosenthal, Sandra Rothe, Andreas Rump, Ruben Schattevoy, Annika Schauer, Markus Schilhabel, Mike Schilling, Liane Schlenkert, Marie-Luise Schmid, Jana Schoemburg, Andreas Schudy, Regina Schulz, Stefan Taudien, Bärbel Tautkus, Margit Teuchtler, Beate Voigt, Jacqueline Weber, Gaiping Wen , Claudia Wenderoth, Daniela Werler, Thomas Wiehe , Nadine Zeise, Renate Zenker and Wolfgang D. Zimmermann

Beijing Genomics Institute/Human Genome Center, *Institute of Genetics, Chinese Academy of Sciences, Beijing 100101, China*: Jingyue Bao, Qiyu Bao, Weidong Bao, Shihua Bi, Xuemen Bian, Lars Bolund[1,2], Tianjing Cai[3], Ting Cao, Yuzhu Cao, Baoxian Chen, Chong Chen, Jianlong Chen, Jie Chen[4], Junbao Chen, Tong Chen[4,5], Yiyu Chen, Zhu Chen[7], Zhihua Cheng[7], Hongjuan Cui, Jinhui Cui, Peng Cui, Li Dai, Hao Ding, Hui Dong[7], Wei Dong, Xiaojia Dong[6], Yutao Du, Hongyuan Fan, Jianqiu Fang, Haiyan Feng, Jie Feng, Xiaoli Feng, Gang Fu[7], Jimei Gao, Quan Gao[6], Yang Gao, Jianing Geng, Guanghui Gong, Jinying Gong[6], Jun Gu, Wenyi Gu[7], Xiaocheng Gu[6], Qiaoning Guan, Qi Gui, Daorong Guo, Fengying He[6], Jiaying He, Lin He[7], Jie Hu, Songnian Hu, Fang Huang, Guyang Huang[4,7], Jia Jia[7], Nan Jia, Lu Jiang, Yetao Jin, Yongsan Jin, Ning Kang, Ning Kang[6], Mary-Clare King[4,8], Yi Kong, Meng Lei, Changfeng Li, Chenji Li, Eryao Li, Gang Li, Jiayang Li, Jihong Li, Jingxiang Li, Li Li, Lili Li, Ming Li[7], Nan Li, Ran Li, Shengbin Li, Shuangding Li, Shuangli Li, Songgang Li, Tao Li, Wei Li[9], Wenjie Li, Yan Li, Yanni Li, Zhijie Li, Jinsong Liao, Wei Lin, Wei Ling[7], Boyong Liu, Haili Liu, Kai Liu, Ning Liu[4,8], Siqi Liu, Wei Liu, Xinshe Liu, Yanhua Liu, Ying Liu, Yu Liu, Zhanwei Liu, Tao Lu[6], Yongxiang Lu, Gang Lv[9], Cheng Ma, Jiao Ma, Qingmei Ma[6], Shanshan Meng, Feng Mu, Yuxin Niu, Jiaofeng Pan, Qiuhui Qi, Xiaohua Qi, Xufang Qian[7], Zengmin Qian, Boqin Qiang[6], Zhenyong Qiao[7], Shuangxi Ren[7], Li Rong[6], Yufen Shao, Fengye Shen[7], Yan Shen[6], Hongfang Shi, Michael Smith[4,10], Liping Song, Shuping Song, Jiajia Sun, Min Sun, Tao Sun, Yongqiao Sun, Yu Sun, Yue Sun, Wei Tan, Xinyu Tan[6], Xiangjun Tang, Ran Tao, Yan Tian, Yuqing Tian[5], Jingli Tong, Yuefeng Tu[7], Ma Wan[7], Dong Wang, Feng Wang, Guangxin Wang, Guihai Wang, Hongjuan Wang[7], Hongwei Wang[6], Huifeng Wang, Jian Wang, Juan Wang, Jun Wang[4,9], Li Wang, Lijie Wang, Lijuan Wang, Liqun Wang[7], Wenjun Wang, Xiaolei Wang, Xiaoning Wang, Xuegang Wang, Yan Wang, Ying Wang, Yuanyuan Wang, Chungen Wu[7], Dongying Wu, Qingfa Wu, Xiaojing Wu, Yingying Xi[6], Fei Xie, Ruqin Xu, Shuhua Xu[7], Wei Xu, Yuning Xu[6], Zhenyu Xuan[12], Rui Xue, Yali Xue, Chunxia Yan, Fei Yan[8], Guangmei Yan[4,11], Huanming Yang4,8, Shudong Yang, Xiaonan Yang, Zhijian Yao6, Haifeng Yin7, Bing Yu, Jun Yu, Kaiwen Yuan, Yixin Zeng, Dong Zhai, Bo Zhang, Fengmei Zhang, Guangyu Zhang, Guohua Zhang, Haiqing Zhang, Hongbo Zhang, Lanzhi Zhang, Li Zhang, Meihua Zhang, Meng Zhang, Ming Zhang[7], Ruhua Zhang, Wei Zhang[7], Xianglin Zhang[7], Xiaoliang Zhang, Xiuqing Zhang, Yan Zhang[5], Yilin Zhang, Ying Zhang, Yuansen Zhang, Yuzhi Zhang, Hongmei Zhao, Lijian Zhao, Zhijing Zhao, Zhicheng Zhen[6], Ming Zhong[7], Haixia Zhou, Nannan Zhou, Xinfeng Zhou[6], Yan Zhou[7], Yi Zhou[6], Bingying Zhu[7], Bofeng Zhu, Genfeng Zhu[7], Ning Zhu[6], Yongge Zhu and Zhen Zhu

Multimegabase Sequencing Center; The Institute for Systems Biology, *4225 Roosevelt Way, NE Suite 200, Seattle, WA 98105, USA*: Nissa Abbasi, Mary Ellen Ahearn, Lida Baradarani, Dale Baskin, Brian Birditt, Scott Bloom, Cecilie Boysen, Roger Bumgarner, Rachel Dickhoff, Monica Dors, Peter Fleetwood, Cynthia Friedman, Grace Harrison, Leroy Hood, Rose James, Amardeep Kaur, Stephen Lasky, Inyoul Lee, Carol Loretz, Anup Madan, Anuradha Madan, Gregory G. Mahairas, Ryan Nesbitt, Shizhen Qin, Amber Ratcliffe, Lee Rowen, Jason Seto, Tristan Shaffer, Arian Smit, Todd Smith, Steven Swartzell, Barbara J. Trask and Kai Wang

Stanford Genome Technology Center, *855 California Avenue, Stanford, CA 94304, USA:* Pia Abola, Scott Argus, V. Babb, Dan Bruno, E. Chung, Lane Conn, Martin Costa, Ronald W. Davis, Joel Elledge, J. Fan, David Faulkner, Nancy

---

[1] Beijing Genomics Institute/Human Genome Center, Institute of Genetics, Chinese Academy of Sciences, Beijing
[2] Institute of Human Genomics Aarhus University, Aarhus, Denmark
[3] Northern National Genome Center, Beijing
[4] Southern National Genome Center, Shanghai
[5] School of Medicine, Southeast University, Nanjing
[6] College of Life Sciences, Peking University, Beijing
[7] Center of Bio-X Life Sciences, University of Communication, Shanghai
[8] Department of Medical Genetics, University of Washington, Seattle, USA
[9]Institute of Biophysics, Chinese Academy of Sciences, Beijing
[10] Genome Sequence Center, BC Cancer Research Center, Vancouver, Canada
[11] Institute of Microbiology, Chinese Academy of Sciences, Beijing

A. Federspiel, Pam Foreman, Slava Glukhov, Nancy Hansen, Zelig Herman, Richard Hyman, Sue Kalman, Omar Kurdi, Jennifer Mao, Rekha Marathe, Michael J. Proctor, Amanda Morehouse, Peter Oefner, Curtis Palm, David Ramirez, M. Rexan, Mitche Dela Rosa, Mary Smith, D. Vollrath, Julie Wilhelmy, Thomas Willis and Susan Yu

Stanford Human Genome Center and Department of Genetics, *Stanford University School of Medicine, Stanford, CA 94305-5120, USA*: Eva Bajorek, Chenier Caoile, Jason Carriere, David R. Cox, Mark Dickson, Kami Dixon, Laurice Fischer, David Flowers, Dea Fotopulos, Carmen Garcia, Darren Gold, Jane Grimwood, Lauren Haydu, Caleb Holtzer, Kathy Litton, Jessica Logan, Jose Lopez, Cathy Medina, Richard M. Myers, Loan Nguyen, Lucia Ramirez, Alex Rodriquez, Stephanie Rogers, Angelica Salazar, Jeremy Schmutz, Jin Shang, Nancy Stone, Ming Tsai, Olivia Valesquez, Steffan Vartanian, Deborah Vitale, Jeremy Wheeler and Joan Yang

University Washington Genome Center, *225 Fluke Hall on Mason Road, Seattle, WA 98195, USA***:** Kerry Bubb, Riza Daza, Cindy Desmarais, Sven Duenwald, Kim Erickson, Thomas Gilbert, Michael Hite, Robert Hubley, Will Huges, Shawn Iodanoto, Don Jewett, Chris Junker, Arnie Kas, Rajinder Kaul, Myphoung Le, Regina Lim, Lloyd Lytle, Charles Magness, Z. Magnesss, Mathew Maza, Erin McClelland, Maynard Olson, Doug Passey, Xuan-Quynh Pham, Karen Avery Phelps, Ruolan Qiu, Stephan Ramsey, Chris Raymond, Bethany Richards, Zohreh Sadhegi, Channakhone Saenphimmachak, Elizabeth Sims, Arian Smit, Mari Stone, Tony Thomas, Gane Ka-Shu Wang, Zaining Wu, Jun Yu and Yang Zhou

Department of Molecular Biology, Keio University School of Medicine, *35 Shinanomachi, Shinjuku-ku, Tokyo 160-8582, Japan:* Norie Aoki, Michi Asahina, Shuichi Asakawa, Kazuhiko Kawasaki, Jun Kudoh, Shinsei Minoshima, Susumu Mitsuyama, Takashi Sasaki, Kazunori Shibuya, Atsushi Shimizu, Nobuyoshi Shimizu, Ai Shintani and Yuko Yoshizaki

University of Texas Southwestern Medical Center at Dallas, *6000 Harry Hines Blvd., Dallas, TX 75235-8591, USA***:** Pablo Aguayo, Sharla Arenare, Drew Armstrong , Maria Athanasiou, Mujeeb Basit, Daina Black, Jessica Brandon, Jill Buettner, Corey Butler, Corey Butler , Paul Card, Sharmaine Chamblis, Joel Dunn, Cynthia English, Shannon Ethridge, Glen A. Evans[12], Nina Federova, Amber Fribish, Monica Garza, Margaret Gordon, Connie Gorman, O'Dell Grant, Lisa Hahner, Susie Hayes, John Joslin, Steven Lam, Thuan Le, Todd Lester, Ed Lewis, Kok Ngai Loo, Meiyu Loo, Tony Major, Tony Major , James McFarland, Minh Nguyen, Sherri Osborne-Lawrence, Igor Rakoshchik, Jeff Schageman , Roger Schultz, Stephen Stimson, Minh Tran , Flora Varghese, Nikki Wagner, Kendra Waller, Travis Ward, John Wharton, John Whitaker, Jacquelyn Newton Willcot and John Zanoni

University of Oklahoma's Advanced Center for Genome Technology, *Dept. of Chemistry and Biochemistry, University of Oklahoma, 620 Parrington Oval, Rm 311, Norman, Oklahoma 73019, USA***:** Mueed Ahmad, Angelica Bodenteich, Feng Chen, Lingzhi Chu, Judy Crabtree, Stephane Deschamps, Anh Do, Trang Do, Joan Dolance, Angela Dorman, Clarence Ducummon, Andrew Duty, Mounir Elharam, Whitney Elkins, Fang Fang, Ying Fu, Glenda Hall, Karen Hartman, Kevin Hill, Ping Hu, Xiaohong Hu, Axin Hua, Emily Huang, Honggui Jia, Xiuhong Jiang, Steve Kenton, Akbar Khan, Doris Kupfer, Hongshing Lai, Lisa Lane, Hio Ieong Lao, Christopher Lau, Jennifer Lewis, Sharon Lewis, Hang Li, Shaoping Lin, Phoebe Loh, Eda Malaj, Jami Milam, Rose Morales-Diaz, Fares Najar, Thuan Nguyen, Ying Ni, Shelly Oommen, Huaqin Pan, Beth Perry, Stacey Phan, Sulan Qi, Yudong Qian, Linda Ray, Qun Ren, Qun Ren, Bruce A. Roe, Steve Shaull, Danica Sloan, Lin Song, Jaime Stone, Jing Tian, Runying Tian, Yonathan Tilahun, Qiaoyan Wang, Ying-Ping Wang, Zhili Wang, Doug White, Jim White, Diana Willingham, Stephen Wong, Heather Wright, Hong Min Wu, Hui Wu, Limei Yang, Ziyun Yao, Younju Yoon, Min Zhan, Guozhong Zhang, Liping Zhou and Hua Zhu

Max Planck Institute for Molecular Genetics, *Ihnestrasse 73, 14195 Berlin, Germany***:** Stefanie Arndt, Alfred Beck, Katja Borzym, Donald Buczek, Jamel Chelly, Fiona Francis, Katja Heitmann, Steffen Hennig, Celine Hoff, Erich Junker, Petra Kioschis, Sven Klages, Marion Klein, Anna Kosiura, Michael Kube, Ines Langer, Hans Lehrach, Silvia Lehrack, Ines Marquard, Nathalie McDonell, Alfons Meindl, Katja Moll, Anthony Monaco, Andrea Nemeth, Annemarie Poustka, Juliane Ramser, Richard Reinhardt, Simone Schuelzchen, Peter Seranski, Anke Starke, Christina Steffens, Ralf Sudbrak, Kieran Todd and Marie Laure Yaspo

[12] Current address: Genome Sequencing Project, Egea Biosciences, Inc., 4178 Sorrento Valley Blvd., Suite F, San Diego, CA 92121, USA

Cold Spring Harbor Laboratory, Lita Annenberg Hazen Genome Center, *1 Bungtown Road, Cold Spring Harbor, NY 11724, USA*: Melissa de la Bastide, Neilay Dedhia, Lidia Gnoj, Tina Gottesman, Susan Granat, Kristina Haberman, Aliya Hameed, Amy Hasegawa, Jane Hoffman, Emily Huang, Kendall Jenson, Arthur Johnson, Nancy Kaplan, Mohammad Lodhi, Anthony Matero, W. Richard McCombie, Andrew O'Shaughnessy, Laurence Parnell, Ray Preston, Milka Rodriguez, Kristin Schutz, Lei Hoon See, Ravi Shah, Monica Shekher, Nadim Shohdy, Lori Spiegel, I'kori Swaby, Sally Till and Danielle Vil

GBF - German Research Centre for Biotechnology, *Mascheroder Weg 1, D-38124 Braunschweig, Germany*: Helmut Blöcker, Petra Brandt, Ansgar Conrad, Simone Dose, Maja Grimm, Klaus Hornischer, Doris Järke, Gerhard Kauer, Tschong-Hun Löhnert, Gabriele Nordsiek, Joachim Reichelt, Maren Scharfe and Oliver Schön

---

Genome Analysis Group. The group consisted of the individuals listed below (in alphabetical order).

Richa Agarwala[13], L. Aravind[16], Jeffrey A. Bailey[14], Alex Bateman[15], Serafim Batzoglou[16], Bruce Birren[19] , Ewan Birney[17], Peer Bork[18,19], John B. Bouck[20], Daniel G. Brown[19], Christopher B. Burge[21], Lorenzo Cerutti[20,22], Hsiu-Chuan Chen[16], Asif T. Chinwalla[23], Deanna Church[16], Michele Clamp[18], Francis S. Collins[24], Richard R. Copley[22], Tobias Doerks[21,22], Richard Durbin[18], Sean R. Eddy[25], Evan E. Eichler[17], William FitzHugh[19], Adam Felsenfeld[27], Terrence S. Furey[26], James Galagan[19], Richard A. Gibbs[23], James G.R. Gilbert[18], Cyrus Harmon[27], Yoshihide Hayashizaki[28], David Haussler[29], Henning Hermjakob[20], LaDeanna Hillier[26], Karsten Hokamp[30], Tim Hubbard[18], Wonhee Jang[16], L. Steven Johnson[28], Thomas A. Jones[28], Simon Kasif[31], Arek Kaspryzk[20], Scot Kennedy[32], W. James Kent[33], Paul Kitts[16], Eugene

---

[13] National Center for Biotechnology Information, National Library of Medicine, National Institutes of Health, Bldg. 38A, 8600 Rockville Pike, Bethesda, MD 20894, USA
[14] Department of Genetics, Case Western Reserve School of Medicine and University Hospitals of Cleveland, BRB 720, 10900 Euclid Ave., Cleveland, OH 44106, USA
[15] The Sanger Centre, Wellcome Trust Genome Campus, Cambridge, CB10 1SA, United Kingdom
[16] Whitehead Institute for Biomedical Research, Center for Genome Research, Nine Cambridge Center Cambridge, MA 02142, USA
[17] EMBL European Bioinformatics Institute, Wellcome Trust Genome Campus, Hinxton, Cambridge CB10 1SD, United Kingdom
[18] Max-Delbruck-Center for Molecular Medicine, Robert-Rossle-Str. 10, 13125 Berlin-Buch, Germany
[19] EMBL Meyerhofstr.1, 69012 Heidelberg, Germany
[20] Baylor College of Medicine Human Genome Sequencing Center, Department of Molecular and Human Genetics, One Baylor Plaza, Houston, TX 77030, USA
[21] Dept. of Biology, Massachusetts Institute of Technology, 77 Massachusetts Ave., Cambridge, MA 02139-4307, USA
[22] Present Address: INRA, Station d'Amelioration des Plantes, 63039 Clermont-Ferrand Cedex 2, France
[23] Washington University Genome Sequencing Center, Box 8501, 4444 Forest Park Avenue, St. Louis, MO 63108, USA
[24] National Human Genome Research Institute, U.S. National Institutes of Health, 31 Center Drive, Bethesda, MD 20892, USA
[25] Howard Hughes Medical Institute, Dept. of Genetics, Washington University School of Medicine, Saint Louis, Missouri 63110. USA
[26] Dept. of Computer Science, University of California at Santa Cruz, Santa Cruz, CA 95064, USA
[27] Affymetrix, Inc., 2612 8th St, Berkeley, CA 94710, USA
[28] Genome Exploration Research Group, Genomic Sciences Center, RIKEN Yokohama Institute, 1-7-22 Suehiro-cho,Tsurumi-ku, Yokohama, Kanagawa 230-0045, Japan
[29] Howard Hughes Medical Institute, Department of Computer Science, University of California at Santa Cruz, CA 95064, USA
[30] University of Dublin, Trinity College, Department of Genetics, Smurfit Institute, Dublin 2, Ireland
[31] Cambridge Research Laboratory, Compaq Computer Corporation and MIT Genome Center, 1 Cambridge Center, Cambridge, MA 02142, USA
[32] Dept. of Mathematics, University of California at Santa Cruz, Santa Cruz, CA 95064. USA
[33] Dept. of Biology, University of California at Santa Cruz, Santa Cruz, CA 95064. USA

V. Koonin[16], Ian Korf[26], David Kulp[30], Doron Lancet[34], Eric S. Lander[19], Todd M. Lowe[35], Aoife McLysaght[33], Jill Mesirov[19], Tarjei Mikkelsen[34], John V. Moran[36], Nicola Mulder[20], James C. Mullikn[18], Chad Nusbaum[19], Victor J. Pollara[19], Chris P. Ponting[37], Greg Schuler[16], Jörg Schultz[22], Guy Slater[20], Arian F.A. Smit[38], Elia Stupka[20], John Sulston[18], Joseph Szustakowki[34], Danielle Thierry-Mieg[16], Jean Thierry-Mieg[16], Lukas Wagner[16], John Wallis[26], Robert Waterston[26], Raymond Wheeler[30], Alan Williams[30] , Yuri I. Wolf[16], Kenneth H. Wolfe[33], Kim C. Worley[23], Shiaw-Pyng Yang[26], Ru-Fang Yeh[24] and Michael C. Zody[19]

DNA Sequence Databases.

GenBank, *National Center for Biotechnology Information, National Library of Medicine, National Institutes of Health, Bldg. 38A, 8600 Rockville Pike, Bethesda, MD 20894, USA*: Richa Agarwala, L. Aravind, Hsiu-Chuan Chen, Deanna Church, Wonhee Jang, Paul Kitts, Eugene V. Koonin, Greg Schuler, Danielle Thierry-Mieg, Jean Thierry-Mieg, Lukas Wagner and Yuri I. Wolf

EMBL, European Bioinformatics Institute, *Wellcome Trust Genome Campus, Hinxton, Cambridge CB10 1SD, United Kingdom*: Ewan Birney, Nicole Reashci and Peter Sterk

DNA Data Bank of Japan, *Center for Information Biology, National Institute of Genetics, 1111 Yata, Mishima-shi, Shizuoka-ken 411-8540, Japan*: Kaoru Fukami-Kobayashi, Takashi Gojobori, Kazuho Ikeo, Tadashi Imanishi, Satoru Miyazaki, Ken Nishikawa, Motonori Ohta, Hideaki Sugawara and Yoshio Tateno

---

Scientific Management.

National Human Genome Research Institute, U.S. National Institutes of Health, *31 Center Drive, Bethesda, MD 20892, USA*: Francis Collins, Mark S. Guyer, Jane Peterson, Adam Felsenfeld and Kris A. Wetterstrand

Office of Science, U.S. Department of Energy, *19901 Germantown Road, Germantown, MD 20874, USA*: Aristides Patrinos

The Wellcome Trust, *183 Euston Road, London, NW1 2BE, United Kingdom*: Michael J. Morgan

---

Additional Acknowledgements

A. The following is a list of the contributors of unpublished human genomic sequence.

---

[34] Crown Human Genetics Center and the Department of Molecular Genetics, the Weizmann Institute of Science, Rehovot 71600, Israel
[35] Dept. of Genetics, Stanford University School of Medicine, Stanford, California 94305. USA
[36] The University of Michigan Medical School, Departments of Human Genetics and Internal Medicine, Ann Arbor, Michigan 48109, USA
[37] MRC Functional Genetics Unit, Department of Human Anatomy and Genetics, University of Oxford, South Parks Road, Oxford OX1 3QX, United Kingdom
[38] Institute for Systems Biology, 4225 Roosevelt Way NE, Seattle, WA 98105, USA

E. Chen et al., Center for Genetic Medicine and Applied Biosystems; USA

S.-F. Tsai, National Yang-Ming University, Institute of Genetics, Taipei, 155 Li-Rong St Section 2, Peitou, Taiwan 11221, Republic of China

Y. Nakamura, K. Koyama, et al., Institute of Medical Science, the University of Tokyo, Human Genome Center, Laboratory of Molecular Medicine, 4-6-1 Shirokanedai, Minato-ku, Tokyo 108-8639, Japan

G. Kremmidiotis and D. Callen, Cytogenetics & Molecular Genetics, Women's & Children's Hospital, 72 King William Rd, Adelaide, SA 5006, Australia

K.T. Montgomery, S.T. Lau and R. Kucherlapati, Albert Einstein College of Medicine, Department of Molecular Genetics, 1300 Morris Park Avenue, Bronx, NY 10461, USA

V. Kodoyianni, Y.Ge, G.K. Krummel, L. Grable, J. Severin, M. Shannon, A. Brower, A.S. Olsen and L.M. Smith, Department of Chemistry, University of Wisconsin, 1101 University Ave., Madison, WI 53706, USA

B. Weiss et al. Human Genetics, University of Utah, 20 S. 2030 E., Rm 308, Salt Lake City, Utah 84112, USA

E.S. Fitzpatrick et al., Department of Human Genetics, Merck & Co. Inc, SumneyTown Pike, West Point, PA 19486, USA

T. Shina, Tokai University School of Medicine, Molecular Life Science, 2; Bohseidai, Isehara, Kanagawa 259-1193, Japan

E. Ben-Asher, N. Avidan, T. Olender, D. Lancet, L. Salmon and H. Tamary, Department of Molecular Genetics, Weizmann Institute of Science, P.O.Box 26, Rehovot 76100, Israel

K. Yoshinaga, K. Sakurada and A. Horii, Tohoku University School of Medicine, Department of Molecular Pathology, 2-1 Seiryo-machi, Aoba-ku, Sendai 980-8575, Japan

R.M. Crowl, D. Luk and M. Milnamow, Arthritis Research, Novartis Pharmaceuticals Corp., 556 Morris Ave., Summit, NJ 07901, USA

L.M. Gouya, c. Martin, J.-C.P. Deybach and H.V. Puy, Biochemistry and Molecular Genetics, INSERM U409, Hopital Louis Mourier, 178, Rue des Renouillers, Colombes, 92700, France

M. Stark, M. Creaven and D. Grafham, Genetic Cancer Susceptibility Unit, International Agency for Research on Cancer, 150 Cours Albert-Thomas, Lyon Cedex 08 69372, France

D. Kedra, J. Trifunovic, E. Seroussi, J. Jacobson, I. Fransson and J. Dumanski, Department of Molecular Medicine, Karolinska Hospital, Stockholm, Sweden

L.K. O'Brien, H.F. Sims and A.W Strauss, Pediatrics, St. Louis Children's Hospital, 1 Children's Place, St. Louis, MO 63110, USA

S. Richards, Baylor College of Medicine, One Baylor Plaza, Houston, TX 77030, USA

E.H. Rozemuller and M.G.J Tilanus, Pathology, University Hospital Utrecht, P.O.Box 85500, Utrecht 3508GA, The Netherlands

T. Nobukani and Y. Murakami, National Cancer Center Research Institute, Oncogene Div.; 5-1-1, Tsukiji, Chuo-ku, Tokyo 104-0045, Japan

P. Verhasselt, Janssen Research Foundation, Beerse, Belgium

B. The following is a partial list of papers in which sequences that have been included in the draft genome sequence were first published.

Bednarek, AK, Laflin, KJ, Daniel RL, Liao, Q, Hawkins, KA, Aldaz, CM Cancer Res 15: 2140-2145 (2000)

Beckmann, J.S. *et al.* Identification of muscle-specific calpain and beta-sarcoglycan genes in progressive autosomal recessive muscular dystrophies. *Neuromuscul Disord*. **6**, 455-462 (1996)

Jou,C. *et al.* Deletion detection in the dystrophin gene by multiplex gap ligase chain reaction and immunochromatographic strip technology. *Hum Mutat.* **5,** 86-93 (1995)

Loftus, B.J. *et al.* Genome duplications and other features in 12 Mb of DNA sequence from human chromosome 16p and 16q. *Genomics.* **60**, 295-308 (1999).

Okamoto S., Matsushima, M. & Nakamura, Y. Identification, genomic organization, and alternative splicing of KNSL3, a novel human gene encoding a kinesin-like protein. *Cytogenet Cell Genet.* **83,** 25-29 (1998)

Ruddy, D.A. *et al.* A 1.1-Mb transcript map of the hereditary hemochromatosis locus. *Genome Res.* **7**, 441-456 (1997)

Corrections and updates

Figure 33. The units on the Y axis are bp, not kb.
The legend should read: Sequence properties of segmental duplications. Distributions of length and per cent nucleotide identity are shown as a function of the number of aligned bp from the finished vs. finished human genomic sequence dataset. Intrachromosomal (blue), interchromosomal (red).

The legend to Figure 41 should read: For each of 27 common domain families, the number of different Pfam domain types that co-occur with the family in each of the five eukaryotic proteomes. The 27 families were chosen to include the 10 most common domain families in each proteome. The data are ranked….

In Table 22 (Properties of the IGI/IPI human protein set), the number of Matches to nonhuman proteins (third column) in the Ensembl data set (third row) should be 8,126, not 81,126.

P. 898, line 31. The final phrase of the sentence"…and the
representativeness of currently 'known' human genes." should be deleted.
The sentence should read "Before discussing the gene predictions for the human genome, it is useful to consider background issues, including previous estimates of the number of human genes and lessons learned from worms and flies."

p. 900, line 38. Remove "…(see above)… "

Supplement to Table 24.
Probable vertebrate-specific horizontal gene transfers in the human genome

Human protein (accession)

gi4505321
gi4759048
gi7656849
gi7662276
gi7705660
gi7705953
gi8922122
gi8922697
gi8922946
gi8923001
gi8923417
IGI_M1_ctg12730_25
IGI_M1_ctg12741_7
IGI_M1_ctg12824_124
IGI_M1_ctg12824_69
IGI_M1_ctg13002_32
IGI_M1_ctg13238_61
IGI_M1_ctg13305_116
IGI_M1_ctg13419_28
IGI_M1_ctg13419_35
IGI_M1_ctg13492_20
IGI_M1_ctg13715_89
IGI_M1_ctg14420_10
IGI_M1_ctg15343_7
IGI_M1_ctg16010_18
IGI_M1_ctg16516_13
IGI_M1_ctg16537_325
IGI_M1_ctg16537_333
IGI_M1_ctg18743_55
IGI_M1_ctg19042_43
IGI_M1_ctg19053_28
IGI_M1_ctg19053_29
IGI_M1_ctg19053_31
IGI_M1_ctg19241_54
IGI_M1_ctg25107_24
IGI_M1_ctg595_96
IGI_M1_ctg_52
O43600
O75588
O76044
P19971
Q16490
Q9ULI2
AAG01853
CAB81772
gi6912516
gi8923543
O43826
P13866

P21397
P27338
P28330
P31639
P53794
IGI_M1_ctg13284_79
IGI_M1_ctg14250_20
IGI_M1_ctg14293_4
IGI_M1_ctg14420_109
IGI_M1_ctg19053_30
IGI_M1_ctg19053_32
Q99540
gi10047132
gi7705582
gi7705929
gi8922911
BAB13402
IGI_M1_ctg17129_30
gi8923844
P10745
AAG09731
BAA91937
CAB96131
IGI_M1_ctg13129_34
IGI_M1_ctg13284_29
IGI_M1_ctg13459_1
IGI_M1_ctg14210_35
IGI_M1_ctg14333_22
IGI_M1_ctg15880_11
IGI_M1_ctg15970_12
IGI_M1_ctg16704_2
IGI_M1_ctg16942_3
IGI_M1_ctg25185_50
O00154
P11245
P16455
P29372
P45381
P46597
P51570
Q14397
Q92819
Q9UBM0
Q9UHN1
gi4885285
gi8850215
gi8923007
O60363
Q9ULF2
AAG01854
AAG01855
CAC00574
IGI_M1_ctg12913_93
IGI_M1_ctg14294_11
IGI_M1_ctg14654_1
IGI_M1_ctg15247_50

IGI_M1_ctg16029_6
IGI_M1_ctg16029_9
IGI_M1_ctg17057_13
IGI_M1_ctg17565_12
IGI_M1_ctg19042_15
O15280
O75202
O75203

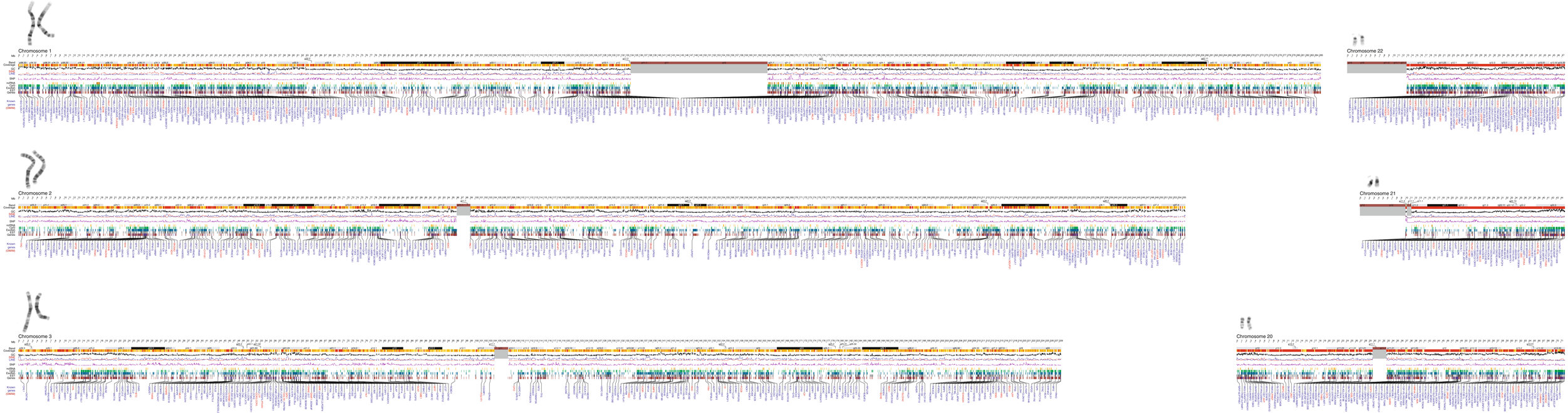
Chromosome 1
Chromosome 2
Chromosome 3
Chromosome 20
Chromosome 21
Chromosome 22

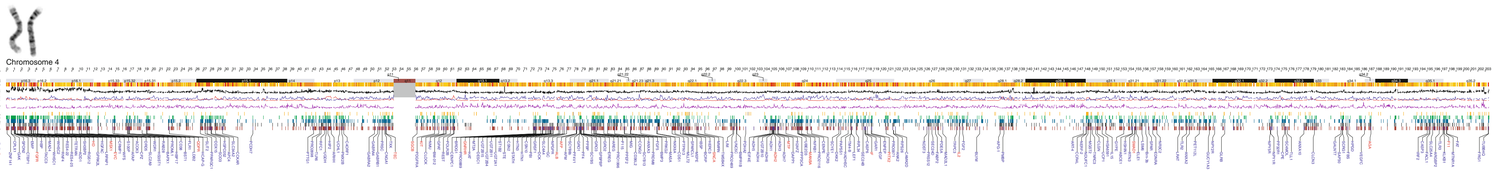
Chromosome 4
Mb
Band
Coverage
DP
LOH
SNP
hetRAT
Exon
Gene
Known gene
(OMIM)

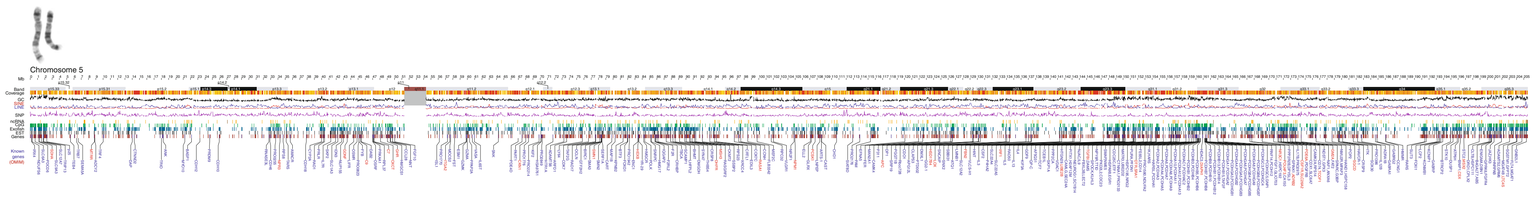
Chromosome 5
Mb
Band
Coverage
DP
LOH
SNP
hetRAT
Exon
Gene
Known gene
(OMIM)

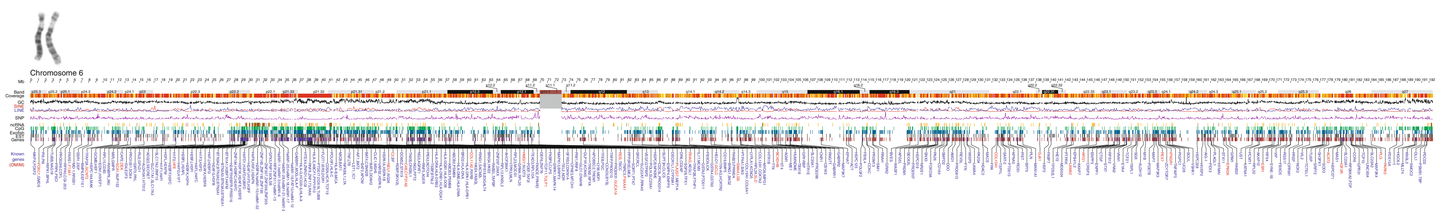
Chromosome 6
Mb
Band
Coverage
DP
LOH
SNP
hetRAT
Exon
Gene
Known gene
(OMIM)

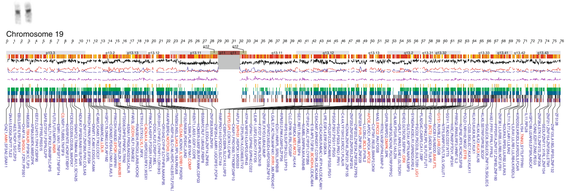
Chromosome 19

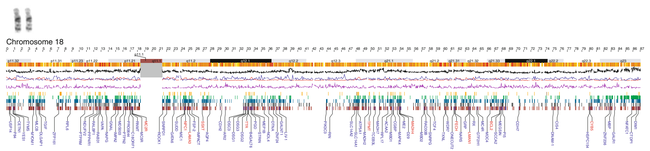
Chromosome 18

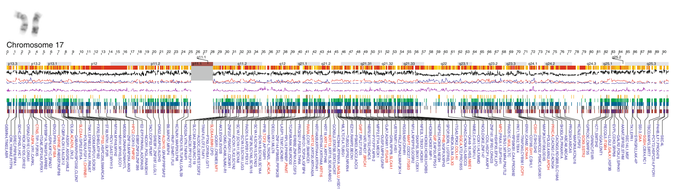
Chromosome 17

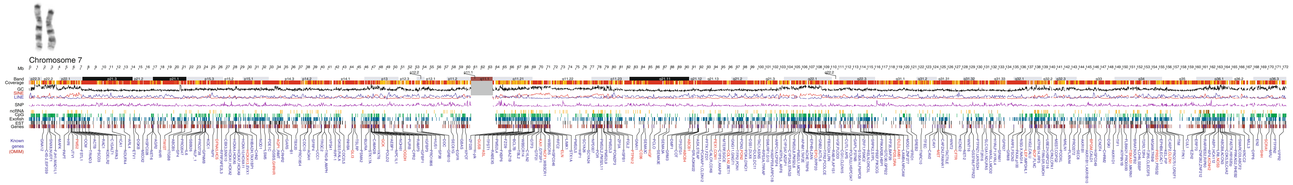
Chromosome 7
Mb
Band
Coverage
GC
LINE
SNP
ncRNA
CpG
Exons
Genes
Known
genes
(OMIM)

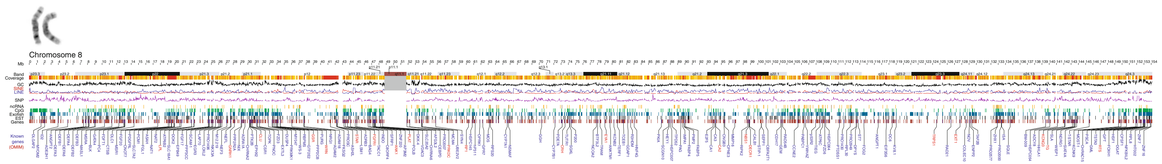
Chromosome 8
Mb
Band
Coverage
GC
LINE
SNP
ncRNA
CpG
Exons
Genes
Known
genes
(OMIM)

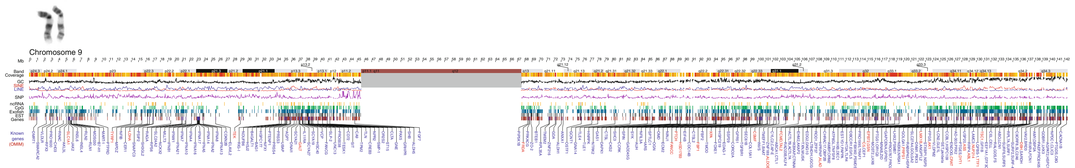
Chromosome 9
Mb
Band
Coverage
GC
LINE
SNP
ncRNA
CpG
Exons
Genes
Known
genes
(OMIM)

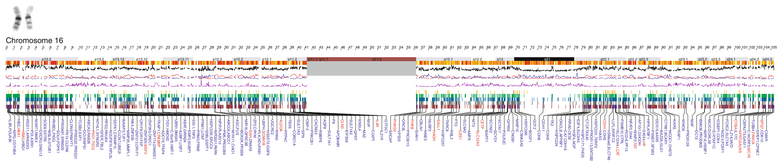
Chromosome 16

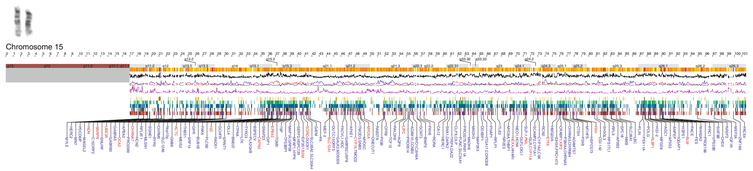
Chromosome 15

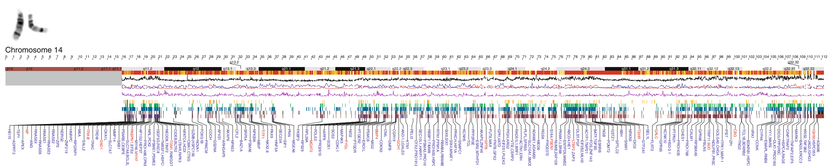
Chromosome 14

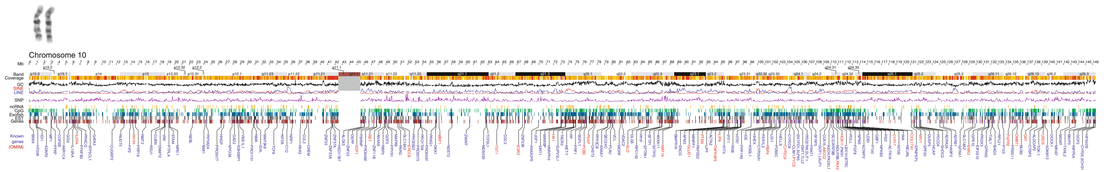
Chromosome 10

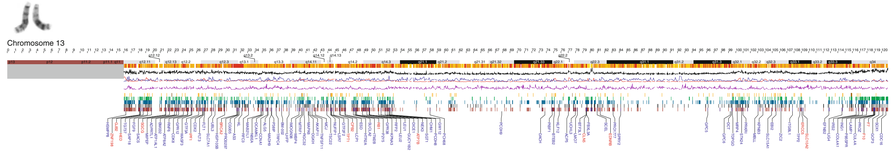
Chromosome 13

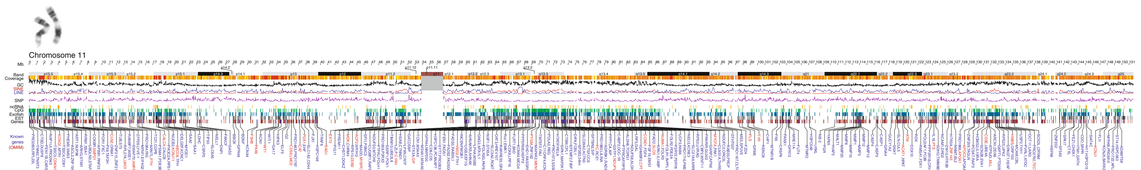
Chromosome 11

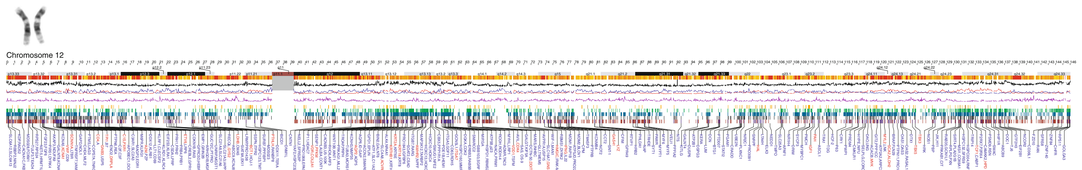
Chromosome 12

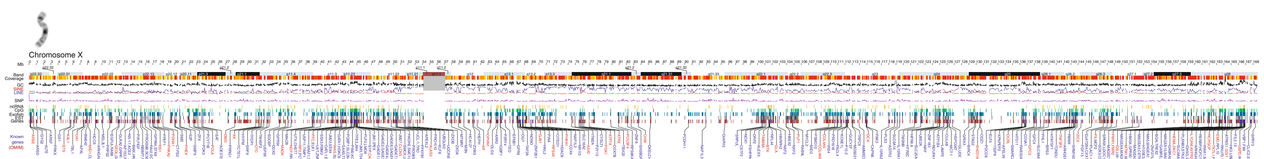
Chromosome X

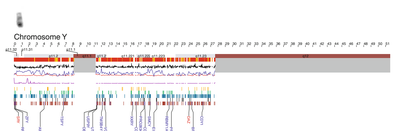
Chromosome Y